

AD-A170 896

A METHOD FOR GOVERNING SPACECRAFT EVASIVE MANEUVERING
(U) AIR FORCE INST OF TECH WRIGHT-PATTERSON AFB OH
K R KELLER JUN 86 AFIT/CI/NR-86-891

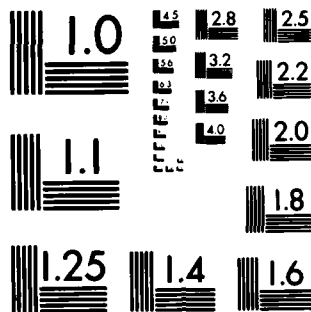
1/3

UNCLASSIFIED

F/G 22/3

ML





MICROCOPY RESOLUTION TEST CHART
NATIONAL BUREAU OF STANDARDS-1963-A

MMIC FILE COPY

AD-A170 896

AD-A170 896

1

SECURITY CLASSIFICATION OF THIS PAGE (When Data Entered)

REPORT DOCUMENTATION PAGE		READ INSTRUCTIONS BEFORE COMPLETING FORM
1. REPORT NUMBER AFIT/CI/NR 86-89T	2. GOVT ACCESSION NO.	3. RECIPIENT'S CATALOG NUMBER
4. TITLE (and Subtitle) A Method for Governing Spacecraft Evasive Maneuvering		5. TYPE OF REPORT & PERIOD COVERED THESIS/DISSERTATION
7. AUTHOR(s) Keith Richard Keller		6. PERFORMING ORG. REPORT NUMBER
9. PERFORMING ORGANIZATION NAME AND ADDRESS AFIT STUDENT AT: Massachusetts Institute of Technology		8. CONTRACT OR GRANT NUMBER(s)
11. CONTROLLING OFFICE NAME AND ADDRESS AFIT/NR WPAFB OH 45433-6583		10. PROGRAM ELEMENT, PROJECT, TASK AREA & WORK UNIT NUMBERS
14. MONITORING AGENCY NAME & ADDRESS (if different from Controlling Office)		12. REPORT DATE 1986
		13. NUMBER OF PAGES 251
		15. SECURITY CLASS. (of this report) UNCLAS
		15a. DECLASSIFICATION/DOWNGRADING SCHEDULE
16. DISTRIBUTION STATEMENT (of this Report) APPROVED FOR PUBLIC RELEASE; DISTRIBUTION UNLIMITED		
17. DISTRIBUTION STATEMENT (of the abstract entered in Block 20, if different from Report) B		
18. SUPPLEMENTARY NOTES APPROVED FOR PUBLIC RELEASE: IAW AFR 190-1 Lynn E. Wolaver 6 AUG 86 Dean for Research and Professional Development AFIT/NR		
19. KEY WORDS (Continue on reverse side if necessary and identify by block number)		
20. ABSTRACT (Continue on reverse side if necessary and identify by block number) ATTACHED.		

DD FORM 1 JAN 73 1473

EDITION OF 1 NOV 65 IS OBSOLETE

86 8 12 026

SECURITY CLASSIFICATION OF THIS PAGE (When Data Entered)

A METHOD FOR GOVERNING SPACECRAFT EVASIVE MANEUVERING

by

KEITH RICHARD KELLER

Bachelor of Aerospace Engineering and Mechanics
University of Minnesota, Institute of Technology
(1982)

SUBMITTED IN PARTIAL FULFILLMENT
OF THE REQUIREMENTS FOR THE
DEGREE OF

MASTER OF SCIENCE IN
AERONAUTICS AND ASTRONAUTICS

at the

MASSACHUSETTS INSTITUTE OF TECHNOLOGY
June 1986

© Keith Richard Keller 1986

The author hereby grants to M.I.T. permission to reproduce and to distribute copies of this thesis document in whole or in part.

Signature of Author _____

Keith R. Keller

Department of Aeronautics and Astronautics
May 9, 1986

Certified by _____

Antonio L. Elias

Assistant Professor Antonio L. Elias
Thesis Supervisor, Department of Aeronautics and Astronautics

Accepted By _____

Harold Y. Wachman

Professor Harold Y. Wachman
Chairman, Department Graduate Committee

A METHOD FOR GOVERNING SPACECRAFT EVASIVE MANEUVERING

by

KEITH RICHARD KELLER

Submitted to the Department of Aeronautics and Astronautics

on May 9, 1986

in partial fulfillment of the requirements

for the degree of

Master of Science in Aeronautics and Astronautics

ABSTRACT

A computer program is developed to govern the evasive maneuvering of a spacecraft in response to an anti-spacecraft missile threat in regions of space where drag is not significant. With a view to circumventing the need to numerically integrate the equations of motion for both vehicles to predict future position and velocity along their trajectories, the methods of astrodynamics are used to determine the missile's orbit from two vector position fixes over time so it can be compared to the spacecraft's orbit, determined from a position and velocity vector. The transfer time required for the missile to reach the spacecraft's altitude is determined and the future position of the missile is predicted so that a future relative position vector between the spacecraft and missile can be found. If it is found that the missile will intercept the spacecraft at the future time, appropriate evasive action is initiated for the spacecraft. A maneuver to any point in three-dimensional space can be targeted by specifying the magnitude and direction of the miss-distance desired, and velocity-to-be-gained calculations are done as an aid to making maneuvering decisions. To test the assumptions of the astrodynamic techniques in the program, a fourth-order Runge-Kutta numerical integration technique was implemented in the program and is used to update all current trajectory data points. Spacecraft engine thrust, if an impulsive maneuver is not selected, atmospheric drag, and higher order gravitational harmonics are modelled and included in the integration of the equations of motion for both vehicles. When the trajectories of the vehicles were fully integrated to the predicted intercept time, the integrated data points could then be compared to those generated through the astrodynamic techniques. It was found that agreement between integrated and astrodynamic data points could typically be obtained to the third or fourth decimal place in kilometers in scenarios where drag was not significant. The astrodynamic techniques were found to be able to predict intercept and provide information for maneuvering the spacecraft in real-time for simulations run on a VAX 11/750, while the integration techniques experienced a time lag in updating trajectories which was dependent on the integration step size used.

Thesis Supervisor: Dr. Antonio L. Elias

Title: Assistant Professor of Aeronautics and Astronautics

Acknowledgements

I would like to thank Dr. Antonio Elias for making the facilities of the Flight Transportation Lab available to me to use in the development of the computer program I am about to describe and in the preparation of this document. I would also like to thank General Dynamics Space Systems Division for the support they provided in the initial phases of this research. Finally, I would especially like to thank Dr. Richard H. Battin, without whose instruction in the methods of astrodynamics this research would not have been possible.



Accession For	
NTIS	<input checked="" type="checkbox"/>
DTIC	<input type="checkbox"/>
Univ.	<input type="checkbox"/>
JPL	<input type="checkbox"/>
BY	
Dist	
Av.	
Dist	
A-1	

Contents

Abstract	2
Acknowledgements	3
List of Figures	7
List of Tables	8
1 Introduction	9
2 Background	12
2.1 Satellite Roles And Vulnerability	12
2.2 Anti-Satellite Systems	15
2.2.1 Soviet ASAT Capabilities	15
2.2.2 U.S. ASAT Capabilities	18
2.2.3 Assessment of Soviet ASAT Capability	20
2.2.3.1 Altitude Limitation	20
2.2.3.2 Launch Constraints	22
2.2.3.3 Homing and Maneuvering Constraints	23
2.2.4 Future ASAT Trends	24
2.3 Defensive Countermeasures	26
2.3.1 Non-maneuvering Countermeasures	29
2.3.2 Evasive Maneuvering as a Countermeasure	32
2.4 Other Research Applicable to Evasive Maneuvering	36
3 Description of Program EVADER	41
3.1 Overview of Evasive Maneuvering Requirements	41
3.2 EVADER's Predictive Astrodynamic Techniques	43
3.2.1 Coordinate System Used	44
3.2.2 Geometry of an Ellipse	47

3.2.3	Program Inputs	49
3.2.4	The Lambert Algorithm	50
3.2.4.1	Lambert Algorithm Equations	51
3.2.5	The Transfer Time Algorithm	54
3.2.5.1	Transfer Time Equations	56
3.2.6	The Extended Gauss Method	58
3.2.6.1	Extended Gauss Equations	59
3.3	Taking Evasive Action	62
3.3.1	Evasive Maneuvering in EVADER	62
3.3.2	Assessing the Operator's Role in Evasive Action Decisions	69
3.4	Testing Evader	72
3.4.1	Vector Equation of Orbital Motion	73
3.4.2	Picking a Numerical Integration Technique	74
3.4.3	Fourth-Order Runge-Kutta Method	76
3.4.4	The Gravity Model	79
3.4.5	The Drag Model	82
3.4.6	The Spacecraft Thrust Model	85
3.4.7	Vehicle Baseline Configurations	89
3.4.8	Setting Up an Evasion Scenario	94
4	Results	102
5	Conclusions	127
APPENDIX		
A	Program Listing of EVADER	132
B	Program Output of EVADER	167
B.1	Non-Retrograde Co-orbital Injection Intercept Scenario	168
B.2	Retrograde Co-orbital Injection Intercept Scenario	178

B.3 Non-Retrograde Direct-Ascent Intercept Scenario	188
B.4 Retrograde Direct-Ascent Intercept Scenario	200
B.5 Retrograde Direct-Ascent Scenario with No Drag	212
B.6 Delta V Required vs. Separation Distance	222
B.7 Scenario Demonstrating Options Available in EVADER	236
Bibliography	249

List of Figures

1	Coordinate System Geometry	46
2	Geometry of an Ellipse	48
3	Stages of an Invocation of EVADER	68
4	Axisymmetric Gravity as a Function of Position	80
5	Non-Retrograde Co-Orbital Injection Intercept Scenario	115
6	Closeup of Non-Retrograde Co-Orbital Injection Intercept Geometry	116
7	Retrograde Co-Orbital Injection Intercept Scenario	117
8	Closeup of Retrograde Co-Orbital Injection Intercept Geometry . . .	118
9	Non-Retrograde Direct-Ascent Intercept Scenario	119
10	Closeup of Non-Retrograde Direct-Ascent Plane Change Geometry .	120
11	Closeup of Non-Retrograde Direct-Ascent Intercept Geometry	121
12	Retrograde Direct-Ascent Intercept Scenario	122
13	Closeup of Retrograde Direct-Ascent Intercept Geometry	123
14	Δv Required vs. Separation Distance from the Missile	124
15	Intercept Scenario with a Three-Dimensional Aim-Point Maneuver .	125
16	Closeup of Three-Dimensional Maneuver Planar Geometry	126

List of Tables

1	Soviet ASAT Tests Conducted To Date	16
2	Default Vehicle Parameters for Drag Calculations	93
3	Spacecraft Propulsion System Default Characteristics	93
4	Breakdown of Spacecraft Mass	93

1 Introduction

For a spacecraft to survive an anti-spacecraft missile attack, it must be able to maneuver evasively if other defensive countermeasures fail to prevent detection of the spacecraft, or fail to deceive, confuse, or destroy the attacker. To maneuver effectively, the spacecraft must be able to detect an attack, determine the attacking missile's orbit, and predict the likelihood of intercept at some future time. If intercept is concluded to be imminent, the spacecraft must be able to plan and carry-out effective evasive maneuvers based on information which is timely, accurate, quantifiable, and realistic. The planning and execution of these maneuvers must take into account the orbital, fuel, and mission constraints which restrict the spacecraft, and the ability to choose a maneuver which is advantageous to the spacecraft and exploits any deficiencies in the missile's maneuverability, range, or homing devices is vital. Thus, to avoid intercept, the spacecraft must be able to maneuver to any point in three-dimensional space based on calculations that must be done on-board in real-time, based on reliable predicted missile position information derived from information available to the spacecraft through its sensors.

In this paper, I will describe research I conducted to develop a method for governing spacecraft evasive maneuvering through a computer program incorporating many of the techniques of astrodynamics. Because of the critical time constraints prevailing in a typical intercept scenario, a means of providing information to the spacecraft concerning the predicted position of the missile and the transfer time-to-intercept is required. I intend to show that the methods of astrodynamics can provide the timely, accurate information needed by the spacecraft to predict intercept and calculate velocity-to-be-gained requirements to achieve a miss-distance of a desired magnitude and direction at the predicted intercept time. These calculations will be based on two vector position fixes of the missile over time, which could be obtained from an infrared detector and a laser-rangefinder, and the position and velocity vectors of the spacecraft, as could be obtained from on-board guidance and

navigation instruments.

The beauty of using astrodynamic techniques to predict future position and velocity information to warn of intercept and to target evasive maneuvers is that they can provide information for future points in time with only one pass of their algorithms. If the same information for points hundreds of seconds in the future had to be found through numerically integrating the equations of motion for both vehicles using small integration time steps, the computational task would most likely prevent on-board computation in real-time, when real-time responses are imperative. Furthermore, if the missile maneuvers, and predicted trajectory point updates are needed, or if updates for the sake of improving the accuracy of missile position information are desired every second or less, the task of integrating trajectories out hundreds of seconds every second would clearly be prohibitive.

In addition, I intend to show that for scenarios where drag is not significant, numerically integrating trajectories is no more accurate than using methods of astrodynamics to predict intercept and plan maneuvers, despite the fact that drag is ignored completely and uniform gravity, two-body motion, and impulsive maneuvers are assumed in the astrodynamic techniques. In fact, a fourth-order Runge-Kutta numerical integration technique will be used to update current trajectory values so that they can be compared to predicted trajectory values generated through the astrodynamic techniques, once the current trajectories are fully integrated to the predicted times. Models for spacecraft engine thrust, atmospheric drag, and gravitational perturbations due to higher order zonal harmonics will be included in the integration of the equations of motion for current trajectory updates, in order to test the assumptions innate to the astrodynamic techniques.

In order to set the stage for the presentation of the astrodynamic techniques, and in order to give the reader a perspective on the assumptions and important considerations incorporated in the computer program, background information on the roles and vulnerability of satellites, anti-satellite systems, and defensive countermeasures will first be presented. Other research that has some applicability to

this project will also be discussed.

A description of the astrodynamic methods used in the program will then ensue, and the pertinent equations to be calculated for each method employed will be briefly presented. This will be followed by an explanation of the ways in which evasive maneuvers are initiated and performed in the program. The role of the operator in making evasive maneuvering decisions will also be discussed.

Then, the vector differential equation of motion governing the trajectories of both vehicles in the presence of external perturbative accelerations will be presented, and the way in which the method of solving this equation numerically was chosen and implemented will be discussed. The models for drag, gravitational anomalies, and spacecraft thrust that are used in the integration of the vehicles' equations of motion will then be described as will the assumptions that were made in the selection of these models. The baseline configurations chosen to represent the missile and spacecraft in numerical calculations will also be presented.

Finally, the way in which scenarios were setup to properly test the program will be examined, followed by the presentation of the results that were obtained through the simulations of a number of scenarios. Four basic types of intercept scenarios which are representative of the methods of attack used by anti-satellite missiles will be presented, along with other scenarios that can provide an insight into the capabilities and assumptions of the program and the geometry and properties of the different stages of an anti-spacecraft missile attack.

All simulations performed with the computer program described in this paper were run on a VAX 11/750, which supports a number of users in the Flight Transportation Laboratory (FTL) of the Department of Aeronautics and Astronautics. The background research for this paper was largely derived from sources obtained through the Aeronautics and Astronautics departmental library.

2 Background

2.1 Satellite Roles And Vulnerability

Today, the use of space-based systems to provide intelligence information and support operational military capabilities and planning is vital to U.S. national security. Furthermore, reliance of nations on their satellites for many critical tasks is continually increasing, since no other means can provide the kind of timely, accurate and global information that space-based systems can provide.

Among the many important global functions satellites perform are communications, navigation and positioning, surveillance, meteorology, mapping, and search and rescue. In peacetime, for example, both electronic and optical surveillance are used to verify compliance with treaties and monitor the exercises, movements, and plans of military forces. During times of crisis and conflict, satellites become essential to give early warning of attack, provide assessment of counter-attack damage, monitor hostile force deployments, and support the command and control of military operations. In fact, an effective and survivable satellite network is essential today in providing the overall command, control, communications, and intelligence (C³I) needs of a large, global military force in modern military combat. If essential satellite systems are vulnerable to attack, denial or destruction by opposing forces at the beginning or during a conflict, at a time when these assets become most necessary, the resulting loss of C³I abilities would be catastrophic. Therefore, it is prudent to develop means of defending U.S. satellites against attack in order to increase their chances of survival.

As stated by Lt Col John E. Angell [2], Deputy Chief of Space Plans Division at HQ USAF,

The increasing capabilities of current and future satellites to perform such critical military missions as communications, navigation, surveillance, and weather monitoring have made them central elements in our national security posture. To accommodate the growing role of space

systems in military operations, the Air Force is modernizing the infrastructure used to support space activities, [and] acquiring a capability to defend U.S. space assets ...

In order to assess the threat to U.S. satellites and determine their vulnerability to attack, it is first necessary to understand in more detail the roles of military satellites and the kinds of orbits they occupy.

Most military satellites can be divided, according to the orbits they occupy, into four general categories [9]:

1) low-Earth orbits

These are generally circular, roughly polar orbits having an inclination with respect to the equator of between 65 and 115 degrees. Orbital periods are usually on the order of 100 minutes and orbital altitudes generally fall into a range of 100 to several thousand kilometers.

2) highly elliptical orbits

Here satellites move in orbits with a perigee (lowest point) of several hundred kilometers in altitude and an apogee (highest point) of up to 40,000 kilometers. These orbits generally have an inclination of between 60 and 65 degrees with the perigee occurring over the Southern Hemisphere and the apogee over the Northern Hemisphere.

3) semisynchronous orbits

Roughly circular and having an altitude of about 20,000 kilometers, these orbits are inclined from the Equator by 63 to 65 degrees.

4) geosynchronous orbits

Satellites in these orbits, which have an altitude of about 36,000 kilometers, move in the Earth's equatorial plane and have an angular velocity which is the same as the Earth's rate of rotation. For this reason, satellites in these orbits remain fixed above a point on the Equator.

The particular orbit in which a satellite operates is dictated by its mission. As a result, satellites performing photoreconnaissance and electronic intelligence tend to be in low-Earth orbits, where better photographic resolution of ground features can be obtained and weak electronic signals are more easily monitored. The inclination of these low orbits, as well as that of the elliptical and semisynchronous orbits, allows a satellite to have coverage of different parts of the globe as the Earth rotates and the satellite moves in its path. In fact, the higher the inclination of the orbit, the more complete the coverage of the globe over several orbits becomes. This can be better understood by realizing that the ground track of a satellite in an inclined orbit resembles a sine wave. The larger the inclination, the larger the amplitude of the sine wave becomes.

Thus, low-orbit satellites provide an important means of gathering routine intelligence data on a day-to-day basis, as well as providing time-critical information for battle management during a conflict. Such tasks as monitoring troop and equipment deployments, ocean surveillance, intercepting weak communications signals, and providing some meteorology and navigation information are examples of missions well suited to low-orbit satellites. Presently, the U.S. Transit Navigation System, which supports the Navy's ballistic missile submarines, is located in a low orbit. However, this task will soon be transferred to NAVSTAR satellites operating in semisynchronous orbits [7].

When communication with facilities farther north toward the Arctic Circle is desired, as is often the case with the U.S.S.R. and some U.S. facilities, an elliptical, highly inclined orbit is used. Thus, many of the U.S.S.R.'s communication and strategic early warning satellites are in such orbits. Satellites of the U.S. Satellite Data System are also in such orbits to facilitate communication with forces in the Arctic.[9] Because the apogee of such orbits is high over the Northern Hemisphere, satellites can be within contact range of ground stations for up to 8 hours of a 12 hour orbital period.

Semisynchronous orbits will be used for the new, highly accurate global nav-

igation systems of the U.S. such as the Global Positioning System (GPS). With GPS, planned to be deployed by the late 1980's, 18 satellites will provide nearly complete global coverage, furnishing navigation information to both military and civilian users. A similar Russian system, the Glonass navigation satellites, is also being deployed in the same type of orbit.[7]

Geosynchronous orbits are preferred for applications where continuous coverage of large areas, or continuous communication with a particular set of ground stations is desired. This is possible because satellites in these orbits remain fixed above a point on the Equator, as previously mentioned. U.S. infrared ballistic missile early warning satellites are in these orbits, as are most U.S. communication satellites for civilian and military use. Certain U.S. electronic intelligence (ELINT) satellites are also deployed in these orbits, as are some Soviet communication satellites.[9]

2.2 Anti-Satellite Systems

To better understand the nature of the threat to U.S. satellites, and to devise appropriate defensive countermeasures, it is necessary to characterize the current operational anti-satellite (ASAT) capability possessed by the Soviets. Furthermore, the future ASAT capabilities they are developing or might achieve must also be considered. This is best done in the context of a comparison between present and projected Soviet and U.S. ASAT capabilities.

2.2.1 Soviet ASAT Capabilities

The currently operational Soviet ASAT system consists of a modified, liquid-fueled, three-stage, SS-9 ballistic missile booster, which is approximately 45 meters long, and its interceptor vehicle payload. The interceptor weighs more than 2,000 kilograms and is about 6 meters long and 3 meters in diameter. It has an engine for maneuvering and a conventional explosive fragmentation warhead[9].

The mode of interception used by the Soviet ASAT weapon is co-orbital injection; that is, the interceptor is launched into an orbit which closely matches the

TEST	DATE	INTERCEPTOR COSMOS NUMBER	INTERCEPT ALTITUDE (KILOMETERS)	ORBITS BEFORE INTERCEPT	TEST RESULT
1	20 OCT 68	249	525	2	FAILURE
2	1 NOV 68	252	535	2	SUCCESS
3	23 OCT 70	374	530	2	FAILURE
4	30 OCT 70	375	535	2	SUCCESS
5	25 FEB 71	397	585	2	SUCCESS
6	4 APR 71	404	1,005	2	SUCCESS
7	3 DEC 71	462	230	2	SUCCESS
8	16 FEB 76	804	575	1	FAILURE
9	13 APR 76	814	590	1	SUCCESS
10	21 JUL 76	843	1,630	2	FAILURE
11 ^a	27 DEC 76	886	570	2	FAILURE
12	23 MAY 77	910	1,710	1	FAILURE
13	17 JUN 77	918	1,575	1	SUCCESS
14	26 OCT 77	961	150	2	SUCCESS
15 ^a	21 DEC 77	970	995	2	FAILURE
16 ^a	19 MAY 78	1,009	985	2	FAILURE
17 ^a	18 APR 80	1,174	1,000	2	FAILURE
18 ^a	2 FEB 81	1,243	1,005	2	FAILURE
19	14 MAR 81	1,258	1,005	2	SUCCESS
20 ^a	18 JUN 82	1,379	1,005	2	FAILURE

^aThe optical/infrared homing device was used and failed for these tests.

Table 1: Soviet ASAT Tests Conducted To Date

orbit of its target. To do this, the interceptor literally rendezvous with its target over a period of up to three hours. Interception is usually completed after one or sometimes two orbital revolutions, once the target's altitude is achieved. Since its inception in 1968, the Soviet system has been tested over 20 times, with varying degrees of success. A list of Soviet ASAT tests, the data for which are from reference [9], is shown as Table 1.

Early tests of the Soviet system through 1971 relied on active radar homing for guidance to an intercept, which occurred after two orbits. Since 1976, two types of guidance have been tested. The first uses active radar homing to perform a quicker

intercept on the first orbit. This approach has worked in two of four attempts. The second guidance technique employs an optical/infrared homing device with the intercept attempted after two orbits. This method has failed in all six of its tests. As shown in Table 1, intercept altitude, which is dependent on the limited range of the SS-9 booster, has been as high as 1,710 kilometers. To illustrate in more detail the way in which a typical Soviet ASAT mission would proceed, it is useful to review the events of a recent ASAT test conducted by the Soviets on June 18, 1982. As reported in the June 28, 1982 issue of *Aviation Week & Space Technology* [34], this test was conducted as part of a demonstration by the Soviet Union of its strategic nuclear weapons offensive and defensive capability integrated with command, control and communications over a 7-hour period on June 18, 1982.

In preparation for the test, an ASAT target, Cosmos 1375, was launched on June 6 into a 1,021×990-km (634×615-miles) orbit inclined 65.9 degrees.[32] The seven hour exercise began on June 18 with the launching of two SS-11 intercontinental ballistic missiles (ICBMs) from operational silos toward the Kamchatka test range, followed almost simultaneously by the launch of an operational SS-20, an intermediate range ballistic missile (IRBM) designed for the European theater.

As the exercise unfolded, the ASAT attack against Cosmos 1375 was performed, followed by two anti-ballistic missile (ABM) intercepts. For the ABM intercepts, two target intercontinental ballistic missiles (ICBMs), which had been fired from Kapustin Yar and retrofired back into the atmosphere over Saryshagan, were intercepted by a new hypersonic interceptor missile. This new missile, which is similar to the U.S. Sprint missile, is designated the ABM-X-3 by the U.S. Department of Defense (DOD) and is controlled by a phased-array radar.[27] A sea-launched ballistic missile (SLBM) was also fired from a Delta class submarine in the White Sea as part of the exercise.

By this exercise, analysts believe the U.S.S.R. demonstrated in logical sequence: a first-strike attack on the U.S. and Europe combined with an ASAT attack, followed by a demonstration of ABM intercepts to thwart a potential U.S. retaliatory strike,

and finally a Soviet second strike capability using SLBMs. The ASAT attack would be designed to destroy U.S. reconnaissance spacecraft in low-orbit, thereby denying the U.S. the ability to detect time-critical targets and to determine which ICBMs have been launched and which remain for a follow-on strike. Detection of silo reloads would also be denied, as would the the ability to monitor the dispersal of ballistic missile submarines and the immediate deployment and movements of conventional forces.

To perform the ASAT attack, the interceptor vehicle, Cosmos 1379, was launched from Tyuratam at 11:10 a.m. GMT in to an initial low-Earth orbit. Then, at 12:26 p.m. GMT, the ASAT vehicle performed a plane change of 0.7 degrees and maneuvered into an elliptical orbit of 1,010×977-km (628×607-miles). As both platforms were passing over Europe at 2:20 p.m. GMT, the intercept of the target vehicle occurred as the ASAT vehicle approached orbital apogee. Thus, the total elapsed time to intercept was 3 hr 10 min. Although the ASAT vehicle was to fly well within lethal range of the target, the warhead's fuzing malfunctioned, causing the warhead to fire early and to fail to damage the target.

2.2.2 U.S. ASAT Capabilities

The U.S. ASAT system, which is air-launched form a modified USAF/McDonnell Douglas F-15 Eagle, is 17 ft (5.18 m) in length, 18 in. (0.457 m) in diameter, and weighs 2,700 lb (1,224 kg). The missile consists of a Boeing short-range attack missile (SRAM) first stage motor, an LTV Altair second-stage motor and an LTV miniature homing vehicle (MHV) interceptor in the nose.[16] Minimal modification is needed to make a standard F-15 capable of carrying the ASAT weapon. Primary additional elements include an interface hardware pallet, a special centerline pylon to carry the missile, and certain F-15 computer software modifications.

The MHV weighs about 35 lb (15.9 kg) and is about 12 in. (30 cm) long. It has 64 small single-shot solid rocket motors around its circumference which fire by computer control for lateral adjustments to the intercept trajectory. The MHV also

carries a laser gyro for guidance and has 8 cryogenically cooled, infrared detection telescopes for homing in on the target.[36,7]

The method of attack used by this vehicle is a direct-ascent interception. That is, destruction of the target satellite is achieved by launching the missile directly into the path of the on-coming satellite, with destruction occurring by collision alone. No explosive is necessary, since the combined velocity of the MHV and target at impact is about 27,000 miles/hr (12.07 km/sec).

A typical ASAT mission proceeds in the following manner.[16] Before takeoff, initial targeting, navigation and launch data, based on information supplied to the F-15 from Space Command's Space Defense Operations Center (SPADOC), is fed into the F-15's mission computer. SPADOC would provide overall coordination of U.S. ASAT attack operations in a conflict.[36] After takeoff, the mission is flown autonomously by the pilot without any need for a data, radar control, or guidance link from the ground. The F-15 mission computer and data from the missile itself provide all guidance and waypoint information needed by the pilot to fly the aircraft so that it will arrive at the correct three-dimensional launch window position at a precise time. Position and timing at missile launch are critical, since the trajectory of the missile must be such that it will place the third-stage MHV in a position from which its infrared detectors can acquire the target. All steering cues, distance, and time to navigation waypoints are displayed to the pilot on the aircraft's head-up display (HUD).

After the aircraft has been navigated to the final waypoint, a maneuvering point, where the aircraft will begin an acceleration and pull-up for launch, is computed. At the maneuvering point, approximately 19-20 sec before launch, the HUD displays cues for a 3.5 g pull-up to establish a 60-65 degree climb angle. Shortly after pull-up, a series of automatic pre-launch sequences are conducted, committing the missile to launch. The launch point is reached and the missile released as the aircraft attains an altitude of 35,000-40,000 ft, after allowing airspeed to bleed off to slightly below Mach 1.

After release, the first and second stage motors ignite and burn in sequence, boosting the third stage MHV into the proper position for target acquisition. The MHV then follows a ballistic trajectory to impact, with lateral homing adjustments being made with the MHV's single-shot solid motors. Elapsed time from missile launch to intercept is about 10 minutes.

On September 13, 1985, the U.S. conducted a successful ASAT mission, like the one just described, over the Western Test Range in California. In the test [30], a 1,936-lb (878 kg), 11.3-ft (3.44 m) long, 6.8-ft (2.07 m) diameter satellite built by Ball Aerospace was destroyed by direct impact. The satellite, which had been launched in 1979 to perform gamma ray spectrometry experiments for the Defense Advanced Research Projects Agency (DARPA) and had outlived its useful life, was in a circular, polar orbit inclined 97.7 degrees at an altitude of 320 nautical miles (593 km).

2.2.3 Assessment of Soviet ASAT Capability

The Soviet ASAT system, first tested in 1968, is rather crude in comparison to the more technologically sophisticated U.S. ASAT system. However, despite its many shortcomings, the Soviet system still remains an effective threat, especially when combined with the formidable Soviet space launch capacity and their continuing efforts to develop an improved infrared homing system.

2.2.3.1 Altitude Limitation

The primary limitation of both the Soviet and U.S. ASAT missiles is their altitude capability. Presently, both systems can only reach spacecraft which operate in low-Earth orbit. Even so, the Soviet system actually has an advantage in this category. Their system has an operational altitude approaching 2,000 km, as judged from their testing to date, while the U.S. system can most likely go no higher than 400 miles (644 km).[7] In view of the present altitude limitation of both systems, according to John Pike of the Federation of American Scientists,

The number of American satellites in orbits within range of the Soviet ASAT will decline from 29 (out of a total of 94) in 1983 to 24 (out of 141) by 1989. Similarly, the number of vulnerable Soviet satellites will decline from 26 (out of 90) to 10 (out of 67) over the same period.[7]

This estimate does not, of course, take into account the possibility that the Soviets could increase the range of their system without much difficulty, while the U.S. ASAT missile's size and air-launched capability, although offering great launch flexibility, fundamentally constrains its altitude reach. Since the Soviet ASAT weapon's intercept altitude is limited primarily because of the SS-9 booster's limited range, it would be possible to simply mount the interceptor vehicle on a booster possessing greater range capacity. In this way, with a large enough booster, even satellites at geostationary altitudes could be threatened.

In Fact, it has been reported [34] that the U.S. intelligence community has known for some time that the capability exists in the Soviet Union to launch nuclear warheads in a direct-ascent attack against spacecraft such as the U.S. early warning satellites at geostationary altitudes. According to a DOD nuclear weapons expert,

They [Soviets] clearly have demonstrated on a number of occasions the capability for accurate point-in-space intercepts, the capability to place a smaller, lighter nuclear warhead on a booster for a geostationary intercept, even though this has not been tested. The yield of the nuclear warhead would provide a sufficiently lethal radius to compensate for any intercept inaccuracies. This is routine technology and would not require any tests prior to a direct-ascent attack.

If the projected ability of the Soviet's to attack spacecraft in geostationary orbits existed, satellites at all altitudes would then be vulnerable to attack. It should be noted, however, that resorting to a nuclear warhead to compensate for guidance inaccuracies might not be in the Soviet's best interest, since the operation of their own satellites might be interfered with by nuclear blast effects such as electromagnetic

pulse (EMP).

2.2.3.2 Launch Constraints

The Soviet system has certain constraints on its flexibility since it must be launched from one of only a few ground launch facilities located in Soviet territory. Because of this, and the interceptor vehicle's limited plane change capacity, only satellites within a small range of inclinations from the latitude of the launch site can be attacked. Moreover, the target must pass directly over the launch point, which can mean a wait of up to 12 hr and only two opportunities per day for a launch window.[7] Herein lies one of the great advantages of the airborne U.S. system. An F-15 with aerial refueling has virtually unlimited range. Therefore, an ASAT equipped F-15 could conceivably attack satellites in orbits of any inclination by simply flying to a point where a launch window was available. Thus, a globally based F-15 ASAT fleet would allow the U.S. maximum attack flexibility.

The fast attack capability of the Soviets should not be underestimated, however. Even though they must launch from a limited number of sites in serial fashion, their launch surge capacity is formidable. A rapid launch operational capability with the SS-9 booster has been demonstrated. The U.S. has observed SS-9 boosters for ASAT missiles being wheeled from shelters at Tyuratam and erected for launch in less than 90 minutes.[34] The ability of the Soviets to launch large numbers of satellites into space has also been demonstrated. From 1983 to 1985 the Soviets averaged 97 space launches per year to orbit and beyond.[31] The U.S., by comparison, will be capable of launching 10-15 missions per year in the short term with the three-orbiter Space Shuttle fleet after it regains operational status, along with a similar number of expendable launch vehicle missions.

Viewed in perspective, however, the main driver behind the high Soviet launch rate is the relatively short life of their satellites. Life expectancy of a Soviet satellite is on the order of months, while most U.S. satellites last for many years. U.S. satellites, on an individual basis, are also more expensive, due largely to the greater

level of reliability, sophistication, and flexibility required of a long duration satellite. As a result of the relatively low cost of their satellites and the high Soviet launch rate capacity, regardless of the shortcomings contributing to the existence of these factors, the U.S.S.R. would actually be at an advantage in the event its satellite network had to be replenished following an attack. This makes it imperative that the U.S., which in contrast to the Soviets does not produce satellites in production line numbers and has a limited launch rate, should provide its critical, difficult to replace, space-based assets with the ability to defend themselves against an ASAT attack. In this way, the U.S. could rely on the inherent survivability of its satellites, rather than having to face the problem of replenishing an unprotected, almost irreplaceable satellite network.

2.2.3.3 Homing and Maneuvering Constraints

Two major flaws in the Soviet ASAT system arise as much from constraints imposed by the method chosen to launch their interceptor as from the shortcomings of their guidance and homing devices. That is, it can take up to 3 hr or more from rocket launch to target intercept, since their attack method of co-orbital injection requires the interceptor to rendezvous with the target, and as judged from the results of Soviet ASAT tests, their system has experienced difficulty in reliably intercepting and destroying even a stationary target. Thus, more than ample time is available for the target to detect and track the interceptor and employ defensive countermeasures. Furthermore, especially in the interceptor's terminal guidance phase where fuel remaining for course changes would be limited, evasive maneuvering by the target would greatly complicate the interceptor's task of tracking the target and coming within lethal range.

In all of its *successful* tests to date, the Soviet interceptor has used radar homing to close in on its target. Radar homing is easy to detect, has high power requirements, and is susceptible to electronic countermeasures (ECM) such as deception and noise jamming. Because of these shortcomings of radar, a passive, optical

infrared homing system, as used successfully on the U.S. MHV, is considered far superior for an ASAT application. Consequently, the Soviets have attempted to develop an infrared (IR) homing device, but as noted in Table 1, page 16, all six tests of their IR homing system have failed. This, of course, does not mean that it will continue to fail. Even IR homing, though, is susceptible to deception, through the use of decoys, for instance, but the passive nature of IR scanning does not alert the target to the presence of a threat. For the same reason, it would also be preferred to use IR sensors for detection and tracking of the interceptor by the target, as will be discussed later.

The U.S. technological lead in microelectronics, computers, and proven IR homing equipment gives the U.S. a clear advantage in the development of miniature, on-board acquisition and tracking equipment for spacecraft. Moreover, the more capable guidance systems and on-board computing capacity of the U.S. ASAT system allows a direct-ascent intercept, reducing the time for target response to 10 minutes or less. With sufficient on-board computing capacity, effective sensors, and a propulsion system for maneuvering, however, it is still possible to perform effective evasive maneuvers even within this shorter time interval, as this paper will attempt to show.

2.2.4 Future ASAT Trends

An appropriate measure by which to estimate future improvements in Soviet ASAT technology is the current level of expertise demonstrated by the U.S. in this arena. That is, in order to plan effectively to counter future Soviet systems, we must plan to defend against not only their present level of capability, but also against the presently superior level of ability already demonstrated by U.S. systems, since the Soviets continue to attempt improvements in their systems along U.S. lines. Thus, assuming continued progress by the Soviets in component miniaturization, guidance and infrared systems, and warhead accuracy and effectiveness, and upgrades in launch flexibility and altitude reach, it should be possible for them to achieve a

direct-ascent, all-altitude attack capability in the near term.

There are other developments on both sides which have inherent application to the ASAT mission - namely, anti-ballistic missile (ABM) systems. The U.S.S.R. maintains the world's only operational ABM system deployed around Moscow. This system consists of 100 silo-based launchers for long-range 'Galosh' interceptors, which are designed to engage targets outside the atmosphere, and high-acceleration interceptors to engage targets within the atmosphere. These missiles are supported by engagement and guidance radars along with a large, new radar at Pushkino designed to control ABM engagements. A nuclear warhead is fitted to the Galosh, which is said to have a range of more than 200 miles (322 km).[27] The technology incorporated in the Soviet ABM system has obvious usefulness for ASAT applications, and indeed the system already possesses some low-altitude ASAT capability.

The Soviets are also believed by the U.S. to have two new ABM development programs in progress. One of these, designated by the U.S. DOD as the ABM-X-3, is said to be rapidly deployable and uses a phased-array radar for missile tracking.[27] This is the system believed to have been successfully tested against two re-entry vehicles during the U.S.S.R.'s integrated nuclear forces demonstration of June 18, 1982, as described in Section 2.2.1.

The U.S. has also conducted a successful demonstration of ABM technology in the Army's recent Homing Overlay Experiment (HOE).[21] In this test on June 10, 1984, the optical homing technology of a Honeywell long-wavelength infrared sensor, similar to that used on the U.S. MHV, was used successfully to intercept and destroy a re-entry vehicle in space. The non-explosive warhead for the HOE missile contains a guidance computer and the IR sensor to lock on to the target, which is destroyed by impact alone. Intercept occurred in the test at a closing velocity of more than 20,000 ft/sec (6.1 km/sec) and an altitude of more than 100 miles (161 km). The interceptor missile was fired from Mech Island in the Kwajalein Atoll after ground-based radars detected the launch of the USAF/Boeing Minuteman I ballistic missile re-entry vehicle from Vandenberg AFB, California.

The technology used in this demonstration will flow directly into the Army's exoatmospheric re-entry vehicle interceptor system (ERIS) in support of the U.S. Strategic Defense Initiative (SDI). Many of the technologies being investigated under the SDI program, although primarily directed to the defense of the U.S. and its allies against a nuclear missile attack, could also prove useful in providing a first layer of defense for satellites as well. Such developments as space-based lasers, anti-missile missiles, and kinetic energy railguns could not only be used against ballistic missiles and re-entry vehicles, but could also be directed against approaching ASAT missiles. Furthermore, the proposed distributed network of acquisition, tracking, and battle management stations in space needed under SDI to support ABM operations could also be used in a complementary fashion to supply critical information to satellites, which could then take individual defensive actions if any ASAT missile penetrated the first layer of defense supplied by SDI battle stations.

Thus, if the multiple defensive layers envisioned under SDI were deployed, the survivability of our satellites and the ability to detect and counter a threat would be greatly enhanced. Of course, there would also be many more satellites to defend under SDI, but the battle stations of SDI would already possess the necessary means to carry out that defense. Therefore, the integrated use of an SDI network along with passive and active countermeasures employed by individual satellites for their separate defense would represent the ultimate defense against an ASAT threat.

2.3 Defensive Countermeasures

In a 1978 White House paper outlining U.S. national space policy, a statement was included dealing with the topic of defending space systems:

The U.S. space defense program shall include an integrated attack warning, notification, verification, and contingency reaction capability which can effectively detect and react to threats to U.S. space systems.[10]

This statement still applies to U.S. space policy and is being even more actively

pursued today through research into systems not only designed to protect space assets, but also through research under SDI designed to protect ground and space-based assets from space.

Within the context of defending satellites in space, Col Donald W. Henderson of HQ U.S. Space Division stated the problem this way:

The major challenges that face us now are: to determine the various levels of survivability needed for our space assets; to sort out the most effective and efficient means to accomplish them; and to incorporate the necessary changes and improvements as quickly as possible consistent with policy, technology, and funding priorities.[10]

Consistent with Col Henderson's statement of the problem, it is necessary to delineate and assess the means through which the survivability of our space assets can be enhanced.

There are several types of defensive countermeasures which can prove effective in solving the problem of satellite survivability. As expressed by Gerald Yonas, chief scientist and deputy director of SDI, "You use decoys, you use deception and maneuver, you harden your satellites. There is much you can do." [14] These and other methods of defense can be broken down into two categories: those that require notification of an impending attack and those that do not. Among the defensive tactics which fall into the former category requiring attack warning are deception and noise jamming ECM, deployment of decoys, attacking the attacker, and maneuver. In the latter, no-notice category are included hardening of the electronics against EMP effects, stealth technology to reduce the spacecraft's IR and radar signature, and relatively permanent, towed decoys.

Another way of viewing defensive countermeasures is according to the active or passive nature of the tactics they employ. Here, active measures are considered to be those tactics in which the spacecraft takes a specific action to defend itself against a threat, while passive measures are those which provide built-in protection or allow

the spacecraft to observe the external environment unobtrusively. Thus, countermeasures requiring attack warning are active, while no-notice countermeasures are passive.

Active measures would generally be undertaken when passive measures have failed to prevent detection of the spacecraft by the interceptor. Because active measures involve using expendable resources such as fuel or electrical power, and changing a satellite's orbit can degrade its mission effectiveness, these tactics should only be used when it is determined that the individual spacecraft is actually under attack. Furthermore, a limited supply of decoys, defensive rockets, and fuel would be available for defense in future engagements, and adequate reserves of fuel must be maintained to re-establish the spacecraft's original orbit if desired.

No matter what combination of countermeasures is employed, it soon becomes apparent that the most effective defense of individual satellites is that which can operate autonomously on-board the spacecraft itself. Although this complicates the design and increases the cost of the spacecraft, the reduced reliance on ground-based sources for attack warning, tracking, and maneuver control is necessary to allow an adequate response within critical time constraints. Also, providing individual satellites with the ability to determine whether or not they are specifically under attack allows a discrete response to a coordinated attack. Thus, if only one part of a satellite network or only one satellite is under attack, minimum disruption will occur in other regions of the net. Furthermore, a central command center, which could nevertheless retain authority to activate or override evasive responses in regions of the net, could very well be overwhelmed during a massive attack if it was required to coordinate all offensive and defensive operations for all systems in space. For our most important military early warning, communications, reconnaissance and navigation satellites at least, the added expense of on-board defensive systems would be well worth the cost if they could make the difference between survival and certain destruction.

In many cases, the technology required for on-board systems is already in hand.

Indeed, in the areas of acquisition, tracking, guidance, on-board computation, propulsive systems and ECM, much of the hardware exists or is under development in the U.S. It is therefore the software needed for battle management, discrimination of attackers, attack assessment, and control of evasive action which is critical in providing satellites with an autonomous defensive capability.

Keeping in mind the need for defensive countermeasures to be available on-board the spacecraft, it is useful to discuss each of the important defensive techniques mentioned so far and assess their effectiveness. Once this has been done, the role software development can play in controlling engagements can be better understood. For the following discussion, evasive maneuvering will be treated separately from all other countermeasures, whether active or passive, since it is the only defensive technique which involves purposefully changing the orbit of the satellite. Changing a satellite's orbit has many unique constraints and requirements which other countermeasures do not have to deal with.

2.3.1 Non-maneuvering Countermeasures

Even though the set of constraints involved with maneuvering a satellite do not necessarily come into play in the use of non-maneuvering countermeasures (NMC), the requirements of detection, acquisition, tracking, and attack assessment leading up to the use of active NMC still apply. That is, with the exception of passive methods of deception and concealment, which are always in place and require no attack warning, the satellite must be able to discover an attack, determine the attacker's trajectory, and initiate an appropriate response.

As mentioned before, the NMC methods requiring no attack warning include stealth, electronic hardening, and towed decoys. Each method operates on a different principle to enhance defense. With stealth, the main concern is to reduce the radar cross-section, infrared, and electromagnetic emissions of the target. Such signatures as provided by the target in the radio frequency (RF), visible, and IR ranges, for instance, are what the interceptor uses to home in on the target. If

these signatures can be reduced, the tasks faced by the interceptor of tracking and homing in on the target become much more difficult.

Electronic hardening of a satellite's circuits is useful to counter the EMP effects associated with a nuclear blast. If a nuclear blast occurs in the proximity of a satellite which is not hardened, the resulting surge of electromagnetic energy created by the blast can disrupt or overload and burn out the satellite's circuits. This effect is closely tied to the concept of lethal intercept volume, which will be discussed later in the section on maneuvering as a countermeasure.

Towed decoys operate in a complementary, though opposite, way with stealth. In the case of any decoy, whether towed or deployed in response to a threat, it attempts to create an electromagnetic environment or IR environment around itself which overwhelms or simulates the target's signature, hoping to deceive the interceptor's homing device into attacking it instead of the real target. This method of deception is very effective if the attacker's homing device is not sufficiently sensitive or has no means of distinguishing between the the real target and the decoy. Towed decoys, although offering constant protection, would not, of course be the preferred method of deception if the attacker's warhead was nuclear. Towed decoys can also cause instability problems for the host satellite, especially if it needs to maneuver.

NMC methods which require attack warning to be effectively employed were listed as active deception and noise jamming ECM, deployment of decoys, and attacking the attacker. These methods are closely tied to constraints such as allowable weight and available power, and the fact that the supply of decoys and defensive missiles would be limited. These active measures come into play when stealth has failed to prevent detection of the satellite.

There are two categories of ECM: deception and noise jamming. In deception jamming, the target attempts to confuse the attacker's radar by actually delivering false range and bearing information to the attacker's radar. To do this, the target must have fairly good knowledge of the adversary's radar and counter-countermeasures (CCM), or the target's ECM system must be sophisticated and

adaptive enough to determine the nature and content of the opposing radar signal to counter it effectively. Noise jamming is less sophisticated, in that the target simply attempts to overwhelm the enemy's radar by radiating large amounts of noise over a range of frequencies. This method, although not requiring extensive knowledge of the enemy's radar, does require a substantial supply of electrical power, something typically in short supply on satellites.

The effect of a decoy deployed in response to an attack is, of course, the same as that of a decoy that is towed. There are some important differences, however, which have an impact on the target. By deploying a decoy which is physically separated from the target, the target is free to maneuver under cover of the decoy's deception. Also, multiple decoys can be deployed as needed, although the number of decoys available is limited and cannot be re-used following a false alarm. Towed decoys could also be ejected in response to a threat, of course, but the power drain associated with operating an active towed decoy and the constraint imposed on maneuvering would reduce its usefulness. Ejected decoys, mainly flairs for IR deception, are used successfully today by aircraft under attack by heat-seeking missiles. Physical decoys are also ejected from ICBMs in their post-boost phase as penetration aids for deployed warheads. In the case of ICBM decoys, they can be discriminated from the real warheads through the effects of drag during re-entry, since decoys of necessity weigh less than the real warheads. In the absence of drag, however, separating out decoys is more difficult, although it can be done by characterizing the decoy's IR signature more closely, say.

Shooting back at an attacker could be accomplished with an anti-missile missile based on-board the target or on an escorting vehicle or battle station. Anti-missile rockets [15] would have to be light-weight, and would be limited in number and range. They would also probably be the most costly of the NMC methods, since many of the same capabilities required of an attacking ASAT missile would also be required of an anti-missile missile. In fact, the defensive missile might even have the added difficulty of performing an intercept with the Earth or Sun, which would

represent sources of IR and electromagnetic interference, in its field of view. Active radar or extremely sensitive IR sensors for the rockets could be used to overcome this tracking difficulty, but because of the associated high radar power requirements or the cost and cooling needs of a sophisticated IR sensor, these sensors might have to be based on the satellite, which would then guide the rocket to its target. If a satellite-based radar were used, however, it might also have the undesirable effect of aiding an attacker having the capability to home in on a radar signal. This would then negate the advantage gained by the target through the sole use of passive, optical on-board sensors, which can provide long-range acquisition and tracking data without revealing the target's position. Firing rockets from a satellite would also introduce unwanted perturbations and instabilities in the satellite's orbit which could in turn cause attitude control problems and reaction control system fuel expenditures. A successful use of defensive rockets would have one chief advantage, however, in that the threat would be removed altogether.

2.3.2 Evasive Maneuvering as a Countermeasure

If all NMC methods fail to defeat the ASAT missile, the targeted spacecraft will be destroyed – unless it has the ability to change its orbit so that a miss will occur. This ability to maneuver evasively can be used alone or in conjunction with NMC methods to enhance the overall chances of survival under many scenarios. As described by Col Henderson in his article[10] concerning the defense of space assets,

A defending satellite can maneuver to avoid acquisition by the ASAT sensor, or with adequate acceleration capability, outrun the ASAT missile's terminal thrust capability. For a laser attack, maneuver can be used to evade acquisition or to increase the distance of closest approach. For a nuclear or laser threat, maneuver must place the spacecraft outside the lethal volume. The lethal volume can be reduced by increasing nuclear and laser hardness of the spacecraft. In some instances, a restoration maneuver would be required in order to resume the mission.

[...] In order for maneuver to be effective, there must be timely surveillance warning and attack characterization. In addition, provision must exist for timely command and control of the targeted satellite.

The concept of *lethal volume*, as alluded to by Col Henderson, is described in more detail by Salkeld [23]:

The effectiveness of an interceptor can be measured by the volume within which it can perform intercept in a given time. This *reach* is in general made up of two components: 1) the destructive mechanism of the warhead, which establishes a kill-radius r_k about the interceptor, and 2) the propulsive maneuvering capability by which the interceptor moves to the target vicinity.

Thus, the sum of the kill-radius r_k and the range of the interceptor r_i gives the radius of the sphere of lethal volume as $r_l = r_k + r_i$. If a target falls within the lethal volume, it is vulnerable to attack. A successful intercept does not occur, however, unless the interceptor can maneuver itself to within r_k of the target. In the case of a nuclear warhead, r_k for a lethal dosage of gamma and neutron radiation to be delivered to an unshielded target can be on the order of hundreds of miles.[23]

The effective kill-radius of the missile can be substantially reduced, however, by appropriate spacecraft shielding and electronics hardening. The present Soviet ASAT system is non-nuclear, however, and uses a conventional warhead (ref. Sec. 2.2.1). For a non-nuclear, conventional warhead, r_k is quite limited, usually on the order of a mile.[23] The U.S. system, of course, uses no explosives at all, and the trend for all ASAT systems seems to be in this direction as IR homing techniques become more reliable. (ref. Sec. 2.2.4) By not using an explosive warhead, the possibility of collateral damage to friendly satellites is reduced. The kill radius of a non-explosive warhead, however, is on the order of meters. With $r_k \approx 0$ though, the difficulty of homing to intercept is greatly increased, while at the same time, evasive maneuvering by the spacecraft becomes much more effective.

For evasive maneuvering to be effective, the spacecraft must be able to remain outside the missile's kill radius. This means that the spacecraft must maneuver to place itself at least a mile, for a conventional warhead, or less, for a point intercept, from the predicted position of the missile at any future intercept time. For the spacecraft to do this, it must be able to perform certain tasks. First, it must detect an approaching missile, or be warned by an independent source of an impending attack. Second, it must be able to acquire the attacking missile and determine its trajectory. Third, it must be able to confirm or negate the possibility that the missile is on a course that will result in an intercept at some future time. And finally, the spacecraft must be able to maneuver effectively to achieve a miss-distance greater than r_k at the intercept time.

Detecting and acquiring a missile can be done on-board with a long-range, optical, infrared sensor. In fact, it was demonstrated in the U.S. Army's Homing Overlay Experiment (HOE) (ref. Sec. 2.2.4) that an infrared sensor can acquire targets at hundreds of miles in distance and provide the precision required to lock on to the opposing vehicle and transmit data to an on-board computer for tracking.[21] The intense IR signature of a rocket during its boost phase is easy to detect, and this is routinely done by U.S. early warning satellites from geosynchronous altitudes. Tracking the interceptor missile after it is released from its booster rocket would not present a problem either, as this is exactly what was done in the HOE test with respect to a re-entry vehicle.

Here, it is useful to note that if greater control by a ground facility was desired over the actual enabling of evasive responses by an individual satellite or an entire region of a network, the command to enable such responses to be used could be given by a ground control center after it detected an unidentified launch through its own means. In this scenario, upon notice from early warning satellites that an attack was under way, Space Command's SPADOC, which presently would coordinate a U.S. attack (ref. Sec. 2.2.2), could enable evasive sequences to ensue on-board spacecraft in affected quadrants. Furthermore, SPADOC could also provide initial coordinates

of the detected missile to satellites in all regions within the proximity of the attack. Each satellite could then separately acquire and monitor the missile's trajectory to determine if evasive action by that particular satellite was called for.

On-board the spacecraft, once the relative angular position of the missile from the spacecraft was determined with the IR sensor, the precise range from spacecraft to missile would also be determined. Range data could be obtained with a laser range-finder, or if unavoidable, a radar could be used. Use of either device, especially radar, would only be needed for short periods of time at certain intervals when updated trajectory information on the missile was needed. Only vector position data on the missile over time is needed to establish the trajectory of the missile, as will be shown later in this paper. Position vectors could, of course, be obtained with radar alone, but this would not be as accurate as an IR sensor/laser range-finder combination, and radar emissions could assist the missile in determining the spacecraft's position.

Updates on the missile's trajectory would not only be used to update the accuracy of the predicted intercept point, but would especially be needed to establish the missile's new trajectory if it performs a maneuver. An alert to maneuvering by the missile could in most cases be given by the IR sensor upon detecting missile thrust, but a maneuver need not be detected if essentially continuous updating of the missile's trajectory is performed. Updating the missile's trajectory continuously in real-time is not unreasonable either, with the right software and computational capacity, as I will attempt to show later in this paper.

Maneuvering to avoid intercept is especially effective where high closing rates are involved, or when intercept must occur at high altitudes at the limit of the ASAT missile's range. In the first case, the ASAT missile's homing and response time capability are severely taxed. In the second, limited fuel reserves can constrain the missile's maneuvering envelope considerably, while at the same time any imprecision in the missile's long-range sensors would increase the need for corrective expenditures of fuel.

Maneuvering to avoid intercept, or to intercept, is subject to many constraints. In the spacecraft's case, characterization of the threat, adequate tracking, remaining time-to-intercept, fuel available, and maneuverability are all critical. In the missile's case, homing accuracy, range capability, and maneuvering envelope limitations are critical. Subject to these constraints, among others, it is the job of the spacecraft to survive. To do this, it must be able to hide from or deceive the missile, destroy the missile, or place itself out of the missile's kill radius through maneuver. In the balance of this paper, I will investigate evasive maneuvering as a defensive countermeasure and present a method I designed for governing spacecraft evasive maneuvering which would allow a spacecraft to avoid intercept by an attacking ASAT missile.

2.4 Other Research Applicable to Evasive Maneuvering

A number of authors have investigated pursuit-evasion problems between two spacecraft, with the majority of references located approaching the problem from the interceptor's point of view [8,1,20,3,22]. Overall, many of the authors placed restrictions on the orbits or capabilities of the spacecraft in their proposed scenarios. This was often done to facilitate the investigation of a particular property of pursuit-evasion problems, or to simplify the model and avoid intractable computational situations. Several papers [8,1,13,22] treated the interception of a target in the context of differential games¹ or an optimization problem with the intent of developing a control scheme which would minimize the cost to the offense of achieving intercept based on the optimization of some quantity.

Rosenbaum [22] considered the problem where an interceptor desires to reach

¹According to Rosenbaum [22], "A differential game can be regarded as a two-sided optimization problem. One side uses the controls available to it to minimize a payoff function while the other side uses its controls to maximize the payoff. When each side uses its optimal control, a minimax solution is obtained. The necessary conditions for a minimax solution are analogous to those for a one-sided optimal control problem."

the target as quickly as possible, while the target seeks to delay the the encounter. His objective was to determine the minimum time-to-intercept as a function of the initial relative position and velocity. In his analysis, he assumes that the two vehicles are relatively close to one another in near-circular, coplanar orbits. He then uses equations of motion for the interceptor relative to the target which describe the relative motion of the vehicles with respect to a reference circular orbit. Constant thrust acceleration is assumed for both vehicles.

Fitzgerald [8] considers the development of an optimized strategy which minimizes the total energy required of the interceptor to achieve an intercept of a deorbiting target. Control parameters he uses are the initial position of the interceptor, the acceleration of the interceptor during the engagement, and the time and duration of the constant acceleration retro thrust of the target. He assumes that the target is constrained to its orbital plane, while the interceptor may approach from any direction. It is also assumed that control accelerations for both vehicles act normal to the relative velocity vector and that the intercept time remains fixed. Moreover, it is assumed that the offense has full knowledge of the defense's strategy and instantaneously recognizes defensive action.

Anderson and Bohn [1] implement a simulation using near-optimal feedback solutions to a nonlinear differential game where it is desired that the interceptor take advantage of nonoptimal maneuvers by the target in order to reduce the final miss-distance between the two vehicles. In their simulations, it is assumed that the pursuing vehicle employs the near-optimal techniques, while the evader always uses nonoptimal strategies. Both coplanar and non-coplanar problems were investigated for vehicles using constant thrust. In the implementation of their simulations, they found that in some cases the numerical integration of a large set of equations needed to update a transition matrix could not be done in real-time. Also, their techniques proved to be less effective in reducing miss-distances as the predicted final range approached zero.

The guidance and control of an interceptor vehicle in space is considered by

Reiss [20] from a fire control viewpoint. He develops a kinematic equation of relative motion for the interceptor with respect to the target from considerations of a typical intercept geometry and the forces acting on the two vehicles. He then performs a computer analysis of the problem of intercepting an ICBM during the portion of its boost phase above the atmosphere with an interceptor missile fired from a satellite. In his analysis he uses a modified proportional form of guidance in which the acceleration of the missile normal to the line-of-sight to the target is proportional to the product of the closing velocity and the angular velocity of the line-of-sight. Line-of-sight direction information was assumed to be available through a tracking system which would monitor ICBM radiation emissions. Angular velocity of the line-of-sight was then determined in missile coordinates with respect to an inertial reference frame. In the event that the acceleration required of the missile was more than the propulsion system could provide, a condition of 'acceleration saturation' would result, in which a non-zero miss-distance would occur. Thus, a trade-off between miss-distance, flight time, and missile system size had to be made. He found that a simple form of modified proportional guidance resulted in excessive maneuvering which wasted fuel, and that if *predicted* target position information were available, considerably less maneuvering resulted. With predicted information, a velocity increment in the proper direction would allow a ballistic path to the impact area, where a terminal homing phase could then take over. In fact, he found that if target position could be predicted, a choice of navigation course and parameters could be made to allow for a minimum miss-distance in the time available for a given situation.

A means of calculating velocity requirements for rapid intercepts of a satellite by a rocket fired from Earth or space is presented by Ash [3]. In his analysis, the problem is approached as a two-body astrodynamics problem, where both the satellite and rocket are assumed to be moving in conic section orbits about a spherical Earth. Atmospheric effects are ignored as are the higher harmonics of Earth's gravitational field. Impulsive velocity changes are assumed for both vehicles. He

uses equations of orbital mechanics to perform three kinds of calculations: finding position and velocity when given the orbital elements, determination of the orbital elements when given position and velocity, and solving Lambert's problem for the travel time between two points in a conic section orbit. In all three of the above cases, he treats elliptic, parabolic, and hyperbolic motion separately, leading to the necessity for three groups of equations for each kind of calculation. Time-to-intercept is calculated iteratively as the target moves in its orbit.

A guidance algorithm for targeting spacecraft was implemented in a computer simulation by Stuart [26]. His objective was to find a way of generating feasible trajectories which satisfied a given set of conditions for the spacecraft's orbit at the target point. His orbit-fitting targeting technique used methods of astrodynamics to ensure that a given combination of target parameters such as position and velocity magnitude, flight path angle, and transfer angle were satisfied. The starting point for his technique was the classical orbital boundary-value problem, where it is desired to find the feasible orbits which pass through a given initial and final position as well as the velocity vectors at the initial point corresponding to these orbits. To develop his technique, which is applicable to two-dimensional, two-body targeting problems, he relaxed the requirement that the resulting trajectories be optimum. Trajectory simulations were performed to test his technique by numerically integrating the spacecraft equations of motion based on the desired initial position and velocity vectors supplied by his targeting technique. Two test cases were used: a launch from Earth to low-Earth orbit (LEO), and a transfer from LEO to geosynchronous orbit. In the guidance algorithm simulations, the thrust vector was aligned along the velocity-to-be-gained² vector. It was found that good targeting accuracy could be achieved and velocity requirements were close to optimal.

The problem of evasive maneuvering by the target as a means of protecting

²The velocity-to-be-gained is the vector difference between the velocity needed at the present point and the current velocity at that point required to achieve a desired target position at some future time, assuming an impulsive velocity change. The magnitude of the velocity-to-be-gained vector is analogous to the concept of required δv .

space assets from an ASAT threat was examined by Kelley, Cliff, and Lutze [13] with a simplified near-circular orbit model. In this model, the pursuer and evader were assumed to be in coplanar orbits, and the pursuer was allocated two impulsive burns to rendezvous with the evader and match its velocity. According to the authors, they specified *rendezvous* with the target because "terminal guidance of the threat ASAT [Soviet] is ineffective at high closing rates." To maximize its closest approach distance to the interceptor, the target was allowed one impulsive burn, which was of fixed magnitude and could be applied in any direction and at any time. Mathematically, the equations of relative motion between the two vehicles were approximated in a linearized, near-circular orbit form. With the simplifications of their model in mind, it was found that optimal evasion was provided by an early, in-plane thrusting maneuver.

3 Description of Program EVADER

3.1 Overview of Evasive Maneuvering Requirements

For a spacecraft in Earth orbit to take appropriate evasive action in response to an approaching anti-spacecraft missile, it is first necessary to determine whether or not the approaching missile is on an intercept course with the spacecraft. If so, a timely evasive maneuver must be performed by the spacecraft so that it can achieve a desired miss-distance from the missile at the predicted intercept time. Following evasion, the spacecraft must continue to monitor the missile's course, so that additional maneuvering can be initiated if necessary. In the balance of this paper, I will outline a computer program I developed to govern the evasive maneuvering of a spacecraft in response to such an anti-spacecraft missile threat.

In order to determine whether or not an approaching missile is on an intercept course with a spacecraft, the orbit of the missile must be determined and compared to the future path of the spacecraft. If interception is concluded to be imminent, by an inspection of the magnitude of the relative position vector between the spacecraft and missile at some future time, an appropriate evasive maneuver must be initiated. For this maneuver, a velocity vector increment can be calculated that, if applied by the spacecraft, would allow it to evade the missile at the future intercept time by a pre-determined miss-distance relative position vector. The requirement that the spacecraft be allowed to achieve a miss-distance of a certain magnitude is based on the concepts of the missile's lethal volume and kill-radius, as discussed in Sec. 2.3.2. Furthermore, being able to choose the direction from the missile in which the miss-distance will be achieved allows the spacecraft to alter its orbit in a way that is acceptable and advantageous to it.

Following any evasive thrusting, the new current and future relative position vectors between the two vehicles must be calculated from their updated trajectories. The magnitude of the future relative position vector can then be monitored to see if it is still decreasing with time, possibly dictating additional evasion, or is

increasing with time, indicating a successful evasion has been achieved. Monitoring the vehicles' relative position vector in this way provides a means of taking into account missile maneuvers designed to re-target the spacecraft.

Establishing the future position and velocity of the missile and spacecraft in order to predict interception and plan maneuvers can be done in one of two ways: by repeatedly integrating the equations of motion for both vehicles, or by using the techniques of astrodynamics to perform a series of predictive analyses for the two-body problem, where the motion of one body with respect to another, such as the Earth, is governed solely by their mutual gravitational attraction. In this paper, I will show that for spacecraft operating in regions where atmospheric drag is not significant, it is essentially as accurate, and certainly more efficient and flexible, to use astrodynamic techniques rather than the brute force methods of numerical integration to predict interception and govern spacecraft maneuvers.

In fact, it might be expected that ignoring drag, higher order gravitational anomalies, and other lesser perturbative accelerations in the astrodynamic techniques would present no problem in a typical intercept scenario, since time-to-intercept is usually less than one orbital period and almost all spacecraft and satellites operate primarily above the appreciable atmosphere (ref. Sec. 2.1). Even in cases where a spacecraft is subject to some drag when operating in the upper atmosphere, say, or operates above the atmosphere for only a portion of its mission, astrodynamic techniques would still be useful, although their utility would decrease as non-trivial perturbations and vehicle lift become more significant.

Astrodynamic techniques can be used to predict time-to-intercept and the position and velocity vectors of a vehicle at any point in its orbit at any future time. Herein lies the real beauty and efficiency of these predictive methods. The position and velocity vectors of a vehicle at a point in space at some future time can be calculated in one pass of the algorithms. This circumvents the need to integrate numerically the equations of motion over the entire future trajectory in small time steps. After all, only the values of the vectors at the end points are needed and it

is desired to make evasive action decisions on-board in real-time.

For example, say the transfer time-to-intercept was 600 sec. Each second, a program using the methods of astrodynamics would be predicting accurately the position and velocity of the missile and target at a point in space 600 sec in the future. In conjunction, any evasive trajectories designed to avoid the missile at the intercept point would also need to be repeatedly computed. To obtain the same future point information to the same order of accuracy by integration, however, would require that the equations of motion governing the future trajectories be fully integrated 600 times every second (if updates were desired every sec and an integration time step of one second, say, was used)! This kind of computation can clearly lead to program output which is not in real-time, in a critical situation where real-time responses are imperative. Integrating the equations of motions does not more realistically model the situation either, since the same initial conditions are used as with the predictive methods, and possible future maneuvering by the missile along its path can not be premeditated in any case. Furthermore, numerical integration schemes carry with them some added internal sources of error such as round-off and truncation error, which increase as the step size of the integration is reduced to improve accuracy.

3.2 EVADER's Predictive Astrodynamic Techniques

The techniques and algorithms of astrodynamics incorporated into the program written to govern evasive maneuvering, a program which will be referred to subsequently by its name EVADER, were selected and implemented in the most generally applicable vector forms available. This was done so as not to restrict the trajectories of either the spacecraft or missile to coplanar orbits of limited eccentricity or small transfer time intervals. That is, EVADER has the capability to deal with orbits that can be elliptic, parabolic, or hyperbolic, using time intervals of arbitrary size where time need not be reckoned from pericenter, and where the position and velocity of either vehicle are unrestricted in three-dimensional space.

The general forms of the astrodynamic techniques which were applied in EVADER are fully derived by Dr. Richard H. Battin [4] in his book, *An Introduction to the Mathematics and Methods of Astrodynamics* (1984). Many of these methods, which originate in the work of such men as Gauss, Lambert, Lagrange, Euler, and Kepler have been improved in convergence and extended in applicability by Dr. Battin in a form useful to a mechanized computation involving orbits of arbitrary conic section.

It is not the intent of this paper to fully derive the mathematical techniques and equations used in EVADER, rather it is desired to outline the general structure and flow of the programs control, and to explore the current capabilities, methods, and assumptions incorporated in the program. For the reader's interest, however, the algorithms used in EVADER and the pertinent equations to be calculated for each are briefly presented. As a reference for the reader throughout the discussion to follow, a program listing of EVADER is provided in Appendix A, pp. 133-166.

3.2.1 Coordinate System Used

Before proceeding, a note on the coordinate system adopted for all calculations in EVADER is in order. The coordinate system used, as shown in Figure 1, p. 46, is an Earth-centered, right-handed, inertial system with the x - and y -axes in the plane of the Equator and the positive z -axis pointing along the Earth's north polar axis. The Earth is assumed to be non-rotating and the position and velocity of a vehicle is expressed in inertial coordinates, while no further locational references such as latitude or longitude are used since this is not important to the study at hand. If desired, though, vehicle position with respect to a point on the Earth's surface could be obtained from the orbital elements that are provided and by fixing the x -axis in the direction of the *vernal equinox*³ and taking into account the angular velocity of the Earth's rotation.

³The vernal equinox is the point of intersection of the plane of the Earth's orbit, or ecliptic plane, and the plane of the Equator where the sun crosses the Equator from south to north in its apparent annual motion along the ecliptic.

In Figure 1, the *line of nodes*, denoted by the unit vector \hat{i}_n , is the line of intersection of the vehicle's orbital plane and the plane of the Equator. The inclination of the the vehicle's orbital plane is given by i . The unit vector \hat{i}_h is perpendicular to the vehicle's orbital plane and gives the direction of the angular momentum vector of the orbit. The *ascending node* is the point at which the vehicle in its orbit crosses the plane of the Equator with a positive z component of velocity. Positive rotation is determined by the 'right-hand rule' with the thumb along the positive z -axis. The direction of the point of closest approach, or perigee, of the vehicle to the Earth is given by the unit vector \hat{i}_p . The line from the origin to perigee is known as the *line of apsides* or the *apsidal line*. The angle ω from the line of nodes to the apsidal line is known as the *argument of perigee*. The angle Ω from the inertial x -axis to the line of nodes lies in the Equatorial plane and is known as the *longitude of the ascending node*, with \hat{i}_x pointing in the direction of the vernal equinox. The three angles i, ω, Ω are known collectively as Euler angles and are considered to be orbital elements of the orbit. The direction of the vehicle, or body, from the origin is shown as the unit vector \hat{i}_r .

Thus, the position and velocity of a vehicle in orbit would each have three components and would be respectively given by

$$\vec{r} = r_x \hat{i}_x + r_y \hat{i}_y + r_z \hat{i}_z \quad \text{and} \quad \vec{v} = v_x \hat{i}_x + v_y \hat{i}_y + v_z \hat{i}_z \quad (1)$$

The magnitudes of the position and velocity vectors would then be

$$r = \sqrt{r_x^2 + r_y^2 + r_z^2} \quad \text{and} \quad v = \sqrt{v_x^2 + v_y^2 + v_z^2} \quad (2)$$

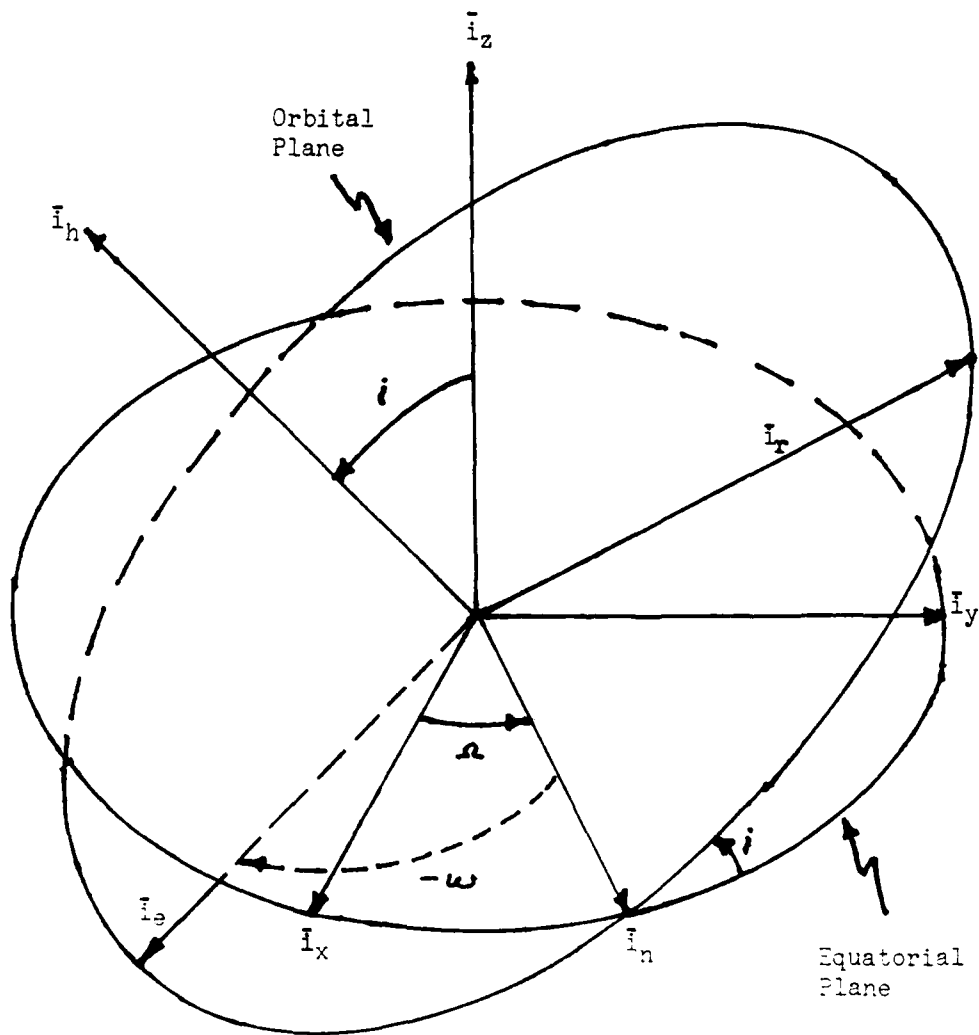


Figure 1: Coordinate System Geometry

3.2.2 Geometry of an Ellipse

The eccentricity e of an orbit determines whether it is classified as a circle ($e = 0$), ellipse ($0 < e < 1$), parabola ($e = 1$), or hyperbola ($e > 1$). If the orbit of an Earth satellite is not circular, and the satellite is not on an escape trajectory, it will be elliptical. The geometry of an ellipse is shown in Figure 2, p. 48.

The focus F of the ellipse is occupied by the Earth and is the origin of coordinates for the inertial system described in Sec. 3.2.1, while the focus F^* is referred to as the *unoccupied focus*. The line drawn from the pericenter at P through F , the center C , and F^* intersects the ellipse at its apocenter at A . This line is known as the *major axis* of the ellipse and therefore the distance a from C to the pericenter is the *semimajor axis*. Similarly, the chord drawn through C and perpendicular to the major axis is the *minor axis*, and the distance along this chord from C to the ellipse is the *semiminor axis* b . The quantity ae represents the distance from either focus to the center. A line drawn from F to a point on the ellipse, say the position of a vehicle in its orbit, represents a radius vector \vec{r} whose magnitude is r , as in Eqs. (1) and (2). The eccentricity vector \vec{e} points from F to P , and the angle from \vec{e} to \vec{r} is the *true anomaly* f . Thus, when $f = 0$ the vehicle is at perigee and when $f = \pi$ the vehicle is at apogee. Finally, a line drawn from F to the ellipse and perpendicular to the major axis is known as the *semilatus rectum* and has length p , where p is also known as the *parameter*. The quantities a, e, p and f , along with the Euler angles Ω, ω and i of Sec. 3.2.1, are known as *orbital elements*.

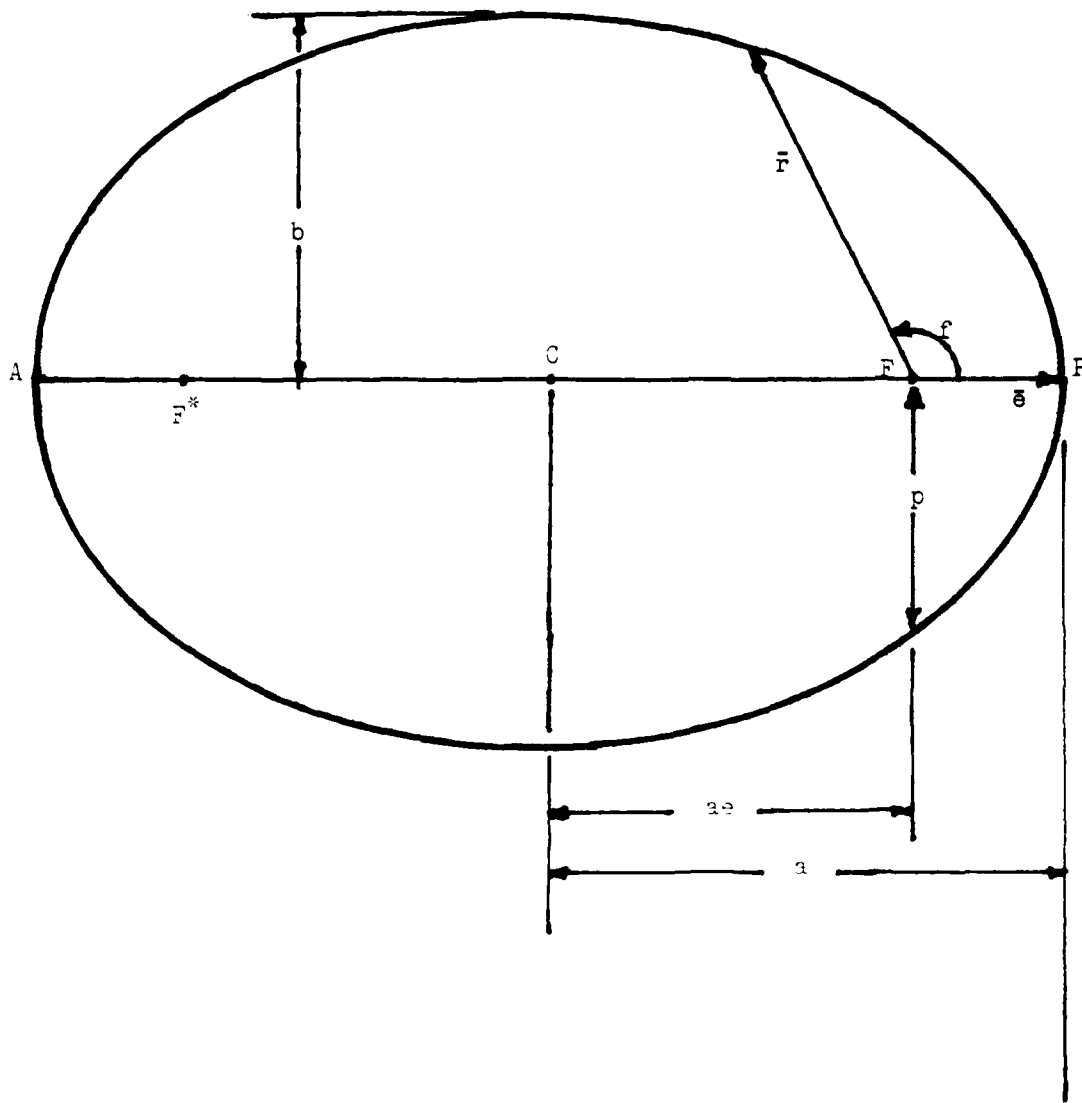


Figure 1: Geometry of an Ellipse

3.2.3 Program Inputs

The required inputs to EVADER were selected on the basis of their being representative of realistic inputs which could be expected to be available to a spacecraft through the use of its on-board sensors and navigation instruments. Sensors available, as discussed in Sec. 2.3.2, might include infrared detectors and a laser range-finder or radar, while navigation instruments would include an inertial navigation set and a star tracker.

As an example of the use of these instruments, a possible scenario might proceed as follows. IR detectors sense a sudden and intense heat signature of an object rising from hostile territory. This heat source, say an ASAT rocket in its boost phase, is monitored until booster cut-off and ASAT missile deployment, at which time the spacecraft uses its instruments to obtain two position fixes in inertial space of the missile over time. The vector position \vec{r}_M of the missile in inertial space can be obtained as the sum of the spacecraft's, or target's, inertial position vector \vec{r}_T , which is known from the spacecraft's navigation instruments, and the relative position vector \vec{r}_{MT} from the target to the missile as found with on-board sensors. Thus,

$$\vec{r}_M = \vec{r}_T + \vec{r}_{MT} \quad (3)$$

As discussed in Sec. 2.3.2, to obtain the relative position vector fixes of the missile with the spacecraft's sensors, infrared detectors could be used to establish the angular position of the line-of-sight from spacecraft to missile while a laser range-finder would establish distance. Radar could also be used to provide missile position information if stealth was not desired or IR interference from the Earth or Sun was too great. Spacecraft velocity, as well as position, would be available from navigation instruments.

Thus, inputs to EVADER consist of the components of two missile position vector fixes, \vec{r}_{M0} and \vec{r}_{M1} , along with the magnitude of the time interval, $t_1 - t_0$ over which the position fixes were taken. The velocity vector \vec{v}_{M1} of the missile

at time t_1 can then be calculated from the position fixes, as will be shown. The position and velocity vectors, \vec{r}_{T1} and \vec{v}_{T1} , for the target at time t_1 are also input. This is all the information that is needed to establish the orbits of both the missile and target. Other inputs, used only to set up and run test scenarios for EVADER, are discussed in the section on testing.

All calculations in EVADER are based on the assumption that the missile and target are in unaccelerated, 'coasting' orbits, or that engine cut-off has just occurred. In an actual situation, however, missile maneuvering would be taken into account by EVADER by requiring new missile position fixes every second or less, so that essentially continuously updated missile position and velocity vectors would be available. Missile trajectory updates could also be commanded only in response to a detected missile engine burn or as a means of improving the accuracy of the predicted trajectory values of the missile as it approached. In this way, predicted positions of the interceptor would be continuously produced and evaluated based on the most recent data available.

3.2.4 The Lambert Algorithm

From \vec{r}_{M0} , \vec{r}_{M1} , and the associated time interval between the fixes, the semimajor axis a , parameter p , and eccentricity e , which are orbital elements of the missile's orbit, can be calculated. Then, knowing the parameter of the orbit and the transfer angle θ between the two position vectors from their dot product, the velocity vectors, \vec{v}_{M0} at time t_0 and, more importantly, \vec{v}_{M1} at time t_1 , of the missile can be found.

This calculation is implemented in the subroutine LAMBERT (ref. Appendix A, pp. 137- 140), where a Lambert algorithm is used to find a and p for the missile. This algorithm was developed by Battin [4,5] from a method first derived by Carl Friedrich Gauss to solve Lambert's Problem for near parabolic orbits. Lambert's Problem, which is the determination of an orbit connecting two position vectors with a specified transfer time, is the result of Lambert's Theorem, which states that "the orbital transfer time depends only upon the semimajor axis, the sum of

the distances of the initial and final points of the arc from the center of force and the length of the chord joining these points."

Battin's improved method, as used in EVADER, exhibits faster convergence than Gauss' original method, is not singular for a transfer angle of 180 degrees, and is applicable to orbits of arbitrary conic section. The ability to determine the precise velocity vectors of an object in space from only two position fixes over time thus circumvents the need to require velocity vector information from a radar sensor, which might at best be only able to give approximate velocity vector component information, depending on the range and sensitivity of the radar.

3.2.4.1 Lambert Algorithm Equations

The following equations for the Lambert algorithm are to be calculated in the order shown.

If Given: $\vec{r}_0, \vec{r}_1, \|t_1 - t_0\|, \mu = 3.981 \times 10^6 \text{ km}^3/\text{sec}^2$

$$\theta = \arccos \left(\frac{\vec{r}_0 \cdot \vec{r}_1}{r_0 r_1} \right) = \text{transfer angle} \quad (4)$$

$$c = (r_0^2 + r_1^2 - 2r_0 r_1 \cos \theta)^{1/2} = \text{chord} \quad (5)$$

$$s = \frac{1}{2}(r_0 + r_1 + c) = \text{semiperimeter} \quad (6)$$

$$\lambda = \frac{\sqrt{r_0 r_1}}{s} \cos \frac{1}{2} \theta \quad (7)$$

$$\epsilon = \frac{r_1}{r_0} - 1 \quad (8)$$

$$\tan 2\omega = \frac{\epsilon}{2(1 + \epsilon)^{1/4} [(1 + \epsilon)^{1/2} + 1]} \quad (9)$$

$$\ell = \frac{\sin^2 \frac{1}{4} \theta + \tan^2 2\omega}{\sin^2 \frac{1}{4} \theta + \tan^2 2\omega + \cos \frac{1}{2} \theta} \quad (10)$$

Then, calculate the transfer time for a parabolic arc as

$$t_{1p} - t_{0p} = \frac{(r_0 + r_1 + c)^{3/2} \pm (r_0 + r_1 - c)^{3/2}}{6\sqrt{\mu}} \quad (11)$$

where the (-) sign is used for $\theta \leq \pi$ and the (+) sign is used for $\theta > \pi$. Next, set

$$x = \begin{cases} \ell & \text{if } \|t_{1p} - t_{0p}\| > \|t_1 - t_0\| \\ 0 & \text{otherwise} \end{cases} \quad (12)$$

and continue by calculating

$$m = \frac{8\mu(t_1 - t_0)^2}{s^3(1 + \lambda)^6} \quad (13)$$

$$\eta = \frac{x}{(\sqrt{1+x} + 1)^2} \quad (14)$$

where: $-1 < \eta < 1$

Using an appropriate top-down or bottom-up method, calculate the continued fraction given by

$$\xi(x) = \frac{8(\sqrt{1+x} + 1)}{3 + \frac{1}{5 + \eta + \frac{\frac{9}{7}\eta}{1 + \frac{\frac{16}{63}\eta}{1 + \frac{\frac{25}{99}\eta}{1 + \dots}}}}} \quad (15)$$

and continue with

$$h_1 = \frac{(\ell + x)^2(1 + 3x + \xi)}{(1 + 2x + \ell)[4x + \xi(3 + x)]} \quad (16)$$

$$h_2 = \frac{m(x - \ell + \xi)}{(1 + 2x + \ell)[4x + \xi(3 + x)]} \quad (17)$$

$$B = \frac{27h_2}{4(1 + h_1)^3} \quad (18)$$

$$u = -\frac{B}{2(\sqrt{1+B} + 1)} \quad (19)$$

Using the top-down method, calculate the continued fraction given by

$$K(u) = \frac{\frac{1}{3}}{1 - \frac{\frac{4}{27}u}{1 - \frac{\frac{8}{27}u}{1 - \frac{\frac{2}{9}u}{1 - \frac{\frac{22}{81}u}{1 - \frac{\frac{208}{891}u}{1 - \dots}}}}}} \quad (20)$$

The top-down method, as used for calculating the value of a continued fraction having the form of Eq. (20), is performed as follows. If given a continued fraction of the form

$$F(3, 1; \frac{5}{2}; z) = \frac{1}{1 - \frac{\gamma_1 z}{1 - \frac{\gamma_2 z}{1 - \frac{\gamma_3 z}{1 - \frac{\gamma_4 z}{1 - \dots}}}}} \quad (21)$$

begin by calculating the γ_1 coefficient. In the case of Eq. (20), γ_1 and subsequent γ coefficients are given by

$$\gamma_{2n+1} = \frac{2(3n+2)(6n+1)}{9(4n+1)(4n+3)} \quad \text{for } \gamma \text{ odd, where } n = 0, 1, 2, 3, \dots \quad (22)$$

$$\gamma_{2n} = \frac{2(3n+1)(6n-1)}{9(4n-1)(4n+1)} \quad \text{for } \gamma \text{ even, where } n = 1, 2, 3, 4, \dots \quad (23)$$

Next, for $n = 1, 2, 3, \dots$, calculate

$$\delta_{n+1} = \frac{1}{1 - \gamma_n z \delta_n} \quad (24)$$

$$\tau_{n+1} = \tau_n (\delta_{n+1} - 1) \quad (25)$$

$$\sigma_{n+1} = \sigma_n + \tau_{n+1} \quad (26)$$

where $\delta_1 = \tau_1 = \sigma_1 = 1$ for the first step when $n = 1$. Finally, increment n , and repeat the calculations, starting with Eq. (22) or (23), until σ ceases to change within a preassigned amount. Then, the value of the continued fraction is given by

$$F(3, 1; \frac{5}{2}; z) = \lim_{n \rightarrow \infty} \sigma_n \quad (27)$$

where $z < 1$. Thus, for Eq. (20), z of Eqs. (21), (24) and (27) is simply replaced by u of Eq. (19) in the iterative calculations.

Once a value for Eq. (20) has been found, calculate

$$y = \frac{1 + h_1}{3} \left(2 + \frac{\sqrt{1+B}}{1 - 2uK^2} \right) \quad (28)$$

$$x = \sqrt{\left(\frac{1-\ell}{2} \right)^2 + \frac{m}{y^2}} - \frac{1+\ell}{2} \quad (29)$$

Repeat the calculations, starting with Eq. (14), until y ceases to change within a preassigned amount.

Then, the orbital elements can be calculated as

$$a = \frac{ms(1 + \lambda)^2}{8xy^2} = \text{semimajor axis} \quad (30)$$

$$p = \frac{2r_1r_0y^2(1 + x)^2 \sin^2 \frac{1}{2}\theta}{ms(1 + \lambda)^2} = \text{parameter} \quad (31)$$

$$e = \sqrt{1 - \frac{p}{a}} = \text{eccentricity} \quad (32)$$

Thus, the velocity vectors at times t_0 and t_1 are given by

$$\vec{v}_0 = \frac{\sqrt{\mu p}}{r_0 r_1 \sin \theta} [(\vec{r}_1 - \vec{r}_0) + \frac{r_1}{p}(1 - \cos \theta)\vec{r}_0] \quad (33)$$

$$\vec{v}_1 = \frac{\sqrt{\mu p}}{r_0 r_1 \sin \theta} [(\vec{r}_1 - \vec{r}_0) - \frac{r_0}{p}(1 - \cos \theta)\vec{r}_1] \quad (34)$$

3.2.5 The Transfer Time Algorithm

Another result of Lambert's Theorem is that when given the orbital elements and geometry of a trajectory, the transfer time between two points on the trajectory can be found. Solutions to this problem for an ellipse were first obtained by Lagrange and also by Gauss, while Euler developed a solution for parabolic orbits. A method combining aspects of Gauss' and Lagrange's methods was developed by Battin [4] which does not involve ambiguities of quadrant or sign and is valid for orbits of any eccentricity.

This combined method was implemented in the subroutine having the name TRANST (ref. Appendix A, pp. 140-141), where knowing the orbital elements of the missile trajectory and the magnitudes of the radial position vectors of the missile and target at time t_1 , it is possible to determine the transfer time $t_2 - t_1$ required for the missile to reach the target's altitude at time t_2 . That is, the transfer time is the time required for the missile to reach some point on the spherical surface containing the target in its orbit, and is considered to be the minimum time to a

possible intercept. Exactly where the missile will penetrate the sphere of radius r_{T2} is not yet known, but will be found next.

It should be noted here that in order for this method of calculating the transfer time-to-intercept to be strictly valid, the target must be moving in a circular orbit. If it is not, the transfer time calculated would still be the *minimum* time-to-intercept if the radius of the sphere at time t_2 was taken to be the radius of the target's orbit at perigee, say, but would not necessarily represent the total time required for the interceptor to effect an intercept. In the case of a non-circular target orbit, if intercept was not predicted on the first pass of the algorithms, a new criterion for establishing transfer time-to-intercept might be required, since target altitude as well as velocity would be a function of time. Regardless, though, the time to a possible intercept could be updated by the target as it moves in its orbit by simply choosing a new altitude acceptable to the target for determining when and where the missile would reach that altitude.

Therefore, in order to establish a criterion to determine the initial transfer time-to-intercept, the target is assumed to be in an initially circular orbit. This is not an unrealistic assumption either, since most satellites that would be likely to come under attack do operate in nearly circular orbits, with a range of inclinations. (ref. Sec. 2.1) Furthermore, this assumption allows a more straightforward initial setup of EVADER, in that it is conducive to designing intercept scenarios. In setting up these scenarios, as will be discussed later in the sections on setting up and testing EVADER, the target's orbit was not restricted in inclination, however.

Despite the simplifications to be had by allowing the initial target orbit to be circular, a circular orbit restriction is not required by the algorithms used in EVADER to update predicted position and velocity vectors. In fact, the same routines which are used to calculate the missile's position and velocity vectors in its unrestricted orbit are also used to calculate the predicted position and velocity of the target before and after it has maneuvered out of its initially circular orbit.

As stated at the outset of this section, in order to determine the transfer time

along an orbital path, the orbital elements of the particular orbit joining two points on the path must be known. After all, an infinite number of paths, each having a different transfer time, could conceivably join any two points in space. Fortunately, the missile position vector \vec{r}_{M1} is known and the missile velocity vector \vec{v}_{M1} at the same point is available through the Lambert algorithm of the previous section. This is all that is needed to determine the missile's orbit uniquely and find the orbital elements.

3.2.5.1 Transfer Time Equations

The equations that follow should be calculated in the order shown. First, the orbital elements of the orbit under question are determined as follows.

If Given: \vec{r} , \vec{v} , $\mu = 3.981 \times 10^5 \text{ km}^3/\text{sec}^2$

$$\vec{h} = \vec{r} \times \vec{v} = \text{angular momentum vector} \quad (35)$$

$$p = \frac{h^2}{\mu} = \text{parameter} \quad (36)$$

From the *vis-viva integral*,

$$a = \left(\frac{2}{r} - \frac{v^2}{\mu} \right) = \text{semimajor axis} \quad (37)$$

$$e = \sqrt{1 - \frac{p}{a}} = \text{eccentricity} \quad (38)$$

The orbit is then classified according to its eccentricity as a(n)

- circle for $e = 0$
- ellipse for $0 < e < 1$
- parabola for $e = 1$
- hyperbola for $1 < e < \infty$

Next, the transfer angle θ can be found in one of two ways.

If given r_1 , r_2 , p and e , and using the equation of orbit:

$$f_1 = \arccos \left[\frac{1}{e} \left(\frac{p}{r_1} - 1 \right) \right] = \text{true anomaly at time } t_1 \quad (39)$$

$$f_2 = \arccos \left[\frac{1}{c} \left(\frac{p}{r_2} - 1 \right) \right] = \text{true anomaly at time } t_2 \quad (40)$$

$$\theta = f_2 - f_1 = \text{transfer angle} \quad (41)$$

otherwise, if given \vec{r}_1, \vec{r}_2 :

$$\theta = \frac{\vec{r}_1 \cdot \vec{r}_2}{r_1 r_2} \quad (42)$$

Then, continue with

$$c = \sqrt{r_1^2 + r_2^2 - 2r_1 r_2 \cos \theta} = \text{chord} \quad (43)$$

$$s = \frac{1}{2}(r_1 + r_2 + c) = \text{semiperimeter} \quad (44)$$

$$a_m = \frac{1}{2}s = \text{semimajor axis of the minimum energy orbit} \quad (45)$$

$$\lambda = \frac{\sqrt{r_1 r_2}}{s} \cos \frac{1}{2}\theta \quad (46)$$

$$x = \sqrt{1 - \frac{a_m}{a}} \quad (47)$$

$$y = \sqrt{1 - \lambda^2(1 - x^2)} \quad (48)$$

$$S_1 = \frac{1}{2}(1 - \lambda - x\eta) \quad (49)$$

where: $0 < S_1 < 1$ for elliptical orbits
 $S_1 = 0$ for parabolic orbits
 $-\infty < S_1 < 0$ for hyperbolic orbits

The top-down method, as described in Eqs. (21) through (27) of Sec. (3.2.4), is then used to evaluate the continued fraction given by

$$Q = \frac{4}{3} F\left(3, 1; \frac{5}{2}; S_1\right) \quad (50)$$

Eq. (50) is of the same form as Eq. (21), with S_1 substituted for z , and is given in expanded form as

$$Q = \frac{\frac{4}{3}}{1 - \frac{\gamma_1 S_1}{1 - \frac{\gamma_2 S_1}{1 - \frac{\gamma_3 S_1}{1 - \frac{\gamma_4 S_1}{1 - \dots}}}}} \quad (51)$$

In the case of Eq. (51), however, the following equations are used for the γ_n values in the top-down method calculations instead of Eqs. (22) and (23):

$$\gamma_n = \left\{ \begin{array}{ll} \frac{(n+2)(n+5)}{(2n+1)(2n+3)} & \text{for } n \text{ odd} \\ \frac{n(n-3)}{(2n+1)(2n+3)} & \text{for } n \text{ even} \end{array} \right\} \quad n = 1, 2, 3, \dots \quad (52)$$

Thus, the transfer time is given as

$$\|t_2 - t_1\| = \sqrt{\frac{a_m^3}{\mu}(\eta^3 Q + 4\lambda\eta)} \quad (53)$$

3.2.6 The Extended Gauss Method

Once the position and velocity vectors of the missile at time t_1 , along with the transfer time to intercept are known, it is possible to employ a third technique known as the Extended Gauss method. This method, as implemented in the subroutine EXGAUSS (ref. Appendix A, pp. 141-144), is used to solve Kepler's Problem, where it is desired to calculate the position and velocity vectors \vec{r}_2 and \vec{v}_2 at a time t_2 for a body in its orbit when the initial state vectors \vec{r}_1 and \vec{v}_1 are known at time t_1 . In his *Theoria Motus*, Gauss first gave an efficient technique for solving Kepler's Problem for near parabolic orbits, with time required to be reckoned from pericenter passage. The Extended Gauss method, as used in EVADER and developed by Battin and T.J. Fill [4], is not restricted to either of these constraints.

Thus, through the use of this method, the position and velocity, \vec{r}_{M2} and \vec{v}_{M2} , of the missile in space can be calculated for the projected time t_2 , which is equal to the sum of t_1 and the transfer time and is the time when the missile achieves the altitude of the target. Use of the Extended Gauss algorithm in EVADER is not limited to the missile alone, and is also used to obtain target position and velocity vectors, \vec{r}_{T2} and \vec{v}_{T2} , at the future time t_2 , since \vec{r}_{T1} and \vec{v}_{T1} are known at time t_1 and the transfer time is the same as for the missile. In actuality, the more involved computations of the Extended Gauss method would not be needed to predict vectors for the initially circular target orbit. Since the velocity magnitude and orbital radius are constant for a circular orbit, only the transfer time is required to find \vec{r}_{T2} and \vec{v}_{T2} for the

initial target orbit from geometrical considerations and simple orbital mechanics relations when \vec{r}_{T1} is known. Moreover, it is only the vector components of position and velocity that change for a body in a circular orbit, and the angular velocity of the body is constant. These properties of a circular orbit are not exploited when initially predicting target vectors in a run of EVADER, however, since it is desired to allow EVADER to deal with initial target input vectors which are not for a circular orbit, if desired. Rather, the Extended Gauss method is used to predict vectors for both vehicles in all phases of the program. The simplifications entailed by a circular orbit are employed for the target when setting up test scenarios for EVADER, but this will be discussed later in Sec. 3.4.8.

3.2.6.1 Extended Gauss Equations

The following equations of the Extended Gauss method should be calculated in the order presented.

If Given: $\vec{r}_1, \vec{v}_1, t_2 - t_1, \mu = 3.981 \times 10^6 \text{ km}^3/\text{sec}^2$

$$T = \sqrt{\mu}(t_2 - t_1) \quad (54)$$

$$\sigma_1 = \vec{r}_1 \cdot \frac{\vec{v}_1}{\sqrt{\mu}} \quad (55)$$

$$\gamma_1 = 2 - \frac{r_1 v_1^2}{\mu} \quad (56)$$

$$\chi_1 = \frac{1}{2} - \frac{9}{20} \gamma_1 \quad (57)$$

Then, initializing $D = \delta = 1$,

$$\xi = \frac{3\delta DT}{r_1} \quad \eta = \frac{\xi}{r_1} \quad \zeta = \frac{\sigma_1 D}{2} \quad (58)$$

$$\epsilon = 1 + \eta \zeta \quad b = \epsilon + \frac{1}{2} \eta (\zeta + \chi_1 \xi) \quad (59)$$

Next, solve the Newton iteration for x_n recursively as shown below until it converges to a desired number of decimal places.

$$x_{n+1} = \frac{2x_n^3 + |b|}{3x_n^2 - \epsilon} \quad (60)$$

$$\text{where: } n = 0, 1, 2, 3, \dots$$

$$x_0 = 1 + |\epsilon|$$

Continue with

$$\theta = \frac{\xi}{1 \pm x} \quad \phi = \frac{\theta^2}{r_1} \quad y = \gamma_1 \phi \quad (61)$$

$$\text{where for } \theta \text{ use } \begin{cases} (+) \text{ sign for } b > 0 \\ (-) \text{ sign for } b \leq 0 \end{cases}$$

Then, if $|y| \leq 1$, skip to Eq. (65). Otherwise, if $y > 1$, which can occur for large time intervals, set $y = 1$ and calculate

$$\phi = \frac{y}{\gamma_1} \quad \theta = \sqrt{\phi r_1} \quad (62)$$

After calculating Eqs. (62), calculate in order Eqs. (65), (66), (67), (68), and (69). After calculating Eq. (69), return to this part of the algorithm and continue with Eq. (63). In Eqs. (64), use the old values of σ_1 and γ_1 to find new values for these variables. All transition matrices thus generated from Eq. (69) because of this part of the algorithm will be sequentially multiplied with any initial transition matrix generated to obtain the final transition matrix.

$$T_m = \frac{\theta \left[\left(\frac{1}{3} \chi_1 \theta + \frac{1}{2} \sigma_1 D \right) \theta + r_1 \right]}{\delta D} \quad (63)$$

$$r_1 = r_2 \quad \sigma_1 = \sigma_1 \kappa + (1 - \gamma_1) \omega \quad \gamma_1 = \frac{r_2 \gamma_1}{r_1} \quad (64)$$

Now, replace T by $T - T_m$ and restart the algorithm beginning with Eq. (57).

Calculate the economized power series for $K(y)$ where:

$$K = \sum_{n=0}^6 k_n y^n \quad (65)$$

where: $k_0^* = 1.00000000001$
 $k_1^* = -0.10000000174$
 $k_2^* = -0.00357142897$
 $k_3^* = -0.00023808136$
 $k_4^* = -0.00001919250$
 $k_5^* = -0.00000172916$
 $k_6^* = -0.00000016292$

Now, calculate new values for D and δ from

$$D = \frac{1 - \frac{3}{20}y}{K} \quad \delta = K^2 + \frac{1}{4}y \quad (66)$$

Once this point is reached, repeat the computations of the algorithm starting with Eq. (58), using the values of D and δ from Eqs. (66), until y of Eqs. (61) ceases to change within a preassigned amount. For subsequent algorithm cycles, the convergence of x in Eq. (60) will be improved by selecting for x_0 the value of x determined during the previous algorithm cycle. After y ceases to change, continue by calculating

$$\lambda = \frac{\phi}{2\delta} \quad \kappa = 1 - \gamma_1\lambda \quad \psi = r_1\lambda \quad (67)$$

$$\omega = \frac{\theta K}{\delta} \quad r_2 = r_1\kappa + \psi + \sigma_1\omega \quad (68)$$

The state transition matrix, the elements of which are known as Lagrangian coefficients, is then given by

$$\Phi(t_2, t_1) = \begin{bmatrix} 1 - \lambda & \frac{r_1\omega + \sigma_1\psi}{\sqrt{\mu}} \\ \frac{-\omega\sqrt{\mu}}{r_1r_2} & 1 - \frac{\psi}{r_2} \end{bmatrix} = \begin{bmatrix} F & G \\ F_t & G_t \end{bmatrix} \quad (69)$$

Finally, the position and velocity vectors at time t_2 are given by

$$\vec{r}_2 = F\vec{r}_1 + G\vec{v}_1 \quad (70)$$

$$\vec{v}_2 = F_t\vec{r}_1 + G_t\vec{v}_1 \quad (71)$$

It is interesting to note by an examination of the Extended Gauss equations that a negative time interval is not precluded. Indeed, if a negative time interval is used, the position and velocity vectors of previous points along a trajectory can be found. In fact, this property is used to facilitate the setup of test scenarios for EVADER, as will be discussed in Sec. 3.4.8.

3.3 Taking Evasive Action

3.3.1 Evasive Maneuvering in EVADER

Each time step, the current and future relative position vectors between the missile and target are calculated based on the vehicles' current and predicted positions at the current time t_1 and future intercept time t_2 and are given by

$$\vec{r}_{MT1} = \vec{r}_{M1} - \vec{r}_{T1} \quad \text{and} \quad \vec{r}_{MT2} = \vec{r}_{M2} - \vec{r}_{T2} \quad (72)$$

If the magnitude of the predicted relative vector r_{MT2} is found to be less than 1 km, subroutine EVADE (ref. Appendix A, pp. 153-155) is called in order to initiate an evasive maneuver. Thus, a warning sphere of 1 km radius surrounds the target's predicted positions, and evasive maneuvering is triggered by predicting the entry of the missile into the warning sphere at a future time. This method of triggering evasion is based on the concepts of lethal volume and missile kill-radius (ref. Sec. 2.3.2). A 1 km radius for the target's warning sphere was chosen to be representative of the current ASAT threat's (Soviet) conventional warhead kill-radius, and represents a satellite's minimum survivable distance of approach to a conventionally armed ASAT weapon.

Once the need for evasive maneuvering has been established, the operator is queried to select one, among several, options. Maneuvering is based on the idea that the target would like to occupy a position in space at the future intercept time which would place it outside of the missile's kill-radius. Furthermore, it is advantageous for the target to be able to select both the direction and magnitude of the future miss-distance vector. In this way, the target can change its orbit in

ways that best use its maneuvering capability and that limit the degradation to mission effectiveness caused by altering the target's operational orbit. Moreover, the target may wish to maneuver in ways which might exploit deficiencies in the attacker's altitude reach, plane change, or homing capabilities. Thus, a maneuver to any point in three-dimensional space might be desired, and in fact, this is what EVADER allows.

Rather than requiring the coordinates of a desired aim-point to be input, which would be needlessly opaque to the operator from a qualitative point of view, EVADER provides for five maneuvering options from which the necessary computations are made internally following a selection. The options provide for maneuvering the target away from the predicted missile position at intercept by a selected magnitude and direction. The maneuvering options are as follows:

1) Option R

Aim the spacecraft for a point which is a specified distance from the missile's predicted position r_{M2} and is in the \pm direction of the target's predicted radial position vector r_{T2} . Thus,

$$\vec{r}_{T2_{aim}} = \vec{r}_{M2} \pm d_{miss} \left(\frac{\vec{r}_{T2}}{r_{T2}} \right) \quad (73)$$

This would be an in-plane altitude change for the target in a zero predicted miss-distance case.

2) Option V

Aim the spacecraft for a point which is a specified distance from the missile's predicted position r_{M2} and is in the \pm direction of the target's predicted velocity \vec{v}_{T2} . Thus,

$$\vec{r}_{T2_{aim}} = \vec{r}_{M2} \pm d_{miss} \left(\frac{\vec{v}_{T2}}{v_{T2}} \right) \quad (74)$$

This would move the target's predicted position essentially ahead of or behind the predicted intercept point.

3) Option H

Aim the spacecraft for a point which is a specified distance from the missile's predicted position \vec{r}_{M2} and is in the \pm direction of the target's angular momentum vector \vec{h}_T , where $\vec{h}_T = \vec{r}_{T1} \times \vec{v}_{T1} = \vec{r}_{T2} \times \vec{v}_{T2}$ and is perpendicular to the target's orbital plane. Thus,

$$\vec{r}_{T2aim} = \vec{r}_{M2} \pm d_{miss} \left(\frac{\vec{h}_T}{h_T} \right) \quad (75)$$

This would represent a pure plane change for the target in a zero predicted miss-distance case.

4) Option E (Extend)

Aim the spacecraft for a point which is a specified distance from the missile's predicted position \vec{r}_{M2} and is in the direction opposite to the presently calculated predicted miss-distance vector \vec{r}_{M2} of Eqs. (72). This option could be used in a non-zero predicted miss-distance case when it is desired to move to a point just outside the missile's kill radius, say, in a way requiring the least additional miss-distance increment. Thus,

$$\vec{r}_{T2aim} = \vec{r}_{M2} - d_{miss} \left(\frac{\vec{r}_{MT2}}{r_{MT2}} \right) \quad (76)$$

5) Option C (Combined)

Aim the spacecraft for a point which is determined by any combination of options R, V, and H. For this option, the magnitude of the miss-distance desired in each of the $\pm R$, $\pm V$, and $\pm H$ directions is input. Thus,

$$\vec{r}_{T2aim} = \vec{r}_{M2} + d_{Hmiss} \left(\frac{\vec{h}_T}{h_T} \right) + d_{Rmiss} \left(\frac{\vec{r}_{T2}}{r_{T2}} \right) + d_{Vmiss} \left(\frac{\vec{v}_{T2}}{v_{T2}} \right) \quad (77)$$

The total resulting straight line miss-distance is then displayed to the operator.

Once the new aim-point for the target has been calculated by EVADER, the velocity-to-be-gained vector \vec{v}_{T1to} , at the present position that will place the spacecraft on a coasting trajectory to the aim-point in the previously specified transfer

time-to-intercept is calculated. The velocity-to-be-gained in this case is simply the vector difference between the velocity required by the target to reach the aim-point from its present position in the specified time and the current velocity of the target at its present position. Thus,

$$\vec{v}_{T1,tt} = \vec{v}_{T1,tt} - \vec{v}_{T1} \quad (78)$$

The magnitude of the vector $\vec{v}_{T1,tt}$ is equivalent to the total *delta v* required to make the maneuver. The actual calculation of the $\vec{v}_{T1,tt}$ vector is made by calling the LAMBERT subroutine with \vec{r}_{T1} , $\vec{r}_{T2,aim}$, and the transfer time-to-intercept, as calculated in subroutine TRANST, as inputs, since the Lambert method requires two position fixes over time from which velocity vectors at the two positions can be found (ref. Sec. 3.2.4). Thus, the Lambert algorithm is used to find velocity vectors for both the missile and target.

After $\vec{v}_{T1,tt}$ is calculated, its magnitude and vector components are displayed to the operator so that a decision on implementation of the maneuver can be made. EVADER offers three options for implementing a calculated maneuver.

1) Option I (Impulsive)

This option performs the maneuver impulsively by simply adding $\vec{v}_{T1,tt}$ to \vec{v}_{T1} . This is useful in testing the program or when only a short engine burn, which can realistically be modelled by an impulsive velocity addition, is required.

2) Option E (Engine Burn)

This option invokes routines which numerically integrate an engine burn based on actual vehicle and propulsion parameters. The model for vehicle propulsion, along with other numerical integration techniques used to test EVADER, will be discussed later in Sec. 3.4.

3) Option N (No Maneuver)

This option negates the planned maneuver altogether. In this case, EVADER then numerically updates the trajectories another time step, as will be ex-

plained in Sec. 3.4, decrements the transfer time accordingly, uses the predictive techniques to sense that interception is still imminent, and again warns the operator that an evasive maneuver is required. This option is useful in exploring various maneuver scenarios and in seeing how the Δv required for maneuvering increases when evasive action is delayed and the time required to achieve a desired miss-distance diminishes as the missile approaches (ref. Sec. 4).

During and after an evasive maneuver, or following a decision not to maneuver, numerically integrated updates to the current position and velocity vectors of the spacecraft and missile are performed. These current vector updates are performed by numerically integrating the vehicles' equations of motion with drag, thrust, and higher order gravitational harmonics taken into account (ref. Sec. 3.4).

Also during and after an evasive maneuver by the spacecraft, the Extended Gauss method (ref. Sec. 3.2.6) is used to update the position and velocity vectors of both the missile and spacecraft. The process of updating current and predicted position and velocity vectors and monitoring the predicted magnitude and direction of change of the relative position vector \vec{r}_{MT2} continues, until the relative vector is found to be strictly increasing in magnitude over time. At that point in EVADER, subroutine SAFE (ref. Appendix A, pp. 155 and 156) is called and a successful evasion is declared for that scenario. SAFE calculates the orbital elements, including the inclination, of the final orbits of both vehicles based on their current position and velocity vectors⁴. Thus, if it was desired to maneuver the spacecraft back to its initial, or some alternate orbit, an appropriate maneuvering schedule could be planned.

The transfer time used in updating future positions is the initial time-to-intercept, appropriately decremented as the trajectories are updated, as was calculated when EVADER first detected an intercept. This transfer time is used for all predicted

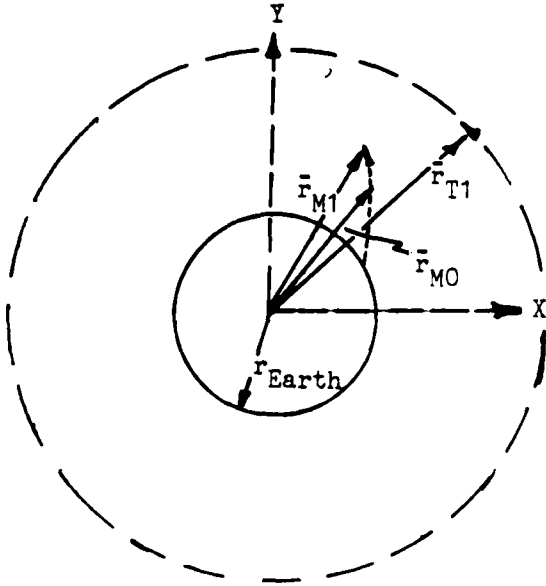
⁴Reference the transfer time algorithm equations of Sec. 3.2.5 for an example of how this kind of calculation is made.

trajectory endpoint calculations following a maneuver, since it is these endpoints that are used to determine the magnitude and direction of change of the relative distance separating the vehicles at a future time $t_{2post-ev}$ after evasion. The relative vector \vec{r}_{MT1} separating the vehicles at the current time is also updated and could be monitored, if desired.

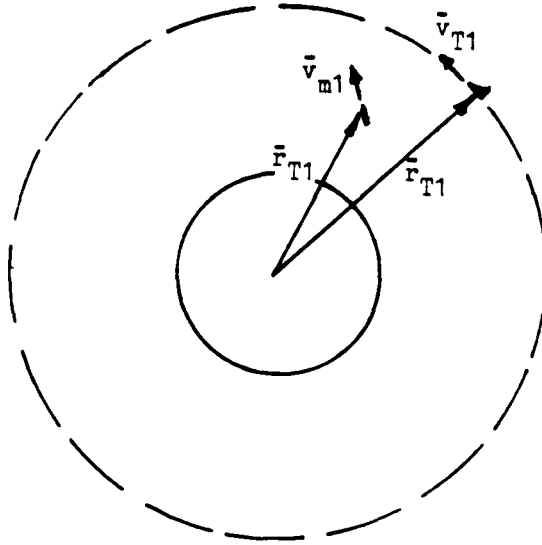
Thus, the initial transfer time is considered to be a minimum value for initial intercept and a constant. If this were not the case, for a missile that was maneuvering or accelerating, the transfer time would be updated by requiring the spacecraft to query its sensors for new missile position vectors each time step or in response to a detected missile engine burn (ref. Sec. 2.3.2).

The astrodynamic techniques are solely responsible for governing an evasive maneuver in EVADER, and the numerical integration techniques to be subsequently discussed are used to calculate current trajectory points which can be compared, once the current trajectory is integrated out to the predicted time, to the trajectory points generated by the astrodynamic techniques. In this way, the accuracy and usefulness of relying on an evasive maneuvering method which ignores drag and gravitational anomalies and assumes impulsive velocity changes can be judged. The various stages of an invocation of the astrodynamic techniques governing an evasive maneuver in EVADER are illustrated in Fig. 3, page 68.

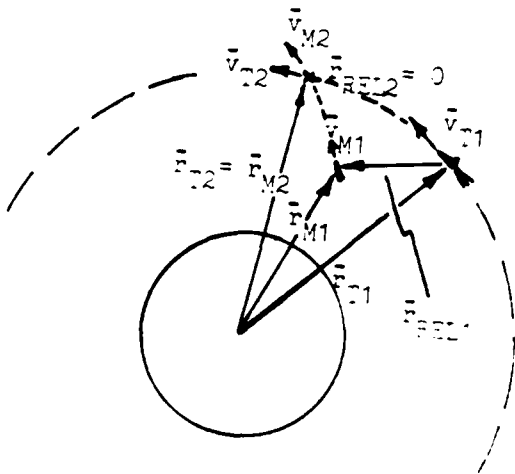
1) Missile position fixes taken following threat alert.



2) Missile velocity vector calculated for time t_1 . Missile transfer time to target altitude determined.



3) Position and Velocity vectors predicted for time t_2 . Intercept predicted. Evasive maneuver initiated.



4) Vectors updated for time t_1 and predicted for time t_2 . Increasing, non-zero r_{REL2} confirmed. Successful evasion declared.

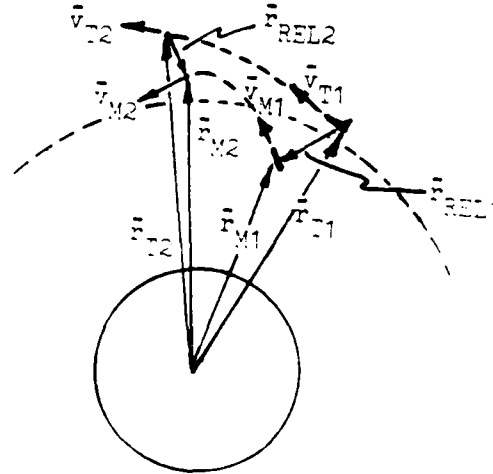


Figure 1: Stages of an Invocation of EVADER

3.3.2 Assessing the Operator's Role in Evasive Action Decisions

To provide a further insight into the implementation of an evasive action method, it is useful to discuss briefly the role of the operator in making evasive action decisions. For a manned spacecraft system, the pilot would be the executive authority in planning an overall evasive strategy, based on data and recommendations from the system, and in deciding to implement it. An autonomous system, however, presents many new problems. How does a spacecraft control itself 'intelligently' in response to a threat when the human operator is not available? Furthermore, how can the system effectively identify and classify the threat so that an appropriate evasive response is taken? These are questions which are well-suited to the techniques of *artificial intelligence*.

For a computer system or a human to exhibit intelligent behavior in a particular domain, it must have a store of knowledge to draw on in performing tasks, drawing conclusions and making inferences about that domain. When a computer is capable of demonstrating such behavior, as judged by comparing its behavior and responses to those of a human in the same situation, its behavior is said to exhibit *artificial intelligence*. The problem of representing knowledge in a computer program can be viewed as the implementation of appropriate data structures and inference and control mechanisms, such that 'knowledgeable' action results in the application domain.

A system demonstrating artificial intelligence in its domain of application is often termed an *expert system*. This is because the computer program draws on a knowledge base compiled from information supplied from human experts in the domain. The inferences and decisions made by the program are thus designed to reflect those made by human experts. The knowledge base of such expert systems is often in the form of *If-Then* rules of thumb, or heuristics, and other data or even calculations which the program can call up or perform, evaluate, and act on.

There are currently under development certain expert systems which have a direct application to the problem of spacecraft evasive maneuvering. Among these

are three research programs being sponsored by the U.S. Defense Advanced Research Projects Agency (DARPA) under its Strategic Computing Program (SCP) [17]. Among these three, the Air Force's Pilot's Associate (PA) program is most applicable⁵. According to DARPA's director of the engineering applications office for the SCP, the PA program will explore the application of artificial intelligence to four distinct functions typically required of a combat pilot [29]:

- 1) monitoring aircraft systems in the role of a flight engineer,
- 2) mission planning and re-planning in flight,
- 3) external situation assessment, based on information obtained from the aircraft's radar and other sensors,
- 4) and tactical mission management, to rapidly devise an optimum strategy for coping with external threats.

All four of these functions, which are so vital to a pilot's and aircraft's survivability and mission success, are also critical to a spacecraft in avoiding an ASAT threat while maintaining mission effectiveness.

As an example of external situation assessment, let's examine the role a spacecraft's sensors would play in supplying the information necessary to deciding the form of evasive action to be taken. If the spacecraft could identify an approaching vehicle and characterize its armament and maneuverability, based on a comparison of information in the target's on-board data banks with sensor data, it could select an action that would have the best chance of defeating the threat. Pope [19] has performed research using artificial intelligence techniques to classify aerial threats according to type based on processing data from radar and infrared sensors and comparing the results to known characteristics of specific threats as stored in a data-base. As his subject area, he chose the problem of identifying Soviet fighter and

⁵The Army is developing a land vehicle which navigates autonomously, while the Navy is developing a battle management system for carrier battle groups.

bomber aircraft based on their radar and infrared emissions and radar cross-section as determined by long-range sensors on-board an aircraft. The radar emissions and cross-section, and infrared signature of a specific vehicle, when taken together can often serve to uniquely identify an opposing vehicle to a high confidence level. The vehicle's characteristics can then be referenced from a data-base and exploited advantageously.

In the ASAT case, a hostile vehicle might be identified as one which carries a nuclear warhead, as opposed to a conventional or direct intercept one. As discussed in Sec. 2.3.2, a miss-distance acceptable to the target would be on the order of meters for a non-explosive, direct intercept weapon, while hundreds of kilometers might be required to escape a nuclear-tipped weapon. Thus, for the target to ensure its survivability, while avoiding unnecessarily large orbital changes, it should have the capability to change the radius of its warning sphere (ref. Sec. 3.3.1) and decide on appropriate miss-distances. This is an example of threat or situation assessment. For an effective decision to be made, however, the capabilities of the spacecraft and its options must also be assessed in addition to the capability of the target.

The making of decisions, based on situation assessment, falls under the tactical management function. The spacecraft may decide that an effective near-term evasive action may be to employ ECM or decoys (ref. Sec. 2.3.1), if susceptibility to these types of countermeasures were indicated for the missile, and postpone a maneuver. If maneuverability and homing were considered to be the missile's primary weaknesses, a strategy of maneuver could be employed to exploit these weaknesses, while maximizing the effectiveness of the spacecraft's maneuverability and position. Furthermore, an evasive strategy intended to optimize some quantity (ref. Sec. 2.4) such as fuel use might be employed if a protracted engagement was expected.

In order for any evasive action decision to be effective in an overall sense, it must be prudently planned. Although survival is the primary objective, a decision must also take into account mission degradation due to orbital changes, as well as the need to re-plan the mission or return to the original orbit once evasive maneuvers

have been completed. Planning the use and conservation of limited stores such as fuel and electrical power is especially critical if subsequent hostile encounters are expected. Thus, the planning function, which must take into account mission, vehicle, and trajectory constraints, lends an overall perspective to the decision to be made.

Thus, a good and realistic evasive maneuvering decision cannot be made unless it is founded in a reliable assessment of the capabilities of both the threat and the target, is done in the context of an effective overall plan, and is founded in a cognizance of spacecraft trajectory and maneuvering constraints. In the case of a program like EVADER, it would fulfill the role of supplying to an expert system or pilot the accurate, timely, realistic data required to predict intercepts, and evaluate and plan evasive maneuvers based on vehicle and trajectory constraints.

3.4 Testing Evader

In order to properly test the accuracy and usefulness of the two-body motion astrodynamics techniques used in EVADER to predict trajectory points, it was decided to numerically integrate the vector equations of motion for both vehicles to update current trajectory values. In this way, the perturbative forces of thrust and drag, as well as higher order gravitational harmonics, could be included in the model of the actual trajectories to see if ignoring these perturbations in the astrodynamics techniques was an acceptable assumption. Thus, the predicted position and velocity vectors generated through astrodynamics methods could be compared to vectors generated through integration once the current trajectories were fully integrated to the predicted time.

Also, the ability to turn the drag and non-uniform gravity models 'on' or 'off' at the start of a scenario was included so that the effect of each model could be determined separately if desired. Moreover, by integrating the trajectories with both drag and non-uniform gravity 'off', and using the impulsive velocity change maneuver option, a convenient means could be had of judging the agreement be-

tween trajectory points which should agree even though they were generated in two completely separate ways. If agreement between both methods was achieved to a significant number of decimal places, a high confidence in the correctness of both implementations would be justified. The sensitivity of the numerical integration scheme to the integration step size could also be judged if integrated values could be made to converge to the astrodynamic values for small enough time steps.

3.4.1 Vector Equation of Orbital Motion

The vector form of the differential equation of motion of a body in orbit about the Earth in the presence of perturbative accelerations is given by

$$\frac{d^2\vec{r}}{dt^2} + \frac{\mu}{r^3}\vec{r} = \vec{a}_{pert} \quad (79)$$

where \vec{r} is the vector position of the body with respect to the origin of an Earth-centered coordinate system (ref. Sec. 3.2.1), μ is the Earth's gravitational constant for uniform gravity, and \vec{a}_{pert} is the resultant acceleration vector due to thrust, drag, or other perturbative forces, and t is time. It should be remembered that since

$$\vec{r} = r_x\hat{i}_x + r_y\hat{i}_y + r_z\hat{i}_z \quad \text{and} \quad \vec{a}_{pert} = a_x\hat{i}_x + a_y\hat{i}_y + a_z\hat{i}_z \quad (80)$$

Eq. (79) is actually the vector form of three simultaneous second-order, non-linear, non-homogeneous, scalar differential equations given by

$$\frac{d^2r_x}{dt^2} + \mu\frac{r_x}{r^3} = a_x \quad \frac{d^2r_y}{dt^2} + \mu\frac{r_y}{r^3} = a_y \quad \frac{d^2r_z}{dt^2} + \mu\frac{r_z}{r^3} = a_z \quad (81)$$

where as in Eqs. (2): $r = \sqrt{r_x^2 + r_y^2 + r_z^2}$

Therefore, to numerically integrate the vector equation of motion of Eq. (79), the three scalar differential equations of Eqs. (81) must be integrated successively to obtain solutions for each of the vector components.

In Eq. (79), the acceleration due to gravity along the direction of the radial position vector \vec{r} is given by the quantity

$$\vec{a}_g = -\frac{\mu}{r^2}\frac{\vec{r}}{r} = -\frac{\mu}{r^3}\vec{r} \quad (82)$$

Thus, for a uniform gravity model \vec{a}_g is a function of position with μ remaining constant. For a non-uniform gravity model, however, μ is also a function of position, as will be discussed further in Sec. 3.4.4.

The acceleration vector \vec{a}_{pert} , as modelled in EVADER, consists of two components: acceleration due to thrust \vec{a}_{th} during an engine burn, and acceleration (in actuality a deceleration) due to drag \vec{a}_d . For the missile, \vec{a}_{th} is, of course, set to zero since no propulsion system was modelled for it. For both vehicles respectively, \vec{a}_d is always a function of position and velocity, while for the target, both drag and thrust acceleration are functions of time as well when the engine is thrusting, since the target's mass decreases as propellant is used. Further details of the functional relationships of the drag and thrust models will be discussed later in Secs. 3.4.5 and 3.4.6, respectively. Thus, we have the functional relationship for \vec{a}_{pert} of Eq. (79)

$$\vec{a}_{pert}(t, \vec{r}, \vec{v}) = \vec{a}_{th}(t) + \vec{a}_d(t, \vec{r}, \vec{v}) \quad (83)$$

where for the missile: $\vec{a}_{th} = \vec{0}$

It now becomes evident that the vector differential equation of Eq. (79) is a function of time t , position \vec{r} , and velocity \vec{v} , and that a numerical integration technique capable of handling equations of this form is required.

3.4.2 Picking a Numerical Integration Technique

To select a numerical integration technique appropriate to a particular application, certain requirements of the application have to be delineated. The order of accuracy desired, computational speed and complexity, and ease and efficiency of controlling the step size are all factors to be considered.

All numerical integration techniques model a function by approximating that function through such means as a Taylor series expansion. The accuracy of the approximation is judged by the number of terms retained in the expansion and the size of the step size used. For example, a second-order Taylor series approximation

for vector position and velocity would be given by

$$\vec{r} = \vec{r}_0 + h\vec{v}_0 + \frac{1}{2}h^2\vec{a}_0 + O(h^3) \quad (84)$$

$$\vec{v} = \vec{v}_0 + h\vec{a}_0 + \frac{1}{2}h^2\vec{a}'_0 + O(h^3) \quad (85)$$

and would have an error of order h^3 as indicated by the notation. In Eqs. (84) and (85), \vec{a} is acceleration, and h denotes the time interval step size $t - t_0$, while \vec{a}'_0 is

$$\vec{a}'_0 = \left. \frac{\partial \vec{a}}{\partial \vec{r}} \right|_{t=t_0} \quad (86)$$

The higher the order of the method, the more accurately it approximates a function. Generally speaking, the higher the order, the more 'stages' of intermediate calculation required, and with an increase in the number of stages to be calculated, the computational time increases, especially if a small step size is used.

Integration techniques can also be broken down into one of two general methods [25]: one-step (O-S), and predictor-corrector (P-C) methods. One-step methods use information at one point to calculate information for the next point, so they are termed 'self-starting'. They may require several evaluations of the function at intermediate points to converge at the desired point, which can be time-consuming. The step size for these methods can be easily modified, however. One-step techniques include Euler, Modified Euler, and Runge-Kutta methods.

Predictor-corrector methods require information about points prior to a current point in order to calculate information at a succeeding point, so these methods are not self-starting. They must, in fact, rely on a one-step method to get there start. Changing the step size in a P-C method is rather involved and requires a temporary reversion to a O-S starting method. Although P-C methods are more complex, their chief advantage is that they require fewer stages of calculation than O-S methods. In a typical fourth-order O-S method, four stages of evaluation are required, while a P-C method of the same order of accuracy requires only two stages and is thus almost twice as fast as the O-S method. Additional memory storage for prior points is required for P-C methods, however, and O-S and P-C methods of the same order

have comparable accuracy. P-C methods include Milne's, Adams-Bashforth, and Hamming's methods.

Therefore, if ease of step size modification is desired or memory space is limited, and integration speed is not critical, the less complex O-S methods would be desired. In EVADER, it was important to be able to change the step size easily for testing and engine burns, and the speed of the astrodynamic techniques used to predict intercept and plan evasion was of more interest than the speed of the numerical integration techniques used simply to update current trajectory points in the simulations. In addition, it was desired to achieve sufficient integration accuracy so that a valid comparison between points generated by the astrodynamic and integration techniques could be made. This accuracy could be had by simply choosing a method of high enough order and reducing the step size sufficiently⁶. Therefore, a fourth-order, Runga-Kutta method, commonly used for engineering applications and valid for functions of time, position and velocity, was selected.

3.4.3 Fourth-Order Runga-Kutta Method

The fourth-order Runga-Kutta numerical integration method chosen to update EVADER's current trajectories, as implemented in subroutine RUNKUT (ref. Appendix A, pp. 144-146), is presented by Shoup [25] and can be used to solve simultaneous differential equations of higher order n which can be broken down into n first-order equations. Thus, for the second-order differential equation of motion of Eq. (79), page 73, with \vec{a}_{pert} and \vec{a}_g as given in Eqs. (83) and (82), we have the functional relationship

$$\frac{d^2 \vec{r}}{dt^2} = \vec{a}_g + \vec{a}_d + \vec{a}_{th} = \vec{G}(t, \vec{r}, \vec{v}) \quad (87)$$

Then, since

$$\vec{v} = \frac{d\vec{r}}{dt} \quad (88)$$

⁶Truncation and round-off errors can become significant, however, if the step size chosen is too small. Computational speed also decreases dramatically as the step size decreases.

we have

$$\frac{d\vec{v}}{dt} = \frac{d^2\vec{r}}{dt^2} \quad (89)$$

Thus, two first-order equations can be written having the functional form

$$\frac{d\vec{v}}{dt} = \vec{G}(t, \vec{r}, \vec{v}) \quad \text{and} \quad \frac{d\vec{r}}{dt} = \vec{F}(t, \vec{r}, \vec{v}) \quad (90)$$

where in this case

$$\vec{F}(t, \vec{r}, \vec{v}) = \vec{v} \quad (91)$$

The Runge-Kutta formulas for position and velocity of a vehicle in its orbit are then given by

$$\vec{r}_{n+1} = \vec{r}_n + \vec{K} \quad (92)$$

$$\vec{v}_{n+1} = \vec{v}_n + \vec{L} \quad (93)$$

where $n = 0, 1, 2, 3, \dots$ and

$$\vec{K} = \frac{(\vec{K}_1 + 2\vec{K}_2 + 2\vec{K}_3 + \vec{K}_4)}{6} \quad (94)$$

$$\vec{L} = \frac{(\vec{L}_1 + 2\vec{L}_2 + 2\vec{L}_3 + \vec{L}_4)}{6} \quad (95)$$

In Eqs. (94) and (95), \vec{K}_1 through \vec{K}_4 and \vec{L}_1 through \vec{L}_4 represent the four stages of calculation for intermediate points needed to find the value of the next point from the current point and are given by the following equations, where \vec{r}_n and \vec{v}_n are the current position and velocity vectors at time t_n to be used to find \vec{r}_{n+1} and \vec{v}_{n+1} at time t_{n+1} , \vec{r}_{s_i} and \vec{v}_{s_i} are the intermediate position and velocity vectors to be used in calculations for the i th stage, and the step size $h = t_{n+1} - t_n$:

$$\vec{K}_1 = h\vec{F}(t_n, \vec{r}_n, \vec{v}_n) = h\vec{v}_n \quad (96)$$

$$\vec{L}_1 = h\vec{G}(t_n, \vec{r}_n, \vec{v}_n) = h[\vec{a}_g(\vec{r}_n) + \vec{a}_d(t_n, \vec{r}_n, \vec{v}_n) + \vec{a}_{th}(t_n)] \quad (97)$$

$$\vec{r}_{s_2} = \vec{r}_n + .5\vec{K}_1 \quad \vec{v}_{s_2} = \vec{v}_n + .5\vec{L}_1 \quad (98)$$

$$\vec{K}_2 = h\vec{F}(t_n + .5h, \vec{r}_{s_2}, \vec{v}_{s_2}) = h\vec{v}_{s_2} \quad (99)$$

$$\vec{L}_2 = h\vec{G}(t_n + .5h, \vec{r}_{s_2}, \vec{v}_{s_2}) = h[\vec{a}_g(\vec{r}_{s_2}) + \vec{a}_d(t_n + .5h, \vec{r}_{s_2}, \vec{v}_{s_2}) + \vec{a}_{th}(t_n + .5h)] \quad (100)$$

$$\vec{r}_{s_2} = \vec{r}_n + .5\vec{K}_2 \quad \vec{v}_{s_2} = \vec{v}_n + .5\vec{L}_2 \quad (101)$$

$$\vec{K}_3 = h\vec{F}(t_n + .5h, \vec{r}_{s_2}, \vec{v}_{s_2}) = h\vec{v}_{s_2} \quad (102)$$

$$\vec{L}_3 = h\vec{G}(t_n + .5h, \vec{r}_{s_2}, \vec{v}_{s_2}) = h[\vec{a}_g(\vec{r}_{s_2}) + \vec{a}_d(t_n + .5h, \vec{r}_{s_2}, \vec{v}_{s_2}) + \vec{a}_{th}(t_n + .5h)] \quad (103)$$

$$\vec{r}_{s_4} = \vec{r}_n + .5\vec{K}_3 \quad \vec{v}_{s_4} = \vec{v}_n + .5\vec{L}_3 \quad (104)$$

$$\vec{K}_4 = h\vec{F}(t_n + h, \vec{r}_{s_4}, \vec{v}_{s_4}) = h\vec{v}_{s_4} \quad (105)$$

$$\vec{L}_4 = h\vec{G}(t_n + h, \vec{r}_{s_4}, \vec{v}_{s_4}) = h[\vec{a}_g(\vec{r}_{s_4}) + \vec{a}_d(t_n + h, \vec{r}_{s_4}, \vec{v}_{s_4}) + \vec{a}_{th}(t_n + h)] \quad (106)$$

Thus, for example, to find a position \vec{r}_1 and velocity \vec{v}_1 at time t_1 from a position \vec{r}_0 and velocity \vec{v}_0 at time t_0 :

- 1) evaluate (96) through (106) in order, with the initial conditions

$$\begin{aligned} t_n &= t_0 & t_{n+1} &= t_1 & h &= t_1 - t_0 \\ \vec{r}_n &= \vec{r}_0 & \vec{v}_n &= \vec{v}_0 \end{aligned}$$

- 2) substitute the values obtained for \vec{K}_1 through \vec{K}_4 and \vec{L}_1 through \vec{L}_4 into Eqs. (94) and (95),
- 3) and finally, substitute the values obtained for \vec{K} and \vec{L} into Eqs. (92) and (93) and solve for the position and velocity vectors at time t_{n+1} given by

$$\vec{r}_{n+1} = \vec{r}_1 = \vec{r}_0 + \vec{K} \quad (107)$$

$$\vec{v}_{n+1} = \vec{v}_1 = \vec{v}_0 + \vec{L} \quad (108)$$

It should be kept in mind that the entire integration process just described must be carried out three times in scalar form for each time step, since in actuality three second-order scalar differential equations, one for each vector component as shown in Eqs. (81), must be successively integrated. Furthermore, computations for \vec{a}_g , \vec{a}_d , and \vec{a}_{th} must be carried out for each stage of the integration, as will be discussed in the sections that follow. This can obviously lead to a massive computational effort for the relatively small time steps required to achieve acceptable accuracy over a long run. For instance, even if an integration time step of 1 sec is used

to calculate position and velocity vectors for a point on a trajectory 600 sec in the future, the integration process described must be repeated 1800 times! For a two-body motion trajectory, the same information can be obtained in one pass of EVADER's astrodynamic algorithms. This makes clear the superiority of using one-pass astrodynamic algorithms to calculate trajectory points hundreds of seconds in the future, especially if the effects of drag, higher order gravitational harmonics, and an impulsive velocity change assumption are negligible.

3.4.4 The Gravity Model

In the case of uniform gravitational attraction between two masses m_1 and m_2 , the acceleration due to gravity is given by Eq. (82) on page 73 where

$$\mu = G(m_1 + m_2) \quad (109)$$

and G is the gravitational constant of gravity. For a satellite with mass m_s orbiting the Earth with mass m_E , where $m_s \ll m_E$, Eq. (109) then becomes

$$\mu \approx Gm_E = 3.981 \times 10^5 \text{ km}^3/\text{sec}^2 \quad (110)$$

This is the value used for Earth's gravitational constant in calculations performed with EVADER's astrodynamic techniques. It is also used to calculate gravity for the integration methods when the non-uniform gravity model is turned 'off' by the operator at the start of a run.

For a non-uniform gravity model, which takes into account anomalies in the Earth's gravitational field due to the Earth's oblateness, μ is a function of position \vec{r} . The Earth's oblateness can be modelled in terms of zonal harmonic perturbations. The most significant term in this model is the second zonal harmonic, referred to as the J_2 perturbation. The J_2 term, as well as the less significant higher harmonics, are empirically obtained through the observation of satellite orbits over time.

A number of analytical solutions have been proposed to take into account anomalies in the Earth's gravitational field in the formulation of orbital equations of motion. For instance, Jezewski [12] presents an analytical solution to the J_2 perturbed

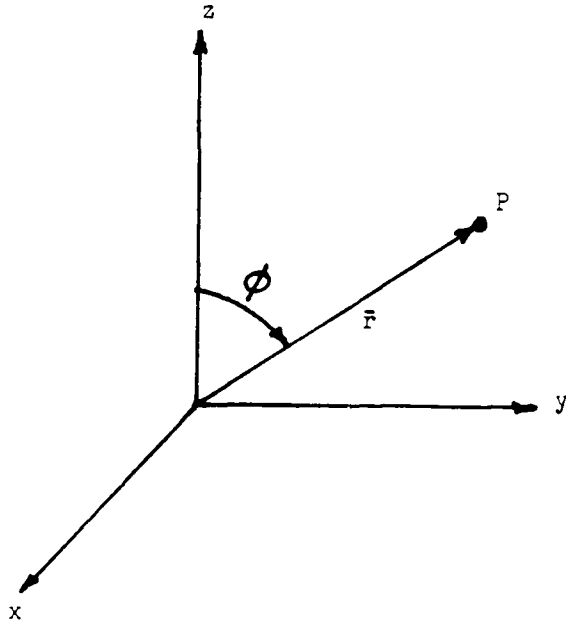


Figure 4: Axisymmetric Gravity as a Function of Position

two-body problem expressed in terms of the true anomaly of a satellite's orbit. He also presents a solution [11] for a J_2 perturbed equatorial orbit in terms of elliptic integrals and functions.

The approach implemented in EVADER's subroutine GRAVITY (ref. Appendix A, pp. 146-147) is presented by Battin [4] and models the gravitational potential of a point external to a body based on a series expansion of Legendre polynomials. In this model, the external potential at a point P is only a function of the magnitude of the radius vector from the center of the body to the satellite and the angle ϕ between \vec{r} and the z -, or polar, axis as shown in Figure 4. This assumes an axially symmetric distribution of mass for the body, an assumption that for practical applications is valid for most bodies in the solar system, including the Earth [4].

For the axisymmetric gravitational model, with r_{eq} , J_k , and P_k denoting respectively Earth's equatorial radius, zonal harmonic terms, and Legendre polynomials, the external potential function is given by

$$V(r, \phi) = \frac{Gm_E}{r} \left[1 - \sum_{k=2}^{\infty} J_k \left(\frac{r_{eq}}{r} \right)^k P_k(\cos \phi) \right] \quad (111)$$

where the values of J_2 through J_6 ($\times 10^6$) for the Earth are

$$\begin{aligned} J_2 &= 1082.28 \pm 0.03 \\ J_3 &= -2.3 \pm 0.2 & J_5 &= -0.2 \pm 0.1 \\ J_4 &= -2.12 \pm 0.05 & J_6 &= 1.0 \pm 0.8 \end{aligned}$$

The Legendre polynomials P_k can be generated by Rodrigues' formula, which is

$$P_k(\nu) = \frac{1}{2^k k!} \frac{d^k}{d\nu^k} (\nu^2 - 1)^k \quad (112)$$

Legendre polynomials through P_6 as used in EVADER and generated by Rodrigues' formula are

$$\begin{aligned} P_2(\nu) &= \frac{1}{3}(3\nu^2 - 1) \\ P_3(\nu) &= \frac{1}{2}(5\nu^3 - 3\nu) \\ P_4(\nu) &= \frac{1}{8}(35\nu^4 - 30\nu^2 + 3) \\ P_5(\nu) &= \frac{1}{8}(63\nu^5 - 70\nu^3 + 15\nu) \\ P_6(\nu) &= \frac{1}{16}(231\nu^6 - 315\nu^4 + 105\nu^2 - 5) \end{aligned} \quad (113)$$

where in the case at hand, ν is given by

$$\nu = \cos \phi \quad (114)$$

The method used to implement the axisymmetric perturbed gravity model proceeds as follows:

- 1) When given the position $\vec{r} = r_x \hat{i}_x + r_y \hat{i}_y + r_z \hat{i}_z$ of a point occupied in space by a vehicle in its trajectory, calculate

$$\cos \phi = \frac{\vec{r} \cdot \hat{i}_z}{r} = \frac{r_z}{r} \quad (115)$$

- 2) Substitute $\cos \phi$ for ν in Eqs. (113) to obtain values for P_2 through P_6 .
- 3) Then, calculate the sum in Eq. (111) and a value for $V(r, \phi)$.
- 4) Finally, the value of μ to be used in calculations for the point is given by

$$\mu = rV \quad (116)$$

In this way, a new value for μ is calculated at each stage of the numerical integration routine for each vehicle. Thus, gravitational perturbations due to the Earth's oblateness through the J_6 zonal harmonic term are taken into account by the numerical integration routines for an Earth assumed to have an axially symmetric mass distribution.

3.4.5 The Drag Model

Since the astrodynamics techniques used in EVADER ignore the effects of atmospheric drag, drag calculations were included in the numerically updated current trajectories to demonstrate that this assumption would not introduce any significant errors in calculations for satellites in low-Earth orbit. Therefore, at each stage of the integration routine in subroutine RUNKUT (ref. Sec. 3.4.3), subroutine DRAG (ref. Appendix A, pp. 147-149) is called to make drag calculations for the appropriate vehicle at that point in its trajectory.

Since all satellites in low-Earth orbit operate primarily above an altitude of 100 km (ref. Sec. 2.1), a lower altitude limit of 100 km was chosen for the drag model. Thus, only density values for regions above 100 km are included in the model. In the future, however, if it was desired to explore the limits of acceptable accuracy of EVADER in regions below 100 km, where drag and possibly lift would become increasingly significant, density values for lower altitudes could simply be added to the those already included in the density values table of subroutine DRAG. In this paper, only conventional intercept scenarios occurring above 100 km will be considered.

The acceleration of the vehicle due to the force of drag, which operates in a direction opposite to the velocity vector \vec{v} , is given by

$$\vec{a}_d = \frac{1}{2} \rho v^2 \frac{C_D A}{m} \left(-\frac{\vec{v}}{v} \right) \quad (117)$$

where: ρ = atmospheric density

C_D = drag coefficient

A = reference area

m = total vehicle mass

At high altitudes, atmospheric constituents are subject to change due to a number of factors, such as solar activity, seasonal changes, and molecular ionization. For these reasons, density at these altitudes is difficult to predict reliably through theoretical means. Because of this, the density of the atmosphere at high altitudes has been traditionally determined through the observation of satellite orbits.[38] To do this, however, a value for the coefficient of drag for the satellite has to be assumed.

In space, where the density above 100 km is 5×10^{-7} kg/m³ or less, Newtonian flow can be assumed for purposes of illustration. In Newtonian flow, the drag force is determined solely by the momentum transfer of individual gas particles impinging on a surface as it moves through the gas. Then, C_D is merely a function of the geometry of the surface facing the flow and its frontal cross-sectional area. It can be shown analytically that for a flat plate in Newtonian flow, $C_D = 4$, while for a cylinder in Newtonian flow, $C_D = \frac{8}{3} \approx 2.67$. Although C_D for a satellite could be expected to be of the same order of magnitude as the C_D values given theoretically for the flat plate and cylinder, a realistic value for a geometrically complex satellite is more difficult to obtain. Furthermore, because of unpredictable changes in the upper atmosphere, ideal Newtonian flow can not necessarily be assumed for practical applications. However, as stated in the *1966 Supplement to the 1962 U.S. Standard Atmosphere* [38], density calculations have been done for satellites assuming a generally accepted, constant satellite drag coefficient of 2.2. It is also stated that this value of C_D is nearly independent of height between altitudes of 140-600 km, and depending on

solar activity, C_D increases only slightly to an asymptotic value of 2.6-2.7 at an altitude of 800 km at times of low solar activity. Furthermore, the likely error in the values assumed for C_D is estimated at between 15 and 30 percent. Therefore, for purposes of a realistic simulation in EVADER, a constant value of $C_D = 2.2$ was assumed for all drag calculations.

The atmospheric density values used in the calculations for each vehicle's current trajectory integrations were interpolated from a table of values selected from the 1976 U.S. Standard Atmosphere tables [37]. Specifically, ρ values between 100 and 1,000 km at 50 km intervals as selected from the Standard Atmosphere were used to determine the appropriate interpolated ρ value to be used for the current altitude of the vehicle. For example, the current ρ value at an altitude of 325 km, say, would be given by

$$\rho_{325} = \rho_{table_{300}} + \frac{325-300}{350-300}(\rho_{table_{350}} - \rho_{table_{300}}) \quad (118)$$

Reference density values used ranged from $5.604 \times 10^{-7} \text{ kg/m}^3$ at 100 km to $3.561 \times 10^{-15} \text{ kg/m}^3$ at 1,000 km. Above 1,000 km, the density was assumed to be zero. As is shown in Eq. (117), the deceleration of a vehicle due to drag is dependent on such vehicle parameters as mass m and reference area A , taken to be the frontal cross-sectional area in this case. For the interceptor, m remains constant for all drag calculations, since no propulsion system is modelled for it. In the case of the target, however, m can decrease during an engine burn, thereby increasing the deceleration of the target due to drag as propellant mass is used. In fact, the total mass figure to be used in drag calculations during integration time steps when the engine is thrusting is actually calculated in the THRUST subroutine. This will be discussed further in Sec. 3.4.6, however.

Values to be used for m and A for the interceptor, and A and the initial mass of the target are supplied in one of two ways: the operator can input new values at the outset of a run, or default values can be used. To establish default vehicle parameters, a baseline configuration for both the interceptor and the target had to be adopted. The vehicle configurations, and their resulting physical parameters will

be discussed later in Sec. 3.4.7.

3.4.6 The Spacecraft Thrust Model

As discussed in Sec. 3.3.1, the velocity-to-be-gained \vec{v}_{ibg} to perform a selected evasive maneuver is calculated through astrodynamic methods. This assumes that the recommended \vec{v}_{ibg} can be applied impulsively. For small velocity increments, this is a valid enough assumption. However, for larger \vec{v}_{ibg} requirements, which would require a longer engine burn, the impulsive velocity addition assumption may not be acceptable. Thus, to demonstrate that no significant targeting error would be introduced by using impulsive \vec{v}_{ibg} calculations to control an engine burn, and to determine how closely a Lambert \vec{v}_{ibg} calculation would agree with Δv calculations based on propellant usage in an integrated engine burn, a spacecraft thrust model was developed and implemented in subroutine THRUST (ref. Appendix A, pp. 149-151).

During an engine burn, the acceleration \vec{a}_{th} due to engine thrust as shown in Eq. (83), p. 74, must be updated at the beginning of each integration step so that the acceleration of the vehicle due to thrust to be used at the beginning of the next integration time step will reflect the loss of propellant mass due to the last time step and any changes in thrust level or direction required at the beginning of the next time step. Thus, \vec{a}_{th} at the beginning of an integration time step is given by

$$\vec{a}_{th} = \frac{T_{curr}}{m_{prev} - \dot{m}_{prev} t_{ts}} \hat{i}_{th} \quad (119)$$

where m_{prev} is the initial mass of the vehicle including propellant at the beginning of the previous time step, and \dot{m}_{prev} and t_{ts} are respectively the mass flow rate used for the previous time step and the constant time step of integration being used for the engine burn. The unit vector \hat{i}_{th} and T_{curr} , are respectively the direction and magnitude of the thrust vector to be used at the beginning of the current time step, since \vec{a}_{th} is being calculated to supply an initial value for the next time interval. Thus, the magnitude and direction of the thrust level can be changed at

the beginning of a time step during an engine burn, and the current total mass of the vehicle is

$$m_{curr} = m_{prev} - \dot{m}_{prev} t_s \quad (120)$$

The value for the current mass of the vehicle as calculated in Eq. (120) is also supplied to subroutine DRAG at the beginning of each integration stage so that drag acceleration calculations will also reflect a change in vehicle mass (ref. Sec. 3.4.5).

For simplicity, and since a smaller time step could be used to integrate trajectory points during an engine burn than was needed for trajectory updates when the engine was off (ref. Secs. 3.4.2 and 3.4.3), a method of guidance was used which aligned the thrust vector with the direction of \vec{v}_{ibg} , which was updated with the Lambert algorithm at the beginning of each integration time step. Thus, it was felt that the added complexity of cross-product steering, say, where the direction of the thrust vector is determined by requiring

$$\frac{d\vec{v}_{ibg}}{dt} \times \vec{v}_{ibg} = \vec{0} \quad (121)$$

was not needed, since the Lambert algorithm was already available to calculate a new \vec{v}_{ibg} at the beginning of every time step, thereby updating the magnitude and direction of the \vec{v}_{ibg} vector needed to achieve the desired aim-point. In this way, accurate targeting for the aim-point could be assured. Even though cross-product steering drives all three components of the \vec{v}_{ibg} vector to zero simultaneously, and is therefore more efficient than aligning \vec{a}_{th} along \vec{v}_{ibg} , the guidance method chosen is optimum for a case where gravity is constant, although gravity is not constant in EVADER. Even so, as mentioned previously the efficiency of the guidance algorithm chosen could be judged by how well Δv calculations based on propellant usage would compare to the magnitude of the total impulsive Δv as calculated by the Lambert algorithm at the initiation of an evasive maneuver. This will be discussed further in Sec. 4.

By choosing a value for the engine thrust T_{curr} and assuming a constant vacuum

specific impulse I_{sp} for the engine, the flow rate \dot{m}_{curr} to be used for the calculation of thrust acceleration following the next integration time step can be determined as

$$\dot{m}_{curr} = \frac{T_{curr}}{g_0 I_{sp}} \quad (122)$$

where $g_0 = 9.81 \text{ m/sec}^2$ and is a reference value for the acceleration of gravity at sea level. Thus, the magnitude of \vec{a}_{th} , and therefore the total Δv to be supplied during the next time step, is controlled by selecting a desired level of thrust. This assumes the engines are throttleable and provides a convenient means of driving the \vec{v}_{ibg} vector to zero and controlling engine cutoff without overshoot or undershoot.

By using a relationship known as the *rocket equation*, the total Δv to be delivered by the engine during the next integration time step can be calculated based on mass flow considerations as

$$\Delta v = g_0 I_{sp} \ln \left(\frac{m_{curr}}{m_{curr} - \dot{m}_{curr} t_{ts}} \right) \quad (123)$$

Thus, the magnitude of the updated \vec{v}_{ibg} vector as calculated at the beginning of each time step by the Lambert algorithm can be compared to the Δv figure from the rocket equation. If it is found that $\Delta v \leq v_{ibg}$, the engine burn over the next time step can go ahead as scheduled at the chosen thrust level. If it is found, however, that $\Delta v > v_{ibg}$, the thrust level to be used for the next time must be reduced appropriately so that overshoot does not occur and v_{ibg} is driven to zero, at which point engine cut-off occurs. The thrust level required to supply a $\Delta v = v_{ibg}$ can be found by combining the rocket equation with Eq. (122). Thus, setting $\Delta v = v_{ibg}$ in the rocket equation and solving for \dot{m}_{curr} yields

$$\dot{m}_{curr} = \frac{m_{curr}}{t_{ts}} \left[1 - \exp \left(-\frac{v_{ibg}}{g_0 I_{sp}} \right) \right] \quad (124)$$

Also, from Eq. (122) we have

$$T_{curr} = g_0 I_{sp} \dot{m}_{curr} \quad (125)$$

Substituting Eq. (124) into Eq. (125) then gives the appropriate level of thrust to be used during the next integration step to drive v_{ibg} to zero as

$$T_{curr} = g_0 I_{sp} \frac{m_{curr}}{t_{ts}} \left[1 - \exp \left(-\frac{v_{ibg}}{g_0 I_{sp}} \right) \right] \quad (126)$$

This method of driving v_{ibj} to zero, which was also used by Stuart [26] in the simulations for his targeting technique (ref. Sec. 2.4), worked quite well. In fact, as will be discussed further in Sec. 4, it was found that of all sources of error in EVADER, not driving v_{ibj} to exactly zero would result in the largest errors in achieving the predicted aim-point. Also, this method of controlling thrust and engine cut-off allowed the target's engine to operate at a selected or maximum level of thrust throughout the entire engine burn, with the exception of the last time step.

Other calculations of interest based on fuel usage and the rocket equation were also made and displayed as output to the operator during an engine burn. To present these relations it is first necessary to describe the way in which total available fuel was determined. Based on the physical configuration of the target vehicle, which will be discussed fully in Sec. 3.4.7, a value for fuel mass fraction M_{Ff} , which is the fraction of the total vehicle mass devoted to fuel, was determined. The THRUST subroutine used M_{Ff} to determine how much of the original vehicle mass was devoted to fuel. In this way, if the operator decided to enter a new total mass figure for the target at the beginning of a simulation, the proportion of the vehicle's mass devoted to fuel was determined by EVADER, since M_{Ff} was considered to be a fixed vehicle design parameter. Thus, with the original vehicle mass denoted by m_0 , the initial mass of fuel available is given by

$$m_{f_i} = M_{Ff} m_0 \quad (127)$$

The total mass of fuel available $m_{f_{avail}}$ at any point during an engine burn is then

$$m_{f_{avail}} = m_{f_{prev}} - \dot{m}_{prev} t_s \quad (128)$$

where $m_{f_{prev}}$ is the mass of fuel that was available at the beginning of the previous time step and is initialized at the beginning of a run to the value of m_{f_i} . The total mass of fuel used so far is then

$$m_{f_{used}} = m_{f_i} - m_{f_{avail}} \quad (129)$$

Total Δv used and available can now be calculated by using Eq. (128) and the rocket equation. Thus, with m_{curr} of Eq. (120) representing the total current mass of the vehicle we have

$$\Delta v_{used} = g_0 I_{sp} \ln \left(\frac{m_0}{m_{curr}} \right) \quad (130)$$

$$\Delta v_{avail} = g_0 I_{sp} \ln \left(\frac{m_{curr}}{m_{curr} - m_{favail}} \right) \quad (131)$$

Burn-time available can also be calculated, based on Eq. (125) and the assumption that future thrusting will occur at the maximum thrust level, as

$$t_{bavail} = \frac{g_0 I_{sp} m_{favail}}{T_{curr}} \quad (132)$$

Thus, if it was found in the THRUST module that the Δv available was insufficient to perform a maneuver or fuel depletion was imminent, a warning could be issued to the operator. Furthermore, for the operator to plan maneuvers and make effective maneuvering decisions, quantitative information on the availability of such resources as Δv , fuel, and remaining burn time is essential.

3.4.7 Vehicle Baseline Configurations

In order to initialize the drag and thrust subroutines, it was necessary to adopt a baseline configuration for the missile and target so that realistic vehicle parameters could be used. As the reader will recall from Secs. 3.4.5 and 3.4.6, only the mass m and cross-sectional area A of each vehicle is needed to initialize drag calculations, while a propulsion system for maneuvering is needed for the target. Furthermore, the missile's mass remains constant, while the target's mass can decrease during an engine burn. Thus, only a total mass and size are needed for the missile model, while a size, initial mass, and propulsion system are needed to fully model the target. In fact, as will be subsequently discussed, the target's propulsion model will largely dictate the size of the target.

For the missile, its configuration was assumed to be similar to the current Soviet ASAT interceptor (ref. Sec. 2.2.1). Thus, the missile's diameter was set at 3 m

and total mass m_M was set at 2,000 kg. The resulting reference area A_M for the missile, as determined by the frontal cross-sectional area, was thus set at $\pi(1.5)^2 \cong 7.07 \text{ m}^2$. This was all that was needed, since only drag and no thrust calculations were required for the missile.

For the target, a propulsion system had to be selected that would be able to provide desired payload and maneuvering capabilities. Then, a reasonable size and mass could be estimated. To select a propulsion system, the following items had to be taken into account:

- 1) Thrust must be sufficient to maneuver with a typical satellite as a payload, and the engine should be preferably man-rated with high reliability.
- 2) The engine must be throttleable and reusable to allow thrust level variation and multiple starts.
- 3) A high vacuum I_{sp} was desired for maximum efficiency and thrust level.
- 4) Sufficient fuel should be available to allow for extended and repeated maneuvers.

Since the above requirements for a spacecraft with maneuvering capability are very much the same as the requirements for NASA's Orbital Transfer Vehicle (OTV), presently under study by various contractors, it was decided to select a propulsion system from among those engine concepts which are being considered for the OTV. Thus, candidate engine concepts were derived from a NASA Conference Publication on the subject entitled, *OTV Propulsion Issues* [6,18,24,28]. A typical payload, or satellite, mass and size was also estimated from this report.

According to the NASA report [18], the current General Dynamics Shuttle/Centaur -G and -G' vehicles have a 15 ft (4.572 m) diameter and are capable of boosting a 10,000 lb (4,536 kg) payload to geosynchronous orbit or an 11,500 lb (5,216 kg) payload to a semisynchronous 12 hr orbit. These stages are designed to be launched from the Space Shuttle's payload bay and can carry such large payloads

as the Tracking and Data Relay Satellite (TDRSS). Thus for EVADER, a satellite payload of 5,000 kg, similar in size to those launched on the Shuttle/Centaur vehicles, is assumed. Furthermore, the target's frontal cross-sectional area A_T was assumed to be 15 m², based on a diameter of 4.37 m, which is slightly less than the diameter of a Shuttle/Centaur vehicle.

The Centaur-G' is powered by a Pratt & Whitney (PW) RL10A-3-3A engine which develops 16,500 lb_f (73,396 N) of thrust and has an I_{sp} of 446.4 sec. The Centaur-G is powered by a PW RL10A-3-3B engine developing 15,000 lb_f (66,723 N) of thrust with an I_{sp} of 440.4 sec. Both engines use LH₂/LO₂ propellant. Although either of these engines could be used for a maneuvering spacecraft, they might prove too large for delicate maneuvers and the use of a single large engine would not provide for backup propulsion in case of main engine failure.

Therefore, to enhance survivability by providing an engine-out capability, smaller, multiple engines will be used. Also, smaller engines can offer higher individual performance and having smaller, multiple engines has only a minor impact on total propulsion system weight [24]. Thus, an advanced, continuously throttleable, man-rated, LH₂/LO₂ fueled engine proposed by Aerojet [24] for the OTV was selected for the spacecraft propulsion model in EVADER. The proposed Aerojet engine will deliver thrust in a range from 200 lb_f (890 N) up to a maximum of 3,000 lb_f (13,345 N). It has a proposed I_{sp} of 483 sec and a mass of 479 lb (217 kg). Thus, if two Aerojet advanced engines were used, the spacecraft's propulsion system would deliver a maximum thrust of 26,690 N (6,000 lb_f). The mass of the two-engine propulsion systems was thus estimated at 500 kg.

Finally, to estimate an initial mass of fuel available, the total initial mass m_0 of the vehicle was first determined by assigning a payload mass fraction M_{Fp} of 0.5 to the vehicle, which was the fraction of the vehicle's mass allocated for the satellite. Then, since a satellite mass of 5,000 kg has been assumed, the total mass of the vehicle can be found from

$$m_0 = \frac{m_{pay}}{M_{Fp}} \quad (133)$$

Thus, with a payload mass of $m_{pay} = 5,000$ kg and $M_{Fp} = 0.5$,

$$m_0 = \frac{5,000 \text{ kg}}{0.5} = 10,000 \text{ kg} \quad (134)$$

Then, since the mass m_{engs} of the engines has been set at 500 kg, and assuming a structural mass fraction M_{Fs} for the vehicle of 0.1, the mass fraction M_{Fe} devoted to the engines, and the structural mass, fuel mass fraction M_{Ff} , and initial mass of fuel available can be found from

$$m_0 = 10,000 \text{ kg} = \frac{m_{engs}}{M_{Fe}} = \frac{m_{struc}}{M_{Fs}} = \frac{m_{fuel}}{M_{Ff}} \quad (135)$$

Thus, we have

$$\begin{aligned} M_{Fe} &= \frac{m_{engs}}{m_0} = \frac{500}{10,000} = 0.05 \\ m_{struc} &= M_{Fs}m_0 = 0.1(10,000) = 1,000 \text{ kg} \\ M_{Ff} &= 1 - (M_{Fp} + M_{Fs} + M_{Fe}) = 1 - 0.65 = 0.35 \\ m_{fuel} &= M_{Ff}m_0 = 0.35(10,000) = 3,500 \text{ kg} \end{aligned} \quad (136)$$

It should be kept in mind that the value of 0.35 found for M_{Ff} in Eq. (136) is also used by the THRUST subroutine to determine the initial mass of fuel available at the beginning of a run if a new total vehicle mass figure is input by the operator. That is, the fraction of any new total spacecraft mass figure available as fuel is simply determined by multiplying 0.35 by the total mass figure input. Furthermore, values for missile mass, target maximum engine thrust, and missile and target cross-sectional area can be input by the operator at the start of a run. Also, as discussed in Sec. 3.4.5, a constant drag coefficient C_D of 2.2 was assumed for both vehicles. Tables 2, 3 and 4 on page 93 list all default vehicle parameters as chosen for both the missile and spacecraft as discussed in this section and Sec. 3.4.5.

	MISSILE	SPACECRAFT
TOTAL MASS (kg)	2,000	10,000 ^a
AREA _{cross-sect} (m ²)	7.07	15.0
C_D	2.2	2.2

^aThe mass of the spacecraft will decrease as propellant is used during an engine burn. See Table 4 for a further breakdown of spacecraft mass.

Table 2: Default Vehicle Parameters for Drag Calculations

NO. OF ENGINES	2
PROPELLANT	LH ₂ /LO ₂
MAXIMUM THRUST (N)	26,690
VACUUM I_{sp} (sec)	483

Table 3: Spacecraft Propulsion System Default Characteristics

	FUEL	PAYLOAD	STRUCTURE	ENGINES
MASS FRACTION	0.35 ^a	0.5	0.1	0.05
MASS ALLOCATED (kg)	3,500	5,000	1,000	500

^aThe fuel mass fraction figure of 0.35 was also used to determine the fraction of any new total mass figure which was available as fuel.

Table 4: Breakdown of Spacecraft Mass

3.4.8 Setting Up an Evasion Scenario

In order to setup an appropriate evasive maneuvering scenario, two vector position fixes over time for the missile and a position and velocity vector for the target had to be input to EVADER. The input of these vectors would thus simulate data EVADER would receive from the spacecraft's sensors (ref. Sec. 3.2.3).

To produce appropriate input vectors, flexible control over the design of realistic target and missile orbits was needed. Furthermore, certain requirements of the orbits had to be met, not the least of which was that a point intercept must occur at some future time in order to invoke EVADER's evasive action routines. A capability to design near-miss orbits, in which case EVADER would only monitor trajectories, was also desired. In addition, the orbital parameters chosen as variables to be set by the operator must be easily understood in terms of relevant requirements and must determine a trajectory uniquely. Finally, it was decided to include the scenario design module in EVADER itself, so that interactive, multiple runs could be conducted without having to manually input new vectors for each scenario, thereby expediting modification and introduction of new scenarios.

The scenario design module written to satisfy the above requirements was given the name SETUP (ref. Appendix A, pp. 164-166). In subroutine SETUP, various orbital mechanics relations, along with calls to the LAMBERT and EXGAUSS subroutines (ref. Secs. 3.2.4 and 3.2.6) already incorporated in EVADER, were used to calculate appropriate vectors based on orbital design parameters input by the operator.

Based on the discussion of ASAT systems in Sec. 2.2 and the methods of intercept they employ, four types of intercept modes were made available for setup:

1) a direct-ascent, non-retrograde intercept

In this mode of attack, the missile is launched directly under the path of the target and in the same orbital direction as the target and attempts an intercept by ascending directly to the altitude of the target. Since an explicit

AD-A170 896

A METHOD FOR GOVERNING SPACECRAFT EVASIVE MANEUVERING
(U) AIR FORCE INST OF TECH WRIGHT-PATTERSON AFB OH
K R KELLER JUN 86 AFIT/CI/NR-86-891

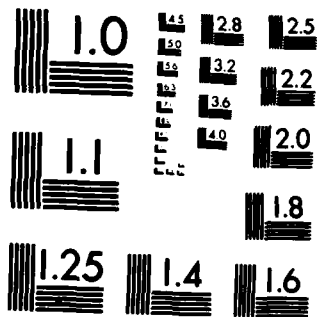
2/3

UNCLASSIFIED

F/G 22/3

NL





MICROCOPY RESOLUTION TEST CHART
NATIONAL BUREAU OF STANDARDS-1963-A

rendezvous is not attempted, the magnitude and direction of the missile's velocity vector is not constrained to that of the target at intercept.

2) a direct-ascent retrograde intercept

This method is similar to that of Item (1), but in this case the missile's orbital direction is opposite to that of the target. Thus, the missile and target velocities add to increase the magnitude of the closing velocity at impact. This is the method of intercept used by the current U.S. ASAT interceptor.

3) a non-retrograde co-orbital injection

In this method, the missile actually rendezvous with the target as if it were performing a two-burn Hohmann transfer, except the second circularizing maneuver is not performed for the missile. Thus, a ballistic trajectory is found which causes the intercept to occur when the missile is at the apogee of its orbit. In this way, the missile's velocity vector is parallel to the target's velocity vector at intercept, since the target is in an initially circular orbit, but does not necessarily have the same magnitude. This method of intercept is essentially the method used by the current Soviet ASAT interceptor, except the rendezvous is completed over a longer time and the interceptor attempts to orbit with the target.

4) a retrograde co-orbital injection

Here, the same general method of intercept as in Item (3) is used, except the missile moves in a trajectory which is opposite to the direction of the target's orbit. Because of this, the vehicles' velocity vectors add to increase the closing velocity as in Item (2).

For all intercept scenarios, the spacecraft orbits about the Earth in a counter-clockwise direction if looking down on the Earth from above the north polar axis. Thus, the spacecraft orbital direction is determined by the 'right-hand rule' with the thumb pointing along the positive direction of the orbit's angular momentum

vector, which can, of course, be inclined from the positive z -axis of the inertial coordinate system used (ref. Sec. 3.2.1).

Intercept scenarios in SETUP were designed with both vehicles initially in the same orbital plane, although this plane could have an inclination anywhere between 0 and 90 degrees, a zero degree inclination being an equatorial orbit, with a polar orbit inclined 90 degrees from the Equator. Only circular initial target orbits were used, to simplify the setup, while the missile orbit could be of any eccentricity. The assumptions just stated were only used to make the setup of scenarios straightforward, and were not in any way innate restrictions of the astrodynamics techniques used in EVADER. In fact, as discussed in Sec. 3.3.1, the same astrodynamics techniques are used to plan and perform out-of-plane, non-circular orbital maneuvers for the spacecraft once EVADER's execution is under way.

Generally, the same techniques used to setup intercept trajectories were also used to setup trajectories for cases where a non-zero miss-distance was desired, except the target was moved back in its circular orbit sufficiently so the desired straight-line miss-distance was achieved.

For direct intercept scenarios, values for seven orbital parameter variables could be selected by the operator when designing an intercept. These variables, with their names as used in EVADER shown first, are discussed in the following list: (ref. Secs. 3.2.1 and 3.2.2 for the following discussion)

- 1) $TALT1$ (h_{T1alt}) - the target altitude in kilometers at its position \vec{r}_{T1} at time t_1 . The target was assumed to be in a circular orbit at this altitude.
- 2) $MALT1$ (h_{M1alt}) - the missile altitude in kilometers at its position \vec{r}_{M1} at time t_1 .
- 3) $TN2$ (θ_{T2}) - the angle in degrees from the line of nodes to the position of the target \vec{r}_{T2} in orbit at the intercept time t_2 . The longitude of the ascending node Ω was assumed to be zero so that the line of nodes of the vehicles' orbits was aligned with the inertial x -axis. As shown in Fig. 1, p. 46, the

line of nodes is the line of intersection of the plane of the vehicle's orbit and the plane of the Equator. Thus, the orientation of the vehicles' orbits with respect to the inertial coordinate system was simplified and the orbital plane containing both vehicles could be viewed as rotating around the inertial x -axis for planes of increasing inclination. For example, an intercept with $\theta_{T2} = 90$ degrees would occur when the x -component of position was zero, regardless of the inclination of the orbit.

- 4) *MN1* (θ_{M1}) – the angle in degrees from the line of nodes to the position of the missile in orbit at time t_1 . The discussion in Item (3) concerning the line of nodes applies here as well.
- 5) *FIXTIME* (t_{fix}) – the desired time interval in seconds between missile position fixes at time t_0 and t_1 . The missile position vector \vec{r}_{M1} , and the velocity \vec{v}_{M1} as calculated in subroutine LAMBERT from the two position fixes \vec{r}_{M0} and \vec{r}_{M1} are used by EVADER to predict initial intercept.
- 6) *TRTIME* (t_{tr}) – the transfer time in seconds allowed for the missile to travel along a ballistic trajectory from its position \vec{r}_{M1} at time t_1 to its position \vec{r}_{M2} at the target intercept time t_2 .
- 7) *ORBINCL* (i_{orb}) – the inclination in degrees from the Equator of the plane containing the missile and target.

By choosing θ_{T2} and *MF2* properly, either a retrograde or non-retrograde direct-ascent intercept would result. That is, for $\theta_{M1} > \theta_{T2}$, a retrograde intercept would result, while for $\theta_{T2} > \theta_{M1}$, a non-retrograde intercept would result.

For co-orbital injection scenarios, all orbital parameter variables were the same as for the direct-intercept scenarios, except the desired eccentricity e_M of the missile's orbit, and whether it was to be retrograde or non-retrograde was specified instead of specifying θ_{T1} and h_{M1alt} . Thus, the initial missile altitude and angular

position of missile would be determined in SETUP, with the additional constraint that missile apogee would occur at intercept.

Implementation of the intercept calculations from the inputs to subroutine SETUP begins by calculating the magnitude

$$r_{T1} = h_{T1alt} + r_{Eav} \quad (137)$$

where r_{Eav} is the average radius of the Earth. Then, since the target orbit is circular and both vehicles are moving in the same plane,

$$\begin{aligned} r_T &= r_{T2} = r_{T1} \\ i_{orb} &= i_{Torb} = i_{Morb} = \text{orbital inclination} \end{aligned} \quad (138)$$

Next, calculations based on r_T , θ_{T2} , i , and the transfer time t_{tr} were used to determine position and velocity vectors for the target at time t_1 that were needed as program input.

First, the position of the target in its orbit at time t_2 can be found through geometrical considerations, and with $\Omega = 0$ is given by

$$\vec{r}_{T2} = r_T \cos \theta_{T2} \hat{i}_x + r_T \cos i_{orb} \sin \theta_{T2} \hat{i}_y + r_T \sin i_{orb} \sin \theta_{T2} \hat{i}_z \quad (139)$$

Also, the magnitude of the velocity for the target in its circular orbit is

$$v_T = v_{T2} = v_{T1} = \sqrt{\frac{\mu}{r_T}} \quad (140)$$

where μ is the Earth's gravitational constant. Then, since the constant angular velocity $\dot{\theta}_T$ (in rad/sec) of the target is

$$\dot{\theta}_T = \frac{v_T}{r_T} \quad (141)$$

the transfer angle θ_{tr} for the target from \vec{r}_{T1} to \vec{r}_{T2} would be

$$\theta_{tr} = t_{tr} \left(\frac{v_T}{r_T} \right) \quad (142)$$

The angle (in radians) between the position of the target at time t_1 and the x -axis would then be

$$\theta_{T1} = \theta_{T2} \left(\frac{\pi}{180} \right) - t_{tr} \left(\frac{v_T}{r_T} \right) \quad (143)$$

The position \vec{r}_{T1} of the target at time t_1 is then found in the same manner as for \vec{r}_{T2} by replacing θ_{T2} in Eq. (139) by θ_{T1} , which yields

$$\vec{r}_{T1} = r_T \cos \theta_{T1} \hat{i}_x + r_T \cos i_{orb} \sin \theta_{T1} \hat{i}_y + r_T \sin i_{orb} \sin \theta_{T1} \hat{i}_z \quad (144)$$

Finally, the velocity of the target in its orbit at time t_1 is given for a circular orbit as

$$\vec{v}_{T1} = -v_T \sin \theta_{T1} \hat{i}_x + v_T \cos i_{orb} \cos \theta_{T1} \hat{i}_y + v_T \sin i_{orb} \cos \theta_{T1} \hat{i}_z \quad (145)$$

Thus, as given by Eqs. (144) and (145), the target position and velocity vectors to be input to EVADER for an intercept scenario have been found. Next, two missile position fixes need to be found that will be compatible with the target vectors just calculated and that will result in an intercept as desired.

If a direct-ascent interception is desired, the magnitude of the missile's position vector at time t_1 is first calculated as

$$r_{M1} = h_{M1alt} + r_{Eav} \quad (146)$$

Then, with $\Omega = 0$, the position vector of the missile in its orbit at time t_1 can be found from Eq. (139) by replacing θ_{T2} by θ_{T1} , since Eq. (139) is not limited to use for circular orbits alone. Thus,

$$\vec{r}_{M1} = r_{M1} \cos \theta_{T1} \hat{i}_x + r_{M1} \cos i_{orb} \sin \theta_{T1} \hat{i}_y + r_{M1} \sin i_{orb} \sin \theta_{T1} \hat{i}_z \quad (147)$$

Next, since $\vec{r}_{M2} = \vec{r}_{T2}$ from Eq. (139) at intercept, the Lambert algorithm can be used to determine \vec{v}_{M1} from \vec{r}_{M1} , \vec{r}_{M2} , and the transfer time t_{tr} . Then, with \vec{r}_{M1} and \vec{v}_{M1} known, \vec{r}_{M0} at time t_0 can be determined with the Extended Gauss method with the transfer time used set equal to $-t_{fis}$. This is possible since by using a negative transfer time in Extended Gauss calculations, previous \vec{r} and \vec{v} vectors in an orbit can be determined from present ones. Thus, two position vectors \vec{r}_{M0} and \vec{r}_{M1} over time t_{fis} have been found that will result in a target intercept.

If a co-orbital injection intercept is specified, calculations following Eq. (145) would begin by calculating the semimajor axis a_M of the missile's desired orbit

from the relation

$$a_M = \frac{r_{M2}}{1 + e_M} \quad (148)$$

where $r_{M2} = r_{T2}$ at intercept and e_M is the desired eccentricity of the missile's orbit as supplied by the operator. Eq. (148) was derived by substituting the relation for an orbit's parameter p , given by,

$$p = a(1 - e^2) \quad (149)$$

into the *equation of orbit*, given by

$$r = \frac{p}{1 + e \cos f} \quad (150)$$

with $\cos f = 1$, since intercept will occur at missile apogee for the co-orbital mode when the true anomaly of the missile's orbit is $f = 180$ degrees. Then, from the *vis-viva* integral, the magnitude of the missile's velocity at intercept can be calculated as

$$v_{M2} = \sqrt{\mu \left(\frac{2}{r_{M2}} - \frac{1}{a_M} \right)} \quad (151)$$

Also, since the missile's velocity vector will be parallel to the target's velocity vector \vec{v}_{T2} at intercept, and

$$\vec{v}_{T2} = -v_T \sin \theta_{T2} \hat{i}_z + v_T \cos i_{orb} \cos \theta_{T2} \hat{i}_y + v_T \sin i_{orb} \cos \theta_{T2} \hat{i}_x \quad (152)$$

we can obtain

$$\vec{v}_{M2} = \pm v_{M2} \frac{\vec{v}_{T2}}{v_T} \quad (153)$$

where the (+) sign is used for a non-retrograde intercept and the (-) sign is used for a retrograde intercept. Then, since \vec{r}_{M2} and \vec{v}_{M2} are known, the Extended Gauss routine can be used to find \vec{r}_{M1} and \vec{v}_{M1} with the transfer time set to $-t_{ir}$. The vectors \vec{r}_{M1} and \vec{v}_{M1} can then in turn be used to find \vec{r}_{M0} with the Extended Gauss routine by using a transfer time of $-t_{is}$. Thus, two position vectors \vec{r}_{M0} and \vec{r}_{M1} over time t_{is} have been found to be input to EVADER for a co-orbital injection scenario.

Finally, if a finite miss-distance is desired, the same process is used as for the intercept cases, except new position and velocity vector components are found for the target after \vec{r}_{M0} and \vec{r}_{M1} have been determined for the missile. To do this, the target's initial position is moved back in its orbit so that over the same transfer time-to-intercept as originally selected, the missile will arrive at a position \vec{r}_{T2miss} which is separated from the previously calculated intercept position \vec{r}_{T2} by a straight line miss-distance d_{miss} input by the operator.

Thus, the included angle θ_{miss} between \vec{r}_{T2} and \vec{r}_{T2miss} is calculated from geometrical considerations as

$$\theta_{miss} = 2 \sin \left(\frac{1}{2} \frac{d_{miss}}{r_T} \right) \quad (154)$$

The new angle from the x -axis at time t_1 required for a miss is then

$$\theta_{T1miss} = \theta_{T1} - \theta_{miss} \quad (155)$$

The new position vector \vec{r}_{T1miss} for a miss is then calculated as in Eq. (144) with θ_{T1} replaced by θ_{T1miss} . Finally, the new velocity vector \vec{v}_{T1miss} for a miss is calculated as in Eq. (145) with θ_{T1} replaced by θ_{T1miss} .

4 Results

To demonstrate the capabilities of EVADER and to show how the program performed in view of the assumptions that have been discussed, seven scenarios will be presented in this section. The objectives of each scenario and the conclusions that were reached will be briefly discussed, while trajectory plots for each scenario will be presented for further illustration. Evader's output for each scenario is presented in Appendix B for the reader to refer to for a more complete and numerically specific understanding of each run. The output data included in the appendix is largely self-explanatory, with additional comments pertaining to variable definitions and the role of each program module in the simulation being further explained through comment statements in the program listing of Appendix A. The input variables required to setup a scenario for EVADER have already been discussed in Sec. 3.4.8, and the content of the output has been discussed from a theoretical point of view throughout Sec. 3 for each of the stages of invocation of the program.

Of the seven scenarios to be discussed, each of the first four will illustrate one of the four possible modes of intercept that could be expected, as discussed in Sec. 3.4.8. In these four scenarios, the two primary types of evasive maneuver, an altitude change and a plane change, will be used by the target to evade intercept. As the reader will recall, the evasive options available to the target were explained in Sec. 3.3.1. The fifth scenario will demonstrate the effect drag has on the accuracy of achieving the target's aim-point. The conclusion that was reached concerning the impact of including gravitational perturbations due to zonal harmonics will also be discussed in conjunction with this scenario. The sixth scenario will illustrate the increase in Δv required for the target to perform a particular maneuver if that maneuver is delayed and the separation distance between the spacecraft and missile is allowed to decrease. One of the intercept modes presented in the first four scenarios will be used as a starting point for this illustration. Finally, the seventh scenario to be presented will demonstrate in one run most of the options available

in EVADER, while the target will employ the 'combined' maneuver option in which an altitude change, plane change and movement 'ahead' or 'behind' the intercept point will all be made simultaneously by asking EVADER to target a particular point in three-dimensional space. A general discussion concerning the overall accuracy and usefulness of using astrodynamic techniques to predict intercept and perform maneuvers will also be discussed in conjunction with the presentation of the scenarios. Conclusions concerning this accuracy will be drawn by comparing trajectory points generated with the astrodynamic techniques with points generated through numerical integration where perturbations are included. For all scenarios presented, an integration time step of 1 sec was used to update trajectories, while a 0.1 sec time step was used to integrate engine burns. It was found that these integration steps would provide the required accuracy while limiting the run-time of the simulations to a reasonable length.

All trajectory plots used to illustrate the discussion of the intercept scenarios are presented together at the end of this section. For the coordinate system adopted (ref. Sec. 3.2.1) and the plotting routines used, three planes in inertial space could be plotted, the x - y , x - z , and y - z planes, which are respectively the Equatorial plane, and two perpendicular polar planes. Because the line of nodes of both orbits was assumed to be coincident with the inertial x -axis when setting up scenarios, as discussed in Sec. 3.4.8, orbits in the Equatorial plane could be shown by plotting the x - y plane, while polar orbits with an inclination of 90 degrees could be seen by plotting the x - z plane. For orbits inclined somewhere between zero and 90 degrees, only the projection of the orbits onto the x - y and x - z planes could be plotted, while a y - z plot could show the relative separation of the target and missile if a plane change maneuver was performed by the target.

The first scenario to be discussed is the mode of intercept that is essentially the same as that used by the present Soviet ASAT interceptor (ref. Sec. 2.2.1). This mode is a non-retrograde, co-orbital injection, in which both vehicles move in the same direction and the missile's orbit is tangent to the target's orbit at intercept.

The output data chronicling this scenario is given in Appendix B.1, on pp. 168-177.

Although in actuality, the Soviet interceptor goes through a series of maneuvers in order to rendezvous with its target, in the simulation performed, the missile's trajectory could be viewed as simply the first half of a Hohmann transfer. Thus, the missile's orbit is elliptical with the apogee of the orbit occurring at the target's altitude and position. The trajectories of the missile and target for this mode of intercept are shown in Figure 5, page 115. In this figure, as in all subsequent trajectory plots, lines of constant time, or timelines, are used to connect the points on the target and missile trajectories which occur at the same time. In this way, it is possible to see where each vehicle is with respect to the other as they move in their orbits. Thus, the timelines serve to give the relative position and its direction of change in the plane of the orbits that is plotted.

For an intercept to occur, it is, of course, not sufficient for the trajectories to simply cross, rather both vehicles must cross each other's path at the same point in time. Thus, when the timelines separating the vehicles simultaneously decrease to zero length in all three coordinate planes, an intercept has occurred. In the scenario shown in Figure 5, intercept was setup to occur in a plane inclined 90 degrees to the Equator - that is, in a polar orbit. In fact, five of the seven intercept scenarios run were performed in a polar orbit plane, so that any effects due to gravitational anomalies would be maximized. This is because the gravity model chosen, as explained in Sec. 3.4.4, is axisymmetric and perturbations in gravity are solely a function of the cosine of the angle between the orbital position and the polar axis of the Earth. Thus, in a polar orbit this angle ranges continuously from zero to 90 degrees, while in an equatorial orbit this angle is always 90 degrees so that the cosine of the angle is always zero. In the latter case the gravity model simply reverts to a uniform gravity model.

For the first scenario, the target performed an evasive maneuver designed to place it 2 km above the missile at the predicted intercept time. Thus, an altitude change along the positive direction of the radius vector from Earth-center to the

position of the missile at intercept was performed. A close-up view of the trajectories of both vehicles and their relative separation in the $x-z$ plane, which is the plane in which the maneuver occurred, is shown as Figure 6, page 116. In this figure, the coordinates of both vehicles in inertial space are given at the moment of the predicted intercept. As can be seen from the figure, the 2 km miss-distance requested by the operator was achieved in the manner specified.

It should be noted that in Figure 6, as in all subsequent close-up figures, that the evasive maneuver illustrated is also incorporated in the first larger scale figure of the trajectories, as in Figure 5, and that the scales and output time steps for the data have simply been changed to allow a closer up view on the smaller scale. Thus, in the close-up figures, the scale of one axis is frequently much different than the scale of the other axis in order to accentuate the maneuver under study, although the data being plotted is the same as for the larger scale figures.

It is interesting to note that the timelines plotted with the trajectories can dramatically illustrate the properties of each vehicle's orbit and the way in which each vehicle moves with respect to the other. In Figure 6, for example, the skew of the timelines changes as the target passes the interceptor below it. Thus; it can be seen that the target actually closes with the missile, overtakes it, and proceeds beyond it, since the velocity of the missile in its circular orbit is higher than the velocity of the missile in its elliptical orbit. Furthermore, the fact that the missile is at the apogee of its orbit, and the way in which its velocity decreases to a minimum and then begins to increase, is shown by the decreasing and increasing length of the lines connecting each point on the missile's orbit to the next point in its orbit. Also, as setup at the beginning of the run (ref. Appendix B.1), the predicted intercept point does occur at a 90 degree angle from the line of nodes when the x -component of position is zero. The aim-point of the missile's maneuver has also been achieved, since the timeline separating the vehicles at the predicted intercept time is vertical, as it should be since the aim-point was chosen along the missile's radius vector and $r_{Tz} = r_{Mz} = 0$.

By an inspection of the scenario output in the appendix, the magnitude of the relative separation vector for the current trajectory points at the requested intercept time of 400 sec is 1.9998 km. This value for separation distance was calculated by finding the magnitude of the vector difference between the positions of the missile and target as had been determined through *integrating* the trajectories to the intercept time. Thus, the accuracy of using predictive astrodynamic techniques to plan and perform evasive maneuvers was established! Despite the inclusion of drag, gravitational anomalies, and integrating the entire engine burn, the integrated trajectory in this scenario agrees with astrodynamic predictions to at least the third decimal place in kilometers. This was true for not only the relative vectors, but also for the components of individual position vectors. Furthermore, velocity vector components computed separately by the integration and astrodynamic techniques typically agreed to the fourth decimal place or better.

Thus, the analytical accuracy of the simulations was shown to be useful for targeting and intercept prediction when accuracy on the order of meters is required. It should be noted that for this particular scenario, the initial altitude of the missile was just over 408 km, while intercept was to occur at 900 km altitude. Thus, drag should have been negligible, and was shown to be so. In subsequent scenarios, which will be discussed later, operating at lower altitudes can introduce some small errors due to drag, however. Also, the time between the missile position fixes used by EVADER to establish the missile's orbit was only 1 sec, illustrating that the missile's orbit can be accurately determined very quickly if accurate missile position information is available, and that the missile's trajectory could be updated essentially continuously to account for missile maneuvers.

As concerns the engine burn, it was found that 1.8 sec was required for the vehicle to achieve the necessary velocity-to-be-gained, with 10.0534 kg of fuel needed to deliver 0.004766 km/sec in Δv as computed from the rocket equation and actual fuel expenditures. This value of Δv computed from the integrated engine burn was just 100.25% of the impulsive velocity-to-be-gained of 0.004754 km/sec as computed

at the start of the maneuver with the astrodynamics techniques. Thus, at least for short burns such as this, an impulsive velocity addition would certainly be an adequate assumption if it was not desired to integrate the engine burn.

Finally for this scenario, the final orbital elements calculated for the missile and target reflect the changes that have occurred for the target. The target's orbit is shown to have some slight eccentricity, with $e = 0.0008$, as a result of its altitude change from a circular orbit, while the missile's eccentricity remains at 0.8, as setup at the start of the run. Both vehicles remain in a plane with an inclination of 90 degrees, since a plane change maneuver was not used in this scenario.

The second scenario presented illustrates the mode of intercept known as a retrograde co-orbital injection, where the manner of intercept is similar to the first scenario discussed, except the missile is moving in a trajectory opposite to the direction of motion of the target. The program output for this second scenario is included as Appendix B.2, on pp. 178-187, while plots of the trajectories made from EVADER's output data are shown in Figs. 7 and 8 on pp. 117 and 118.

For this scenario, an altitude change of 2 km was also made as in the first scenario discussed. In fact, the entire discussion for the first scenario also applies to this scenario since the only difference between them is that the missile uses a retrograde orbit to intercept the target. The geometry resulting from a retrograde intercept is quite different than for a non-retrograde scenario, however, and this is clearly illustrated in Figure 8. In that figure, it is evident that the target does not overtake the missile, but would collide head-on if an intercept were successfully achieved. Thus, the closing velocities add, making a retrograde intercept the preferred method for an ASAT missile which destroys its target by impact alone, as in the case of the U.S. ASAT vehicle (ref. Sec. 2.2.2). For instance, in the case of this particular scenario, the combined velocity of the missile and target at intercept would be almost 10.7 km/sec.

As shown in Figure 8, the length of the timelines, and therefore the separation distance between the missile and target, decreases much more rapidly for a retro-

grade intercept than for the intercept as shown in Figure 6. Because of this, the demands on the maneuverability and guidance system of the missile greatly increase, as a result of which any maneuvers by the target become even more effective.

The third scenario to be presented is called a non-retrograde direct-ascent intercept. This mode uses a non-retrograde intercept as discussed in the first scenario, except the direction and velocity of the missile at intercept is not constrained with respect to the orbit of the target. Thus, the interceptor is not required to explicitly rendezvous with the target, but rather intercepts the target in a direct ascent trajectory from launch to impact. A large-scale view of the trajectories for this scenario is shown as Figure 9 on page 119, and the associated program output is presented in Appendix B.3, pp. 188-199.

For the third scenario, the maneuver chosen for the target was a plane change which was performed by requiring the spacecraft to achieve an aim-point which was 5 km from the predicted intercept point and in the positive direction of the angular momentum vector of the target's orbit. The plane change maneuver performed by the target is clearly shown in Figure 10, page 120, where the y -axis of the plot of the y - z plane is shown on a much smaller scale than the z -axis to aid in the illustration of the maneuver. It is interesting to note that in Figure 10 the timeline connecting the trajectories of the missile and target at the altitude of the predicted intercept is parallel to the y -axis, since the plane of the polar orbit is perpendicular to the y -axis and no altitude change has been made with respect to the missile. Because of this, the trajectories as shown in the x - z plane of Figure 9 appear to intersect exactly, when in fact the vehicles are separated by the 5 km miss-distance as shown in Figure 10. This makes clear the three dimensional nature of intercept scenarios and the virtually unlimited combinations of intercept geometry and maneuvering possibilities that could be explored. Figure 11, page 121, looks down on the trajectories as seen from above the x - y plane. In this figure, the 5 km miss-distance is clearly seen at the time of predicted intercept, while following that time, the distance separating the target from the plane of the missile's orbit

continues to increase, since the target is now in a new orbit inclined from its original one.

Since a larger miss-distance of 5 km and an out-of-plane maneuver were required of the target, it would stand to reason that a larger Δv , and therefore a longer duration engine burn, would be required than for the 2 km in-plane maneuver in the first and second scenarios. This was in fact the case, and an engine burn of 4 sec with a Δv expenditure of 0.010502 km/sec was recorded for the plane change maneuver, which is roughly 2.2 times the Δv required for the maneuver of the first two scenarios. Due in part to the longer duration of the engine burn, a slightly larger discrepancy might also be expected in a comparison of the velocity-to-be-gained calculated with the astrodynamic techniques at the outset of the maneuver and the Δv actually expended, as calculated from fuel mass usage. The program output bears this out, with the actual Δv calculated from fuel mass usage being 100.36 % of the impulsive value. This is still a very small discrepancy, however, making any impulsive maneuvering assumptions completely valid.

In the fourth scenario presented, a retrograde direct-ascent scenario is used. This is the same type of intercept mode used by the U.S. ASAT missile (ref. Sec. 2.2.2). As in the third intercept scenario presented, the direct-ascent mode of intercept does not restrict the direction and magnitude of the missile's velocity at intercept, but here, as in the second scenario presented, the missile is moving in a direction opposite to that of the target. The output data for this scenario is included as Appendix B.4, pp. 200-211, and the associated trajectory plots are shown as Figs. 12 and 13, on pp. 122 and 123.

The same maneuver as was used in the third scenario was also used here and the discussion for that scenario applies here as well. In Figure 13, however, the differences in approach geometry at intercept are illustrated, as the rotation of the timelines connecting trajectory points of the missile and target paths show the manner in which the vehicles approach and pass each other. Again, the 5 km miss-distance achieved through a plane change maneuver is clearly shown.

From an examination of the output data for both the third and fourth scenarios, it is seen that the actual value of the miss-distance achieved was 5.0401 km. Thus, an error of 40 m was introduced in some way during the calculations from time zero to the intercept point. The fifth scenario, as presented in Appendix B.5, helps to explain the origin of this discrepancy between the targeted position and the position values calculated through integration. In the fifth scenario, the same setup was used as for the third and fourth scenarios, except the drag model was turned off. It was found in this way that the discrepancy in the miss-distance disappeared in the absence of drag, even though the axisymmetric gravity model was still being used. But in the first and second scenarios, drag seemingly had no effect, while in the third and fourth runs it did. This might be expected, though, since in the latter runs the missile's initial altitude was 110 km, while in the former runs, the missile operated at altitudes greater than 400 km exclusively. Thus, if discrepancies due to drag were being introduced, they would most likely show up in differences in the missile's trajectory values and not the target's, since the target operated at 900 km for the first two runs and at 800 km in the second two. This was in fact found to be the case, and as can be seen by a comparison between the fourth scenario and the fifth, scenarios for which the same setup had been used except drag was turned off in the fifth, the position and velocity vectors were slightly different in each scenario for the missile at the intercept time. Specifically, when drag was used, the magnitude of the velocity vector for the missile at the intercept time decreased from 6.9181 to 6.9171 km/sec and the x and z components of position changed to -0.4493 and 7170.8677 km respectively from 0.0001 and 7171.3150. The y -component of the missile's position remained unchanged from zero, however, whether or not drag was included. This would be expected, since the missile was in a polar orbit in the x - z plane, and any acceleration due to drag would be operating strictly opposite and parallel to the direction of the missile's velocity vector and would therefore have no effect on the y components of position or velocity which are perpendicular to the orbital plane.

Furthermore, since the target's orbit at the higher altitudes did not seem to be perturbed by drag, it might be assumed that any perturbations in the missile's orbit had been introduced early in its orbit while it was still operating at relatively low altitudes. This was verified in a way by the astrodynamic techniques. It was found that at the current time of 100 sec, when the missile was passing 267 km in altitude, the position predicted for the missile already reflected the changes in its orbit that would occur based on calculations made from the vectors of the missile's orbit at the current time of 100 seconds. In fact, the separation distance was already projected to be 5.0400, which was correct to the third decimal place. Although the output in Appendix B.5, pp. 212-221, for this simulation is only given for time steps of 100 sec, other runs were made with the same setup and smaller output time steps which backed up this conclusion and showed that the predicted miss-distance gradually increased to the value shown at 100 seconds. Thus, it was established that for scenarios where operations at low altitudes were performed, drag could have some noticeable effect, while the effect of gravitational perturbations was found to be negligible and undetectable in the simulations that were run.

The sixth scenario is presented to demonstrate the way in which Δv requirements increase for the target to perform a given maneuver if a maneuver is delayed as the target approaches the intercept point. The output for this run is given as Appendix B.6, starting on p. 222. Some of the simpler options available in EVADER were also demonstrated in this scenario, such as the impulsive maneuver option. An equatorial orbit was also used and the gravity model was turned off, since as discussed previously in this section, the gravity model is reduced to a uniform gravity field anyway. Furthermore, the way in which EVADER decrements the transfer time and continues to predict intercept if no action is taken is also demonstrated.

In Figure 14, p. 124, a plot of Δv required for the missile to perform a 2 km altitude change, as in the first two scenarios, versus the separation distance between missile and target is shown. Separation distance was chosen as the independent variable merely to illustrate the urgency of the maneuver and the increasing cost

of maneuvering evasively if the missile is not promptly detected and reacted to. As can be seen from the plot and the data in the appendix, Δv requirements begin to grow exponentially from a low value of 0.004754 km/sec 400 sec before intercept to a high value of .039965 km/sec as intercept becomes imminent. This is more than an 840% increase in Δv required! Furthermore, from the plot it can be seen that an acceleration in the growth of Δv requirements begins to be noticeable when the missile is about 500 km away. This is not necessarily out of the range of long-wave infrared detectors (ref. Sec. 2.3.2), and if a spacecraft was afforded the capability to track threats at long range, its survivability and effective use of propellant would be greatly enhanced.

The seventh and final scenario to be discussed is one in which many of the options available in EVADER are exercised to demonstrate the program's versatility. For this scenario, the output of which is presented in Appendix B.7, pp. 236-248 and two trajectory plots are shown as Figs. 15 and 16 on pp. 125 and 126, the target was setup to operate in a low circular orbit at 300 km altitude similar to a typical Space Shuttle orbit, while the missile was assumed to be detected at an altitude of 105 km, or just as it was breaching the upper atmosphere and presumably entering its post-boost phase. The mode of intercept was chosen to be that of a retrograde direct-ascent missile trajectory, where closing velocities and guidance problems are greatest for the missile, but the effectiveness of intercept by impact is enhanced. The plane in which the scenario was performed was set at 28.5 degrees, which is the latitude of Kennedy Space Center. A transfer time of 125 sec was chosen to minimize the reaction time for the target, even though the operator's responses are assumed to be instantaneous in the simulations. Both the gravity and drag models were used and the initial cross-sectional areas and total masses of the missile and target were changed at the outset of the run. Even though the mass of the target was doubled, its available thrust was only slightly increased to 30,000 Newtons. Thus, a longer engine burn would be expected to accelerate the target and complete a given maneuver. The output step for the engine data was also changed to 5 sec.

To begin the simulation, a predicted miss-distance of 0.01 km was requested so that the 'Extend' maneuver option could be employed. In this option, which was requested and then negated in the scenario after Δv calculations were made, simply extends the magnitude of the miss-distance in the direction of the presently predicted relative position vector to calculate an aim-point. After another data block was run and output, the program again advised that an evasive maneuver was required, at which time the 'Combined' maneuver option was selected. For this option, a maneuver was requested that would place the target at a point in space at the future intercept time that was respectively 4, 3, and 1 km away from the missile in the -H, +R, and -V directions. Thus, a plane change, altitude change, and position change behind the predicted intercept point was targeted and performed simultaneously. The engine was then used to provide thrust to achieve the necessary velocity-to-be-gained.

As can be seen from the data in the appendix, a relative predicted separation distance for the maneuver was predicted to be 5.0990 km, and an actual miss-distance of 5.0992 km was achieved. The impulsive velocity-to-be-gained was calculated at the maneuver's outset as 0.050541 km/sec, and after an engine burn of 42.6 sec, actual Δv expenditure was calculated to be 0.064235 km/sec, which is 127% of the impulsive value. Thus, for a long duration engine burn such as this, an impulsive velocity assumption, at least for judging fuel expenditure, approaches the limits of its usefulness. Finally, by an examination of the orbital elements as calculated for the target at the end of the run, the target's orbit is shown to have some slight eccentricity due to the altitude change, and a plane change of 0.4029 degrees has occurred.

Since only views of three coordinate planes could be plotted for the scenario and the plane of the vehicles' orbits was inclined from the Equator by 28.5 degrees, it was difficult to clearly illustrate the geometry of the three-dimensional intercept by only plotting the projection of the orbits onto a coordinate plane. Even so, it is possible for the reader to gain an understanding of the way in which a miss

would conceivably occur from a plot of the view in the $x-y$ plane for the scenario as shown in Figure 16. From the figure, it appears as if the target passes over the missile at intercept and is slightly skewed in position with respect to the point of closest approach since a plane change, and a movement slightly back from the intercept point along the target's velocity vector, has occurred in conjunction with an altitude change. As in the second and fourth scenarios discussed, the rapid change in the direction of of the timelines and the quickly decreasing and increasing separation distance is illustrated for a retrograde intercept. Thus, the missile has only one chance to achieve intercept, while evasive maneuvers by the target can serve to greatly increase the load on the missile's terminal maneuvering and homing capabilities.

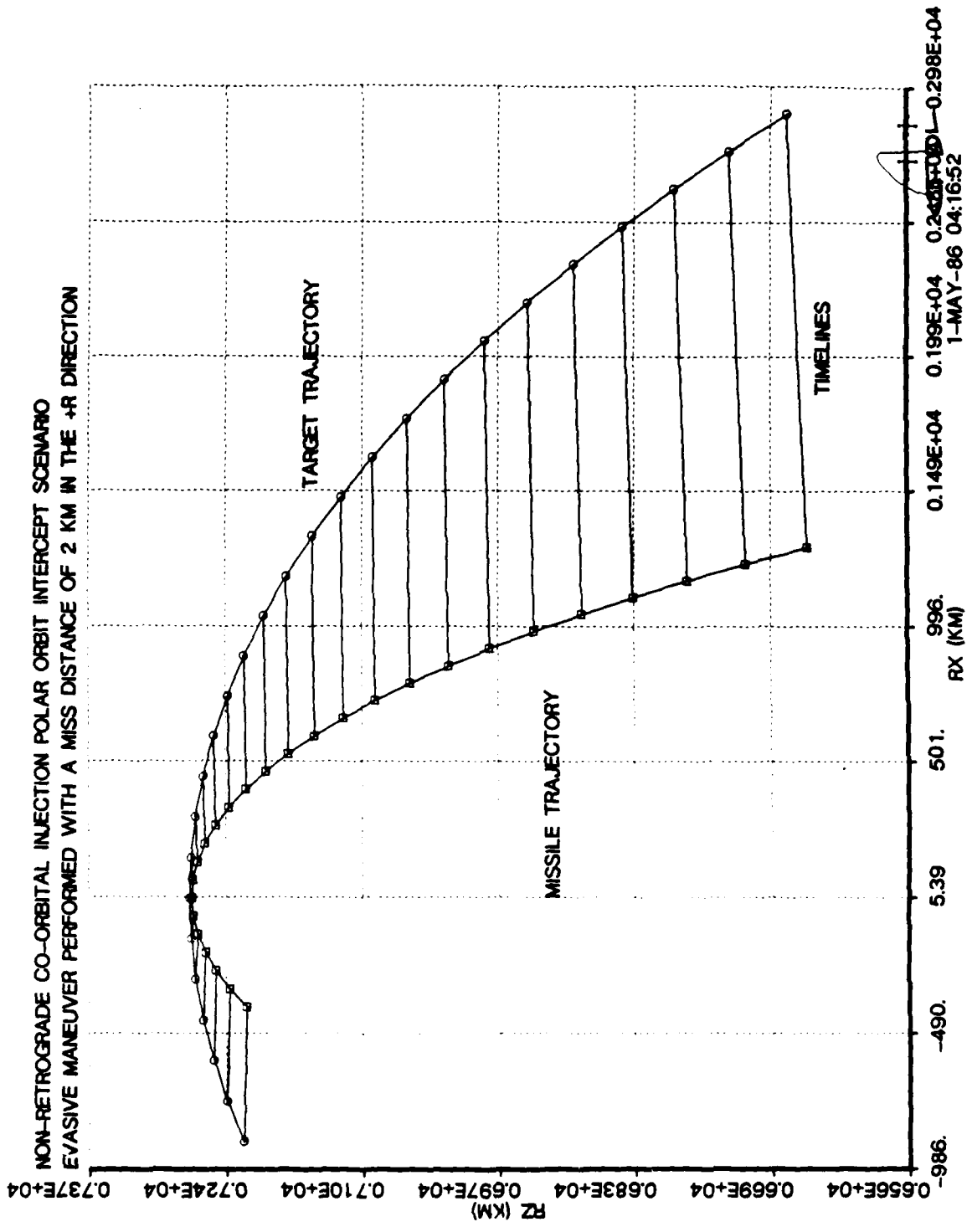


Figure 5: Non-Retrograde Co-Orbital Injection Intercept Scenario

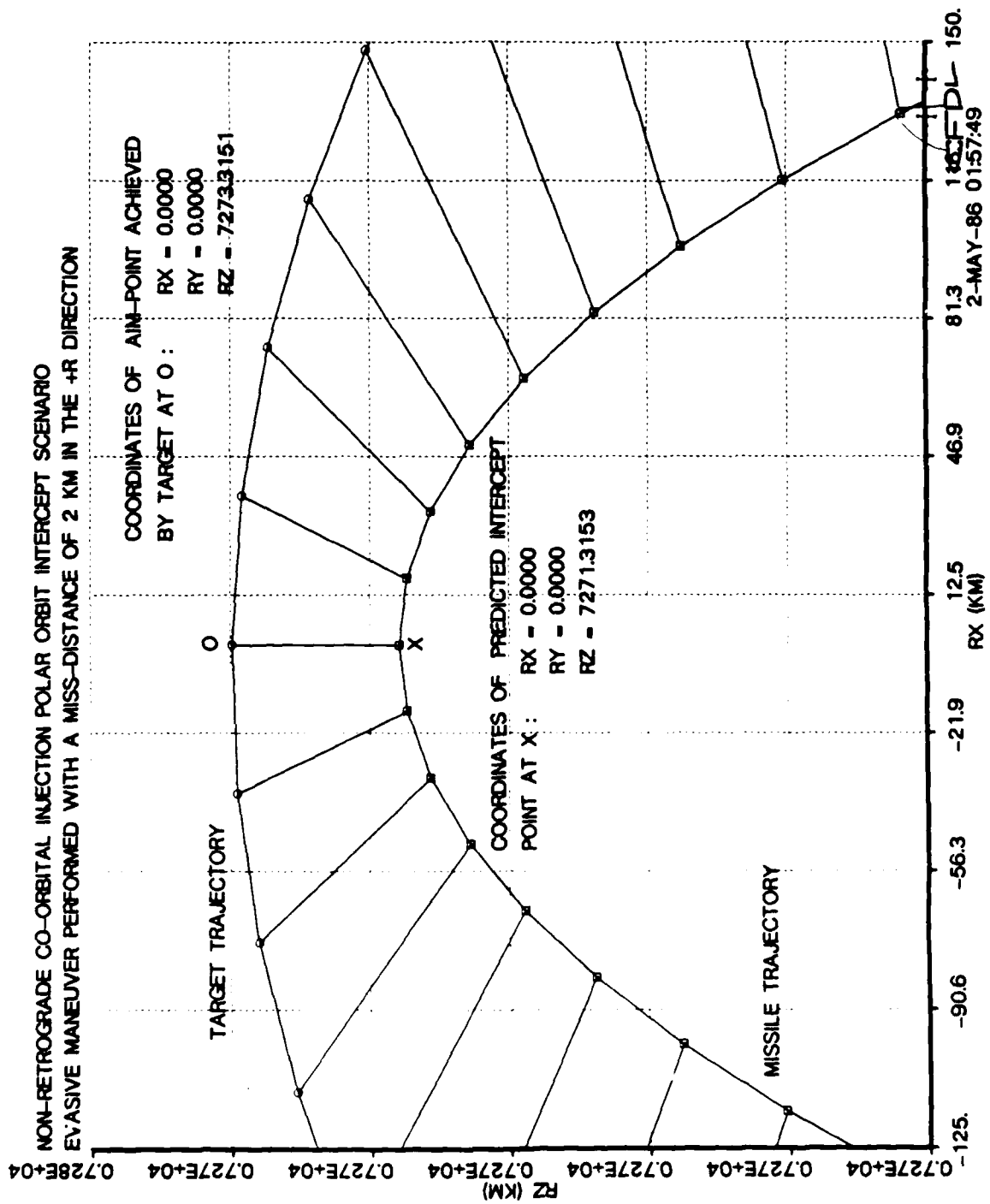


Figure 6: Closeup of Non-Retrograde Co-Orbital Injection Intercept Geometry

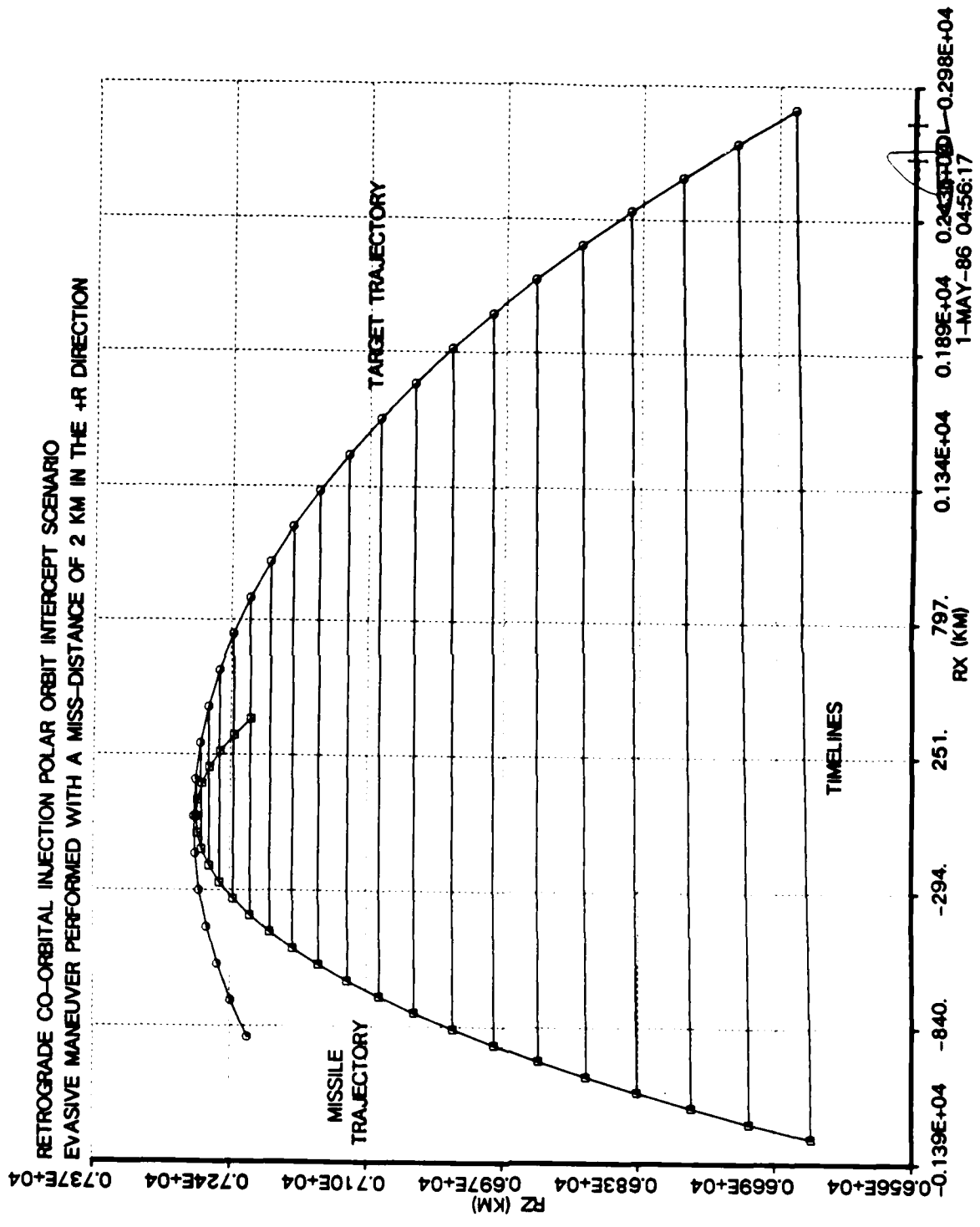


Figure 7: Retrograde Co-Orbital Injection Intercept Scenario

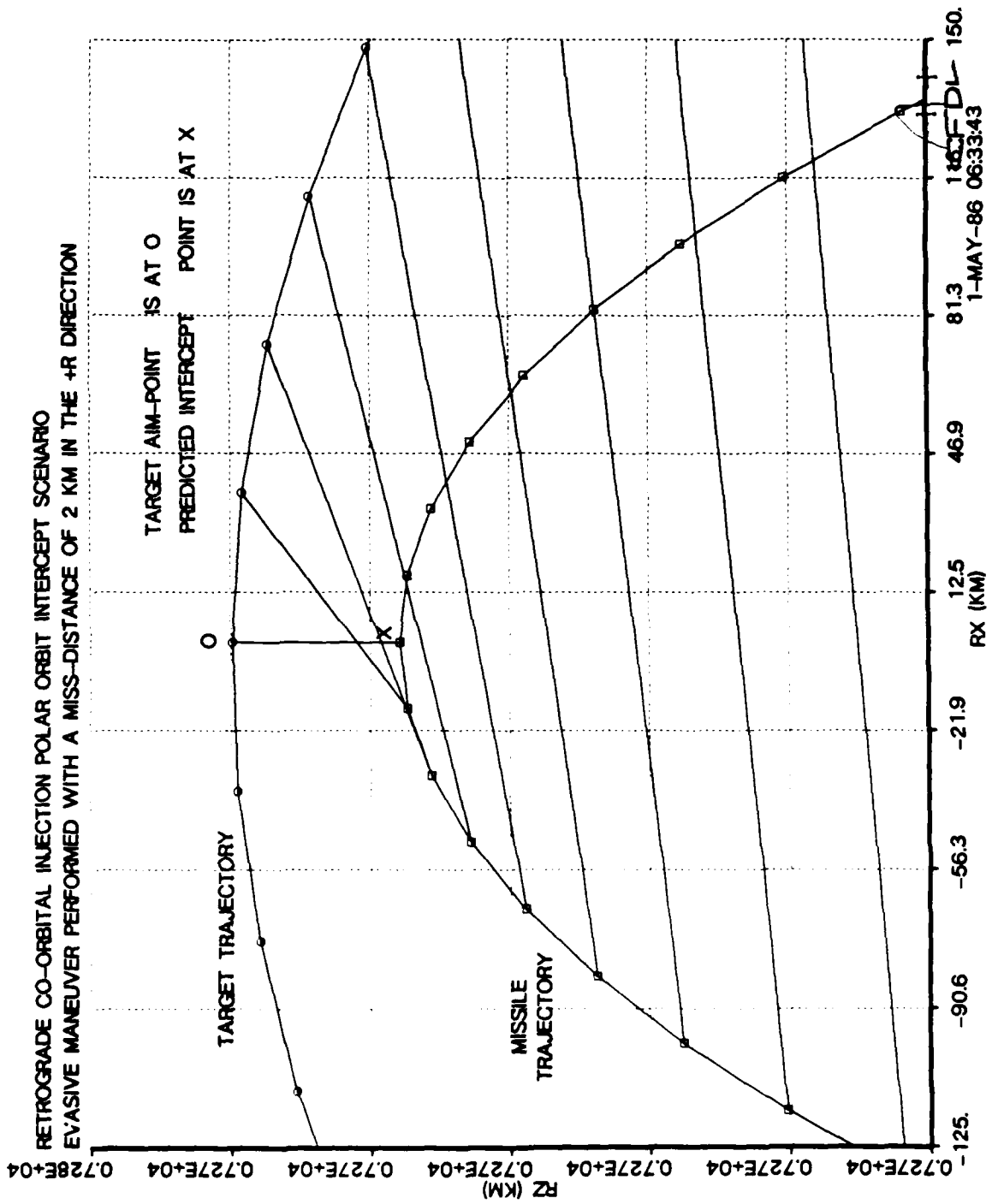


Figure 8: Closeup of Retrograde Co-Orbital Injection Intercept Geometry

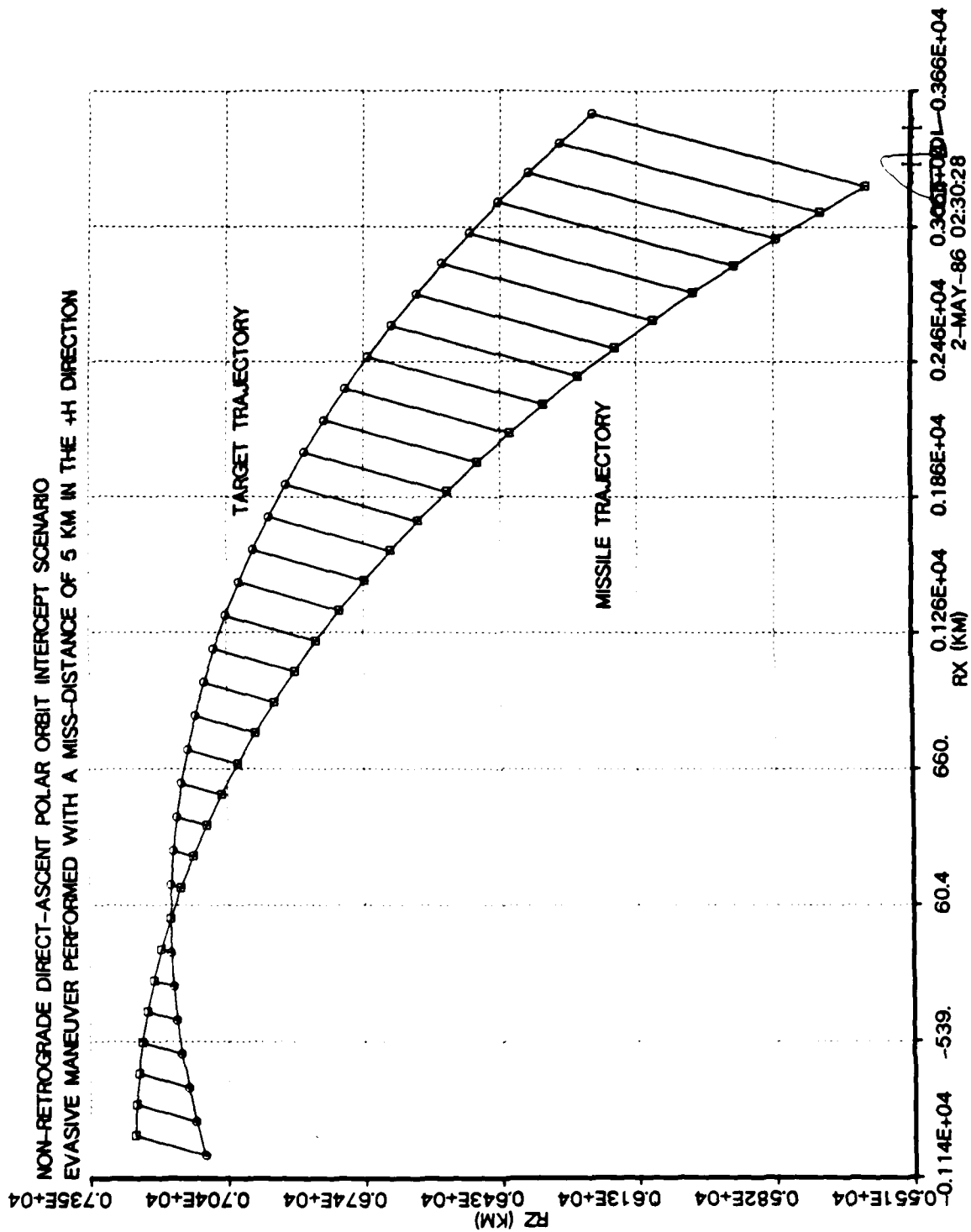


Figure 9: Non-Retrograde Direct-Ascent Intercept Scenario

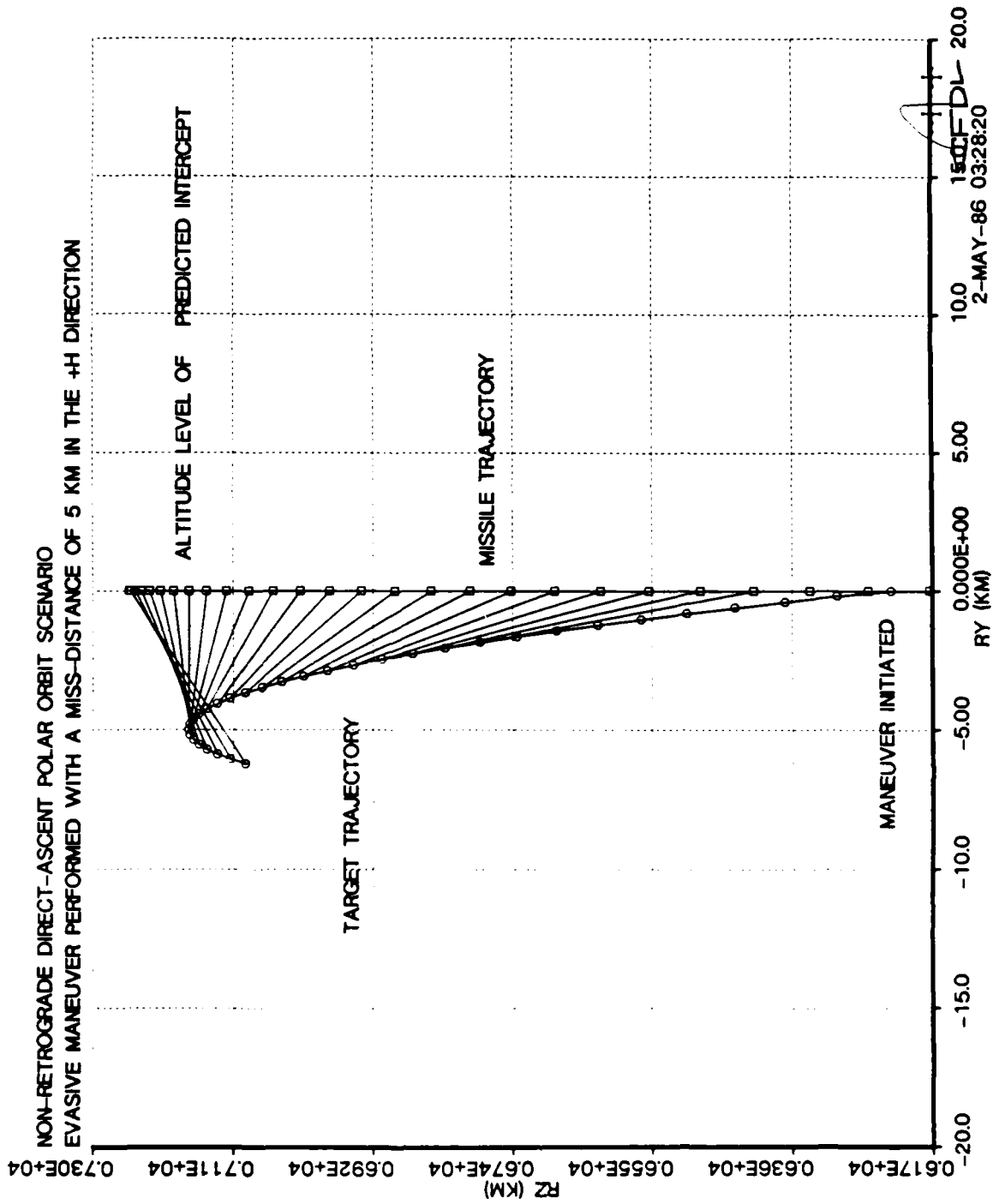


Figure 10: Closeup of Non-Retrograde Direct-Ascent Plane Change Geometry

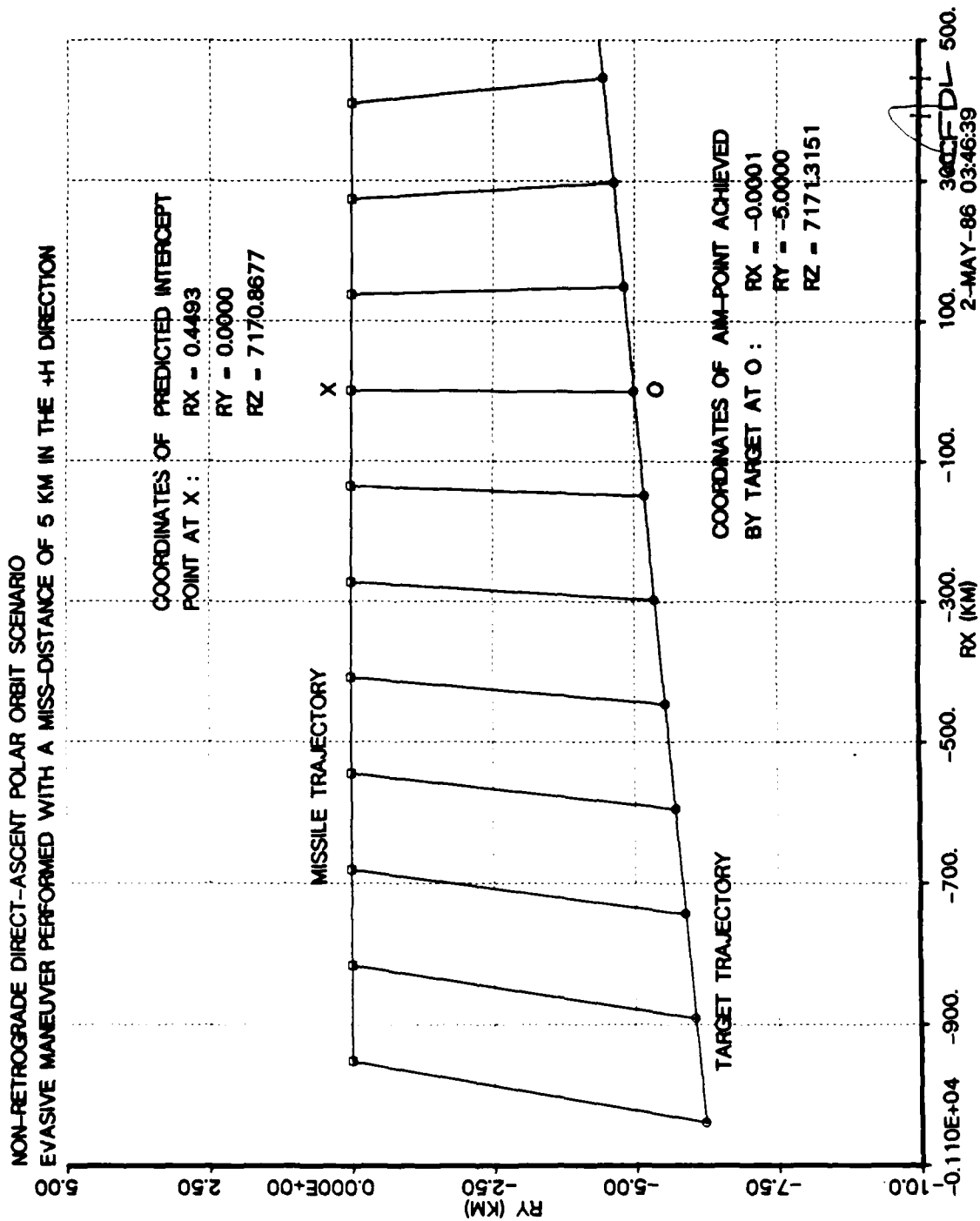


Figure 11: Closeup of Non-Retrograde Direct-Ascent Intercept Geometry

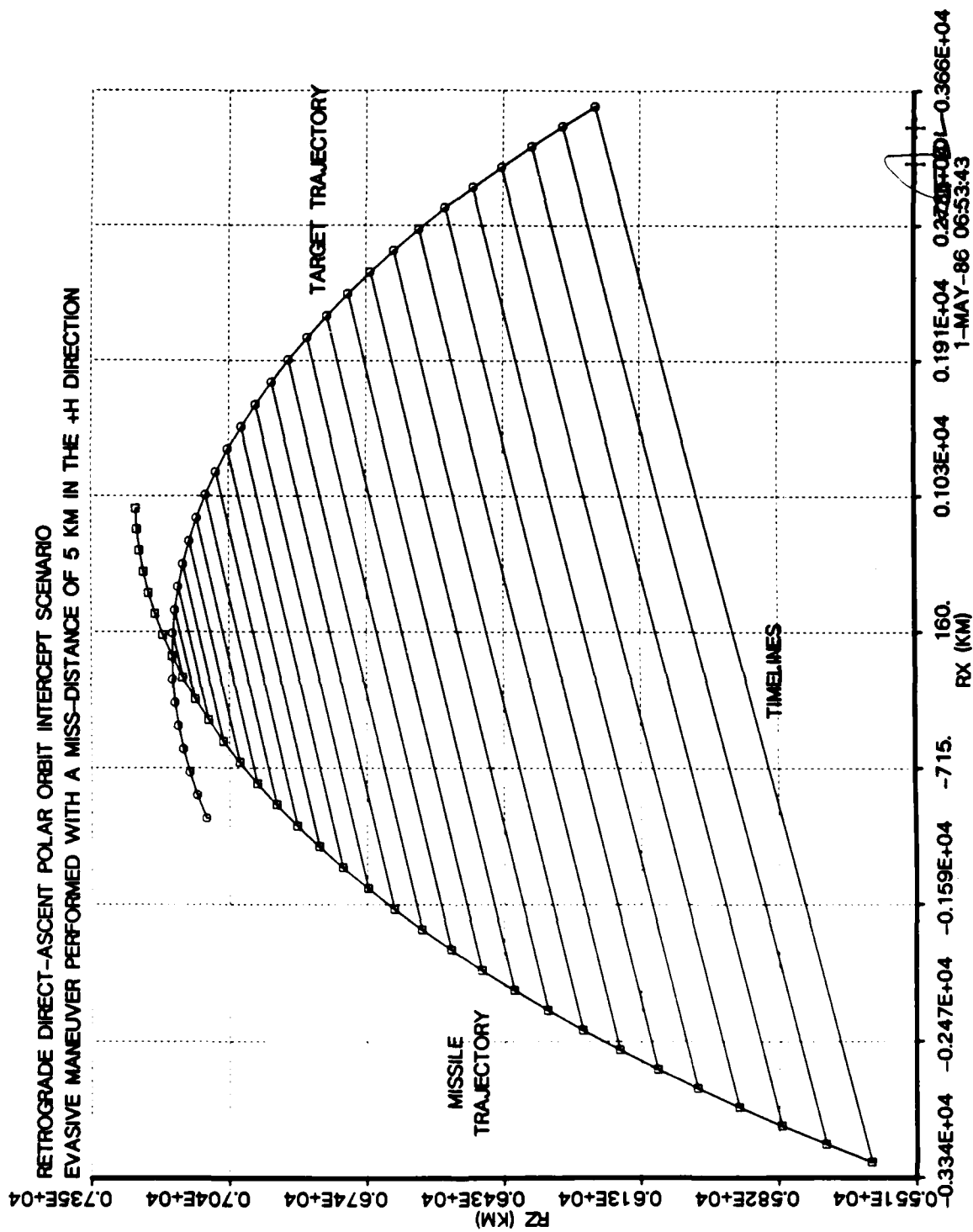


Figure 12: Retrograde Direct-Ascent Intercept Scenario

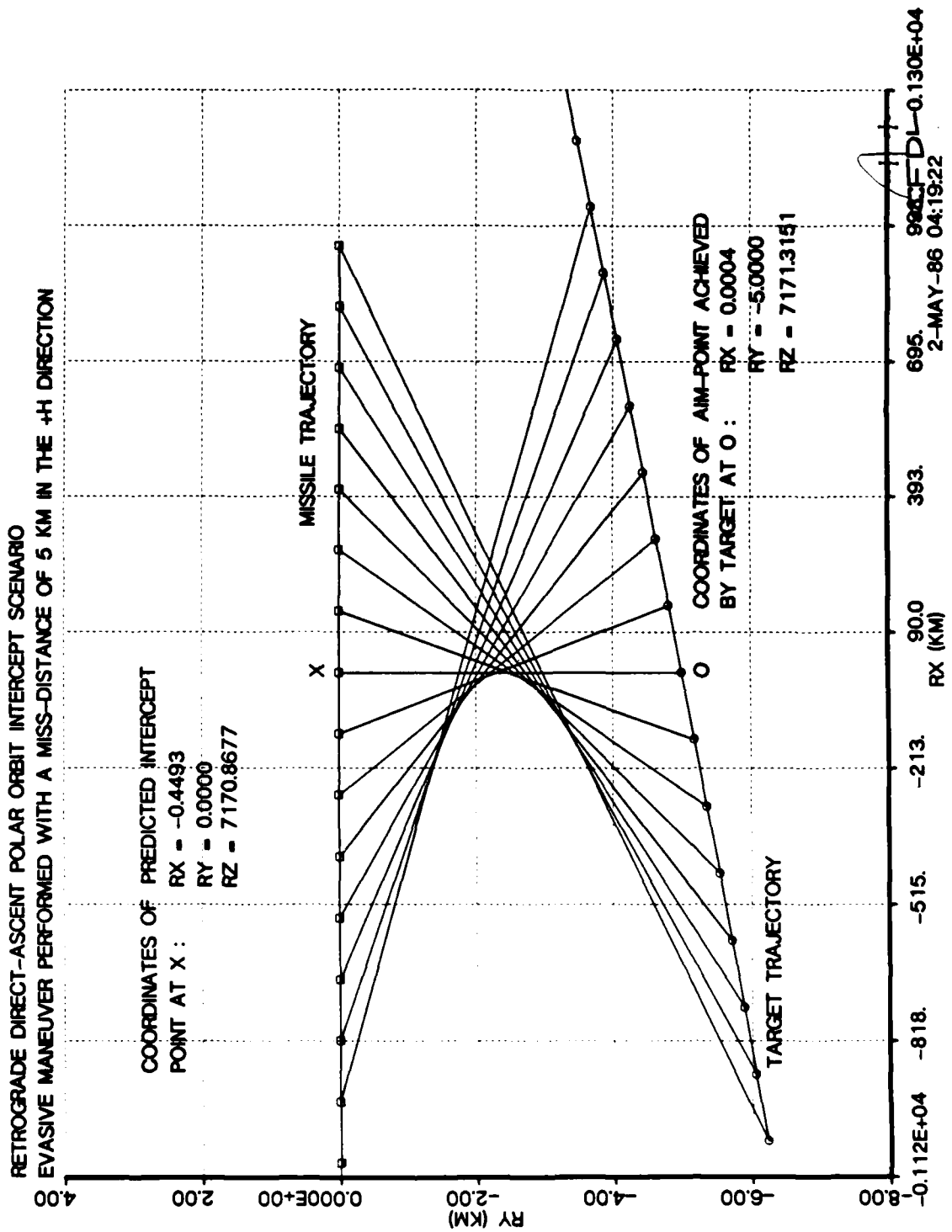


Figure 13: Closeup of Retrograde Direct-Ascent Intercept Geometry

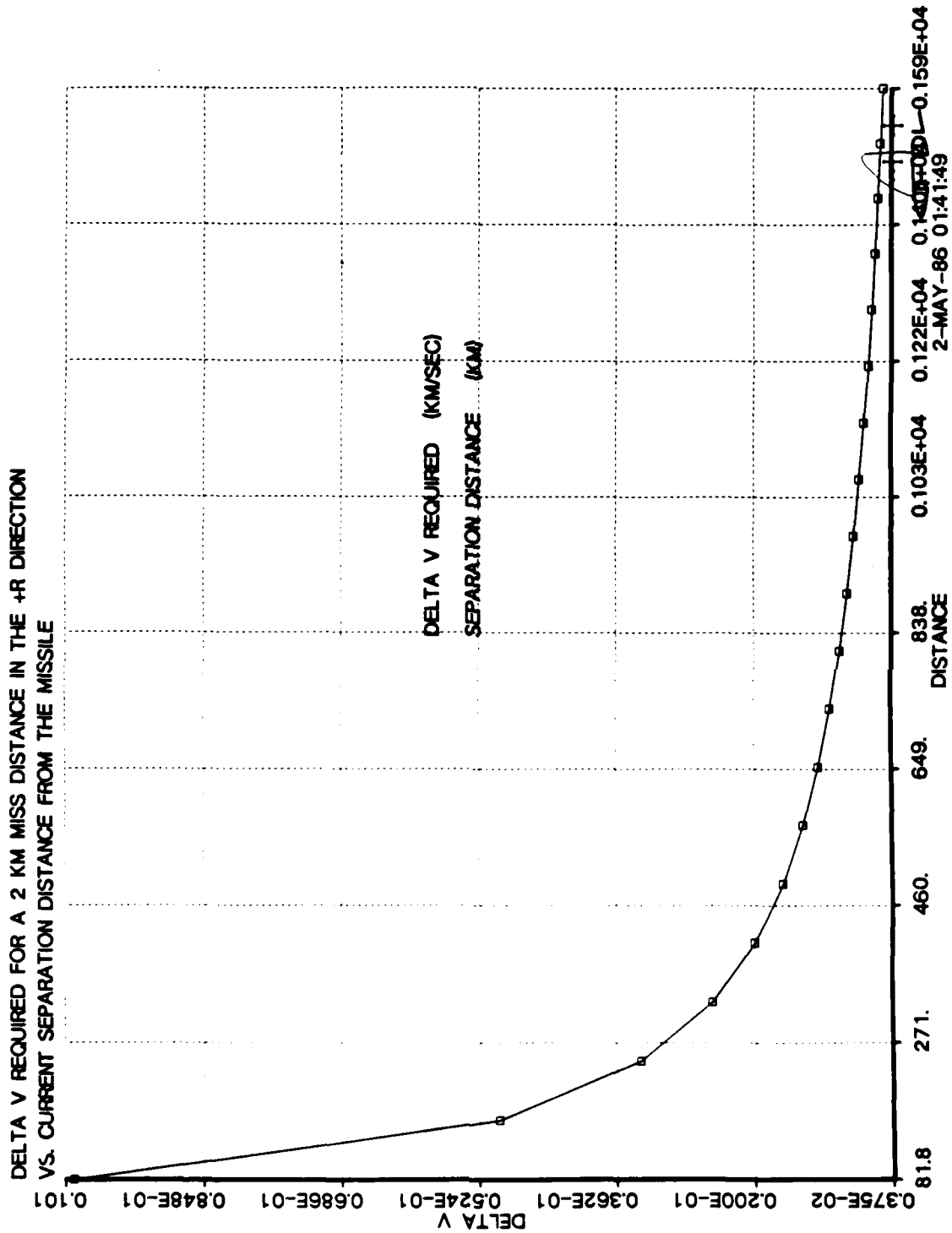


Figure 14: Δv Required vs. Separation Distance from the Missile

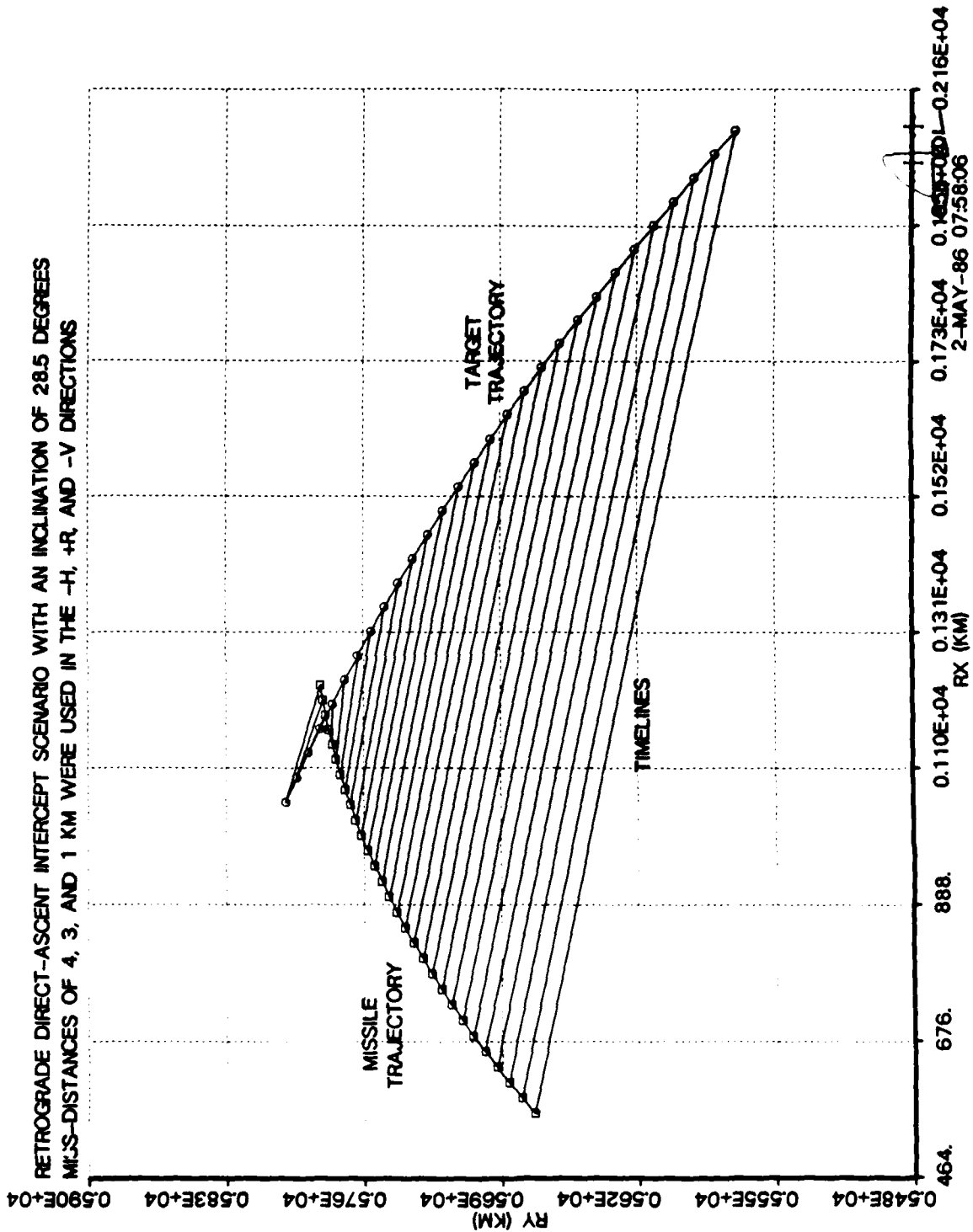


Figure 15: Intercept Scenario with a Three-Dimensional Aim-Point Maneuver

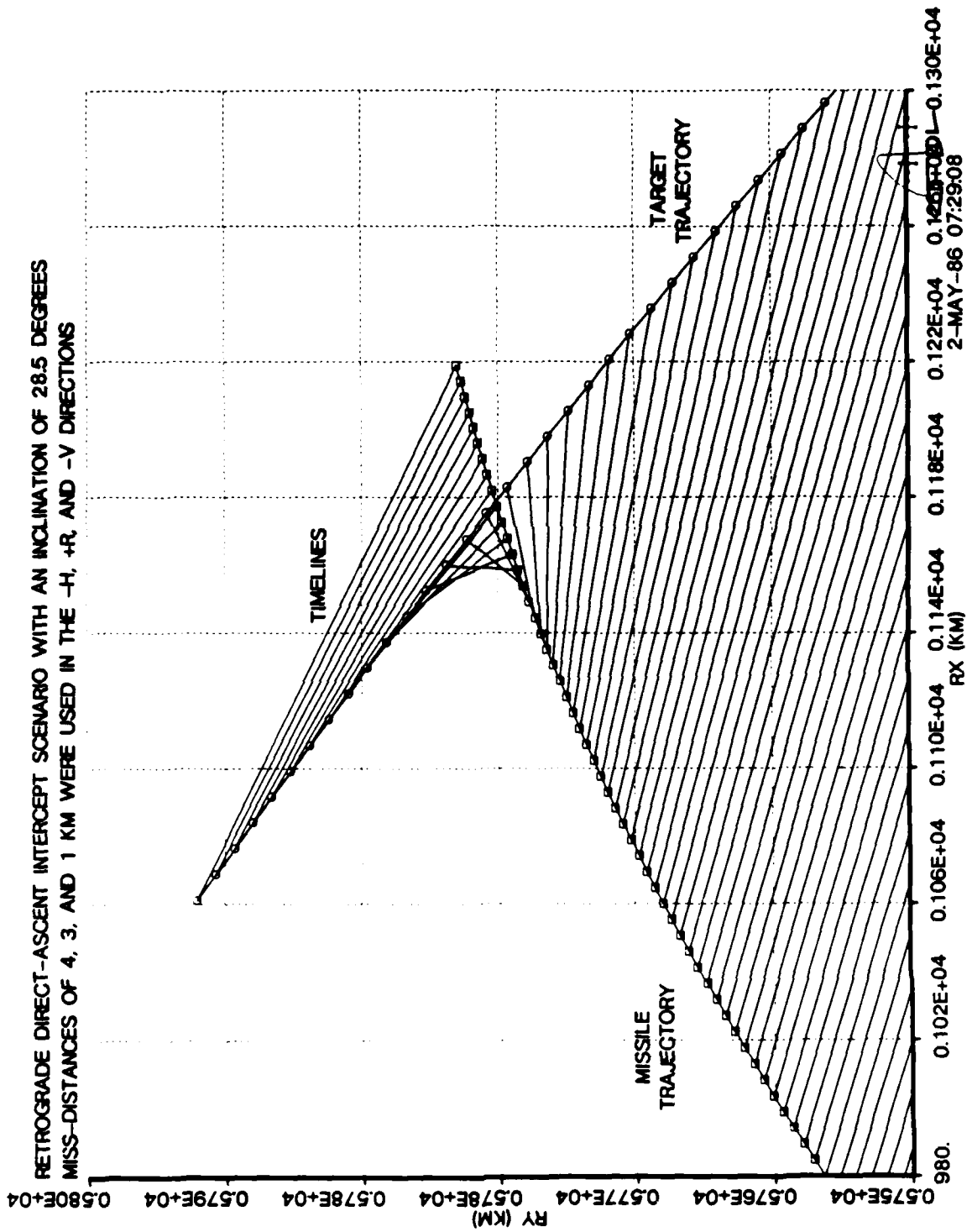


Figure 16: Closeup of Three-Dimensional Maneuver Planar Geometry

5 Conclusions

In order to enhance the survivability of vital U.S. space-based systems, it is imperative that they be provided with an effective means of defensive countermeasure against an anti-spacecraft missile threat. In order for a spacecraft to react appropriately to an imminent danger, it must have access to timely, quantifiable, accurate information on which to base evasive action decisions. To select and employ an appropriate countermeasure to an approaching anti-spacecraft missile, the target must be able to detect the missile, determine its trajectory, and predict whether or not the missile is likely to intercept the spacecraft at some future time. If an intercept is predicted, the spacecraft must select one or a combination of several defensive countermeasures that will effectively confuse, deceive, destroy, or evade the attacker.

If all non-maneuvering countermeasures fail to defeat the missile, the spacecraft will be destroyed - unless it can maneuver to avoid intercept. To maneuver effectively, calculations must be made on-board the spacecraft in real-time to enable a selection of possible maneuvering aim-points, and to determine velocity-to-be-gained requirements to perform selected maneuvers. These calculations must be accurate and provide realistic data based on actual spacecraft orbital maneuvering constraints and reliable predictions of missile position and transfer time-to-intercept. Maneuvers to any point in three-dimensional space must be provided for, so that the spacecraft can effectively exploit any limitations in the missile's maneuverability, range, or homing capabilities. Furthermore, the missile must be able to select the direction and magnitude of any changes to its orbit, so that its own maneuvering capability and fuel reserves can be used to advantage, while limiting the degradation to its mission effectiveness and retaining the ability to re-establish its operational orbit if desired.

Through the research described in this paper, it was found that the methods of astrodynamics as implemented in the program EVADER could provide the kind of

accurate, quantitative, real-time data required to determine a missile's trajectory, predict intercept and determine the transfer time-to-intercept, and to plan and carry-out evasive maneuvers to any point in three-dimensional space. Based on two position fixes over time for the missile, which could be realistically obtained from sensors on-board a spacecraft, and information on spacecraft position and velocity, which could be obtained from spacecraft guidance and navigation instruments, it was possible to determine the missile and spacecraft trajectories and compare their relative position vectors in inertial space at present and future predicted times.

Based on the magnitude and direction of change of the future relative position vector between the vehicles, an evasive maneuver was initiated and the operator was provided with the means to select the magnitude and direction of the aim-point to be achieved at the future intercept time. Based on the operator's selections, the program was able to calculate vector aim-points and supply velocity-to-be-gained information to the operator so that a decision on implementation of the maneuver could be made.

If the maneuver was approved, it was carried out either impulsively or through a numerically integrated engine burn. This engine burn, along with current trajectory point updates was numerically integrated with a fourth-order Runge-Kutta integration technique. In conjunction with the model for spacecraft thrust, models for atmospheric drag and gravitational perturbations due to higher order zonal harmonics were included in the integration of current trajectories. In this way, it was possible to judge the accuracy and usefulness of the astrodynamic techniques in predicting future positions of the spacecraft and missile.

It was found that in scenarios where drag was negligible, above say 200 km, the position information provided by the astrodynamic techniques up to 500 or 600 sec in the future for the simulations that were run generally agreed to within the third or fourth decimal place in kilometers with the values for position provided through the integration techniques, once the current trajectories had been integrated out to the predicted times. Velocity information provided through the astrodynamic

techniques typically agreed with the integrated values to 4 decimal places or better in kilometers per second. Thus, for aim-point targeting and vehicle position predictions, it was found that accuracy to within the range of meters could be achieved in the regions of space in which the majority of a typical spacecraft's operational mission is carried out.

It was determined that some slight errors could be introduced through perturbations due to drag at altitudes in the region between 100 and 200 km. At those altitudes, position discrepancies between integrated and astrodynamical calculations could occur in the second or third decimal place in kilometers, while velocity information discrepancies could occur in the third or fourth decimal place in km/sec. In all trajectories run, it was found that perturbations due to axisymmetric gravity as modelled were always negligible and were, in fact, undetectable.

Transfer times-to-intercept used in scenarios ranged from 125 sec for a 100 to 300 km low-altitude intercept scenario to 500 to 600 sec for higher altitude simulations at 800 to 1000 km. For evasive maneuvers when transfer times were on the order of 400 to 500 seconds and the separation distance from target to missile was say 400 km or more, moderate Δv requirements were placed on the engine in the range of 0.001 to 0.01 km/sec for miss-distances of 2 to 5 km. Burn times averaged on the order of 2 to 10 seconds, when default vehicle and propulsion parameters were used. For these types of engine burns, it was found that Δv expenditures as calculated from fuel mass usage were typically 100.25 to 101% of the impulsive velocity-to-be-gained calculations made at the outset of a maneuver, so that an impulsive velocity addition assumption would be completely adequate in typical short burn situations with sufficient attack warning.

In situations where maneuvering was delayed, however, Δv requirements could increase by as much as 840% to achieve a miss-distance of 2 km as time-to-intercept decreases to 50 sec and separation distance decreases to less than 100 km. In this case, an engine burn of up to 40 to 45 sec might be required. For one scenario, an engine burn of 42.6 sec was required in just such a situation, with the Δv

calculations based on fuel usage exceeding the impulsive calculations by 27%. Thus, for longer duration burns of more than 15 to 20 sec say, an impulsive velocity addition assumption might not be adequate.

Through multiple simulation runs, it was found that an integration time-step of 1 sec could provide acceptable accuracy for the integration of trajectory updates, while an integration time step of 0.1 sec was typically required for an engine to be able to reduce velocity-to-be-gained to essentially zero in the sixth or seventh decimal place in km/sec. If engine cut-off was allowed to occur with any significant amount of velocity-to-be-gained left to be supplied, it was found that this would by far be the most significant contributor to any resulting discrepancies in achieving predicted aim-points as planned.

As an overall relative comparison between run-times of the astrodynamic and integration techniques in a typical simulation scenario, as performed on a VAX 11/750 which was usually supporting competing multiple users, it was found that the astrodynamic techniques could supply intercept prediction data, maneuvering aim-points, and velocity-to-be-gained information for trajectory points 500 to 600 sec in the future essentially instantaneously in real-time. Integration routines, however, would usually produce information for just 100 sec in the future with a time-lag of up to 15 to 20 seconds. Thus, the astrodynamic techniques were shown to be able to supply information that was typically as accurate as the integration techniques, but could be delivered in real-time on the computer system used, while the integration techniques could not supply the same information in real-time. In fact, for integration time steps smaller than 1 sec for trajectory updates and 0.1 sec for engine burns, response times of the integration routines became inordinate.

Scenarios successfully demonstrated included retrograde and non-retrograde co-orbital injection and direct-ascent intercepts. It was found that the techniques used in subroutine SETUP to design scenarios worked well, provided accurate vector information for input to EVADER, and allowed the operator great flexibility in designing intercept scenarios that had the properties desired and would test EVADER

properly. As demonstrated in Sec. 4, maneuvers to any point in three-dimensional space could be made, with any combination of plane, altitude, or further position change being possible by choosing the direction and magnitude of the aim-point.

Thus, integration techniques, although providing a convenient and useful means of testing the astrodynamics techniques in EVADER and having applicability in situations where time constraints are not critical, were not found to be able to provide the kind of timely, information that would be required on-board a spacecraft maneuvering evasively, where computational resources and time available is limited. The use of predictive astrodynamics techniques to govern the evasive maneuvering of a spacecraft in response to an anti-spacecraft missile threat, however, were found to be accurate, efficient and flexible, and could deliver the timely information required for the spacecraft to avoid intercept and to survive.

Appendix A

Program Listing of EVADER

PROGRAM EVADER

```

C*****
C
C          LIST OF VARIABLES
C*****
C  ADRAG(3) - DRAG ACCELERATION VECTOR OF EITHER VEHICLE AS USED
C            IN RUNKUT
C  ANDRAGM(2),ATDRAGM(2) - ARRAYS CONTAINING MAGNITUDE OF DRAG
C                        ACCELERATION ACTING ON MISSILE AND TARGET AT
C                        CURRENT AND PREDICTED TIME FOR DATA OUTPUT
C  ANGRAVM(2),ATGRAVM(2) - ARRAYS CONTAINING MAGNITUDE OF GRAVITY ACCELERATION
C                        ACTING ON MISSILE AND TARGET AT CURRENT AND
C                        PREDICTED TIME FOR DATA OUTPUT
C  AREAM,AREAT - CROSS-SECTIONAL AREA OF THE MISSILE AND TARGET. THESE CAN
C                BE CHANGED BY THE OPERATOR AT THE START OF A RUN.
C  ATHRUST(3),ATHRM - THRUST ACCELERATION OF TARGET AS USED IN RUNKUT
C  BTAVAIL - TOTAL ENGINE BURN TIME AVAILABLE
C  BTIME - ELAPSED BURN-TIME SINCE ENGINE BEGAN THRUSTING
C  DELVIMP - IMPULSIVE DELTA V REQUIRED FOR REQUESTED MANEUVER
C  DELVUSE,DVAVAIL - TOTAL DELTA V USED AND AVAILABLE
C  DRAGOPT,GRAVOPT - USED TO TURN DRAG AND AXISYMMETRIC GRAVITY INTEGRATION
C                   MODELS 'ON' OR 'OFF' BY THE OPERATOR AT THE START OF A RUN
C  FIXTIME - TIME INTERVAL BETWEEN MISSILE POSITION FIXES RMO AND RM1
C  FUELUSE - MASS OF FUEL USED
C  HM,PM,AM,EM,MI - ANGULAR MOMENTUM, PARAMETER, SEMIMAJOR AXIS, ECCENTRICITY,
C                   AND INCLINATION OF THE MISSILE'S ORBIT
C  HT,PT,AT,ET,TI - ANGULAR MOMENTUM, PARAMETER, SEMIMAJOR AXIS, ECCENTRICITY,
C                   AND INCLINATION OF THE TARGET'S ORBIT
C  HRK - INTEGRATION TIME STEP TO BE USED IN RUNKUT FOR TRAJECTORY
C        CALCULATIONS. IT IS ASSIGNED THE VALUE OF HRKNOM FOR BALLISTIC
C        TRAJECTORY UPDATES AND IS SET TO HRKBURN DURING AN ENGINE BURN.
C  HRKBURN - (BURNSTEP) - INTEGRATION TIME STEP TO BE USED DURING AN ENGINE
C            BURN AS SET BY THE OPERATOR. THIS IS NOT THE TIME STEP USED FOR
C            ENGINE DATA OUTPUT.
C  HRKNOM - (INTSTEP) - INTEGRATION TIME STEP TO BE USED FOR BALLISTIC
C            TRAJECTORY CALCULATIONS AS SET BY THE OPERATOR AT THE START OF A
C            RUN. THIS IS NOT THE TIME STEP USED FOR DATA OUTPUT.
C  MALT(2),TALT(2) - ARRAYS CONTAINING MISSILE AND TARGET ALTITUDE AT
C                   THE CURRENT AND PREDICTED TIMES
C  MASSM,MASST - TOTAL MISSILE MASS AND CURRENT MASS OF THE TARGET. THESE
C                CAN BE CHANGED BY THE OPERATOR AT THE OUTSET OF A RUN.
C  MDOT,THRUSTM,VACISP - MASS FLOW RATE, THRUST LEVEL, AND ISP OF THE
C                       TARGET'S ENGINE. THRUSTM CAN BE SET BY THE
C                       OPERATOR AT THE STRART OF A RUN.
C  MFUEL - MASS OF FUEL REMAINING FOR THE TARGET
C  MRHO(2),TRHO(2) - ARRAYS CONTAINING THE ATMOSPHERIC DENSITIES FOR THE
C                   MISSILE AND TARGET AT THEIR CURRENT AND PREDICTED
C                   ALTITUDES.
C  MU - GRAVITATIONAL CONSTANT OF EARTH
C  MULTOUT - USED TO CONTROL THRUST DATA OUTPUT
C  MUVAL - CURRENT VALUE OF EARTH'S GRAVITATIONAL CONSTANT AS CALCULATED BY
C          SUBROUTINE GRAVITY
C  NRUNS - TOTAL NUMBER OF DATA OUTPUT BLOCKS TO BE RUN AS SET BY THE OPERATOR
C  OUTSTEP - TIME STEP TO BE USED FOR OUTPUTTING DATA AS SET BY
C            THE OPERATOR

```

C OUTTIME = CURRENT TIME STEP FOR WHICH DATA IS BEING OUTPUT
C PHASE = CURRENT PHASE OF CALCULATION OF THE PROGRAM. POSSIBLE PHASES ARE
C SETUP, PRE-EVADE, EVADING, POST-EVADE, AND MAXRUNS (NRUNS REACHED)
C PI = 3.141592654
C RAVE,REQE = AVERAGE AND EQUATORIAL RADIUS OF THE EARTH
C RMO(3),RNOM = COMPONENTS AND MAGNITUDE OF FIRST MISSILE POSITION VECTOR
C FIX AT TIME TO
C RM1(3),RM1M = COMPONENTS AND MAGNITUDE OF MISSILE POSITION VECTOR
C AT THE CURRENT TIME T1
C RM2(3),RN2M = COMPONENTS AND MAGNITUDE OF MISSILE POSITION VECTOR
C AT THE PREDICTED TIME T2
C RMISS(3),MISSD = COMPONENTS AND MAGNITUDE OF DESIRED MISS DISTANCE VECTOR
C AT PREDICTED INTERCEPT TIME
C RMTACT(3),RMTACTM = COMPONENTS AND MAGNITUDE OF RELATIVE POSITION VECTOR
C ACTUALLY SEPARATING THE MISSILE AND TARGET AT THE
C CURRENT TIME T1
C RMPRE(3),RMPREM = COMPONENTS AND MAGNITUDE OF PREDICTED RELATIVE POSITION
C VECTOR SEPARATING THE MISSILE AND TARGET AT
C THE PREDICTED TIME T2
C RT1(3),RT1M = COMPONENTS AND MAGNITUDE OF TARGET POSITION VECTOR AT THE
C CURRENT TIME T1
C RT2(3),RT2M = COMPONENTS AND MAGNITUDE OF TARGET POSITION VECTOR AT THE
C PREDICTED TIME T2
C SETOPT = SET TO 'Y' BY THE OPERATOR IF A NEW SETUP IS DESIRED
C TCHANGE = SET TO .TRUE. INTERNALLY IF THE MAGNITUDE OF THE THRUST NEEDS
C TO BE REDUCED FOR THE LAST INTEGRATION STEP OF AN ENGINE BURN
C TERMOUT = SET TO 'Y' BY THE OPERATOR IF OUTPUT IS TO BE DISPLAYED AT THE
C TERMINAL
C THROPT = SET BY THE OPERATOR TO 'E' FOR AN ENGINE BURN, 'I' FOR IMPULSIVE
C CALCULATIONS, AND 'N' IF NO MANEUVER IS DESIRED
C TINTER = ORIGINAL TIME-TO-INTERCEPT
C TOSTEP = (THOUTSTEP) = THRUST DATA OUTPUT STEP AS SET BY THE OPERATOR AT
C THE OUTSET OF A RUN
C TOTTIME = TOTAL ELAPSED TIME OF THE RUN
C TRIME = CURRENT TRANSFER TIME BEING USED FOR PREDICTED VECTOR CALCULATIONS
C VM1(3),VM1M = COMPONENTS AND MAGNITUDE OF THE CURRENT MISSILE VELOCITY
C VECTOR AT TIME T1
C VM2(3),VM2M = COMPONENTS AND MAGNITUDE OF THE PREDICTED MISSILE VELOCITY
C VECTOR AT TIME T2
C VT1(3),VT1M = COMPONENTS AND MAGNITUDE OF THE CURRENT TARGET VELOCITY VECTOR
C AT TIME T1
C VT2(3),VT2M = COMPONENTS AND MAGNITUDE OF THE PREDICTED TARGET VELOCITY
C VECTOR AT TIME T2
C VTBGAIN,TDIRECT(3) = MAGNITUDE OF THE CURRENT VELOCITY-TO-BE-GAINED VECTOR
C AND THE DIRECTION OF THE CURRENT THRUST VECTOR. THESE
C ARE UPDATED EVERY INTEGRATION STEP DURING AN ENGINE
C BURN.
C*****
IMPLICIT DOUBLE PRECISION (A-H,K-M,O-Z)
CHARACTER PHASE*9, IDM*7, IDT*7, IDMP*7, IDTP*7,
+ GRAVOPT, DRAGOPT, THROPT
COMMON/BLOK1/ RM1(3),RM1M
COMMON/BLOK2/ RT1(3),RT1M
COMMON/BLOK3/ RM2(3),RN2M

```

COMMON/BLOK4/ RT2(3),RT2M
COMMON/BLOK5/ VM1(3),VM1M
COMMON/BLOK6/ VT1(3),VT1M
COMMON/BLOK7/ VM2(3),VM2M
COMMON/BLOK8/ VT2(3),VT2M
COMMON/BLOK10/ PI,MU
COMMON/BLOK11/ TRTIME,TINTER
COMMON/BLOK12/ HM,PM,AM,EM,MI
COMMON/BLOK13/ HT,PT,AT,ET,TI
COMMON/BLOK14/ RMTACT(3),RMTACTM
COMMON/BLOK15/ RMTPRE(3),RMTPREM
COMMON/BLOK16/ RMISS(3),MISSD
COMMON/BLOK17/ OUTTIME,TOTTIME
COMMON/BLOK18/ RMO(3),RMON,FIXTIME
COMMON/BLOK19/ PHASE
COMMON/BLOK20/ HRK,NRUNS,OUTSTEP,HRKNOM,HRKBURN
COMMON/BLOK22/ GRAVOPT,DRAGOPT,THROPT
COMMON/BLOK23/ ATHRUST(3),ATHRM,ADRAG(3),BTIME
COMMON/BLOK24/ AREAM,AREAT
COMMON/BLOK25/ MASSM,MASST
COMMON/BLOK29/ THRUSTM,MDOT,VACISP
COMMON/BLOK33/ RAVE,REQE

```

```

OPEN (UNIT=1, FILE='EVADE.DAT;1', STATUS='UNKNOWN')
OPEN (UNIT=3, FILE='AEPLT.DAT;1', STATUS='UNKNOWN')
OPEN (UNIT=4, FILE='P2EPLT.DAT;1', STATUS='UNKNOWN')
OPEN (UNIT=7, FILE='P1EPLT.DAT;1', STATUS='UNKNOWN')
OPEN (UNIT=8, FILE='DVDIST.DAT;1', STATUS='UNKNOWN')
C*****
C - UNITS OF DEFAULT DATA BELOW: TIME (SEC), DISTANCE (KM),
C VELOCITY (KM/SEC), ACCELERATION (KM/SEC**2), MU (KM**3/SEC**2)
C AREA (KM**2), MASS (KG), THRUST (KILONEWTONS),VACISP (SEC)
C*****
DATA RT1 /6400.399648763481,2875.838048518093,251.603227381849/
DATA VT1 /-3.095911960380,6.837852390940,0.598234567071/
DATA MISSD /2./
DATA RMO /5912.285346269399,2738.312028374148,239.571259679416/
DATA RM1 /5910.318566218911,2745.539295485917,240.203563619970/
DATA FIXTIME /1.0/
DATA RAVE,REQE /6371.315,6378.533/
DATA MU,PI /3.981D5,3.141592654/
DATA ATHRUST,ADRAG,TOTTIME,OUTTIME,BTIME,IRUNS,OUTTIME /11*0./
DATA AREAM,AREAT,MASSM,MASST /.00000707,.000015,2000.,10000./
DATA THRUSTM,VACISP /26.69,483./
C*****SETTING UP NEW SCENARIO INPUT VECTORS IF DESIRED
CALL SETUP
C*****INPUTTING INTEGRATON AND OUTPUT STEPS; SPECIFYING OUTPUT; SELECTING
C GRAVITY AND DRAG MODELS; INPUTTING NEW VEHICLE PARAMETERS IF DESIRED
CALL PUTIN
IDM = 'MISSILE'
IDT = 'TARGET '
IDMP = 'MPREDIC'
IDTP = 'TPREDIC'
PHASE = 'PREEVADE '

```

```

CALL RELVECT(RM1,RT1,'ACTUAL  ')
RMTTEST = RMTACTM
C*****CALCULATING MISSILE VELOCITY FROM POSITION FIXES
CALL LAMBERT(RMO,RM1,FIXTIME)
C*****CALCULATING MISSILE ORBITAL ELEMENTS AND TRANSFER TIME TO
C   TARGET ALTITUDE
CALL ORBELS(RM1,VM1,IDM)
CALL TRANST
TINTER = TRTIME
C*****CALCULATING GRAVITY AND DRAG FOR FIRST CURRENT VECTOR DATA BLOCK
CALL GRAVITY (RM1M,RM1(3),IDM)
CALL DRAG (RM1M,VM1,IDM)
C*****TARGET CURRENT GRAVITY AND DRAG RE-CALCULATED IF NO MANEUVER WAS
C   PERFORMED
10 CALL GRAVITY (RT1M,RT1(3),IDT)
CALL DRAG (RT1M,VT1,IDT)
IF(PHASE .EQ. 'EVADING  ') GOTO 30
C*****DECREMENTING TRANSFER TIME IF APPROPRIATE
20 IF((PHASE .EQ. 'EVADING  ').AND.((THROPT .EQ. 'N')
+   .OR.(THROPT .EQ. 'E')))) TRTIME = TINTER-TOTTIME
C*****CALCULATING PREDICTED MISSILE VECTORS, GRAVITY, AND DRAG
CALL EXGAUSS(RM1,VM1,TRTIME,IDM)
CALL GRAVITY (RM2M,RM2(3),IDMP)
CALL DRAG (RM2M,VM1,IDMP)
C*****CALCULATING PREDICTED TARGET VECTORS, GRAVITY, AND DRAG
30 CALL EXGAUSS(RT1,VT1,TRTIME,IDT)
CALL GRAVITY (RT2M,RT2(3),IDTP)
CALL DRAG (RT2M,VT1,IDTP)
CALL RELVECT(RM2,RT2,'PREDICTED')
C*****INCREMENTING OUTPUT DATA BLOCK COUNTER AND OUTPUTTING
C   CURRENT AND PREDICTED DATA
40 IRUNS = IRUNS+1
CALL PUTOUT('ACTUAL  ')
CALL PUTOUT('PREDICTED')
C*****CHECKING FOR MISSILE PENETRATION OF PREDICTED WARNING SPHERE
C   TO INDICATE ATTEMPTED INTERCEPT
IF((RMTPREM .LE. 1.).AND.((PHASE .EQ. 'PREEVADE  ').OR.
+   (THROPT .EQ. 'N')))) THEN
PHASE = 'EVADING  '
C*****ENTERING INTERACTIVE EVASIVE MANEUVERING MODE
CALL EVADE
C*****IF IMPULSIVE MANEUVER, UPDATE CURRENT TARGET VELOCITY AT CURRENT
C   POSITION
IF(THROPT .EQ. 'I') THEN
GOTO 10
C*****IF ENGINE BURN, INITIATE THRUST AT CURRENT STEP AND CONTINUE
ELSE IF(THROPT .EQ. 'E') THEN
CALL THRUST(BTIME,0.,1)
GOTO 40
C*****IF NO MANEUVER, CONTINUE UPDATING TRAJECTORIES AND DECREMENT
C   TRANSFER TIME
ELSE IF(THROPT .EQ. 'N') THEN
GOTO 50
ENDIF

```

```

ENDIF
C*****INITIATE SCENARIO TERMINATION IF REQUESTED NUMBER OF OUTPUT
C   DATA BLOCKS HAVE BEEN RUN
C   50 IF(IRUNS .EQ. NRUNS) THEN
C*****IF PREDICTED SEPARATION DISTANCE IS INCREASING, DECLARE A SUCCESSFUL
C   EVASION AND CALCULATE FINAL ORBITAL ELEMENTS FOR BOTH VEHICLES
C   IF(RMTPREM .GT. RMTTEST) THEN
C       PHASE = 'POSTEVADE'
C*****IF PREDICTED SEPARATION DISTANCE IS DECREASING, TERMINATE SCENARIO,
C   ISSUE WARNING TO THE OPERATOR, AND CALCULATE ORBITAL ELEMENTS
C   ELSE
C       PHASE = 'MAXRUNS '
C   ENDIF
C   CALL SAFE(NRUNS)
C       GOTO 100

ENDIF
C*****RESET RMTTEST TO CHECK FOR INCREASING OR DECREASING PREDICTED
C   SEPARATION DISTANCE
RMTTEST = RMTPREM
C*****INTEGRATE THE CURRENT TRAJECTORIES TO THE NEXT OUTPUT STEP.
C*****THE INTEGRATION TIME STEP USED IS THE CURRENT VALUE OF VARIABLE HRK.
C   IF THE ENGINE IS ON, HRK=HRKBURN, OTHERWISE, HRK=HRKNOM.
CALL RUNKUT(RM1,VM1,IDM)
CALL RUNKUT(RT1,VT1,IDT)
OUTTIME = OUTTIME+OUTSTEP
CALL RELVECT(RM1,RT1,'ACTUAL ')
GOTO 20
    100 STOP
END
C
C

SUBROUTINE LAMBERT(RO,R1,FIXTIME)
C
C
C*****
C   WHEN GIVEN TWO VECTOR POSITION FIXES OVER TIME, THIS SUBROUTINE
C   CALCULATES THE VELOCITY VECTORS OF THE ORBIT AT EACH OF THE
C   POSITIONS GIVEN. SUBROUTINE LAMBERT IS USED TO CALCULATE
C   MISSILE VELOCITIES BASED ON TWO POSITION FIXES OVER TIME AND IS
C   USED TO PERFORM VELOCITY-TO-BE-GAINED CALCULATIONS FOR THE
C   TARGET TO PLAN MANEUVERS AND DURING AN ENGINE BURN. LAMBERT
C   IS ALSO USED IN SETTING UP SCENARIOS IN SUBROUTINE SETUP.
C*****
IMPLICIT DOUBLE PRECISION (A-H,K-M,O-Z)
CHARACTER PHASE*9
COMMON/BLOK5/ VM1(3),VM1M
COMMON/BLOK6/ VT1(3),VT1M
COMMON/BLOK10/ PI,MU
COMMON/BLOK19/ PHASE
DIMENSION RO(3),R1(3),VO(3),V1(3)
ROM = MAGN(RO)
R1M = MAGN(R1)
THETA1 = DACOS((RO(1)*R1(1)+RO(2)*R1(2)+RO(3)*R1(3))/

```

```

      +          (RON+R1M)
C = DSQRT(ROM**2+R1M**2-2.*ROM*R1M+DCOS(THETA))
S = .5*(ROM+R1M+C)
LAMBDA = (DSQRT(ROM*R1M)*DCOS(.5*THETA))/S
EPS = R1M/ROM-1.
T2OMEG = EPS/(2.*DSQRT(DSQRT(1.+EPS))*(DSQRT(1.+EPS)+1.))
L = ((DSIN(.25*THETA))**2+T2OMEG**2)/((DSIN(.25*THETA))**2
      +T2OMEG**2+DCOS(.5*THETA))
MULT = -1.
IF(THETA .GT. PI) MULT = 1.
DTPARA = 1./(6.*DSQRT(MU))*(DSQRT(ROM+R1M+C))**3+
      +MULT*(DSQRT(ROM+R1M-C))**3)
IF(DTPARA .GT. FIXTIME) THEN
  X = L
ELSE
  X = 0.
ENDIF
M = 8.*MU*FIXTIME**2/(8**3*(1.+LAMBDA)**6)
INUM = 0
  5 INUM = INUM+1
  ETA = X/(DSQRT(1.+X)+1.))**2
  ZI = 6.
  Z = ZI
  ICNT = 0
    10 FACT = Z**2-(Z-1.))**2
  ICNT = ICNT+1
    20 Z = Z-1.
  FACT = 1./FACT+Z**2*ETA+Z**2-(Z-1.))**2
  IF(Z .NE. 3.) GOTO 20
  ZI = ZI+1.
  Z = ZI
  IF(ICNT .EQ. 1) THEN
    FACTI = FACT
    GOTO 10
  ENDIF
  FDIFF = FACT-FACTI
  IF(DABS(FDIFF) .GT. 1.D-12) THEN
    FACTI = FACT
    GOTO 10
  ENDIF
  E = 1./(1./(FACT+ETA)+3.)*8.*(DSQRT(1.+X)+1.)
  DENOM = (1.+2.*X+L)*(4.*X+E*(3.+X))
  H1 = (L+X)**2*(1.+3.*X+E)/DENOM
  H2 = M*(X-L+E)/DENOM
  B = 27.*H2/(4.*(1.+H1)**3)
  U = -B/(2.*(DSQRT(1.+B)+1.))
  DELTAN = 1.
  UN = 1.
  SIGMAN = 1.
    SIGT = 1.
  DO 30 N=1,20
    NODD = N/2
    W = DFLOAT(N)-1.
    IF(NODD .EQ. 0) THEN

```



```

      GAMN = 2.*(3.*W+2.)*(6.*W+1.)/(9.*(4.*W+1.)
      +
      *(4.*W+3.))
ELSE
      GAMN = 2.*(3.*W+1.)*(6.*W-1.)/(9.*(4.*N-1.)
      +
      *(4.*N+1.))
ENDIF
DELTAN = 1./(1.-GAMN*U*DELTAN)
UN = UN*(DELTAN-1.)
SIGMAN = SIGMAN+UN
SIGT = DABS(SIGMAN-SIGT)
      IF(SIGT .LT. 1.D-12) GOTO 40
30  CONTINUE
40  KU = 1./3.*SIGMAN
Y = (1.+H1)/3.*(2.+DSQRT(1.+B)/(1.-2.*U*KU**2))
      X = DSQRT((.5*(1.-L))**2+M/Y**2)-.5*(1.+L)
IF(INUM .EQ. 1) THEN
      YTEST = Y
      GOTO 5
ENDIF
YDIFF = Y-YTEST
IF(DABS(YDIFF) .LT. 1.D-12) GOTO 60
YTEST = Y
GOTO 5
60  A = M*S*(1.+LAMBDA)**2/(8.*X*Y**2)
P = 2.*ROM*R1M*Y**2*(1.+X)**2*(DSIN(.5*THETA)
      +
      )**2/(M*S*(1.+LAMBDA)**2)
COEFF = DSQRT(MU*P)/(ROM*R1M*DSIN(THETA))
DO 70 I=1,3
      VO(I) = COEFF*(R1(I)-RO(I)+R1M/P*(1.-
      +
      DCOS(THETA))*RO(I))
      V1(I) = COEFF*(R1(I)-RO(I)-ROM/P*(1.-
      +
      DCOS(THETA))*R1(I))
70  CONTINUE
C*****ASSIGN VELOCITY VECTORS CALCULATED FOR THE MISSILE
IF(PHASE .EQ. 'SETUP ') THEN
      DO 75 I=1,3
      VM1(I) = VO(I)
75  CONTINUE
      VM1M = MAGN(VM1)
ELSE IF(PHASE .EQ. 'PREEVADE ') THEN
      DO 80 I=1,3
      VM1(I) = V1(I)
80  CONTINUE
      VM1M = MAGN(VM1)
C*****ASSIGN VELOCITY VECTORS CALCULATED FOR IMPULSIVE
C      VELOCITY-TO-BE-GAINED MANEUVERS, THRUST VECTOR
C      CONTROL AND ENGINE CUTOFF FOR THE TARGET.
ELSE
      DO 90 I=1,3
      VT1(I) = VO(I)
90  CONTINUE
      VT1M = MAGN(VT1)
ENDIF
RETURN

```

```

END
C
C

SUBROUTINE TRANST
C
C
C*****
C THIS SUBROUTINE CALCULATES THE TRANSFER TIME BETWEEN TWO POINTS
C IN A TWO-BODY ORBIT. TRANST IS USED TO FIND THE TIME FOR THE
C MISSILE TO REACH THE TARGET'S ALTITUDE.
C*****
IMPLICIT DOUBLE PRECISION (A-H,K-M,O-Z)
COMMON/BLOK1/ RM1(3),RM1M
COMMON/BLOK2/ RT1(3),RT1M
COMMON/BLOK10/ PI,MU
COMMON/BLOK11/ TRTIME,TINTER
COMMON/BLOK12/ HM,PM,AM,EM,MI
COMMON/BLOK33/ RAVE,REQE
RM1M = MAGN(RM1)
RT1M = MAGN(RT1)
FO = DACOS(1./EM*(PM/RM1M-1.))
IF(DABS(1./EM*(PM/RT1M-1.)) .GE. 1.) THEN
F1 = PI
ELSE
F1 = DACOS(1./EM*(PM/RT1M-1.))
ENDIF
THETA = F1-FO
C = DSQRT(RM1M**2+RT1M**2-2.*RM1M*RT1M*DCOS(THETA))
S = .5*(RM1M+RT1M+C)
AMIN = .5*S
LAMBDA = DSQRT(RM1M*RT1M)*DCOS(.5*THETA)/S
X = DSQRT(1.-AMIN/AM)
Y = DSQRT(1.-LAMBDA**2*(1.-X**2))
ETA = Y-LAMBDA*X
S1 = .5*(1.-LAMBDA-X*ETA)
DELTAN = 1.
UN = 1.
SIGMAN = 1.
SIGT = 1.
DO 10 N=1,20
NODD = N/2
Z = DFLOAT(N)
IF(NODD .EQ. 0) THEN
GAMN = (Z+2.)*(Z+5.)/((2.*Z+1.)*(2.*Z+3.))
ELSE
GAMN = Z*(Z-3.)/((2.*Z+1.)*(2.*Z+3.))
ENDIF
DELTAN = 1./(1.-GAMN*S1*DELTAN)
UN = UN*(DELTAN-1.)
SIGMAN = SIGMAN+UN
SIGT = DABS(SIGMAN-SIGT)
IF(SIGT .LT. 1.D-12) GOTO 20
10 CONTINUE

```

```

20   Q = 4./3.*SIGMAN
TRTIME = DSQRT(AMIN**3/MU)*(ETA**3+Q+4.*LAMBDA*ETA)
MAPOALT = AM*(1.+EM)-RAVE
C*****OUTPUT INITIAL INTERCEPT TRANSFER TIME AND MISSILE APOGEE ALTITUDE
WRITE(6,1000)
WRITE(6,1100) TRTIME,MAPOALT
WRITE(1,1000)
WRITE(1,1100) TRTIME,MAPOALT
RETURN
1000  FORMAT(/8X,'INITIAL PREDICTED INTERCEPT TIME',4X,
+      'MISSILE APOGEE ALTITUDE')
1100  FORMAT(16X,F12.4,19X,F12.4/)
END
C
C

```

```

SUBROUTINE EXGAUSS(R1,V1,TRTIME, ID)
C
C
C*****
C THIS SUBROUTINE CALCULATES THE POSITION AND VELOCITY
C VECTORS IN AN ORBIT AT A FUTURE OR PREVIOUS TIME
C FROM THE CURRENT POSITION AND VELOCITY VECTORS. EXGAUSS
C IS USED TO CALCULATE THE PREDICTED POSITION AND VELOCITY
C VECTORS OF THE MISSILE AND TARGET AT THE PREDICTED TIME.
C EXGAUSS IS ALSO USED IN SETTING UP SCENARIOS IN
C SUBROUTINE SETUP.
C*****
IMPLICIT DOUBLE PRECISION (A-H,K-M,O-Z)
CHARACTER ID*7
COMMON/BLOK1/ RM1(3),RM1M
COMMON/BLOK3/ RM2(3),RM2M
COMMON/BLOK4/ RT2(3),RT2M
COMMON/BLOK5/ VM1(3),VM1M
COMMON/BLOK7/ VM2(3),VM2M
COMMON/BLOK8/ VT2(3),VT2M
COMMON/BLOK10/ PI,MU
COMMON/BLOK18/ RMO(3),RMOM, FIXTIME
DIMENSION R1(3),V1(3),R2(3),V2(3)
R1M = MAGN(R1)
V1M = MAGN(V1)
T = DSQRT(MU)*TRTIME
SIGMAO = (R1(1)*V1(1)+R1(2)*V1(2)+R1(3)*V1(3))/DSQRT(MU)
GAMMAO = 2.-R1M*V1M**2/MU
FI = 1.
FTI = 0.
GI = 0.
GTI = 1.
5 CHIO = .5-9./20.*GAMMAO
D = 1.
DELTA = 1.
ICOUNT = -1
10 ICOUNT = ICOUNT+1
E = 3.*DELTA*D*T/R1M

```

```

ETA = E/R1M
ZETA = SIGMAO*D/2.
EPS = 1.+ETA*ZETA
B = EPS+.5*ETA*(ZETA+CHIO*E)
IF(ICOUNT .EQ. 0) THEN
    XN = 1.+DABS(EPS)
    XNT = XN
ENDIF
DO 20 N=1,10
    XN = 2./3.*(XN**3+DABS(B))/(XN**2-EPS)
    XDIFF = XN-XNT
    IF(DABS(XDIFF) .LT. 1.D-12) GOTO 30
    XNT = XN
    20 CONTINUE
    30 THETA = E/(1.+DSIGN(XN,B))
    PHI = THETA**2/R1M
Y = GAMMAO*PHI
IF(DABS(Y) .GT. 1.) THEN
    YSW = DABS(Y)
    YM = 1.
    Y = DSIGN(YM,Y)
    PHI = Y/GAMMAO
    THETA = DSQRT(PHI*R1M)
ENDIF
K = 1.00000000001-0.10000000174*Y
    + -0.00357142897*Y**2
    + -0.00023808136*Y**3-0.00001919250*Y**4
    + -0.00000172916*Y**5-0.00000016292*Y**6
D = (1.-3./20.*Y)/K
DELTA = K**2+.25*Y
IF(YSW .GT. 1.) THEN
    TM = ((1./3.*CHIO*THETA+.5*SIGMAO*D)*THETA+R1M)*THETA
    + /((DELTA*D)
GOTO 40
ENDIF
IF(ICOUNT .EQ. 0) THEN
    YM1 = Y
    GOTO 10
ENDIF
YDIFF = Y-YM1
YM1 = Y
IF(DABS(YDIFF) .GE. 1.D-12) GOTO 10
    40 LAMBDA = PHI/(2.*DELTA)
KAPPA = 1.-GAMMAO*LAMBDA
PSI = R1M*LAMBDA
OMEGA = THETA*K/DELTA
    R2M = R1M*KAPPA*PSI+SIGMAO*OMEGA
F = 1.-LAMBDA
GMU = R1M*OMEGA*SIGMAO*PSI
FTDMU = -OMEGA/(R1M*R2M)
GT = 1.-PSI/R2M
FT = FTDMU*DSQRT(MU)
G = GMU/DSQRT(MU)
F = F*FI+G*FTI

```

```

FT = FT+FI+GT+FTI
G = F+GI+G+GTI
GT = FT+GI+GT+GTI
IF(YSW .GT. 1.) THEN
  SIGMAO = SIGMAO*KAPPA+(1.-GAMMAO)*OMEGA
  GAMMAO = R2M*GAMMAO/R1M
  R1M = R2M
  T = T-TM
  FI = F
  FTI = FT
  GI = G
  GTI = GT
  YSW = 0.
  GOTO 5
ENDIF
R1M = MAGN(R1)
R2(1) = F*R1(1)+G*V1(1)
R2(2) = F*R1(2)+G*V1(2)
R2(3) = F*R1(3)+G*V1(3)
V2(1) = FT*R1(1)+GT*V1(1)
V2(2) = FT*R1(2)+GT*V1(2)
V2(3) = FT*R1(3)+GT*V1(3)
C*****ASSIGN POSITION AND VELOCITY VECTORS CALCULATED FOR TIME T2
C   TO THE MISSILE
IF(ID .EQ. 'MISSILE') THEN
  DO 50 I=1,3
    RM2(I) = R2(I)
    VM2(I) = V2(I)
  50 CONTINUE
  RM2M = MAGN(RM2)
  VM2M = MAGN(VM2)
C*****ASSIGN POSITION AND VELOCITY VECTORS CALCULATED FOR TIME T2
C   TO THE TARGET
ELSE IF(ID .EQ. 'TARGET ') THEN
  DO 60 I=1,3
    RT2(I) = R2(I)
    VT2(I) = V2(I)
  60 CONTINUE
  RT2M = MAGN(RT2)
  VT2M = MAGN(VT2)
C*****ASSIGN THE MISSILE POSITION FIX AT TIME TO AS CALCULATED FOR SETUP
ELSE IF(ID .EQ. 'SETHIT ') THEN
  DO 70 I=1,3
    RMO(I) = R2(I)
  70 CONTINUE
  RMO = MAGN(RMO)
C*****ASSIGN THE MISSILE POSITION REQUIRED AT TIME T1 AS CALCULATED FOR
C   SETUP
ELSE IF(ID .EQ. 'INJECT ') THEN
  DO 80 I=1,3
    RM1(I) = R2(I)
    VM1(I) = V2(I)
  80 CONTINUE
  RM1M = MAGN(RM1)

```

```

      VM1M = MAGN(VM1)
ENDIF
RETURN
END
C
C

```

```

SUBROUTINE RUNKUT(R1,V1,ID)

```

```

C
C
C*****
C THIS SUBROUTINE NUMERICALLY INTEGRATES THE VECTOR EQUATIONS
C OF MOTION OF THE CURRENT MISSILE AND TARGET TRAJECTORIES USING
C A FOURTH-ORDER RUNGA-KUTTA TECHNIQUE. HIGHER ORDER GRAVITATIONAL
C HARMONICS AND DRAG ARE TAKEN INTO ACCOUNT FOR BOTH VEHICLES.
C AN INTEGRATED ENGINE BURN IS PERFORMED FOR THE TARGET. THE
C INTEGRATION TIME STEP TO BE USED FOR BALLISTIC TRAJECTORIES AND
C DURING A TARGET ENGINE BURN CAN BE SEPARATELY DESIGNATED BY THE
C OPERATOR AT THE OUTSET OF A SCENARIO.
C*****
IMPLICIT DOUBLE PRECISION (A-H,K-M,O-Z)
CHARACTER ID*7,GRAVOPT,DRAGOPT,THROPT
COMMON/BLOK1/ RM1(3),RM1M
COMMON/BLOK2/ RT1(3),RT1M
COMMON/BLOK5/ VM1(3),VM1M
COMMON/BLOK6/ VT1(3),VT1M
COMMON/BLOK10/ PI,MU
COMMON/BLOK17/ OUTTIME,TOTTIME
COMMON/BLOK20/ HRK,NRUNS,OUTSTEP,HRKNOM,HRKBURN
COMMON/BLOK22/ GRAVOPT,DRAGOPT,THROPT
COMMON/BLOK23/ ATHRUST(3),ATHRM,ADRAG(3),BTIME
COMMON/BLOK30/ NUVAL
DIMENSION R1(3),V1(3),RK2(3),RK3(3),RK4(3),VK2(3),
+          VK3(3),VK4(3),K1(3),K2(3),K3(3),K4(3),
+          L1(3),L2(3),L3(3),L4(3)
C*****RESET THE TIME STEP FOR THE MISSILE FOR BALLISTIC CALCULATIONS
C WHILE THE TARGET IS USING THE SMALLER THRUSTING TIME STEP
IF((ID.EQ.'MISSILE').AND.(THROPT.NE.'I')) THEN
  HRK = HRKNOM
  DO 10 I=1,3
    ATHRUST(I) = 0.
  10 CONTINUE
C*****SETUP FOR TARGET ENGINE BURN
ELSE IF((ID.EQ.'TARGET').AND.(THROPT.EQ.'E')) THEN
  HRK = HRKBURN
  CALL THRUST(BTIME,0.,1)
C*****SETUP FOR BALLISTIC CALCULATIONS
ELSE
  HRK = HRKNOM
ENDIF
C*****DETERMINE THE NUMBER OF INTEGRATION ITERATIONS THAT WILL OCCUR TO
C INTEGRATE THE TRAJECTORY TO THE NEXT OUTPUT STEP
NSTEPS = IDNINT(OUTSTEP/HRK)
DO 50 J=1,NSTEPS

```

```

MUVAL = MU
RK1M = MAGN(R1)
IF(GRAVOPT .EQ. 'Y') CALL GRAVITY(RK1M,R1(3),ID)
IF(DRAGOPT .EQ. 'Y') CALL DRAG(RK1M,V1,ID)
MURMC = MUVAL/RK1M**3
DO 15 I=1,3
  K1(I) = HRK*V1(I)
  L1(I) = HRK*(ATHRUST(I)+ADRAG(I)-MURMC*R1(I))
  RK2(I) = R1(I)+.5*K1(I)
  VK2(I) = V1(I)+.5*L1(I)
15 CONTINUE
RK2M = MAGN(RK2)
IF(GRAVOPT .EQ. 'Y') CALL GRAVITY(RK2M,RK2(3),ID)
IF((THROPT .EQ. 'E').AND.(ID .EQ. 'TARGET '))
  + CALL THRUST(BTIME,.5*HRK,2)
IF(DRAGOPT .EQ. 'Y') CALL DRAG(RK2M,VK2,ID)
MURMC = MUVAL/RK2M**3
DO 20 I=1,3
  K2(I) = HRK*VK2(I)
  L2(I) = HRK*(ATHRUST(I)+ADRAG(I)-MURMC*VK2(I))
  RK3(I) = R1(I)+.5*K2(I)
  VK3(I) = V1(I)+.5*L2(I)
20 CONTINUE
RK3M = MAGN(RK3)
IF(GRAVOPT .EQ. 'Y') CALL GRAVITY(RK3M,RK3(3),ID)
IF((THROPT .EQ. 'E').AND.(ID .EQ. 'TARGET '))
  + CALL THRUST(BTIME,.5*HRK,3)
IF(DRAGOPT .EQ. 'Y') CALL DRAG(RK3M,VK3,ID)
MURMC = MUVAL/RK3M**3
DO 30 I=1,3
  K3(I) = HRK*VK3(I)
  L3(I) = HRK*(ATHRUST(I)+ADRAG(I)-MURMC*VK3(I))
  RK4(I) = R1(I)+K3(I)
  VK4(I) = V1(I)+L3(I)
30 CONTINUE
RK4M = MAGN(RK4)
IF(GRAVOPT .EQ. 'Y') CALL GRAVITY(RK4M,RK4(3),ID)
IF((THROPT .EQ. 'E').AND.(ID .EQ. 'TARGET '))
  + CALL THRUST(BTIME,HRK,4)
IF(DRAGOPT .EQ. 'Y') CALL DRAG(RK4M,VK4,ID)
MURMC = MUVAL/RK4M**3
DO 40 I=1,3
  K4(I) = HRK*VK4(I)
  L4(I) = HRK*(ATHRUST(I)+ADRAG(I)-MURMC*VK4(I))
  R1(I) = R1(I)+(K1(I)+2.*K2(I)+2.*K3(I)+K4(I))/6.
  V1(I) = V1(I)+(L1(I)+2.*L2(I)+2.*L3(I)+L4(I))/6.
40 CONTINUE
IF(ID .EQ. 'TARGET ') THEN
  TOTTIME = TOTTIME+HRK
  IF(THROPT .EQ. 'E') THEN
    BTIME = BTIME+HRK
    CALL THRUST(BTIME,0.,1)
  IF((J .NE. NSTEPS).AND.(THROPT .NE. '0'))
    + CALL THROUT

```

```

ENDIF
ENDIF
50 CONTINUE
R1M = MAGN(R1)
CALL GRAVITY(R1M,R1(3),ID)
IF(DRAGOPT .EQ. 'Y') CALL DRAG(R1M,V1,ID)
C*****ASSIGN INTEGRATED VECTORS TO THE APPROPRIATE VEHICLE
IF(ID .EQ. 'MISSILE') THEN
DO 60 I=1,3
RM1(I) = R1(I)
VM1(I) = V1(I)
60 CONTINUE
RM1M = MAGN(RM1)
VM1M = MAGN(VM1)
ELSE
DO 70 I=1,3
RT1(I) = R1(I)
VT1(I) = V1(I)
70 CONTINUE
RT1M = MAGN(RT1)
VT1M = MAGN(VT1)
ENDIF
RETURN
END
C
C

```

```

SUBROUTINE GRAVITY(RM,RZ,ID)

```

```

C
C
C*****
C THIS SUBROUTINE CALCULATES A VALUE FOR ACCELERATION DUE TO
C GRAVITY FOR EACH VEHICLE AT ITS CURRENT AND PREDICTED POSITION.
C CURRENT GRAVITY ACCELERATION VALUES ARE USED AT EACH
C STAGE OF THE INTEGRATION SUBROUTINE RUNKUT FOR EACH VEHICLE.
C EITHER UNIFORM GRAVITY OR AN AXISYMMETRIC GRAVITY MODEL IS USED
C AS DESIGNATED BY THE OPERATOR AT THE OUTSET OF A SCENARIO.
C*****
IMPLICIT DOUBLE PRECISION (A-H,K-M,O-Z)
CHARACTER ID*7, GRAVOPT, DRAGOPT, THROPT
COMMON/BLOK10/ PI,MU
COMMON/BLOK22/ GRAVOPT, DRAGOPT, THROPT
COMMON/BLOK27/ ANGRAVM(2), ATGRAVM(2)
COMMON/BLOK30/ MUVAL
COMMON/BLOK33/ RAVE,REQE
DIMENSION GJ(2:6),P(2:6)
DATA GJ/1082.28D-6,-2.3D-6,-2.12D-6,-0.2D-6,1.0D-6/
C*****DEFAULT VALUE FOR GRAVITATIONAL CONSTANT IS THAT OF
C A SPHERICAL EARTH WITH UNIFORM GRAVITY
C*****CALCULATE AXISYMMETRIC GRAVITY VALUE IF REQUIRED AND ASSIGN
C APPROPRIATE VALUE TO GRAVITATIONAL CONSTANT FOR RUNKUT
IF(GRAVOPT .EQ. 'Y') THEN
C*****AXISYMMETRIC GRAVITY COEFFICIENTS FOR EARTH THROUGH
C J6 ARE USED

```



```

      COSPHI = RZ/RM
P(2) = .5*(3.*COSPHI**2-1.)
P(3) = .5*(5.*COSPHI**3-3.*COSPHI)
P(4) = 1./8.*(35.*COSPHI**4-30.*COSPHI**2+3.)
P(5) = 1./8.*(63.*COSPHI**5-70.*COSPHI**3
+
+15.*COSPHI)
P(6) = 1./16.*(231.*COSPHI**6-315.*COSPHI**4
+
+105.*COSPHI**2-5.)
DO 10 I=2,6
  PJSUM = GJ(I)*(REQE/RM)**I*P(I)
  10 CONTINUE
MUVAL = NU*(1.-PJSUM)
ELSE
  MUVAL = MU
ENDIF
C*****CONVERT ACCEL FROM KM/S**2 TO M/S**2 FOR OUTPUT
C*****ASSIGN GRAVITATIONAL ACCELERATION VALUES TO APPROPRIATE
C VEHICLE FOR OUTPUT
IF(ID .EQ. 'MISSILE') THEN
  ANGRAVM(1) = (MUVAL/RM**2)*1000.
ELSE IF(ID .EQ. 'TARGET ') THEN
  ATGRAVM(1) = (MUVAL/RM**2)*1000.
  ELSE IF(ID .EQ. 'MPREDIC') THEN
  ANGRAVM(2) = (MUVAL/RM**2)*1000.
ELSE IF(ID .EQ. 'TPREDIC') THEN
  ATGRAVM(2) = (MUVAL/RM**2)*1000.
ENDIF
40 RETURN
END
C
C

```

```

SUBROUTINE DRAG(R1M,V1, ID)
C
C
C*****
C THIS SUBROUTINE CALCULATES THE VECTOR ACCELERATION DUE TO DRAG
C ACTING ON EACH VEHICLE AT THE CURRENT AND PREDICTED TIMES BASED
C ON THE CURRENT AND PREDICTED POSITION AND VELOCITY VECTORS OF
C EACH VEHICLE. PRESENT TIME DRAG CALCULATIONS ARE PERFORMED FOR
C EACH STAGE OF SUBROUTINE RUNKUT.
C*****
IMPLICIT DOUBLE PRECISION (A-H,K-M,O-Z)
CHARACTER ID*7
COMMON/BLOK23/ ATHRUST(3),ATHRM,ADrag(3),BTIME
COMMON/BLOK24/ AREAM,AREAT
COMMON/BLOK25/ MASSM,MASST
COMMON/BLOK26/ MALT(2),TALT(2),MRHO(2),TRHO(2),
+
+ AMDRAGM(2),ATDRAGM(2)
COMMON/BLOK33/ RAVE,REQE
DIMENSION R1(3),V1(3),RHO(19,2)
DATA CD/2.2/
C*****RHO DATA VALUES IN KG/M**3
DATA RHO/100.,150.,200.,250.,300.,350.,400.,450.,

```

```

+           500.,550.,600.,650.,700.,750.,800.,850.,
+ 900.,950.,1000.,
+ 5.604D-7,2.076D-9,2.541D-10,6.073D-11,
+       1.916D-11,7.014D-12,2.803D-12,1.184D-12,
+ 5.215D-13,2.384D-13,1.137D-13,5.712D-14,
+       3.070D-14,1.788D-14,1.136D-14,7.824D-15,
+       5.759D-15,4.453D-15,3.561D-15/
C*****DENSITY AT PRESENT ALTITUDE IS FOUND FROM RHO DATA
C       BY INTERPOLATION
ALT = R1M-RAVE
C*****IF ALTITUDE IS BELOW 100 KM, DENSITY IS SET TO ZERO AND
C       A WARNING IS ISSUED TO THE OPERATOR.
IF(ALT .LE. 100.) THEN
  WRITE(6,1000)
  RHOALT = 0.
  GOTO 10
ENDIF
C*****ABOVE 100 KM, DENSITY IS ASSUMED TO BE ZERO.
IF(ALT .GT. 1000.) THEN
  RHOALT = 0.
  GOTO 10
ENDIF
IALT = INT(ALT/50.)
RHO1 = RHO(IALT-1,2)
RHO2 = RHO(IALT,2)
ALT1 = RHO(IALT-1,1)
ALT2 = RHO(IALT,1)
RHOALT = RHO1+(ALT-ALT1)/(ALT2-ALT1)*(RHO2-RHO1)
10  V1M = MAGN(V1)
C*****CONVERT RHOALT FROM KG/M**3 TO KG/KM**3
RHOALT = 1.D9*RHOALT
C*****DETERMINE DRAG MAGNITUDE FOR APPROPRIATE VEHICLE AND CONVERT
C       ACCELERATION TO M/S**2 AND DENSITY TO KG/M**3 FOR OUTPUT
DCOEFF = .5*RHOALT*V1M**2*CD
IF(ID .EQ. 'MISSILE') THEN
  DRAGM = DCOEFF*AREAM/MASSM
  AMDRAGM(1) = DRAGM/1000.
  MALT(1) = ALT
  MRHO(1) = RHOALT/1.D9
ELSE IF(ID .EQ. 'TARGET ') THEN
  DRAGM = DCOEFF*AREAT/MASST
  ATDRAGM(1) = DRAGM/1000.
  TALT(1) = ALT
  TRHO(1) = RHOALT/1.D9
ELSE IF(ID .EQ. 'MPREDIC') THEN
  DRAGM = DCOEFF*AREAM/MASSM
  AMDRAGM(2) = DRAGM/1000.
  MALT(2) = ALT
  MRHO(2) = RHOALT/1.D9
ELSE IF(ID .EQ. 'TPREDIC') THEN
  DRAGM = DCOEFF*AREAT/MASST
  ATDRAGM(2) = DRAGM/1000.
  TALT(2) = ALT
  TRHO(2) = RHOALT/1.D9

```

```

ENDIF
IF((ID .EQ. 'MISSILE').OR.(ID .EQ. 'TARGET ')) THEN
    DO 20 I=1,3
        ADRAG(I) = DRAGM*(-V1(I)/V1M)
    20    CONTINUE
ENDIF
RETURN
1000    FORMAT(/5X,'WARNING - ALTITUDE IS LESS THAN 100. KM'/)
END
C
C

```

```

SUBROUTINE THRUST(TBTIME,BTINC,ISTAGE)

```

```

C
C
C*****
C DURING AN INTEGRATED ENGINE BURN FOR THE TARGET, THIS SUBROUTINE
C PERFORMS CALCULATIONS TO PROVIDE A THRUST ACCELERATION VECTOR
C FOR USE IN EACH STAGE OF SUBROUTINE RUNKUT.
C*****
IMPLICIT DOUBLE PRECISION (A-H,K-M,O-Z)
CHARACTER GRAVOPT,DRAGOPT,THROPT
LOGICAL TCHANGE,MULTOUT
COMMON/BLOK2/ RT1(3),RT1M
COMMON/BLOK6/ VT1(3),VT1M
COMMON/BLOK11/ TRTIME,TINTER
COMMON/BLOK16/ RMISS(3),MISSD
COMMON/BLOK17/ OUTTIME,TOTTIME
COMMON/BLOK20/ HRK,NRUNS,OUTSTEP,HRKNOM,HRKBURN
COMMON/BLOK22/ GRAVOPT,DRAGOPT,THROPT
COMMON/BLOK23/ ATHRUST(3),ATHRM,ADRAG(3),BTIME
COMMON/BLOK25/ MASSM,MASST
COMMON/BLOK28/ MFUEL,FUELUSE,VTBGAIN,TDIRECT(3),
+             DELVUSE,DVAVAIL,BTAVAIL,TCHANGE,MULTOUT
COMMON/BLOK29/ THRUSTM,MDOT,VACISP
COMMON/BLOK31/ DELVIMP
DATA TCHANGE /.FALSE./
DIMENSION V1(3),VGAIN(3)
IF(TBTIME+BTINC .EQ. 0.) THEN
    MASSTO = MASST
C*****INITIAL MASS OF FUEL AVAILABLE IS CALCULATED FOR ALL SCENARIOS
C BY USING A FIXED FUEL MASS FRACTION OF 0.35.
    MFUELO = .35*MASSTO
    THRMO = THRUSTM
    MDOT = THRUSTM/(VACISP*.00981)
    MDOTO = MDOT
ENDIF
C*****DETERMINE VELOCITY-TO-BE-GAINED
C*****DETERMINE DIRECTION OF THRUST VECTOR FOR PRESENT
C TIME STEP
IF(ISTAGE .EQ. 1) THEN
    DO 20 I=1,3
        V1(I) = VT1(I)
    20    CONTINUE

```

```

CALL LAMBERT(RT1,RMISS,TINTER-TOTTIME)
DO 25 I=1,3
  VGAIN(I) = VT1(I)-V1(I)
  VT1(I) = V1(I)
  25 CONTINUE
VT1M = MAGN(VT1)
VTBGAIN = MAGN(VGAIN)
DO 30 I=1,3
  TDIRECT(I) = VGAIN(I)/VTBGAIN
  30 CONTINUE
C*****CHECK FOR INSUFFICIENT FUEL
IF(MDOT*(TBTIME+HRK) .GT. MFUELO) THEN
  THROPT = '0'
  CALL THROUT
  WRITE(6,1100)
  WRITE(1,1100)
  TBTIME = TBTIME-OUTSTEP
  DO 40 I=1,3
    ATHRUST(I) = 0.
  40 CONTINUE
  ATHRM = 0.
  GOTO 100
ENDIF
C*****CHECK FOR A THRUST REDUCTION AND USE THE APPROPRIATE EQUATIONS
C      TO DETERMINE FUEL AND DELTA V USED AND AVAILABLE AND
C      BURN TIME AVAILABLE
IF(TCHANGE .EQ. .TRUE.) THEN
  MASS1 = MASSTO-FUELUSE
  MASS2 = MASS1-MDOT*HRK
  MFUEL = MFUELO-MDOT*HRK
  FUELUSE = MFUELO-MFUEL
  DELVUSE = DELVUSE+.00981*VACISP*DLOG(MASS1/MASS2)
  DVAVAIL = .00981*VACISP*DLOG((MASSTO-FUELUSE)
    + /((MASSTO-MFUELO)))
  BTAVAIL = MFUEL*.00981*VACISP/THRMO
ELSE
  MFUEL = MFUELO-MDOT*TBTIME
  FUELUSE = MFUELO-MFUEL
  DELVUSE = .00981*VACISP*DLOG(MASSTO/(MASSTO-FUELUSE))
  DVAVAIL = .00981*VACISP*DLOG((MASSTO-FUELUSE)
    + /((MASSTO-MFUELO)))
  BTAVAIL = MFUEL/MDOT
ENDIF
ENDIF
C*****DETERMINE NEW VEHICLE MASS FOR THRUST AND DRAG CALCULATIONS
IF(TCHANGE .EQ. .TRUE.) THEN
  MINIT = MASSTO-MDOTO*TBTIMEO
  IF(ISTAGE .EQ. 1) MINIT = MINIT-MDOT*HRK
ELSE
  MINIT = MASSTO-MDOT*TBTIME
ENDIF
MASST = MINIT-MDOT*BTINC
C*****CHECK VELOCITY-TO-BE-GAINED MAGNITUDE FOR THRUST REDUCTION
C      AND ENGINE CUTOFF

```

```

      IF((ISTAGE .EQ. 1).AND.(VTBGAIN .LT.
+      .00981*VACISP*DLOG(MASST/(MASST-MDOT*HRK)))) THEN
      IF(TCHANGE .EQ. .FALSE.) THEN
THRUSTM = .00981*VACISP*MASST/HRK*(1.-DEXP(-VTBGAIN/
+      (.00981*VACISP)))
MDOT = THRUSTM/(.00981*VACISP)
ATHRM = THRUSTM/MASST
TBTIMEO = TBTIME
TCHANGE = .TRUE.
CALL THROUT
GOTO 60
ENDIF
THROPT = '0'
DO 50 I=1,3
  ATHRUST(I) = 0.
  50 CONTINUE
ATHRM = 0.
THRUSTM = 0.
MDOT = 0.
  CALL THROUT
WRITE(6,1000)
WRITE(1,1000)
THRUSTM = THRMO
MDOT = MDOTO
TRTIME = TRTIME-OUTSTEP
GOTO 100
  ENDIF
  60 ATHRM = THRUSTM/MASST
C*****DETERMINE THRUST ACCELERATION VECTOR FOR THIS TIME STEP
DO 70 I=1,3
  ATHRUST(I) = ATHRM*TDIRECT(I)
  70 CONTINUE
  100 RETURN
  1000 FORMAT(/5X,'EVASIVE MANEUVER COMPLETED - THRUST TERMINATED'/)
  1100 FORMAT(/5X,'EVASIVE MANEUVER ABORTED - INSUFFICIENT FUEL'/)
END
C
C

```

```

SUBROUTINE ORBELS(R1,V1,ID)

```

```

C

```

```

C

```

```

C*****
C THIS SUBROUTINE CALCULATES THE ORBITAL ELEMENTS OF AN ORBIT FROM
C A POSITION AND VELOCITY VECTOR
C*****

```

```

IMPLICIT DOUBLE PRECISION (A-H,K-M,O-Z)

```

```

CHARACTER ID*7

```

```

DIMENSION R1(3),V1(3)

```

```

COMMON/BLOK10/ PI,MU

```

```

COMMON/BLOK12/ HM,PM,AM,EM,MI

```

```

COMMON/BLOK13/ HT,PT,AT,ET,TI

```

```

DIMENSION HVECT(3)

```

```

R1M = MAGN(R1)

```

```

V1M = MAGN(V1)
H = CPRODM(R1,V1,HVECT)
P = H**2/MU
A = 1./(2./R1M-V1M**2/MU)
E = DSQRT(1.-P/A)
ORBINCL = 180./PI*DACOS(ABS(HVECT(3))/H)
IF(ID .EQ. 'MISSILE') THEN
  HM = H
  PM = P
  AM = A
  EM = E
  MI = ORBINCL
ELSE
  HT = H
  PT = P
  AT = A
  ET = E
  TI = ORBINCL
ENDIF
RETURN
END
C
C
SUBROUTINE CIRCORB(RM,THETA,ORBINCL,R)
C
C
C*****
C THIS SUBROUTINE CALCULATES THE MAGNITUDE OF THE CIRCULAR ORBIT
C VELOCITY OF A VEHICLE AND CALCULATES THE VECTOR POSITION OF A
C VEHICLE FROM ITS ANGULAR POSITION AND INCLINATION FOR USE
C IN SUBROUTINE SETUP.
C*****
IMPLICIT DOUBLE PRECISION (A-H,J-M,O-Z)
COMMON/BLOK10/ PI,MU
DIMENSION R(3)
VM = DSQRT(MU/RM)
R(1) = RM*DCOSD(THETA)
R(2) = RM*DSIND(THETA)*DCOSD(ORBINCL)
R(3) = RM*DSIND(THETA)*DSIND(ORBINCL)
RETURN
END
C
C
SUBROUTINE RELVECT(RM,RT,OUTOPT)
C
C
C*****
C THIS SUBROUTINE CALCULATES THE RELATIVE POSITION VECTORS SEPARATING
C THE MISSILE AND TARGET AT THE CURRENT AND PREDICTED TIMES.
C*****
IMPLICIT DOUBLE PRECISION (A-H,K-M,O-Z)
CHARACTER OUTOPT*9
COMMON/BLOK14/ RMTACT(3),RMTACTM
COMMON/BLOK15/ RMTPRE(3),RMTPREM

```

```

DIMENSION RM(3),RT(3)
IF(OUTOPT .EQ. 'ACTUAL ') THEN
  DO 10 I=1,3
    RMTACT(I) = RM(I)-RT(I)
  10 CONTINUE
  RMTACTM = MAGN(RMTACT)
ELSE
  DO 20 I=1,3
    RMTPRE(I) = RM(I)-RT(I)
  20 CONTINUE
  RMTPREM = MAGN(RMTPRE)
ENDIF
RETURN
END
C
C

```

SUBROUTINE EVADE

```

C
C
C*****
C THIS SUBROUTINE MAKES THE APPROPRIATE POSITION AND VELOCITY CALCULATIONS
C NEEDED TO PERFORM AN EVASIVE MANEUVER BASED ON THE MANEUVERING
C OPTION AND MISS DISTANCE INPUT BY THE OPERATOR. VELOCITY-TO-BE-GAINED
C CALCULATIONS ARE MADE WITH A CALL TO SUBROUTINE LAMBERT.
C*****
IMPLICIT DOUBLE PRECISION (A-H,K-M,O-Z)
CHARACTER GRAVOPT,DRAGOPT,THROPT,MISSOPT
COMMON/BLOK2/ RT1(3),RT1M
COMMON/BLOK3/ RM2(3),RM2M
COMMON/BLOK4/ RT2(3),RT2M
COMMON/BLOK6/ VT1(3),VT1M
COMMON/BLOK8/ VT2(3),VT2M
COMMON/BLOK11/ TRTIME,TINTER
COMMON/BLOK14/ RMTACT(3),RMTACTM
COMMON/BLOK15/ RMTPRE(3),RMTPREM
COMMON/BLOK16/ RMISS(3),MISSD
COMMON/BLOK22/ GRAVOPT,DRAGOPT,THROPT
COMMON/BLOK31/ DELVIMP
DIMENSION V1(3),R2(3),VTBGAIN(3),HVECT(3),MISSDV(3)
WRITE(6,1000)
WRITE(6,1300)
WRITE(1,1000)
C*****INFORM THE OPERATOR AN EVASIVE MANEUVER IS REQUIRED AND ASK
C FOR THE MISS DISTANCE MAGNITUDE AND DIRECTIONAL OPTION
C DESIRED BY THE OPERATOR
READ(5,1400) MISSOPT,MISSD
C*****PERFORM THE APPROPRIATE CALCULATIONS FOR THE SELECTED MANEUVER OPTION
IF(MISSOPT .EQ. 'C') THEN
  WRITE(1,1550) MISSOPT
  WRITE(6,1900)
  READ(5,2000) HMISSD,RMISSD,VMISSD
  WRITE(1,2100) HMISSD,RMISSD,VMISSD
  GOTO 5

```

```

ENDIF
WRITE(1,1500) MISSOPT,MISSD
  5 DO 10 I=1,3
    V1(I) = VT1(I)
    10 CONTINUE
IF((MISSOPT .EQ. 'H').OR.(MISSOPT .EQ. 'C')) THEN
  HVECTM = CPROD(RT2,VT2,HVECT)
  IF(MISSOPT .EQ. 'C') THEN
    DO 30 I=1,3
      RMISS(I) = RM2(I)+HMISSD*HVECT(I)/HVECTM
      RMISS(I) = RMISS(I)+RMISSD*RT2(I)/RT2M
      RMISS(I) = RMISS(I)+VMISSD*VT2(I)/VT2M
      MISSDV(I) = RMISS(I)-RM2(I)
    30 CONTINUE
    MISSD = MAGN(MISSDV)
    WRITE(6,2200) MISSD
    WRITE(1,2200) MISSD
    GOTO 70
  ENDIF
ELSE
  GOTO 50
ENDIF
DO 40 I=1,3
  RMISS(I) = RM2(I)+MISSD*HVECT(I)/HVECTM
40 CONTINUE
  GOTO 70
50 DO 60 I=1,3
  IF(MISSOPT .EQ. 'E') THEN
    RMISS(I) = RM2(I)+MISSD*RMTPRE(I)/RMTPREM
  ELSE IF(MISSOPT .EQ. 'R') THEN
    RMISS(I) = RM2(I)+MISSD*RT2(I)/RT2M
  ELSE IF(MISSOPT .EQ. 'V') THEN
    RMISS(I) = RM2(I)+MISSD*VT2(I)/VT2M
  ENDIF
  60 CONTINUE
  70 CALL LAMBERT(RT1,RMISS,TRTIME)
MISSD = DABS(MISSD)
DO 80 I=1,3
  VTBGAIN(I) = VT1(I)-V1(I)
  80 CONTINUE
DELVIMP = MAGN(VTBGAIN)
*****DISPLAY TO THE OPERATOR THE MAGNITUDE AND COMPONENTS OF THE
C VELOCITY VECTOR REQUIRED TO PERFORM THE DESIGNATED MANEUVER
*****THE OPERATOR WILL DECIDE IF AN IMPULSIVE VELOCITY ADDITION,
C ENGINE BURN, OR NO EVASION WILL BE PERFORMED.
WRITE(6,1100) DELVIMP
WRITE(1,1100) DELVIMP
WRITE(8,1150) RMTACTM, DELVIMP
WRITE(6,1200) VTBGAIN(1),VTBGAIN(2),VTBGAIN(3)
WRITE(1,1200) VTBGAIN(1),VTBGAIN(2),VTBGAIN(3)
WRITE(6,1600)
READ(5,1700) THROPT
WRITE(1,1800) THROPT
*****IF AN IMPULSIVE VELOCITY CHANGE IS DESIRED, UPDATE THE TARGET'S

```



```

C      VELOCITY AT ITS PRESENT POSITION
IF(THROPT .NE. 'I') THEN
  DO 90 I=1,3
    VT1(I) = V1(I)
  90   CONTINUE
  VT1M = MAGN(VT1)
ENDIF
RETURN
1000  FORMAT(/5X,'EVASIVE MANEUVER REQUIRED'/)
1100  FORMAT(/5X,'REQUIRED IMPULSIVE DELV = ',F12.6/)
1150  FORMAT(1X,F10.4,F9.6/)
1200  FORMAT(/5X,'REQUIRED IMPULSIVE '
+      'DELV VECTOR (DELVX,DELVY,DELVZ) = ',3F12.6/)
1300  FORMAT(/1X,'INPUT MANEUVER OPTION (R,V,H,E,C), ',
+      'DESIRED MISS DISTANCE (+KM OR -KM):')
1400  FORMAT(A1,1X,F12.4)
1500  FORMAT(/5X,'INPUT MANEUVER OPTION (R,V,H,E,C), ',
+      'DESIRED MISS DISTANCE (KM): ',A1,F12.4/)
1550  FORMAT(/5X,'INPUT MANEUVER OPTION (R,V,H,E,C): ',A1/)
1600  FORMAT(1X,'SELECT IMPULSIVE DELV, ENGINE BURN OR NO EVASION',
+      ': (I,E OR N)')
1700  FORMAT(A1)
1800  FORMAT(/5X,'SELECT IMPULSIVE DELV, ENGINE BURN OR NO EVASION',
+      ': (I,E OR N) ',A1/)
1900  FORMAT(1X,'INPUT HMISSD,RMISSD,VMISSD: (+KM OR -KM)')
2000  FORMAT(3F12.4)
2100  FORMAT(/5X,'INPUT DESIRED MISS DISTANCES IN THE H,R, AND V',
+      ' DIRECTIONS: (KM) ',3F12.4/)
2200  FORMAT(/5X,'RESULTING MISS DISTANCE = ',F12.4/)
END
C
C

```

SUBROUTINE SAFE(NRUNS)

```

C
C
C*****
C THIS SUBROUTINE CALCULATES THE FINAL ORBITAL ELEMENTS OF THE ORBITS
C OF BOTH VEHICLES WITH A CALL TO SUBROUTINE ORBELS AND PREPARES FOR
C SCENARIO TERMINATION.
C*****
IMPLICIT DOUBLE PRECISION (A-H,K-M,O-Z)
CHARACTER TERMOUT,PHASE*9
COMMON/BLOK1/ RM1(3),RM1M
COMMON/BLOK2/ RT1(3),RT1M
COMMON/BLOK5/ VM1(3),VM1M
COMMON/BLOK6/ VT1(3),VT1M
COMMON/BLOK12/ HM,PH,AM,EM,MI
COMMON/BLOK13/ HT,PT,AT,ET,TT
COMMON/BLOK19/ PHASE
COMMON/BLOK21/ TERMOUT
CALL ORBELS(RM1,VM1,'MISSILE')
CALL ORBELS(RT1,VT1,'TARGET ')
C*****IF THE REQUESTED NUMBER OF DATA BLOCKS HAVE BEEN RUN AND

```

```

C      THE PREDICTED RELATIVE POSITION VECTOR IS STILL DECREASING
C      A WARNING IS ISSUED TO THE OPERATOR.
IF(PHASE .EQ. 'MAXRUNS ') THEN
  WRITE(6,1020) NRUNS
  WRITE(1,1020) NRUNS
  WRITE(6,1025)
  WRITE(1,1025)
  PHASE = 'POSTEVADE'
  GOTO 10
ENDIF
CALL PUTOUT('POSTEVADE')
C*****DECLARE A SUCCESSFUL EVASION IF THE MAGNITUDE OF THE PREDICTED
C      RELATIVE POSITION VECTOR IS INCREASING WITH TIME AS DETERMINED
C      IN THE TOP LEVEL OF THE PROGRAM.
WRITE(6,1010)
WRITE(1,1010)
  10 WRITE(6,1050)
WRITE(6,1060)
WRITE(6,1000) HT,PT,AT,ET,TI
WRITE(6,1100)
WRITE(6,1060)
WRITE(6,1000) HM,PM,AM,EM,MI
WRITE(1,1050)
WRITE(1,1060)
WRITE(1,1000) HT,PT,AT,ET,TI
WRITE(1,1100)
WRITE(1,1060)
WRITE(1,1000) HM,PM,AM,EM,MI
RETURN
  1000 FORMAT(5X,5F12.4/)
  1010 FORMAT(/5X,'MISSILE SUCCESSFULLY EVADED'//)
  1020 FORMAT(/5X,'OUTPUT TERMINATED AFTER ',I4,' RUNS AS ',
+           ' REQUESTED'//)
  1025 FORMAT(/5X,'WARNING - PREDICTED MISS DISTANCE IS ',
+           ' DECREASING'//)
  1050 FORMAT(18X,'FINAL ORBITAL ELEMENTS FOR THE TARGET')
  1060 FORMAT(/12X,'H',11X,'P',11X,'A',11X,'E',11X,'I')
  1100 FORMAT(18X,'FINAL ORBITAL ELEMENTS FOR THE MISSILE')
END
C
C
      FUNCTION MAGN(VECT)
C
C
C*****
C THIS FUNCTION CALCULATES THE MAGNITUDE OF A VECTOR
C*****
IMPLICIT DOUBLE PRECISION (A-H,K-M,O-Z)
DIMENSION VECT(3)
MAGN = DSQRT(VECT(1)**2+VECT(2)**2+VECT(3)**2)
RETURN
END
C

```

```

C
FUNCTION CPROD(VECT1,VECT2,CROSSP)
C
C
C*****
C THIS FUNCTION CALCULATES THE MAGNITUDE OF THE CROSS
C PRODUCT OF TWO VECTORS
C*****
IMPLICIT DOUBLE PRECISION (A-H,K-M,O-Z)
DIMENSION VECT1(3),VECT2(3),CROSSP(3)
CROSSP(1) = VECT1(2)*VECT2(3)-VECT2(2)*VECT1(3)
CROSSP(2) = -(VECT1(1)*VECT2(3)-VECT2(1)*VECT1(3))
CROSSP(3) = VECT1(1)*VECT2(2)-VECT2(1)*VECT1(2)
CPRODM = MAGN(CROSSP)
RETURN
END
C
C

```

SUBROUTINE PUTIN

```

C
C
C*****
C THIS SUBROUTINE IS USED TO INITIALIZE ALL VARIABLES AND OPTIONS WHICH
C THE OPERATOR CAN INPUT AT THE START OF A RUN. IF A NEW SCENARIO WAS
C NOT SETUP FIRST WITH SUBROUTINE SETUP, NEW INPUT VECTORS CAN BE
C MANUALLY INPUT BY THE OPERATOR HERE, IF DESIRED. ALSO, INTEGRATION
C TIME STEPS FOR BALLISTIC AND ENGINE BURN CALCULATIONS, NEW VEHICLE
C MASSES, CROSS-SECTIONAL AREAS, MAXIMUM TARGET THRUST LEVEL, GRAVITY
C AND DRAG OPTIONS, OUTPUT OPTIONS, AND THRUST AND TRAJECTORY OUTPUT
C TIME STEPS ARE ENTERED HERE.
C*****
IMPLICIT DOUBLE PRECISION (A-H,K-M,O-Z)
CHARACTER TERMOUT,PHASE*9,GRAVOPT,DRAGOPT,THROPT,
+
ENGOPT,INPOPT,SETOPT,HEADOPT
COMMON/BLOK1/ RM1(3),RM1M
COMMON/BLOK2/ RT1(3),RT1M
COMMON/BLOK6/ VT1(3),VT1M
COMMON/BLOK16/ RMISS(3),MISSD
COMMON/BLOK18/ RMO(3),RMOM,FIXTIME
COMMON/BLOK19/ PHASE
COMMON/BLOK20/ HRK,NRUNS,OUTSTEP,HRKNOM,HRKBURN
COMMON/BLOK21/ TERMOUT
COMMON/BLOK22/ GRAVOPT,DRAGOPT,THROPT
COMMON/BLOK24/ AREAM,AREAT
COMMON/BLOK25/ MASSM,MASST
COMMON/BLOK29/ THRUSTM,MDOT,VACISP
COMMON/BLOK32/ SETOPT
COMMON/BLOK34/ TOSTEP
IF(SETOPT.EQ.'Y')GOTO 10
WRITE(6,1000)
READ(5,2600) INPOPT
IF(INPOPT.EQ.'N')GOTO 10
WRITE(6,1050)

```

```

READ(5,1100) RT1(1),RT1(2),MISSD
WRITE(6,1200)
READ(5,1100) RMO(1),RMO(2),RMO(3)
WRITE(6,1300)
READ(5,1100) RM1(1),RM1(2),RM1(3)
WRITE(6,1800)
READ(5,2000) FIXTIME
RT1(3) = 0.
WRITE(1,1500) RT1(1),RT1(2),MISSD
WRITE(1,1600) RMO(1),RMO(2),RMO(3)
WRITE(1,1700) RM1(1),RM1(2),RM1(3)
WRITE(1,1900) FIXTIME
10 WRITE(6,4300)
READ(5,4200) IO
WRITE(6,2100)
READ(5,2200) HRKNOM,HRKBURN,TOSTEP,OUTSTEP,NRUNS
HRK = HRKNOM
WRITE(1,2300) HRKNOM,HRKBURN,TOSTEP,OUTSTEP,NRUNS
WRITE(3,2400) NRUNS
WRITE(6,2700)
READ(5,2800) GRAVOPT,DRAGOPT
WRITE(1,2900) GRAVOPT,DRAGOPT
IF(DRAGOPT.EQ.'Y') THEN
WRITE(6,3000)
READ(5,2800) AREAOPT,MASSOPT
IF(AREAOPT.EQ.'Y') THEN
WRITE(6,3100)
READ(5,3500) AREAM,AREAT
WRITE(1,3200) AREAM,AREAT
C*****CONVERT AREAS FROM M**2 TO KM**2
AREAM = 1.D-6*AREAM
AREAT = 1.D-6*AREAT
ENDIF
IF(MASSOPT.EQ.'Y') THEN
WRITE(6,3300)
READ(5,3500) MASSM,MASST
WRITE(1,3400) MASSM,MASST
ENDIF
ENDIF
WRITE(6,3600)
READ(5,2600) ENGOPT
IF(ENGOPT.EQ.'Y') THEN
WRITE(6,3700)
READ(5,2000) THRUSTM
WRITE(1,3800) THRUSTM
C*****CONVERT THRUST FROM NEWTONS TO KILONEWTONS FOR INTERNAL CALCULATION
THRUSTM = THRUSTM/1000.
ENDIF
WRITE(6,2500)
READ(5,2800) TERMOUT,HEADOPT
WRITE(6,3900)
WRITE(1,3900)
WRITE(6,3950) FIXTIME
WRITE(1,3950) FIXTIME

```

```

        WRITE(6,4000) RMO(1),RMO(2),RMO(3),RM1(1),RM1(2),RM1(3)
WRITE(6,4100) RT1(1),RT1(2),RT1(3),VT1(1),VT1(2),VT1(3)
        WRITE(1,4000) RMO(1),RMO(2),RMO(3),RM1(1),RM1(2),RM1(3)
WRITE(1,4100) RT1(1),RT1(2),RT1(3),VT1(1),VT1(2),VT1(3)
IF(HEADOPT .EQ. 'Y') THEN
        WRITE(6,1400)
        WRITE(1,1400)
ENDIF
RETURN
1000  FORMAT(1X,'INPUT NEW INITIAL POSITION VECTORS? (Y OR N)')
1050  FORMAT(/1X,'INPUT RT1X,RT1Y,MISSD:')
1100  FORMAT(3F12.4)
1200  FORMAT(1X,'INPUT RMOX,RMOY,RMOZ:')
1300  FORMAT(1X,'INPUT RM1X,RM1Y,RM1Z:')
1400  FORMAT(/24X,'MISSILE AND TARGET TRAJECTORIES'/,24X,31('-'),
+      /17X,'TIME IN SEC, DISTANCE IN KM, VELOCITY IN KM/S'/,
+      7X,'ACCELERATION DUE TO DRAG AND GRAVITY IN M/S**2, '
+      'DENSITY IN KG/M**3'/,9X,
+      'THRUST ACCELERATION IN KM/S**2, MASS IN KG, '
+      'THRUST IN NEWTONS'/,24X,'VACISP IN SEC, MASSFLOW IN '
+      'KG/S'//)
1500  FORMAT(/5X,'INPUT RT1X,RT1Y,MISSD:',3F12.4)
1600  FORMAT(5X,'INPUT RMOX,RMOY,RMOZ:',3F12.4)
1700  FORMAT(5X,'INPUT RM1X,RM1Y,RM1Z:',3F12.4)
1800  FORMAT(1X,'INPUT TIME BETWEEN FIXES:')
1900  FORMAT(5X,'INPUT TIME BETWEEN FIXES:',F12.4//)
2000  FORMAT(F12.4)
2100  FORMAT(1X,'INPUT INTSTEP,BURNSTEP,THOUTSTEP,OUTSTEP,NRUNS:')
2200  FORMAT(4F12.4,I4)
2300  FORMAT(/5X,'INPUT INTSTEP,BURNSTEP,THOUTSTEP,OUTSTEP,NRUNS:',
+      3F7.3,2X,F8.3,I4/)
2400  FORMAT(1X,I4)
2500  FORMAT(1X,'TERMINAL OUTPUT,HEADING? (Y OR N)')
2600  FORMAT(A1)
2700  FORMAT(1X,'AXISYMMETRIC GRAVITY,DRAG? (Y OR N) ')
2800  FORMAT(A1,1X,A1)
2900  FORMAT(/5X,'AXISYMMETRIC GRAVITY,DRAG? (Y OR N) ',A1',',A1/)
3000  FORMAT(1X,'INPUT VEHICLE AREAS, MASSES? (Y OR N) ')
3100  FORMAT(1X,'INPUT CROSS-SECT AREAS FOR MISSILE AND TARGET ',
+      '(SQUARE METERS):')
3200  FORMAT(/5X,'INPUT CROSS-SECT AREAS FOR MISSILE AND TARGET ',
+      '(SQUARE METERS:',2F12.4/)
3300  FORMAT(1X,'INPUT TOTAL MISSILE AND TARGET MASSES (KG):')
3400  FORMAT(/5X,'INPUT TOTAL MISSILE AND TARGET MASSES (KG):',
+      2F12.4/)
3500  FORMAT(2F12.4)
3600  FORMAT(1X,'SET ENGINE THRUST? (Y OR N)')
3700  FORMAT(1X,'INPUT NEW ENGINE THRUST (NEWTONS):')
3800  FORMAT(/5X,'INPUT NEW ENGINE THRUST (NEWTONS): ',F12.4/)
3900  FORMAT(/24X,'INITIAL INPUT VECTORS FOR THIS RUN',/24X,34('-'))
3950  FORMAT(22X,'(TIME BETWEEN MISSILE FIXES:',F12.4,')')
4000  FORMAT(5X,T6,'RMOX',T<IO*5+18>,'RMOY',T<IO*10+31>,'RMOZ',
+      T<IO*15+42>,'RM1X',T<IO*20+54>,'RM1Y',T<IO*22+67>,
+      'RM1Z'/,6F<IO*4+12>.<IO*4+4>/)

```

```

4100  FORMAT(5X,T6,'RT1X',T<IO*5+18>,'RT1Y',T<IO*10+31>,'RT1Z',
+      T<IO*15+42>,'VT1X',T<IO*20+54>,'VT1Y',T<IO*22+67>,
+      'VT1Z'/.6F<IO*4+12>.<IO*4+4>/)
4200  FORMAT(I1)
4300  FORMAT(1X,'F12.4 OR F16.8 INITIAL VECTORS OUTPUT FORMAT?',
+      ' (0 OR 1)')
      END
C
C

```

SUBROUTINE PUTOUT(OUTOPT)

```

C
C
C*****
C THIS SUBROUTINE PROVIDES FOR THE OUTPUT OF ALL TIME, POSITION, VELOCITY,
C ACCELERATION, AND DENSITY DATA DISPLAYED IN THE CURRENT AND PREDICTED
C TRAJECTORY DATA BLOCKS OF BOTH VEHICLES. DATA SPECIFICALLY PERTAINING
C TO AN ENGINE BURN IS OUTPUT BY SUBROUTINE THROUT. SUBROUTINE PUTOUT IS
C CALLED EACH TIME THE VARIABLE OUTTIME IS INCREMENTED BY THE VALUE OF
C OUTSTEP IN THE TOP LEVEL OF THE PROGRAM AND AT OTHER TIMES WHEN
C APPROPRIATE, SUCH AS AFTER AN IMPULSIVE VELOCITY CHANGE FOR THE TARGET.
C OUTPUT IS SENT TO THE TERMINAL, IF DESIRED, AND TO DATA STORAGE FILES
C FOR MAKING HARDCOPIES AND PLOTS.
C*****
C DIMENSIONAL UNITS OF OUTPUT VARIABLES ARE AS FOLLOWS:
C TIME IN SEC, POSITION IN KM, VELOCITY IN KM/SEC,
C ACCELERATION IN M/SEC**2, AND DENSITY RHO IN KG/M**3.
C*****
IMPLICIT DOUBLE PRECISION (A-H,K-M,O-Z)
CHARACTER OUTOPT*9,PHASE*9,TERMOUT,GRAVOPT,
+      DRAGOPT,THROPT
COMMON/BLOK1/ RM1(3),RM1M
COMMON/BLOK2/ RT1(3),RT1M
COMMON/BLOK3/ RM2(3),RM2M
COMMON/BLOK4/ RT2(3),RT2M
COMMON/BLOK5/ VM1(3),VM1M
COMMON/BLOK6/ VT1(3),VT1M
COMMON/BLOK7/ VM2(3),VM2M
COMMON/BLOK8/ VT2(3),VT2M
COMMON/BLOK10/ PI,MU
COMMON/BLOK11/ TRTIME,TINTER
COMMON/BLOK14/ RMTACT(3),RMTACTM
COMMON/BLOK15/ RMTPRE(3),RMTPREM
COMMON/BLOK17/ OUTTIME,TOTTIME
COMMON/BLOK19/ PHASE
COMMON/BLOK20/ HRK,NRUNS,OUTSTEP,HRKNOM,HRKBURN
COMMON/BLOK21/ TERMOUT
COMMON/BLOK22/ GRAVOPT,DRAGOPT,THROPT
COMMON/BLOK26/ MALT(2),TALT(2),MRHO(2),TRHO(2),
+      AMDRAGM(2),ATDRAGM(2)
COMMON/BLOK27/ AMGRAVM(2),ATGRAVM(2)
DATA IP1RUNS,IP2RUNS/0,0/
      IF(OUTOPT.EQ.'ACTUAL')THEN
          IF(TERMOUT.EQ.'N')THEN

```

```

      I = 1
ELSE
      I = 6
ENDIF
      10      WRITE(I,1000)
      WRITE(I,1100)
      WRITE(I,1500) OUTTIME,RMTACTM,RMTACT(1),RMTACT(2),RMTACT(3)
      WRITE(I,2000)
      WRITE(I,1200)
            WRITE(I,1500) MALT(1),RM1M,RM1(1),RM1(2),RM1(3)
      WRITE(I,1300)
      WRITE(I,1500) VM1M,VM1(1),VM1(2),VM1(3),AMGRAVM(1)
      IF(DRAGOPT .EQ. 'Y') THEN
            WRITE(I,1400)
            WRITE(I,1600) AMDRAGM(1),MRHO(1)
      ENDIF
      WRITE(I,2100)
      WRITE(I,1200)
            WRITE(I,1500) TALT(1),RT1M,RT1(1),RT1(2),RT1(3)
      WRITE(I,1300)
      WRITE(I,1500) VT1M,VT1(1),VT1(2),VT1(3),ATGRAVM(1)
      IF(DRAGOPT .EQ. 'Y') THEN
            WRITE(I,1400)
            WRITE(I,1600) ATDRAGM(1),TRHO(1)
      ENDIF
      IF(I .EQ. 6) THEN
            I = 1
            GOTO 10
      ENDIF
      IF(THROPT .EQ. 'E') CALL THROUT
            WRITE(3,1700) OUTTIME
            WRITE(3,1800) RM1(1),RM1(2),RM1(3),RT1(1),RT1(2),
            +
            RT1(3)
            WRITE(3,1800) VM1(1),VM1(2),VM1(3),VT1(1),VT1(2),
            +
            VT1(3)
      ELSE IF(OUTOPT .EQ. 'PREDICTED') THEN
            TTPRED = OUTTIME+TRTIME
            IF(TERMOUT .EQ. 'N') THEN
                  I = 1
            ELSE
                  I = 6
            ENDIF
            20      WRITE(I,1050)
            WRITE(I,1100)
            WRITE(I,1500) TTPRED,RMTPREM,RMTPRE(1),RMTPRE(2),RMTPRE(3)
            WRITE(I,2000)
            WRITE(I,1200)
                  WRITE(I,1500) MALT(2),RM2M,RM2(1),RM2(2),RM2(3)
            WRITE(I,1300)
            WRITE(I,1500) VM2M,VM2(1),VM2(2),VM2(3),AMGRAVM(2)
            IF(DRAGOPT .EQ. 'Y') THEN
                  WRITE(I,1400)
                  WRITE(I,1600) AMDRAGM(2),MRHO(2)
            ENDIF

```

```

WRITE(I,2100)
WRITE(I,1200)
      WRITE(I,1500) TALT(2),RT2M,RT2(1),RT2(2),RT2(3)
WRITE(I,1300)
WRITE(I,1500) VT2M,VT2(1),VT2(2),VT2(3),ATGRAVM(2)
IF(DRAGOPT .EQ. 'Y') THEN
      WRITE(I,1400)
      WRITE(I,1600) ATDRAGM(2),TRHO(2)
ENDIF
IF(I .EQ. 6) THEN
      I = 1
      GOTO 20
ENDIF
      IF(PHASE .EQ. 'EVADING ') THEN
      IP2RUNS = IP2RUNS+1
      WRITE(4,1700) TTPRED
      WRITE(4,1800) RM2(1),RM2(2),RM2(3),RT2(1),RT2(2),
      +
      RT2(3)
      WRITE(4,1800) VM2(1),VM2(2),VM2(3),VT2(1),VT2(2),
      +
      VT2(3)
      ELSE IF(PHASE .EQ. 'PREEVADE ') THEN
      IP1RUNS = IP1RUNS+1
      WRITE(7,1700) TTPRED
      WRITE(7,1800) RM2(1),RM2(2),RM2(3),RT2(1),RT2(2),
      +
      RT2(3)
      WRITE(7,1800) VM2(1),VM2(2),VM2(3),VT2(1),VT2(2),
      +
      VT2(3)
      ENDIF
      ELSE IF(OUTOPT .EQ. 'POSTEVADE') THEN
      WRITE(4,1900) IP2RUNS
      WRITE(7,1900) IP1RUNS
      ENDIF
      RETURN
      1000  FORMAT(/32X,'CURRENT TIME'/,32X,12('--'))/
      1050  FORMAT(/32X,'PREDICTED TIME'/,32X,14('--'))/
      1100  FORMAT(11X,'TIME',8X,'RREL',8X,'RRELX',7X,'RRELY',7X,
      +
      'RRELZ')
      1200  FORMAT(/11X,'ALT',10X,'R',10X,'RX',10X,'RY',
      +
      10X,'RZ')
      1300  FORMAT(11X,'VMAG',8X,'VX',10X,'VY',10X,'VZ',
      +
      7X,'ACCELGRAV')
      1400  FORMAT(9X,'DECCELDRAG',6X,'RHO')
      1500  FORMAT(5X,5F12.4/)
      1600  FORMAT(5X,2G14.4/)
      1700  FORMAT(1X,F12.4)
      1800  FORMAT(1X,6F12.4)
      1900  FORMAT(1X,I4)
      2000  FORMAT(32X,'MISSILE VALUES')
      2100  FORMAT(32X,'TARGET VALUES')
      END
      C
      C
      SUBROUTINE THROUT
      C

```



```

C
C*****
C THIS SUBROUTINES PROVIDES FOR THE OUTPUT OF ALL PARAMETERS
C SPECIFICALLY PERTAINING TO THE TARGET'S ENGINE WHEN IT IS THRUSTING.
C ELAPSED TIME OF THE CURRENT BURN, TOTAL BURN-TIME OF THE ENGINE IN A
C SCENARIO, IF MULTIPLE ENGINE BURNS WERE LATER PROVIDED FOR IN EVADER,
C FUEL AND DELTA V USED AND AVAILABLE, THRUST LEVEL, DIRECTION AND
C ACCELERATION, CURRENT VELOCITY-TO-BE-GAINED, MASS FLOW, AND ENGINE
C VACUUM ISP ARE ALL OUPUT.
C*****
C DIMENSIONAL UNITS OF THE OUTPUT ARE AS FOLLOWS: TIME IN SEC,
C VELOCITY IN KM/S, ACCELERATION IN KM/SEC, THRUST IN NEWTONS,
C FUEL MASS IN KG, THRUST DIRECTION (UNIT VECTOR), ISP IN SEC,
C MASS FLOW IN KG/S
C*****
IMPLICIT DOUBLE PRECISION (A-H,K-M,O-Z)
CHARACTER TERMOUT, GRAVOPT, DRAGOPT, THROPT
LOGICAL TCHANGE, MULTOUT
COMMON/BLOK17/ OUTTIME, TOTTIME
COMMON/BLOK21/ TERMOUT
COMMON/BLOK22/ GRAVOPT, DRAGOPT, THROPT
COMMON/BLOK23/ ATHRUST(3), ATHRM, ADRAG(3), BTIME
COMMON/BLOK28/ MFUEL, FUELUSE, VTBGAIN, TDIRECT(3),
+ DELVUSE, DVAVAIL, BTAVAIL, TCHANGE, MULTOUT
COMMON/BLOK29/ THRUSTM, MDOT, VACISP
COMMON/BLOK34/ TOSTEP
DATA MULTOUT /.FALSE./
IF((AINT(SNGL(BTIME)/SNGL(TOSTEP)) .LT. SNGL(BTIME/TOSTEP))
+ .AND.(THROPT .NE. '0') .AND.(TCHANGE .EQ. .FALSE.))
+ GOTO 100
IF((TCHANGE .EQ. .FALSE.) .OR. (THROPT .EQ. '0')) GOTO 5
IF((TCHANGE .EQ. .TRUE.) .AND. (MULTOUT .EQ. .FALSE.)) THEN
MULTOUT = .TRUE.
ELSE
GOTO 100
ENDIF
C*****CONVERT THRUST FROM KILONEWTONS TO NEWTONS FOR OUTPUT
5 THRM = THRUSTM*1000.
IF(TERMOUT .EQ. 'N') THEN
I = 1
ELSE
I = 6
ENDIF
10 WRITE(I,1000)
WRITE(I,1100)
WRITE(I,1150) TOTTIME, BTIME, BTAVAIL, DELVUSE, DVAVAIL
WRITE(I,1300)
WRITE(I,1200) FUELUSE, MFUEL, TDIRECT(1), TDIRECT(2),
+ TDIRECT(3)
WRITE(I,1400)
WRITE(I,1500) VTBGAIN, ATHRM, THRM, MDOT, VACISP
IF(I .EQ. 6) THEN
I = 1
GOTO 10

```

```

ENDIF
  100 RETURN
  1000 FORMAT(27X,'CURRENT TARGET ENGINE VALUES'//,27X,28('-'))
  1100 FORMAT(T12,'TIME',T23,'TOTBTIME',T34,'BTAVAIL',T47,'DELVUSED',
    +      T59,'DVAVAIL')
  1150 FORMAT(5X,3F12.4,1X,2F12.6/)
  1200 FORMAT(5X,5F12.4/)
  1300 FORMAT(T11,'FUELUSED',T21,'FUELAVAL',T36,'THDIRX',
    +      T48,'THDIRY',T60,'THDIRZ')
  1400 FORMAT(T11,'VTBAINED',T23,'THACCEL',T36,'THRUST',T48,'MASSFLOW',
    +      T60,'VACISP')
  1500 FORMAT(7X,F12.7,F11.6,F12.2,1X,2F12.4/)
      END

```

```

C
C

```

SUBROUTINE SETUP

```

C
C
C*****
C THIS SUBROUTINE IS USED BY THE OPERATOR TO PROVIDE TWO NEW MISSILE POSITION
C FIXES OVER TIME AND A TARGET POSITION AND VELOCITY VECTOR TO BE INPUT TO
C EVADER TO SETUP A DESIRED INTERCEPT SCENARIO. INTERCEPT MODES WHICH CAN BE
C SETUP INLCUDE DIRECT ASCENT AND CO-ORBITAL INJECTION, WITH THE MISSILE
C MOVING IN A RETROGRADE OR NON-RETROGRADE PATH WITH RESPECT TO THE TARGET.
C TRAJECTORY CALCULATIONS ARE BASED ON OPERATOR CHOICES FOR ALTITUDE,
C ANGULAR POSITION, TRANSFER TIME, FIX TIME, ORBITAL INCLINATION, AND
C RETROGRADE OPTION OR MISSILE ORBIT ECCENTRICITY. VECTOR'S CALCULATED
C THROUGH SUBROUTINE SETUP ARE DISPLAYED TO THE OPERATOR AND SUPPLIED TO
C THE TOP LEVEL OF EVADER AS INPUT.
C*****
C INPUT DIMENSIONAL UNITS ARE AS FOLLOWS: ALTITUDE IN KM, ANGULAR POSITION
C FROM THE LINE OF NODES IN DEGREES, TIME IN SEC, INCLINATION IN DEGREES,
C RETROGRADE OPTION (Y OR N)
C*****
IMPLICIT DOUBLE PRECISION(A-H,K-M,O-Z)
CHARACTER SETOPT,TRAJOPT,SOUTOPT,PHASE*9,ORBOPT,RETROPT
COMMON/BLOK1/ RM1(3),RM1M
COMMON/BLOK2/ RT1(3),RT1M
COMMON/BLOK5/ VM1(3),VM1M
COMMON/BLOK6/ VT1(3),VT1M
COMMON/BLOK10/ PI,MU
COMMON/BLOK11/ TRTIME,TINTER
COMMON/BLOK18/ RMO(3),RMOM,FIXTIME
COMMON/BLOK19/ PHASE
COMMON/BLOK32/ SETOPT
COMMON/BLOK33/ RAVE,REQE
DIMENSION RT2(3),VM2(3)
WRITE(6,1000)
C*****ASK OPERATOR IF SETUP IS DESIRED
READ(5,1100) SETOPT
IF(SETOPT.EQ.'N') GOTO 100
PHASE = 'SETUP'
  10  WRITE(6,1050)

```

```

C*****ASK OPERATOR IF DIRECT-ASCENT (ORBOPT='D') OR CO-ORBITAL INJECTION
C      ('C') IS DESIRED AND ASK FOR APPROPRIATE INPUT DATA
READ (5,1100) ORBOPT
IF(ORBOPT .EQ. 'D') THEN
  WRITE(6,1200)
  READ(5,1300) TALT1,MALT1,TN2,MN1,FIXTIME,TRTIME,ORBINCL
ELSE
  WRITE(6,1800)
  READ(5,1900) TALT1,TN2,EM,FIXTIME,TRTIME,ORBINCL,RETROPT
C*****PREPARE APPROPRIATELY FOR RETROGRADE OPTION
  IF(RETROPT .EQ. 'Y') THEN
    RETRO = -1.
  ELSE
    RETRO = 1.
  ENDIF
ENDIF
WRITE(6,1325)
C*****PROVIDE OUTPUT AS REQUESTED
READ(5,1100) SOUTOPT
IF(SOUTOPT .EQ. 'Y') THEN
  WRITE(1,1150) ORBOPT
  IF(ORBOPT .EQ. 'D') THEN
    WRITE(1,1350) TALT1,MALT1,TN2,MN1,FIXTIME,TRTIME,ORBINCL
  ELSE IF((SOUTOPT .EQ. 'Y').AND.(ORBOPT .EQ. 'C')) THEN
    WRITE(1,2000) TALT1,TN2,EM,FIXTIME,TRTIME,ORBINCL,RETROPT
  ENDIF
ENDIF
WRITE(6,1400)
C*****ASK IF INTERCEPT (TRAJOPT='I') OR NEAR-MISS ('M') SCENARIO IS DESIRED
READ(5,1100) TRAJOPT
WRITE(1,1450) TRAJOPT
  RT2M = TALT1+RAVE
RT1M = RT2M
CALL CIRCORB(RT2M,TN2,ORBINCL,RT2)
C*****CALCULATE TARGET POSITION AND VELOCITY AT TIME T1
VT2M = DSQRT(MU/RT2M)
VT1M = VT2M
  THETA = TN2-TRTIME*VT2M/RT2M*180./PI
  20 CALL CIRCORB(RT1M,THETA,ORBINCL,RT1)
VT1(1) = -VT1M*DSIND(THETA)
VT1(2) = VT1M*DCOSD(THETA)*DCOSD(ORBINCL)
VT1(3) = VT1M*DCOSD(THETA)*DSIND(ORBINCL)
C*****IF DONE (TRAJOPT='D'), RETURN CONTROL TO EVADER
  IF(TRAJOPT .EQ. 'D') GOTO 100
IF(ORBOPT .EQ. 'D') THEN
C*****CALCULATE MISSILE POSITION FIXES AT TIME T1 AND TO
C      FOR DIRECT INTERCEPT
  RM1M = MALT1+RAVE
  CALL CIRCORB(RM1M,MN1,ORBINCL,RM1)
  CALL LAMBERT(RM1,RT2,TRTIME)
  CALL EXGAUSS(RM1,VM1,-FIXTIME,'SETHIT ')
ELSE
C*****CALCULATE MISSILE POSITION FIXES AT TIME T1 AND TO
C      FOR CO-ORBITAL INJECTION

```

```

AM = RT2M/(1.+EM)
VM2M = DSQRT(MU*(2./RT2M-1./AM))
VM2(1) = RETRO*(-VM2M)*DSIND(TN2)
VM2(2) = RETRO*VM2M*DCOSD(TN2)*DCOSD(ORBINCL)
VM2(3) = RETRO*VM2M*DCOSD(TN2)*DSIND(ORBINCL)
CALL EXGAUSS(RT2,VM2,-TRTIME,'INJECT ')
CALL EXGAUSS(RM1,VM1,-FIXTIME,'SETHIT ')
IF(RNON-RAVE .LE. 100.) THEN
  WRITE(6,2100)
  GOTO 10
ENDIF
ENDIF
C*****IF A NEAR-MISS IS DESIRED, MOVE TARGET BACK IN ITS ORBIT AT
C   TIME T1 AND CALCULATE NEW POSITION AND VELOCITY VECTOR COMPONENTS
IF(TRAJOPT .EQ. 'M') THEN
  WRITE(6,1500)
C*****ASK OPERATOR FOR STRAIGHT LINE MISS-DISTANCE
READ(5,1600) MISSD
WRITE(1,1700) MISSD
MTHETA = 2.*DASIN(.5*MISSD/RT2M)
  THETA = THETA-MTHETA*180./PI
TRAJOPT = 'D'
GOTO 20
ENDIF
100  RETURN
1000 FORMAT(/1X,'SETUP NEW INITIAL POSITION VECTORS? (Y OR N)')
1050 FORMAT(1X,'DIRECT INTERCEPT OR CO-ORBITAL INJECTION? (D OR C)')
1100 FORMAT(A1)
1150 FORMAT(5X,'DIRECT INTERCEPT OR CO-ORBITAL INJECTION? (D OR C)',
+       1X,A1/)
1200 FORMAT(1X,'INPUT TALT1,MALT1,TN2,MN1,FIXTIME,TRTIME,ORBINCL:')
1300 FORMAT(7F12.4)
1325 FORMAT(1X,'WRITE INPUT DATA ON HARDCOPY? (Y OR N)')
1350 FORMAT(/29X,'INPUT DATA FOR NEW SETUP',/29X,24('-')/,
+       /T11,'TALT1',T23,'MALT1',T36,'TN2',T48,'MN1',
+       T59,'FIXTIME',T70,'TRTIME',T83,'ORBINCL'/,5X,7F12.4/)
1400 FORMAT(1X,'INTERCEPT OR NEAR-MISS TRAJECTORY? (I OR M)')
1450 FORMAT(5X,'INTERCEPT OR NEAR-MISS TRAJECTORY? (I OR M) ',A1/)
1500 FORMAT(1X,'INPUT DESIRED MISS DISTANCE:')
1600 FORMAT(F12.4)
1700 FORMAT(5X,'INPUT DESIRED MISS DISTANCE:',F12.4)
1800 FORMAT(1X,'INPUT TALT1,TN2,EM,FIXTIME,TRTIME,ORBINCL,RETROPT',
+       '(Y OR N):')
1900 FORMAT(6F12.4,A1)
2000 FORMAT(/29X,'INPUT DATA FOR NEW SETUP',/29X,24('-')/,
+       /T11,'TALT1',T25,'TN2',T36,'ECCENTM',T48,'FIXTIME',
+       T59,'TRTIME',T72,'ORBINCL',T84,'RETROGRADE'/,5X,6F12.4,
+       10X,A1/)
2100 FORMAT(/5X,'WARNING - ALTITUDE IS LESS THAN 100. KM'/)
END

```

Appendix B

Program Output of EVADER

B.1 Non-Retrograde Co-orbital Injection Intercept Scenario

DIRECT INTERCEPT OR CO-ORBITAL INJECTION? (D OR C) C

INPUT DATA FOR NEW SETUP

TALT1	TN2	ECCENTM	FIXTIME	TRTIME	ORBINCL	RETROGRADE
900.0000	90.0000	0.8000	1.0000	400.0000	90.0000	N

INTERCEPT OR NEAR-MISS TRAJECTORY? (I OR M) I

INPUT INTSTEP, BURNSTEP, THOUTSTEP, OUTSTEP, NRUNS: 1.000 0.100 1.000 100.000 7

AXISYMMETRIC GRAVITY, DRAG? (Y OR N) Y, Y

INITIAL INPUT VECTORS FOR THIS RUN

(TIME BETWEEN MISSILE FIXES: 1.0000)

RMOX	RMOY	RMOZ	RM1X	RM1Y	RM1Z
1288.0739	0.0000	6653.6568	1285.0656	0.0000	6656.7972
RT1X	RT1Y	RT1Z	VT1X	VT1Y	VT1Z
2878.6592	0.0000	6677.2257	-6.7947	0.0000	2.9293

MISSILE AND TARGET TRAJECTORIES

TIME IN SEC, DISTANCE IN KM, VELOCITY IN KM/S
ACCELERATION DUE TO DRAG AND GRAVITY IN M/S**2, DENSITY IN KG/M**3
THRUST ACCELERATION IN KM/S**2, MASS IN KG, THRUST IN NEWTONS
VACISP IN SEC, MASSFLOW IN KG/S

INITIAL PREDICTED INTERCEPT TIME	MISSILE APOGEE ALTITUDE
400.0000	900.0000

CURRENT TIME

TIME	RREL	RRELX	RRELY	RRELZ
0.0000	1593.7246	-1593.5937	0.0000	-20.4285

MISSILE VALUES

ALT	R	RX	RY	RZ
408.3857	6779.7007	1285.0656	0.0000	6656.7972

VMAG	VX	VY	VZ	ACCELGRAV
4.3463	-3.0091	0.0000	3.1361	8.6611
DECCELDRAG	RHO			
0.1859E-12	0.2531E-11			

TARGET VALUES

ALT	R	RX	RY	RZ
900.0000	7271.3150	2878.6592	0.0000	6677.2257
VMAG	VX	VY	VZ	ACCELGRAV
7.3993	-6.7947	0.0000	2.9293	7.5295
DECCELDRAG	RHO			
0.5202E-15	0.5759E-14			

PREDICTED TIME

TIME	RREL	RRELX	RRELY	RRELZ
400.0000	0.0001	-0.0001	0.0000	0.0000

MISSILE VALUES

ALT	R	RX	RY	RZ
900.0000	7271.3150	0.0001	0.0000	7271.3150
VMAG	VX	VY	VZ	ACCELGRAV
3.3091	-3.3091	0.0000	0.0000	7.5295
DECCELDRAG	RHO			
0.4230E-15	0.5759E-14			

TARGET VALUES

ALT	R	RX	RY	RZ
900.0000	7271.3150	0.0001	0.0000	7271.3150
VMAG	VX	VY	VZ	ACCELGRAV
7.3993	-7.3993	0.0000	0.0000	7.5295
DECCELDRAG	RHO			
0.5202E-15	0.5759E-14			

EVASIVE MANEUVER REQUIRED

INPUT MANEUVER OPTION (R,V,H,E,C), DESIRED MISS DISTANCE (KM): R 2.0000

REQUIRED IMPULSIVE DELV = 0.004754

REQUIRED IMPULSIVE DELV VECTOR (DELVX,DELVY,DELVZ) = -0.000079 0.000000 0.004754

SELECT IMPULSIVE DELV, ENGINE BURN OR NO EVASION: (I,E OR N) E

CURRENT TIME

TIME RREL RRELX RRELY RRELZ
0.0000 1593.7246 -1593.5937 0.0000 -20.4285

MISSILE VALUES

ALT R RX RY RZ
408.3857 6779.7007 1285.0656 0.0000 6656.7972
VMAG VX VY VZ ACCELGRAV
4.3463 -3.0091 0.0000 3.1361 8.6611
DECCELDRAG RHO
0.1859E-12 0.2531E-11

TARGET VALUES

ALT R RX RY RZ
900.0000 7271.3150 2878.6592 0.0000 6677.2257
VMAG VX VY VZ ACCELGRAV
7.3993 -6.7947 0.0000 2.9293 7.5295
DECCELDRAG RHO
0.5202E-15 0.5759E-14

CURRENT TARGET ENGINE VALUES

TIME TOTBTIME BTAVAIL DELVUSED DVAVAIL
0.0000 0.0000 621.3490 0.000000 2.041149
FUELUSED FUELAVAIL THDIRX THDIRY THDIRZ
0.0000 3500.0000 -0.0165 0.0000 0.9999
VTBAINED THACCEL THRUST MASSFLOW VACISP
0.0047543 0.002669 26690.00 5.6329 483.0000

PREDICTED TIME

TIME RREL RRELX RRELY RRELZ

400.0000 0.0001 -0.0001 0.0000 0.0000

MISSILE VALUES

ALT R RX RY RZ
900.0000 7271.3150 0.0001 0.0000 7271.3150

VMAG VX VY VZ ACCELGRAV
3.3091 -3.3091 0.0000 0.0000 7.5295

DECCELDRAG RHO
0.4230E-15 0.5759E-14

TARGET VALUES

ALT R RX RY RZ
900.0000 7271.3150 0.0001 0.0000 7271.3150

VMAG VX VY VZ ACCELGRAV
7.3993 -7.3993 0.0000 0.0000 7.5295

DECCELDRAG RHO
0.5202E-15 0.5759E-14

CURRENT TARGET ENGINE VALUES

TIME TOTBTIME BTAVAIL DELVUSED DVAVAIL
1.0000 1.0000 620.3490 0.002670 2.038479

FUELUSED FUELAVAIL THDIRX THDIRY THDIRZ
5.6329 3494.3671 -0.0164 0.0000 0.9999

VTBGAINED THACCEL THRUST MASSFLOW VACISP
0.0020939 0.002671 26690.00 5.6329 483.0000

CURRENT TARGET ENGINE VALUES

TIME TOTBTIME BTAVAIL DELVUSED DVAVAIL
1.7000 1.7000 619.6490 0.004539 2.036609

FUELUSED FUELAVAIL THDIRX THDIRY THDIRZ
9.5759 3490.4241 -0.0163 0.0000 0.9999

VTBGAINED THACCEL THRUST MASSFLOW VACISP
0.0002264 0.002264 22622.30 4.7744 483.0000

CURRENT TARGET ENGINE VALUES

TIME TOTBTIME BTAVAIL DELVUSED DVAVAIL
1.8000 1.8000 619.5642 0.004766 2.036383

FUELUSED	FUELAVAIL	THDIRX	THDIRY	THDIRZ
10.0534	3489.9466	0.0313	0.0000	0.9995
VTBGAIND	THACCEL	THRUST	MASSFLOW	VACISP
0.0000000	0.000000	0.00	0.0000	483.0000

EVASIVE MANEUVER COMPLETED - THRUST TERMINATED

CURRENT TIME

TIME	RREL	RRELX	RRELY	RRELZ
100.0000	1208.6426	-1208.6230	0.0000	-6.8702

MISSILE VALUES

ALT	R	RX	RY	RZ
625.9193	6997.2343	976.8360	0.0000	6928.7141

VMAG	VX	VY	VZ	ACCELGRAV
3.9037	-3.1470	0.0000	2.3098	8.1309

DECCELDRAG	RHO
0.4999E-14	0.8437E-13

TARGET VALUES

ALT	R	RX	RY	RZ
900.4496	7271.7646	2185.4590	0.0000	6935.5843

VMAG	VX	VY	VZ	ACCELGRAV
7.4008	-7.0572	0.0000	2.2287	7.5286

DECCELDRAG	RHO
0.5199E-15	0.5747E-14

PREDICTED TIME

TIME	RREL	RRELX	RRELY	RRELZ
400.0000	1.9999	0.0000	0.0000	-1.9999

MISSILE VALUES

ALT	R	RX	RY	RZ
900.0001	7271.3151	0.0001	0.0000	7271.3151

VMAG	VX	VY	VZ	ACCELGRAV
3.3091	-3.3091	0.0000	0.0000	7.5295

DECCELDRAG	RHO
0.3413E-15	0.5759E-14

TARGET VALUES

ALT	R	RX	RY	RZ
902.0000	7273.3150	0.0001	0.0000	7273.3150
VMAG	VX	VY	VZ	ACCELGRAV
7.3992	-7.3992	0.0000	0.0055	7.5254
DECCELDRAG	RHO			
0.5163E-15	0.5707E-14			

CURRENT TIME

TIME	RREL	RRELX	RRELY	RRELZ
200.0000	812.4711	-812.4681	0.0000	-2.2144

MISSILE VALUES

ALT	R	RX	RY	RZ
778.9397	7150.2547	657.1836	0.0000	7119.9896
VMAG	VX	VY	VZ	ACCELGRAV
3.5782	-3.2390	0.0000	1.5207	7.7866
DECCELDRAG	RHO			
0.7023E-15	0.1411E-13			

TARGET VALUES

ALT	R	RX	RY	RZ
900.9381	7272.2531	1469.6517	0.0000	7122.2040
VMAG	VX	VY	VZ	ACCELGRAV
7.4003	-7.2466	0.0000	1.5005	7.5276
DECCELDRAG	RHO			
0.5187E-15	0.5734E-14			

PREDICTED TIME

TIME	RREL	RRELX	RRELY	RRELZ
500.0000	408.3206	408.3120	0.0000	-2.6541

MISSILE VALUES

ALT	R	RX	RY	RZ
869.8458	7241.1608	-330.3329	0.0000	7233.6222
VMAG	VX	VY	VZ	ACCELGRAV

3.3773	-3.2918	0.0000	-0.7548	7.5923
DECCELDRAG	RHO			
0.3487E-15	0.7004E-14			

TARGET VALUES

ALT	R	RX	RY	RZ
902.5623	7273.8773	-738.6450	0.0000	7236.2763
VMAG	VX	VY	VZ	ACCELGRAV
7.3986	-7.3610	0.0000	-0.7456	7.5242
DECCELDRAG	RHO			
0.5149E-15	0.5692E-14			

CURRENT TIME

TIME	RREL	RRELX	RRELY	RRELZ
300.0000	408.3146	-408.3117	0.0000	-1.5430

MISSILE VALUES

ALT	R	RX	RY	RZ
869.8457	7241.1607	330.3331	0.0000	7233.6220
VMAG	VX	VY	VZ	ACCELGRAV
3.3773	-3.2918	0.0000	0.7548	7.5923
DECCELDRAG	RHO			
0.3107E-15	0.7004E-14			

TARGET VALUES

ALT	R	RX	RY	RZ
901.4568	7272.7718	738.6447	0.0000	7235.1650
VMAG	VX	VY	VZ	ACCELGRAV
7.3998	-7.3610	0.0000	0.7568	7.5265
DECCELDRAG	RHO			
0.5174E-15	0.5721E-14			

PREDICTED TIME

TIME	RREL	RRELX	RRELY	RRELZ
600.0000	812.4850	812.4728	0.0000	-4.4591

MISSILE VALUES

ALT	R	RX	RY	RZ
778.9401	7150.2551	-657.1835	0.0000	7119.9900
VMAG	VX	VY	VZ	ACCELGRAV
3.5782	-3.2390	0.0000	-1.5207	7.7866
DECCELDRAG	RHO			
0.6256E-15	0.1411E-13			

TARGET VALUES

ALT	R	RX	RY	RZ
903.1379	7274.4529	-1469.6562	0.0000	7124.4492
VMAG	VX	VY	VZ	ACCELGRAV
7.3980	-7.2467	0.0000	-1.4889	7.5230
DECCELDRAG	RHO			
0.5134E-15	0.5677E-14			

CURRENT TIME

TIME	RREL	RRELX	RRELY	RRELZ
400.0000	1.9998	0.0001	0.0000	-1.9998

MISSILE VALUES

ALT	R	RX	RY	RZ
900.0003	7271.3153	0.0000	0.0000	7271.3153
VMAG	VX	VY	VZ	ACCELGRAV
3.3091	-3.3091	0.0000	0.0000	7.5295
DECCELDRAG	RHO			
0.2452E-15	0.5759E-14			

TARGET VALUES

ALT	R	RX	RY	RZ
902.0001	7273.3151	0.0000	0.0000	7273.3151
VMAG	VX	VY	VZ	ACCELGRAV
7.3992	-7.3992	0.0000	0.0055	7.5254
DECCELDRAG	RHO			
0.5160E-15	0.5707E-14			

PREDICTED TIME

TIME	RREL	RRELX	RRELY	RRELZ
------	------	-------	-------	-------

700.0000 1208.6901 1208.6463 0.0000 -10.2919

MISSILE VALUES

ALT	R	RX	RY	RZ
625.9200	6997.2350	-976.8359	0.0000	6928.7148
VMAG	VX	VY	VZ	ACCELGRAV
3.9037	-3.1470	0.0000	-2.3098	8.1309
DECCELDRAG	RHO			
0.3592E-14	0.8437E-13			

TARGET VALUES

ALT	R	RX	RY	RZ
903.7208	7275.0358	-2185.4822	0.0000	6939.0067
VMAG	VX	VY	VZ	ACCELGRAV
7.3975	-7.0575	0.0000	-2.2167	7.5218
DECCELDRAG	RHO			
0.5120E-15	0.5662E-14			

CURRENT TIME

TIME	RREL	RRELX	RRELY	RRELZ
500.0000	408.3207	408.3121	0.0000	-2.6541

MISSILE VALUES

ALT	R	RX	RY	RZ
869.8459	7241.1609	-330.3330	0.0000	7233.6223
VMAG	VX	VY	VZ	ACCELGRAV
3.3773	-3.2918	0.0000	-0.7548	7.5923
DECCELDRAG	RHO			
0.3107E-15	0.7004E-14			

TARGET VALUES

ALT	R	RX	RY	RZ
902.5624	7273.8774	-738.6451	0.0000	7236.2764
VMAG	VX	VY	VZ	ACCELGRAV
7.3986	-7.3610	0.0000	-0.7456	7.5242
DECCELDRAG	RHO			
0.5146E-15	0.5692E-14			

PREDICTED TIME

TIME	RREL	RRELX	RRELY	RRELZ
800.0000	1593.8637	1593.6663	0.0000	-25.0841

MISSILE VALUES

ALT	R	RX	RY	RZ
408.3867	6779.7017	-1285.0655	0.0000	6656.7982

VMAG	VX	VY	VZ	ACCELGRAV
4.3463	-3.0091	0.0000	-3.1361	8.6611

DECCELDRAG	RHO
0.1123E-12	0.2531E-11

TARGET VALUES

ALT	R	RX	RY	RZ
904.3051	7275.6201	-2878.7318	0.0000	6681.8823

VMAG	VX	VY	VZ	ACCELGRAV
7.3969	-6.7955	0.0000	-2.9213	7.5206

DECCELDRAG	RHO
0.5105E-15	0.5647E-14

MISSILE SUCCESSFULLY EVADED

FINAL ORBITAL ELEMENTS FOR THE TARGET

H	P	A	E	I
53816.7252	7275.1568	7275.1613	0.0008	90.0000

FINAL ORBITAL ELEMENTS FOR THE MISSILE

H	P	A	E	I
24061.2152	1454.2629	4039.6196	0.8000	90.0000

B.2 Retrograde Co-orbital Injection Intercept Scenario

DIRECT INTERCEPT OR CO-ORBITAL INJECTION? (D OR C) C

INPUT DATA FOR NEW SETUP

TALT1 TN2 ECCENTM FIXTIME TRTIME ORBINCL RETROGRADE
900.0000 90.0000 0.8000 1.0000 400.0000 90.0000 Y

INTERCEPT OR NEAR-MISS TRAJECTORY? (I OR M) I

INPUT INTSTEP, BURNSTEP, THOUTSTEP, OUTSTEP, NRUNS: 1.000 0.100 1.000 100.000 7

AXISYMMETRIC GRAVITY, DRAG? (Y OR N) Y, Y

INITIAL INPUT VECTORS FOR THIS RUN

(TIME BETWEEN MISSILE FIXES: 1.0000)

RMOX	RMOY	RMOZ	RM1X	RM1Y	RM1Z
-1288.0739	0.0000	6653.6568	-1285.0656	0.0000	6656.7972
RT1X	RT1Y	RT1Z	VT1X	VT1Y	VT1Z
2878.6592	0.0000	6677.2257	-6.7947	0.0000	2.9293

MISSILE AND TARGET TRAJECTORIES

TIME IN SEC, DISTANCE IN KM, VELOCITY IN KM/S
ACCELERATION DUE TO DRAG AND GRAVITY IN M/S**2, DENSITY IN KG/M**3
THRUST ACCELERATION IN KM/S**2, MASS IN KG, THRUST IN NEWTONS
VACISP IN SEC, MASSFLOW IN KG/S

INITIAL PREDICTED INTERCEPT TIME	MISSILE APOGEE ALTITUDE
400.0000	900.0000

CURRENT TIME

TIME	RREL	RRELX	RRELY	RRELZ
0.0000	4163.7749	-4163.7248	0.0000	-20.4285

MISSILE VALUES

ALT	R	RX	RY	RZ
408.3857	6779.7007	-1285.0656	0.0000	6656.7972

VMAG	VX	VY	VZ	ACCELGRAV
4.3463	3.0091	0.0000	3.1361	8.6611
DECCELDRAG	RHO			
0.1859E-12	0.2531E-11			

TARGET VALUES

ALT	R	RX	RY	RZ
900.0000	7271.3150	2878.6592	0.0000	6677.2257
VMAG	VX	VY	VZ	ACCELGRAV
7.3993	-6.7947	0.0000	2.9293	7.5295
DECCELDRAG	RHO			
0.5202E-15	0.5759E-14			

PREDICTED TIME

TIME	RREL	RRELX	RRELY	RRELZ
400.0000	0.0002	-0.0002	0.0000	0.0000

MISSILE VALUES

ALT	R	RX	RY	RZ
900.0000	7271.3150	-0.0001	0.0000	7271.3150
VMAG	VX	VY	VZ	ACCELGRAV
3.3091	3.3091	0.0000	0.0000	7.5295
DECCELDRAG	RHO			
0.4230E-15	0.5759E-14			

TARGET VALUES

ALT	R	RX	RY	RZ
900.0000	7271.3150	0.0001	0.0000	7271.3150
VMAG	VX	VY	VZ	ACCELGRAV
7.3993	-7.3993	0.0000	0.0000	7.5295
DECCELDRAG	RHO			
0.5202E-15	0.5759E-14			

EVASIVE MANEUVER REQUIRED

INPUT MANEUVER OPTION (R,V,H,E,C), DESIRED MISS DISTANCE (KM): R 2.0000

REQUIRED IMPULSIVE DELV = 0.004754

REQUIRED IMPULSIVE DELV VECTOR (DELVX,DELVY,DELVZ) = -0.000079 0.000000 0.004754

SELECT IMPULSIVE DELV, ENGINE BURN OR NO EVASION: (I,E OR N) E

CURRENT TIME

TIME RREL RRELX RRELY RRELZ
0.0000 4163.7749 -4163.7248 0.0000 -20.4285

MISSILE VALUES

ALT R RX RY RZ
408.3857 6779.7007 -1285.0656 0.0000 6656.7972
VMAG VX VY VZ ACCELGRAV
4.3463 3.0091 0.0000 3.1361 8.6611
DECCELDRAG RHO
0.1859E-12 0.2531E-11

TARGET VALUES

ALT R RX RY RZ
900.0000 7271.3150 2878.6592 0.0000 6677.2257
VMAG VX VY VZ ACCELGRAV
7.3993 -6.7947 0.0000 2.9293 7.5295
DECCELDRAG RHO
0.5202E-15 0.5759E-14

CURRENT TARGET ENGINE VALUES

TIME TOTBTIME BTAVAIL DELVUSED DVAVAIL
0.0000 0.0000 621.3490 0.000000 2.041149
FUELUSED FUELAVAIL THDIRX THDIRY THDIRZ
0.0000 3500.0000 -0.0166 0.0000 0.9999
VTBGAINED THACCEL THRUST MASSFLOW VACISP
0.0047544 0.002669 26690.00 5.6329 483.0000

PREDICTED TIME

TIME RREL RRELX RRELY RRELZ

400.0000 0.0002 -0.0002 0.0000 0.0000

MISSILE VALUES

ALT R RX RY RZ
900.0000 7271.3150 -0.0001 0.0000 7271.3150

VMAG VX VY VZ ACCELGRAV
3.3091 3.3091 0.0000 0.0000 7.5295

DECCELDRAG RHO
0.4230E-15 0.5759E-14

TARGET VALUES

ALT R RX RY RZ
900.0000 7271.3150 0.0001 0.0000 7271.3150

VMAG VX VY VZ ACCELGRAV
7.3993 -7.3993 0.0000 0.0000 7.5295

DECCELDRAG RHO
0.5202E-15 0.5759E-14

CURRENT TARGET ENGINE VALUES

TIME TOTBTIME BTAVAIL DELVUSED DVAVAIL
1.0000 1.0000 620.3490 0.002670 2.038479
FUELUSED FUELAVAIL THDIRX THDIRY THDIRZ
5.6329 3494.3671 -0.0165 0.0000 0.9999
VTBGAINED THACCEL THRUST MASSFLOW VACISP
0.0020940 0.002671 26690.00 5.6329 483.0000

CURRENT TARGET ENGINE VALUES

TIME TOTBTIME BTAVAIL DELVUSED DVAVAIL
1.7000 1.7000 619.6490 0.004539 2.036609
FUELUSED FUELAVAIL THDIRX THDIRY THDIRZ
9.5759 3490.4241 -0.0164 0.0000 0.9999
VTBGAINED THACCEL THRUST MASSFLOW VACISP
0.0002265 0.002264 22623.26 4.7746 483.0000

CURRENT TARGET ENGINE VALUES

TIME TOTBTIME BTAVAIL DELVUSED DVAVAIL
1.8000 1.8000 619.5642 0.004766 2.036383

FUELUSED	FUELAVAIL	THDIRX	THDIRY	THDIRZ
10.0534	3489.9466	0.0313	0.0000	0.9995
VTBAINED	THACCEL	THRUST	MASSFLOW	VACISP
0.0000000	0.000000	0.00	0.0000	483.0000

EVASIVE MANEUVER COMPLETED - THRUST TERMINATED

CURRENT TIME

TIME	RREL	RRELX	RRELY	RRELZ
100.0000	3162.3025	-3162.2950	0.0000	-6.8702

MISSILE VALUES

ALT	R	RX	RY	RZ
625.9193	6997.2343	-976.8360	0.0000	6928.7141
VMAG	VX	VY	VZ	ACCELGRAV
3.9037	3.1470	0.0000	2.3098	8.1309
DECCELDRAG	RHO			
0.4999E-14	0.8437E-13			

TARGET VALUES

ALT	R	RX	RY	RZ
900.4496	7271.7646	2185.4590	0.0000	6935.5843
VMAG	VX	VY	VZ	ACCELGRAV
7.4008	-7.0572	0.0000	2.2287	7.5286
DECCELDRAG	RHO			
0.5199E-15	0.5747E-14			

PREDICTED TIME

TIME	RREL	RRELX	RRELY	RRELZ
400.0000	1.9999	0.0000	0.0000	-1.9999

MISSILE VALUES

ALT	R	RX	RY	RZ
900.0001	7271.3151	-0.0001	0.0000	7271.3151
VMAG	VX	VY	VZ	ACCELGRAV
3.3091	3.3091	0.0000	0.0000	7.5295
DECCELDRAG	RHO			
0.3413E-15	0.5759E-14			

TARGET VALUES

ALT	R	RX	RY	RZ
902.0000	7273.3150	0.0000	0.0000	7273.3150
VMAG	VX	VY	VZ	ACCELGRAV
7.3992	-7.3992	0.0000	0.0055	7.5254
DECCELDRAG	RHO			
0.5163E-15	0.5707E-14			

CURRENT TIME

TIME	RREL	RRELX	RRELY	RRELZ
200.0000	2126.8363	-2126.8352	0.0000	-2.2144

MISSILE VALUES

ALT	R	RX	RY	RZ
778.9397	7150.2547	-657.1836	0.0000	7119.9896
VMAG	VX	VY	VZ	ACCELGRAV
3.5782	3.2390	0.0000	1.5207	7.7866
DECCELDRAG	RHO			
0.7023E-15	0.1411E-13			

TARGET VALUES

ALT	R	RX	RY	RZ
900.9381	7272.2531	1469.6516	0.0000	7122.2040
VMAG	VX	VY	VZ	ACCELGRAV
7.4003	-7.2466	0.0000	1.5005	7.5276
DECCELDRAG	RHO			
0.5187E-15	0.5734E-14			

PREDICTED TIME

TIME	RREL	RRELX	RRELY	RRELZ
500.0000	1068.9813	1068.9780	0.0000	-2.6541

MISSILE VALUES

ALT	R	RX	RY	RZ
869.8458	7241.1608	330.3329	0.0000	7233.6222
VMAG	VX	VY	VZ	ACCELGRAV

3.3773	3.2918	0.0000	-0.7548	7.5923
DECCELDRAG	RHO			
0.3487E-15	0.7004E-14			

TARGET VALUES

ALT	R	RX	RY	RZ
902.5623	7273.8773	-738.6451	0.0000	7236.2763
VMAG	VX	VY	VZ	ACCELGRAV
7.3986	-7.3610	0.0000	-0.7456	7.5242
DECCELDRAG	RHO			
0.5149E-15	0.5692E-14			

CURRENT TIME

TIME	RREL	RRELX	RRELY	RRELZ
300.0000	1068.9788	-1068.9777	0.0000	-1.5430

MISSILE VALUES

ALT	R	RX	RY	RZ
869.8457	7241.1607	-330.3331	0.0000	7233.6220
VMAG	VX	VY	VZ	ACCELGRAV
3.3773	3.2918	0.0000	0.7548	7.5923
DECCELDRAG	RHO			
0.3107E-15	0.7004E-14			

TARGET VALUES

ALT	R	RX	RY	RZ
901.4567	7272.7717	738.6446	0.0000	7235.1650
VMAG	VX	VY	VZ	ACCELGRAV
7.3998	-7.3610	0.0000	0.7568	7.5265
DECCELDRAG	RHO			
0.5174E-15	0.5721E-14			

PREDICTED TIME

TIME	RREL	RRELX	RRELY	RRELZ
600.0000	2126.8445	2126.8399	0.0000	-4.4591

MISSILE VALUES

ALT	R	RX	RY	RZ
778.9401	7150.2551	657.1835	0.0000	7119.9900
VMAG	VX	VY	VZ	ACCELGRAV
3.5782	3.2390	0.0000	-1.5207	7.7866
DECCELDRAG	RHO			
0.6256E-15	0.1411E-13			

TARGET VALUES

ALT	R	RX	RY	RZ
903.1379	7274.4529	-1469.6564	0.0000	7124.4492
VMAG	VX	VY	VZ	ACCELGRAV
7.3980	-7.2467	0.0000	-1.4889	7.5230
DECCELDRAG	RHO			
0.5134E-15	0.5677E-14			

CURRENT TIME

TIME	RREL	RRELX	RRELY	RRELZ
400.0000	1.9998	0.0001	0.0000	-1.9998

MISSILE VALUES

ALT	R	RX	RY	RZ
900.0003	7271.3153	0.0000	0.0000	7271.3153
VMAG	VX	VY	VZ	ACCELGRAV
3.3091	3.3091	0.0000	0.0000	7.5295
DECCELDRAG	RHO			
0.2452E-15	0.5759E-14			

TARGET VALUES

ALT	R	RX	RY	RZ
902.0001	7273.3151	-0.0001	0.0000	7273.3151
VMAG	VX	VY	VZ	ACCELGRAV
7.3992	-7.3992	0.0000	0.0055	7.5254
DECCELDRAG	RHO			
0.5160E-15	0.5707E-14			

PREDICTED TIME

TIME	RREL	RRELX	RRELY	RRELZ
------	------	-------	-------	-------

700.0000 3162.3350 3162.3183 0.0000 -10.2919

MISSILE VALUES

ALT R RX RY RZ
625.9200 6997.2350 976.8359 0.0000 6928.7148

VMAG VX VY VZ ACCELGRAV
3.9037 3.1470 0.0000 -2.3098 8.1309

DECCELDRAG RHO
0.3592E-14 0.8437E-13

TARGET VALUES

ALT R RX RY RZ
903.7209 7275.0359 -2185.4824 0.0000 6939.0067

VMAG VX VY VZ ACCELGRAV
7.3975 -7.0575 0.0000 -2.2167 7.5218

DECCELDRAG RHO
0.5120E-15 0.5662E-14

CURRENT TIME

TIME RREL RRELX RRELY RRELZ
500.0000 1068.9815 1068.9782 0.0000 -2.6541

MISSILE VALUES

ALT R RX RY RZ
869.8459 7241.1609 330.3330 0.0000 7233.6223

VMAG VX VY VZ ACCELGRAV
3.3773 3.2918 0.0000 -0.7548 7.5923

DECCELDRAG RHO
0.3107E-15 0.7004E-14

TARGET VALUES

ALT R RX RY RZ
902.5624 7273.8774 -738.6452 0.0000 7236.2764

VMAG VX VY VZ ACCELGRAV
7.3986 -7.3610 0.0000 -0.7456 7.5242

DECCELDRAG RHO
0.5146E-15 0.5692E-14

PREDICTED TIME

TIME	RREL	RRELX	RRELY	RRELZ
800.0000	4163.8730	4163.7975	0.0000	-25.0841

MISSILE VALUES

ALT	R	RX	RY	RZ
408.3867	6779.7017	1285.0655	0.0000	6656.7982

VMAG	VX	VY	VZ	ACCELGRAV
4.3463	3.0091	0.0000	-3.1361	8.6611

DECCELDRAG	RHO
0.1123E-12	0.2531E-11

TARGET VALUES

ALT	R	RX	RY	RZ
904.3052	7275.6202	-2878.7320	0.0000	6681.8823

VMAG	VX	VY	VZ	ACCELGRAV
7.3969	-6.7955	0.0000	-2.9213	7.5206

DECCELDRAG	RHO
0.5105E-15	0.5647E-14

MISSILE SUCCESSFULLY EVADED

FINAL ORBITAL ELEMENTS FOR THE TARGET

H	P	A	E	I
53816.7272	7275.1573	7275.1619	0.0008	90.0000

FINAL ORBITAL ELEMENTS FOR THE MISSILE

H	P	A	E	I
24061.2152	1454.2629	4039.6196	0.8000	90.0000

B.3 Non-Retrograde Direct-Ascent Intercept Scenario

DIRECT INTERCEPT OR CO-ORBITAL INJECTION? (D OR C) D

INPUT DATA FOR NEW SETUP

TALT1	MALT1	TN2	MN1	FIXTIME	TRTIME	ORBINCL
800.0000	110.0000	90.0000	60.0000	1.0000	500.0000	90.0000

INTERCEPT OR NEAR-MISS TRAJECTORY? (I OR M) I

INPUT INTSTEP,BURNSTEP,THOUTSTEP,OUTSTEP,NRUNS: 1.000 0.100 1.000 100.000 8

AXISYMMETRIC GRAVITY,DRAG? (Y OR N) Y,Y

INITIAL INPUT VECTORS FOR THIS RUN

(TIME BETWEEN MISSILE FIXES: 1.0000)

RMOX	RMOY	RMOZ	RM1X	RM1Y	RM1Z
3246.3952	0.0000	5607.8091	3240.6575	0.0000	5612.9834
RT1X	RT1Y	RT1Z	VT1X	VT1Y	VT1Z
3560.0404	0.0000	6225.2608	-6.4678	0.0000	3.6987

MISSILE AND TARGET TRAJECTORIES

TIME IN SEC, DISTANCE IN KM, VELOCITY IN KM/S
ACCELERATION DUE TO DRAG AND GRAVITY IN M/S**2, DENSITY IN KG/M**3
THRUST ACCELERATION IN KM/S**2, MASS IN KG, THRUST IN NEWTONS
VACISP IN SEC, MASSFLOW IN KG/S

INITIAL PREDICTED INTERCEPT TIME	MISSILE APOGEE ALTITUDE
500.0000	1254.2041

CURRENT TIME

TIME	RREL	RRELX	RRELY	RRELZ
0.0000	690.5714	-319.3829	0.0000	-612.2773

MISSILE VALUES

ALT	R	RX	RY	RZ
110.0000	6481.3150	3240.6575	0.0000	5612.9834

VMAG	VX	VY	VZ	ACCELGRAV
7.7253	-5.7401	0.0000	5.1702	9.4769
DECCELDRAG	RHO			
0.1041E-06	0.4487E-06			

TARGET VALUES

ALT	R	RX	RY	RZ
800.0000	7171.3150	3560.0404	0.0000	6225.2608
VMAG	VX	VY	VZ	ACCELGRAV
7.4507	-6.4678	0.0000	3.6987	7.7410
DECCELDRAG	RHO			
0.1041E-14	0.1136E-13			

PREDICTED TIME

TIME	RREL	RRELX	RRELY	RRELZ
500.0000	0.0001	-0.0001	0.0000	0.0000

MISSILE VALUES

ALT	R	RX	RY	RZ
800.0000	7171.3150	-0.0003	0.0000	7171.3150
VMAG	VX	VY	VZ	ACCELGRAV
6.9181	-6.8291	0.0000	1.1058	7.7410
DECCELDRAG	RHO			
0.2636E-14	0.1136E-13			

TARGET VALUES

ALT	R	RX	RY	RZ
800.0000	7171.3150	-0.0002	0.0000	7171.3150
VMAG	VX	VY	VZ	ACCELGRAV
7.4507	-7.4507	0.0000	0.0000	7.7410
DECCELDRAG	RHO			
0.1041E-14	0.1136E-13			

EVASIVE MANEUVER REQUIRED

INPUT MANEUVER OPTION (R,V,H,E,C), DESIRED MISS DISTANCE (KM): H 5.0000

REQUIRED IMPULSIVE DELV = 0.010464

REQUIRED IMPULSIVE DELV VECTOR (DELVX,DELVY,DELVZ) = 0.000000 -0.010464 0.000000

SELECT IMPULSIVE DELV, ENGINE BURN OR NO EVASION: (I,E OR N) E

CURRENT TIME

TIME RREL RRELX RRELY RRELZ
0.0000 690.5714 -319.3829 0.0000 -612.2773

MISSILE VALUES

ALT R RX RY RZ
110.0000 6481.3150 3240.6575 0.0000 5612.9834
VMAG VX VY VZ ACCELGRAV
7.7253 -5.7401 0.0000 5.1702 9.4769
DECCELDRAG RHO
0.1041E-06 0.4487E-06

TARGET VALUES

ALT R RX RY RZ
800.0000 7171.3150 3560.0404 0.0000 6225.2608
VMAG VX VY VZ ACCELGRAV
7.4507 -6.4678 0.0000 3.6987 7.7410
DECCELDRAG RHO
0.1041E-14 0.1136E-13

CURRENT TARGET ENGINE VALUES

TIME TOTBTIME BTAVAIL DELVUSED DVAVAIL
0.0000 0.0000 621.3490 0.000000 2.041149
FUELUSED FUELAVAIL THDIRX THDIRY THDIRZ
0.0000 3500.0000 0.0000 -1.0000 0.0000
VTBGAINED THACCEL THRUST MASSFLOW VACISP
0.0104643 0.002669 26690.00 5.6329 483.0000

PREDICTED TIME

TIME RREL RRELX RRELY RRELZ

AD-A170 896

A METHOD FOR GOVERNING SPACECRAFT EVASIVE MANEUVERING
(U) AIR FORCE INST OF TECH WRIGHT-PATTERSON AFB OH
K R KELLER JUN 86 AFIT/CI/MR-86-891

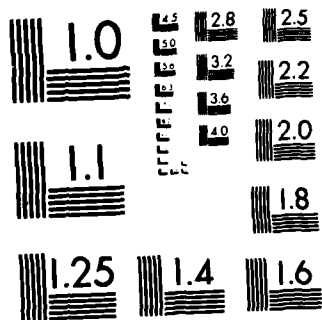
3/3

UNCLASSIFIED

F/G 22/3

NL

END
DATE
FILMED
9-86
DT.



MICROCOPY RESOLUTION TEST CHART
NATIONAL BUREAU OF STANDARDS-1963-A

500.0000 0.0001 -0.0001 0.0000 0.0000

MISSILE VALUES

ALT R RX RY RZ
800.0000 7171.3150 -0.0003 0.0000 7171.3150

VMAG VX VY VZ ACCELGRAV
6.9181 -6.8291 0.0000 1.1058 7.7410

DECCELDRAG RHO
0.2636E-14 0.1136E-13

TARGET VALUES

ALT R RX RY RZ
800.0000 7171.3150 -0.0002 0.0000 7171.3150

VMAG VX VY VZ ACCELGRAV
7.4507 -7.4507 0.0000 0.0000 7.7410

DECCELDRAG RHO
0.1041E-14 0.1136E-13

CURRENT TARGET ENGINE VALUES

TIME TOTBTIME BTAVAIL DELVUSED DVAVAIL
1.0000 1.0000 620.3490 0.002670 2.038479

FUELUSED FUELAVAIL THDIRX THDIRY THDIRZ
5.6329 3494.3671 0.0000 -1.0000 0.0000

VTBGAINED THACCEL THRUST MASSFLOW VACISP
0.0078112 0.002671 26690.00 5.6329 483.0000

CURRENT TARGET ENGINE VALUES

TIME TOTBTIME BTAVAIL DELVUSED DVAVAIL
2.0000 2.0000 619.3490 0.005341 2.035808

FUELUSED FUELAVAIL THDIRX THDIRY THDIRZ
11.2658 3488.7342 0.0000 -1.0000 0.0000

VTBGAINED THACCEL THRUST MASSFLOW VACISP
0.0051518 0.002672 26690.00 5.6329 483.0000

CURRENT TARGET ENGINE VALUES

TIME TOTBTIME BTAVAIL DELVUSED DVAVAIL
3.0000 3.0000 618.3490 0.008014 2.033135

FUELUSED	FUELAVAIL	THDIRX	THDIRY	THDIRZ
16.8987	3483.1013	0.0000	-1.0000	0.0000
VTBGAINED	THACCEL	THRUST	MASSFLOW	VACISP
0.0024860	0.002674	26690.00	5.6329	483.0000

CURRENT TARGET ENGINE VALUES

TIME	TOTBTIME	BTAVAIL	DELVUSED	DVAVAIL
3.9000	3.9000	617.4490	0.010421	2.030728
FUELUSED	FUELAVAIL	THDIRX	THDIRY	THDIRZ
21.9683	3478.0317	0.0000	-1.0000	0.0000
VTBGAINED	THACCEL	THRUST	MASSFLOW	VACISP
0.0000813	0.000813	8114.40	1.7125	483.0000

CURRENT TARGET ENGINE VALUES

TIME	TOTBTIME	BTAVAIL	DELVUSED	DVAVAIL
4.0000	4.0000	617.4186	0.010502	2.030647
FUELUSED	FUELAVAIL	THDIRX	THDIRY	THDIRZ
22.1396	3477.8604	0.0523	-0.9985	0.0150
VTBGAINED	THACCEL	THRUST	MASSFLOW	VACISP
0.0000000	0.000000	0.00	0.0000	483.0000

EVASIVE MANEUVER COMPLETED - THRUST TERMINATED

CURRENT TIME

TIME	RREL	RRELX	RRELY	RRELZ
100.0000	534.4046	-250.2386	1.0278	-472.1948

MISSILE VALUES

ALT	R	RX	RY	RZ
267.0812	6638.3962	2644.9896	0.0000	6088.7055
VMAG	VX	VY	VZ	ACCELGRAV
7.5334	-6.1551	0.0000	4.3436	9.0337
DECCELDRAG	RHO			
0.1027E-10	0.4653E-10			

TARGET VALUES

ALT	R	RX	RY	RZ
800.0000	7171.3150	2895.2281	-1.0278	6560.9003

VMAG	VX	VY	VZ	ACCELGRAV
7.4507	-6.8165	-0.0104	3.0080	7.7410
DECCELDRAG	RHO			
0.1043E-14	0.1136E-13			

PREDICTED TIME

TIME	RREL	RRELX	RRELY	RRELZ
500.0000	5.0400	0.4494	5.0000	-0.4473

MISSILE VALUES

ALT	R	RX	RY	RZ
799.5527	7170.8677	0.4490	0.0000	7170.8677
VMAG	VX	VY	VZ	ACCELGRAV
6.9171	-6.8283	0.0000	1.1048	7.7419
DECCELDRAG	RHO			
0.2520E-14	0.1142E-13			

TARGET VALUES

ALT	R	RX	RY	RZ
800.0017	7171.3167	-0.0003	-5.0000	7171.3150
VMAG	VX	VY	VZ	ACCELGRAV
7.4507	-7.4507	-0.0091	0.0000	7.7409
DECCELDRAG	RHO			
0.1043E-14	0.1136E-13			

CURRENT TIME

TIME	RREL	RRELX	RRELY	RRELZ
200.0000	391.1550	-185.9418	2.0651	-344.1274

MISSILE VALUES

ALT	R	RX	RY	RZ
415.8077	6787.1227	2013.2502	0.0000	6481.6555
VMAG	VX	VY	VZ	ACCELGRAV
7.3569	-6.4624	0.0000	3.5159	8.6421
DECCELDRAG	RHO			
0.4822E-12	0.2291E-11			

TARGET VALUES

ALT	R	RX	RY	RZ
800.0002	7171.3152	2199.1920	-2.0651	6825.7829
VMAG	VX	VY	VZ	ACCELGRAV
7.4507	-7.0917	-0.0103	2.2849	7.7410
DECCELDRAG	RHO			
0.1043E-14	0.1136E-13			

PREDICTED TIME

TIME	RREL	RRELX	RRELY	RRELZ
600.0000	127.0222	62.5449	5.8841	110.4000

MISSILE VALUES

ALT	R	RX	RY	RZ
903.6911	7275.0061	-681.1851	0.0000	7243.0450
VMAG	VX	VY	VZ	ACCELGRAV
6.8013	-6.7926	0.0000	0.3430	7.5219
DECCELDRAG	RHO			
0.1192E-14	0.5663E-14			

TARGET VALUES

ALT	R	RX	RY	RZ
800.0025	7171.3175	-743.7300	-5.8841	7132.6451
VMAG	VX	VY	VZ	ACCELGRAV
7.4507	-7.4105	-0.0085	-0.7727	7.7409
DECCELDRAG	RHO			
0.1043E-14	0.1136E-13			

CURRENT TIME

TIME	RREL	RRELX	RRELY	RRELZ
300.0000	256.6740	-123.6432	3.0801	-224.9097

MISSILE VALUES

ALT	R	RX	RY	RZ
554.8223	6926.1373	1355.7951	0.0000	6792.1423
VMAG	VX	VY	VZ	ACCELGRAV
7.1951	-6.6710	0.0000	2.6958	8.2987

DECCELDRAG RHO
0.4557E-13 0.2264E-12

TARGET VALUES

ALT	R	RX	RY	RZ
800.0006	7171.3156	1479.4383	-3.0801	7017.0521
VMAG	VX	VY	VZ	ACCELGRAV
7.4507	-7.2904	-0.0100	1.5371	7.7410

DECCELDRAG RHO
0.1043E-14 0.1136E-13

PREDICTED TIME

TIME	RREL	RRELX	RRELY	RRELZ
700.0000	255.3216	123.6136	6.7047	223.3021

MISSILE VALUES

ALT	R	RX	RY	RZ
994.8913	7366.2063	-1355.8252	0.0000	7240.3545
VMAG	VX	VY	VZ	ACCELGRAV
6.7009	-6.6894	0.0000	-0.3922	7.3368

DECCELDRAG RHO
0.7352E-15 0.3652E-14

TARGET VALUES

ALT	R	RX	RY	RZ
800.0035	7171.3185	-1479.4388	-6.7047	7017.0524
VMAG	VX	VY	VZ	ACCELGRAV
7.4507	-7.2904	-0.0079	-1.5371	7.7409

DECCELDRAG RHO
0.1043E-14 0.1136E-13

CURRENT TIME

TIME	RREL	RRELX	RRELY	RRELZ
400.0000	127.3674	-61.7076	4.0620	-111.3469

MISSILE VALUES

ALT	R	RX	RY	RZ
-----	---	----	----	----

683.0298	7054.3448	682.0219	0.0000	7021.2981
VMAG	VX	VY	VZ	ACCELGRAV
7.0484	-6.7902	0.0000	1.8903	7.9998
DECCELDRAG	RHO			
0.7663E-14	0.3967E-13			

TARGET VALUES

ALT	R	RX	RY	RZ
800.0011	7171.3161	743.7295	-4.0620	7132.6450
VMAG	VX	VY	VZ	ACCELGRAV
7.4507	-7.4105	-0.0096	0.7727	7.7409
DECCELDRAG	RHO			
0.1043E-14	0.1136E-13			

PREDICTED TIME

TIME	RREL	RRELX	RRELY	RRELZ
800.0000	385.6167	182.1897	7.4531	339.7817

MISSILE VALUES

ALT	R	RX	RY	RZ
1072.7179	7444.0329	-2017.0027	0.0000	7165.5653
VMAG	VX	VY	VZ	ACCELGRAV
6.6161	-6.5242	0.0000	-1.0987	7.1842
DECCELDRAG	RHO			
0.0000E+00	0.0000E+00			

TARGET VALUES

ALT	R	RX	RY	RZ
800.0046	7171.3196	-2199.1924	-7.4531	6825.7836
VMAG	VX	VY	VZ	ACCELGRAV
7.4507	-7.0917	-0.0071	-2.2849	7.7409
DECCELDRAG	RHO			
0.1043E-14	0.1136E-13			

CURRENT TIME

TIME	RREL	RRELX	RRELY	RRELZ
500.0000	5.0400	0.4494	5.0000	-0.4473

MISSILE VALUES

ALT	R	RX	RY	RZ
799.5527	7170.8677	0.4493	0.0000	7170.8677
VMAG	VX	VY	VZ	ACCELGRAV
6.9171	-6.8283	0.0000	1.1048	7.7419
DECCELDRAG	RHO			
0.2124E-14	0.1142E-13			

TARGET VALUES

ALT	R	RX	RY	RZ
800.0018	7171.3168	-0.0001	-5.0000	7171.3151
VMAG	VX	VY	VZ	ACCELGRAV
7.4507	-7.4507	-0.0091	0.0000	7.7409
DECCELDRAG	RHO			
0.1043E-14	0.1136E-13			

PREDICTED TIME

TIME	RREL	RRELX	RRELY	RRELZ
900.0000	517.9414	236.4792	8.1210	460.7330

MISSILE VALUES

ALT	R	RX	RY	RZ
1136.8340	7508.1490	-2658.7494	0.0000	7021.6346
VMAG	VX	VY	VZ	ACCELGRAV
6.5467	-6.3015	0.0000	-1.7748	7.0620
DECCELDRAG	RHO			
0.0000E+00	0.0000E+00			

TARGET VALUES

ALT	R	RX	RY	RZ
800.0059	7171.3209	-2895.2286	-8.1210	6560.9016
VMAG	VX	VY	VZ	ACCELGRAV
7.4507	-6.8165	-0.0063	-3.0080	7.7409
DECCELDRAG	RHO			
0.1043E-14	0.1136E-13			

CURRENT TIME

TIME	RREL	RRELX	RRELY	RRELZ
600.0000	127.0222	62.5449	5.8841	110.4000

MISSILE VALUES

ALT	R	RX	RY	RZ
903.6914	7275.0064	-681.1849	0.0000	7243.0453

VMAG	VX	VY	VZ	ACCELGRAV
6.8013	-6.7926	0.0000	0.3430	7.5219

DECCELDRAG	RHO
0.1019E-14	0.5663E-14

TARGET VALUES

ALT	R	RX	RY	RZ
800.0027	7171.3177	-743.7298	-5.8841	7132.6453

VMAG	VX	VY	VZ	ACCELGRAV
7.4507	-7.4105	-0.0085	-0.7727	7.7409

DECCELDRAG	RHO
0.1043E-14	0.1136E-13

PREDICTED TIME

TIME	RREL	RRELX	RRELY	RRELZ
1000.0000	651.8464	284.5233	8.7014	586.4082

MISSILE VALUES

ALT	R	RX	RY	RZ
1186.9836	7558.2986	-3275.5177	0.0000	6811.6710

VMAG	VX	VY	VZ	ACCELGRAV
6.4927	-6.0252	0.0000	-2.4191	6.9686

DECCELDRAG	RHO
0.0000E+00	0.0000E+00

TARGET VALUES

ALT	R	RX	RY	RZ
800.0074	7171.3224	-3560.0410	-8.7014	6225.2629

VMAG	VX	VY	VZ	ACCELGRAV
7.4507	-6.4678	-0.0053	-3.6987	7.7409

DECCELDRAG	RHO
0.1043E-14	0.1136E-13

MISSILE SUCCESSFULLY EVADED

FINAL ORBITAL ELEMENTS FOR THE TARGET

H	P	A	E	I
53431.3230	7171.3295	7171.3295	0.0000	89.9601

FINAL ORBITAL ELEMENTS FOR THE MISSILE

H	P	A	E	I
48965.5424	6022.6685	6300.4475	0.2100	90.0000

B.4 Retrograde Direct-Ascent Intercept Scenario

DIRECT INTERCEPT OR CO-ORBITAL INJECTION? (D OR C) D

INPUT DATA FOR NEW SETUP

TALT1	MALT1	TN2	MN1	FIXTIME	TRTIME	ORBINCL
800.0000	110.0000	90.0000	120.0000	1.0000	500.0000	90.0000

INTERCEPT OR NEAR-MISS TRAJECTORY? (I OR M) I

INPUT INTSTEP, BURNSTEP, THOUTSTEP, OUTSTEP, NRUNS: 1.000 0.100 1.000 100.000 8

AXISYMMETRIC GRAVITY, DRAG? (Y OR N) Y, Y

INITIAL INPUT VECTORS FOR THIS RUN

(TIME BETWEEN MISSILE FIXES: 1.0000)

RMOX	RMOY	RMOZ	RM1X	RM1Y	RM1Z
-3246.3952	0.0000	5607.8091	-3240.6575	0.0000	5612.9834
RT1X	RT1Y	RT1Z	VT1X	VT1Y	VT1Z
3560.0404	0.0000	6225.2608	-6.4678	0.0000	3.6987

MISSILE AND TARGET TRAJECTORIES

TIME IN SEC, DISTANCE IN KM, VELOCITY IN KM/S
ACCELERATION DUE TO DRAG AND GRAVITY IN M/S**2, DENSITY IN KG/M**3
THRUST ACCELERATION IN KM/S**2, MASS IN KG, THRUST IN NEWTONS
VACISP IN SEC, MASSFLOW IN KG/S

INITIAL PREDICTED INTERCEPT TIME	MISSILE APOGEE ALTITUDE
500.0000	1254.2041

CURRENT TIME

TIME	RREL	RRELX	RRELY	RRELZ
0.0000	6828.2044	-6800.6979	0.0000	-612.2773

MISSILE VALUES

ALT	R	RX	RY	RZ
110.0000	6481.3150	-3240.6575	0.0000	5612.9834

VMAG	VX	VY	VZ	ACCELGRAV
7.7253	5.7401	0.0000	5.1702	9.4769
DECCELDRAG	RHO			
0.1041E-06	0.4487E-06			

TARGET VALUES

ALT	R	RX	RY	RZ
800.0000	7171.3150	3560.0404	0.0000	6225.2608
VMAG	VX	VY	VZ	ACCELGRAV
7.4507	-6.4678	0.0000	3.6987	7.7410
DECCELDRAG	RHO			
0.1041E-14	0.1136E-13			

PREDICTED TIME

TIME	RREL	RRELX	RRELY	RRELZ
500.0000	0.0005	0.0005	0.0000	0.0000

MISSILE VALUES

ALT	R	RX	RY	RZ
800.0000	7171.3150	0.0003	0.0000	7171.3150
VMAG	VX	VY	VZ	ACCELGRAV
6.9181	6.8291	0.0000	1.1058	7.7410
DECCELDRAG	RHO			
0.2636E-14	0.1136E-13			

TARGET VALUES

ALT	R	RX	RY	RZ
800.0000	7171.3150	-0.0002	0.0000	7171.3150
VMAG	VX	VY	VZ	ACCELGRAV
7.4507	-7.4507	0.0000	0.0000	7.7410
DECCELDRAG	RHO			
0.1041E-14	0.1136E-13			

EVASIVE MANEUVER REQUIRED

INPUT MANEUVER OPTION (R,V,H,E,C), DESIRED MISS DISTANCE (KM): H 5.0000

REQUIRED IMPULSIVE DELV = 0.010464

REQUIRED IMPULSIVE DELV VECTOR (DELVX,DELVY,DELVZ) = 0.000001 -0.010464 0.000000

SELECT IMPULSIVE DELV, ENGINE BURN OR NO EVASION: (I,E OR N) E

CURRENT TIME

TIME RREL RRELX RRELY RRELZ
0.0000 6828.2044 -6800.6979 0.0000 -612.2773

MISSILE VALUES

ALT R RX RY RZ
110.0000 6481.3150 -3240.6575 0.0000 5612.9834
VMAG VX VY VZ ACCELGRAV
7.7253 5.7401 0.0000 5.1702 9.4769
DECCELDRAG RHO
0.1041E-06 0.4487E-06

TARGET VALUES

ALT R RX RY RZ
800.0000 7171.3150 3560.0404 0.0000 6225.2608
VMAG VX VY VZ ACCELGRAV
7.4507 -6.4678 0.0000 3.6987 7.7410
DECCELDRAG RHO
0.1041E-14 0.1136E-13

CURRENT TARGET ENGINE VALUES

TIME TOTBTIME BTAVAIL DELVUSED DVAVAIL
0.0000 0.0000 621.3490 0.000000 2.041149
FUELUSED FUELAVAIL THDIRX THDIRY THDIRZ
0.0000 3500.0000 0.0001 -1.0000 0.0000
VTBGAINED THACCEL THRUST MASSFLOW VACISP
0.0104643 0.002669 26690.00 5.6329 483.0000

PREDICTED TIME

TIME RREL RRELX RRELY RRELZ

500.0000 0.0005 0.0005 0.0000 0.0000

MISSILE VALUES

ALT R RX RY RZ
800.0000 7171.3150 0.0003 0.0000 7171.3150

VMAG VX VY VZ ACCELGRAV
6.9181 6.8291 0.0000 1.1058 7.7410

DECCELDRAG RHO
0.2636E-14 0.1136E-13

TARGET VALUES

ALT R RX RY RZ
800.0000 7171.3150 -0.0002 0.0000 7171.3150

VMAG VX VY VZ ACCELGRAV
7.4507 -7.4507 0.0000 0.0000 7.7410

DECCELDRAG RHO
0.1041E-14 0.1136E-13

CURRENT TARGET ENGINE VALUES

TIME TOTBTIME BTAVAIL DELVUSED DVAVAIL
1.0000 1.0000 620.3490 0.002670 2.038479

FUELUSED FUELAVAIL THDIRX THDIRY THDIRZ
5.6329 3494.3671 0.0001 -1.0000 0.0000

VTBGAINED THACCEL THRUST MASSFLOW VACISP
0.0078112 0.002671 26690.00 5.6329 483.0000

CURRENT TARGET ENGINE VALUES

TIME TOTBTIME BTAVAIL DELVUSED DVAVAIL
2.0000 2.0000 619.3490 0.005341 2.035808

FUELUSED FUELAVAIL THDIRX THDIRY THDIRZ
11.2658 3488.7342 0.0001 -1.0000 0.0000

VTBGAINED THACCEL THRUST MASSFLOW VACISP
0.0051518 0.002672 26690.00 5.6329 483.0000

CURRENT TARGET ENGINE VALUES

TIME TOTBTIME BTAVAIL DELVUSED DVAVAIL
3.0000 3.0000 618.3490 0.008014 2.033135

FUELUSED	FUELAFAIL	THDIRX	THDIRY	THDIRZ
16.8987	3483.1013	0.0001	-1.0000	0.0000
VTBGAINED	THACCEL	THRUST	MASSFLOW	VACISP
0.0024860	0.002674	26690.00	5.6329	483.0000

CURRENT TARGET ENGINE VALUES

TIME	TOTBTIME	BTAVAIL	DELVUSED	DVAVAIL
3.9000	3.9000	617.4490	0.010421	2.030728
FUELUSED	FUELAFAIL	THDIRX	THDIRY	THDIRZ
21.9683	3478.0317	0.0001	-1.0000	0.0000
VTBGAINED	THACCEL	THRUST	MASSFLOW	VACISP
0.0000813	0.000813	8114.40	1.7125	483.0000

CURRENT TARGET ENGINE VALUES

TIME	TOTBTIME	BTAVAIL	DELVUSED	DVAVAIL
4.0000	4.0000	617.4186	0.010502	2.030647
FUELUSED	FUELAFAIL	THDIRX	THDIRY	THDIRZ
22.1396	3477.8604	0.0524	-0.9985	0.0150
VTBGAINED	THACCEL	THRUST	MASSFLOW	VACISP
0.0000000	0.000000	0.00	0.0000	483.0000

EVASIVE MANEUVER COMPLETED - THRUST TERMINATED

CURRENT TIME

TIM	RREL	RRELX	RRELY	RRELZ
100.0000	5560.3042	-5540.2178	1.0278	-472.1948

MISSILE VALUES

ALT	R	RX	RY	RZ
267.0812	6638.3962	-2644.9896	0.0000	6088.7055

VMAG	VX	VY	VZ	ACCELGRAV
7.5334	6.1551	0.0000	4.3436	9.0337

DECCELDRAG	RHO
0.1027E-10	0.4653E-10

TARGET VALUES

ALT	R	RX	RY	RZ
-----	---	----	----	----

800.0001	7171.3151	2895.2282	-1.0278	6560.9003
VMAG	VX	VY	VZ	ACCELGRAV
7.4507	-6.8165	-0.0104	3.0080	7.7410
DECCELDRAG	RHO			
0.1043E-14	0.1136E-13			

PREDICTED TIME

TIME	RREL	RRELX	RRELY	RRELZ
500.0000	5.0400	-0.4492	5.0000	-0.4473

MISSILE VALUES

ALT	R	RX	RY	RZ
799.5527	7170.8677	-0.4490	0.0000	7170.8677
VMAG	VX	VY	VZ	ACCELGRAV
6.9171	6.8283	0.0000	1.1048	7.7419
DECCELDRAG	RHO			
0.2520E-14	0.1142E-13			

TARGET VALUES

ALT	R	RX	RY	RZ
800.0017	7171.3167	0.0002	-5.0000	7171.3150
VMAG	VX	VY	VZ	ACCELGRAV
7.4507	-7.4507	-0.0091	0.0000	7.7409
DECCELDRAG	RHO			
0.1043E-14	0.1136E-13			

CURRENT TIME

TIME	RREL	RRELX	RRELY	RRELZ
200.0000	4226.4759	-4212.4424	2.0651	-344.1274

MISSILE VALUES

ALT	R	RX	RY	RZ
415.8077	6787.1227	-2013.2502	0.0000	6481.6555
VMAG	VX	VY	VZ	ACCELGRAV
7.3569	6.4624	0.0000	3.5159	8.6421
DECCELDRAG	RHO			
0.4822E-12	0.2291E-11			

TARGET VALUES

ALT	R	RX	RY	RZ
800.0003	7171.3153	2199.1922	-2.0651	6825.7829
VMAG	VX	VY	VZ	ACCELGRAV
7.4507	-7.0917	-0.0103	2.2849	7.7410
DECCELDRAG	RHO			
0.1043E-14	0.1136E-13			

PREDICTED TIME

TIME	RREL	RRELX	RRELY	RRELZ
600.0000	1429.1970	1424.9145	5.8841	110.4000

MISSILE VALUES

ALT	R	RX	RY	RZ
903.6911	7275.0061	681.1851	0.0000	7243.0450
VMAG	VX	VY	VZ	ACCELGRAV
6.8013	6.7926	0.0000	0.3430	7.5219
DECCELDRAG	RHO			
0.1192E-14	0.5663E-14			

TARGET VALUES

ALT	R	RX	RY	RZ
800.0024	7171.3174	-743.7294	-5.8841	7132.6451
VMAG	VX	VY	VZ	ACCELGRAV
7.4507	-7.4105	-0.0085	-0.7727	7.7409
DECCELDRAG	RHO			
0.1043E-14	0.1136E-13			

CURRENT TIME

TIME	RREL	RRELX	RRELY	RRELZ
300.0000	2844.1421	-2835.2338	3.0801	-224.9097

MISSILE VALUES

ALT	R	RX	RY	RZ
554.8223	6926.1373	-1355.7951	0.0000	6792.1423
VMAG	VX	VY	VZ	ACCELGRAV
7.1951	6.6710	0.0000	2.6958	8.2987

DECCELDRAG RHO
0.4557E-13 0.2264E-12

TARGET VALUES

ALT R RX RY RZ
800.0006 7171.3156 1479.4387 -3.0801 7017.0521

VMAG VX VY VZ ACCELGRAV
7.4507 -7.2904 -0.0100 1.5371 7.7410

DECCELDRAG RHO
0.1043E-14 0.1136E-13

PREDICTED TIME

TIME RREL RRELX RRELY RRELZ
700.0000 2844.0510 2835.2632 6.7047 223.3021

MISSILE VALUES

ALT R RX RY RZ
994.8913 7366.2063 1355.8252 0.0000 7240.3545

VMAG VX VY VZ ACCELGRAV
6.7009 6.6894 0.0000 -0.3922 7.3368

DECCELDRAG RHO
0.7352E-15 0.3652E-14

TARGET VALUES

ALT R RX RY RZ
800.0033 7171.3183 -1479.4381 -6.7047 7017.0524

VMAG VX VY VZ ACCELGRAV
7.4507 -7.2904 -0.0079 -1.5371 7.7409

DECCELDRAG RHO
0.1043E-14 0.1136E-13

CURRENT TIME

TIME RREL RRELX RRELY RRELZ
400.0000 1430.0990 -1425.7519 4.0620 -111.3469

MISSILE VALUES

ALT R RX RY RZ

683.0298	7054.3448	-682.0219	0.0000	7021.2981
VMAG	VX	VY	VZ	ACCELGRAV
7.0484	6.7902	0.0000	1.8903	7.9998
DECCELDRAG	RHO			
0.7663E-14	0.3967E-13			

TARGET VALUES

ALT	R	RX	RY	RZ
800.0011	7171.3161	743.7300	-4.0620	7132.6450
VMAG	VX	VY	VZ	ACCELGRAV
7.4507	-7.4105	-0.0096	0.7727	7.7409
DECCELDRAG	RHO			
0.1043E-14	0.1136E-13			

PREDICTED TIME

TIME	RREL	RRELX	RRELY	RRELZ
800.0000	4229.8702	4216.1943	7.4531	339.7817

MISSILE VALUES

ALT	R	RX	RY	RZ
1072.7179	7444.0329	2017.0027	0.0000	7165.5653
VMAG	VX	VY	VZ	ACCELGRAV
6.6161	6.5242	0.0000	-1.0987	7.1842
DECCELDRAG	RHO			
0.0000E+00	0.0000E+00			

TARGET VALUES

ALT	R	RX	RY	RZ
800.0044	7171.3194	-2199.1916	-7.4531	6825.7836
VMAG	VX	VY	VZ	ACCELGRAV
7.4507	-7.0917	-0.0071	-2.2849	7.7409
DECCELDRAG	RHO			
0.1043E-14	0.1136E-13			

CURRENT TIME

TIME	RREL	RRELX	RRELY	RRELZ
500.0000	5.0401	-0.4498	5.0000	-0.4473

MISSILE VALUES

ALT	R	RX	RY	RZ
799.5527	7170.8677	-0.4493	0.0000	7170.8677
VMAG	VX	VY	VZ	ACCELGRAV
6.9171	6.8283	0.0000	1.1048	7.7419
DECCELDRAG	RHO			
0.2124E-14	0.1142E-13			

TARGET VALUES

ALT	R	RX	RY	RZ
800.0018	7171.3168	0.0004	-5.0000	7171.3151
VMAG	VX	VY	VZ	ACCELGRAV
7.4507	-7.4507	-0.0091	0.0000	7.7409
DECCELDRAG	RHO			
0.1043E-14	0.1136E-13			

PREDICTED TIME

TIME	RREL	RRELX	RRELY	RRELZ
900.0000	5573.0605	5553.9772	8.1210	460.7330

MISSILE VALUES

ALT	R	RX	RY	RZ
1136.8340	7508.1490	2658.7494	0.0000	7021.6346
VMAG	VX	VY	VZ	ACCELGRAV
6.5467	6.3015	0.0000	-1.7748	7.0620
DECCELDRAG	RHO			
0.0000E+00	0.0000E+00			

TARGET VALUES

ALT	R	RX	RY	RZ
800.0056	7171.3206	-2895.2277	-8.1210	6560.9016
VMAG	VX	VY	VZ	ACCELGRAV
7.4507	-6.8165	-0.0063	-3.0080	7.7409
DECCELDRAG	RHO			
0.1043E-14	0.1136E-13			

CURRENT TIME

TIME	RREL	RRELX	RRELY	RRELZ
600.0000	1429.1965	1424.9140	5.8841	110.4000

MISSILE VALUES

ALT	R	RX	RY	RZ
903.6914	7275.0064	681.1849	0.0000	7243.0453

VMAG	VX	VY	VZ	ACCELGRAV
6.8013	6.7926	0.0000	0.3430	7.5219

DECCELDRAG	RHO
0.1019E-14	0.5663E-14

TARGET VALUES

ALT	R	RX	RY	RZ
800.0026	7171.3176	-743.7291	-5.8841	7132.6453

VMAG	VX	VY	VZ	ACCELGRAV
7.4507	-7.4105	-0.0085	-0.7727	7.7409

DECCELDRAG	RHO
0.1043E-14	0.1136E-13

PREDICTED TIME

TIME	RREL	RRELX	RRELY	RRELZ
1000.0000	6860.6705	6835.5577	8.7014	586.4082

MISSILE VALUES

ALT	R	RX	RY	RZ
1186.9836	7558.2986	3275.5177	0.0000	6811.6710

VMAG	VX	VY	VZ	ACCELGRAV
6.4927	6.0252	0.0000	-2.4191	6.9686

DECCELDRAG	RHO
0.0000E+00	0.0000E+00

TARGET VALUES

ALT	R	RX	RY	RZ
800.0069	7171.3219	-3560.0400	-8.7014	6225.2628

VMAG	VX	VY	VZ	ACCELGRAV
7.4507	-6.4678	-0.0053	-3.6987	7.7409

DECCELDRAG	RHO
------------	-----

0.1043E-14 0.1136E-13

MISSILE SUCCESSFULLY EVADED

FINAL ORBITAL ELEMENTS FOR THE TARGET

H	P	A	E	I
53431.3158	7171.3276	7171.3276	0.0000	89.9601

FINAL ORBITAL ELEMENTS FOR THE MISSILE

H	P	A	E	I
48965.5424	6022.6685	6300.4475	0.2100	90.0000

B.5 Retrograde Direct-Ascent Scenario with No Drag

DIRECT INTERCEPT OR CO-ORBITAL INJECTION? (D OR C) D

INPUT DATA FOR NEW SETUP

TALT1	MALT1	TN2	MN1	FIXTIME	TRTIME	ORBINCL
800.0000	110.0000	90.0000	120.0000	1.0000	500.0000	90.0000

INTERCEPT OR NEAR-MISS TRAJECTORY? (I OR M) I

INPUT INTSTEP,BURNSTEP,THOUTSTEP,OUTSTEP,NRUNS: 1.000 0.100 1.000 100.000 8

AXISYMMETRIC GRAVITY,DRAG? (Y OR N) Y,N

INITIAL INPUT VECTORS FOR THIS RUN

(TIME BETWEEN MISSILE FIXES: 1.0000)

RMOX	RMOY	RMOZ	RM1X	RM1Y	RM1Z
-3246.3952	0.0000	5607.8091	-3240.6575	0.0000	5612.9834
RT1X	RT1Y	RT1Z	VT1X	VT1Y	VT1Z
3560.0404	0.0000	6225.2608	-6.4678	0.0000	3.6987

MISSILE AND TARGET TRAJECTORIES

TIME IN SEC, DISTANCE IN KM, VELOCITY IN KM/S
ACCELERATION DUE TO DRAG AND GRAVITY IN M/S**2, DENSITY IN KG/M**3
THRUST ACCELERATION IN KM/S**2, MASS IN KG, THRUST IN NEWTONS
VACISP IN SEC, MASSFLOW IN KG/S

INITIAL PREDICTED INTERCEPT TIME	MISSILE APOGEE ALTITUDE
500.0000	1254.2041

CURRENT TIME

TIME	RREL	RRELX	RRELY	RRELZ
0.0000	6828.2044	-6800.6979	0.0000	-612.2773

MISSILE VALUES

ALT	R	RX	RY	RZ
110.0000	6481.3150	-3240.6575	0.0000	5612.9834

VMAG	VX	VY	VZ	ACCELGRAV
7.7253	5.7401	0.0000	5.1702	9.4769

TARGET VALUES

ALT	R	RX	RY	RZ
800.0000	7171.3150	3560.0404	0.0000	6225.2608

VMAG	VX	VY	VZ	ACCELGRAV
7.4507	-6.4678	0.0000	3.6987	7.7410

PREDICTED TIME

TIME	RREL	RRELX	RRELY	RRELZ
500.0000	0.0005	0.0005	0.0000	0.0000

MISSILE VALUES

ALT	R	RX	RY	RZ
800.0000	7171.3150	0.0003	0.0000	7171.3150

VMAG	VX	VY	VZ	ACCELGRAV
6.9181	6.8291	0.0000	1.1058	7.7410

TARGET VALUES

ALT	R	RX	RY	RZ
800.0000	7171.3150	-0.0002	0.0000	7171.3150

VMAG	VX	VY	VZ	ACCELGRAV
7.4507	-7.4507	0.0000	0.0000	7.7410

EVASIVE MANEUVER REQUIRED

INPUT MANEUVER OPTION (R,V,H,E,C), DESIRED MISS DISTANCE (KM): H 5.0000

REQUIRED IMPULSIVE DELV = 0.010464

REQUIRED IMPULSIVE DELV VECTOR (DELVX,DELVY,DELVZ) = 0.000001 -0.010464 0.000000

SELECT IMPULSIVE DELV, ENGINE BURN OR NO EVASION: (I,E OR N) E

CURRENT TIME

TIME	RREL	RRELX	RRELY	RRELZ
0.0000	6828.2044	-6800.6979	0.0000	-612.2773

MISSILE VALUES

ALT	R	RX	RY	RZ
110.0000	6481.3150	-3240.6575	0.0000	5612.9834
VMAG	VX	VY	VZ	ACCELGRAV
7.7253	5.7401	0.0000	5.1702	9.4769

TARGET VALUES

ALT	R	RX	RY	RZ
800.0000	7171.3150	3560.0404	0.0000	6225.2608
VMAG	VX	VY	VZ	ACCELGRAV
7.4507	-6.4678	0.0000	3.6987	7.7410

CURRENT TARGET ENGINE VALUES

TIME	TOTBTIME	BTAVAIL	DELVUSED	DVAVAIL
0.0000	0.0000	621.3490	0.000000	2.041149
FUELUSED	FUELAVAIL	THDIRX	THDIRY	THDIRZ
0.0000	3500.0000	0.0001	-1.0000	0.0000
VTBAINED	THACCEL	THRUST	MASSFLOW	VACISP
0.0104643	0.002669	26690.00	5.6329	483.0000

PREDICTED TIME

TIME	RREL	RRELX	RRELY	RRELZ
500.0000	0.0005	0.0005	0.0000	0.0000

MISSILE VALUES

ALT	R	RX	RY	RZ
800.0000	7171.3150	0.0003	0.0000	7171.3150
VMAG	VX	VY	VZ	ACCELGRAV
6.9181	6.8291	0.0000	1.1058	7.7410

TARGET VALUES

ALT	R	RX	RY	RZ
800.0000	7171.3150	-0.0002	0.0000	7171.3150
VMAG	VX	VY	VZ	ACCELGRAV
7.4507	-7.4507	0.0000	0.0000	7.7410

CURRENT TARGET ENGINE VALUES

TIME	TOTBTIME	BTAVAIL	DELVUSED	DVAVAIL
1.0000	1.0000	620.3490	0.002670	2.038479
FUELUSED	FUELAVAIL	THDIRX	THDIRY	THDIRZ
5.6329	3494.3671	0.0001	-1.0000	0.0000
VTBGAINED	THACCEL	THRUST	MASSFLOW	VACISP
0.0078112	0.002671	26690.00	5.6329	483.0000

CURRENT TARGET ENGINE VALUES

TIME	TOTBTIME	BTAVAIL	DELVUSED	DVAVAIL
2.0000	2.0000	619.3490	0.005341	2.035808
FUELUSED	FUELAVAIL	THDIRX	THDIRY	THDIRZ
11.2658	3488.7342	0.0001	-1.0000	0.0000
VTBGAINED	THACCEL	THRUST	MASSFLOW	VACISP
0.0051518	0.002672	26690.00	5.6329	483.0000

CURRENT TARGET ENGINE VALUES

TIME	TOTBTIME	BTAVAIL	DELVUSED	DVAVAIL
3.0000	3.0000	618.3490	0.008014	2.033135
FUELUSED	FUELAVAIL	THDIRX	THDIRY	THDIRZ
16.8987	3483.1013	0.0001	-1.0000	0.0000
VTBGAINED	THACCEL	THRUST	MASSFLOW	VACISP
0.0024860	0.002674	26690.00	5.6329	483.0000

CURRENT TARGET ENGINE VALUES

TIME	TOTBTIME	BTAVAIL	DELVUSED	DVAVAIL
3.9000	3.9000	617.4490	0.010421	2.030728
FUELUSED	FUELAVAIL	THDIRX	THDIRY	THDIRZ
21.9683	3478.0317	0.0001	-1.0000	0.0000
VTBGAINED	THACCEL	THRUST	MASSFLOW	VACISP
0.0000813	0.000813	8114.40	1.7125	483.0000

CURRENT TARGET ENGINE VALUES

TIME	TOTBTIME	BTAVAIL	DELVUSED	DVAVAIL
4.0000	4.0000	617.4186	0.010502	2.030647

FUELUSED	FU L AVAIL	THDIRX	THDIRY	THDIRZ
22.1398	3477.8604	0.0524	-0.9985	0.0150
VTB GAINED	THACCEL	THRUST	MASSFLOW	VACISP
0.0000000	0.000000	0.00	0.0000	483.0000

EVASIVE MANEUVER COMPLETED - THRUST TERMINATED

CURRENT TIME

TIME	RREL	RRELX	RRELY	RRELZ
100.0000	5560.2082	-5540.1283	1.0278	-472.1155

MISSILE VALUES

ALT	R	RX	RY	RZ
110.0000	6638.4333	-2644.9001	0.0000	6088.7848
VMAG	VX	VY	VZ	ACCELGRAV
7.5347	6.1561	0.0000	4.3445	9.0336

TARGET VALUES

ALT	R	RX	RY	RZ
800.0000	7171.3151	2895.2282	-1.0278	6560.9003
VMAG	VX	VY	VZ	ACCELGRAV
7.4507	-6.8165	-0.0104	3.0080	7.7410

PREDICTED TIME

TIME	RREL	RRELX	RRELY	RRELZ
500.0000	5.0000	0.0001	5.0000	0.0000

MISSILE VALUES

ALT	R	RX	RY	RZ
799.9999	7171.3149	0.0003	0.0000	7171.3149
VMAG	VX	VY	VZ	ACCELGRAV
6.9181	6.8291	0.0000	1.1058	7.7410

TARGET VALUES

ALT	R	RX	RY	RZ
800.0017	7171.3167	0.0002	-5.0000	7171.3150
VMAG	VX	VY	VZ	ACCELGRAV
7.4507	-7.4507	-0.0091	0.0000	7.7409

CURRENT TIME

TIME	RREL	RRELX	RRELY	RRELZ
200.0000	4226.2773	-4212.2567	2.0651	-343.9610

MISSILE VALUES

ALT	R	RX	RY	RZ
110.0000	6787.2265	-2013.0645	0.0000	6481.8219
VMAG	VX	VY	VZ	ACCELGRAV
7.3582	6.4634	0.0000	3.5168	8.6419

TARGET VALUES

ALT	R	RX	RY	RZ
800.0000	7171.3153	2199.1922	-2.0651	6825.7829
VMAG	VX	VY	VZ	ACCELGRAV
7.4507	-7.0917	-0.0103	2.2849	7.7410

PREDICTED TIME

TIME	RREL	RRELX	RRELY	RRELZ
600.0000	1429.7661	1425.4421	5.8841	110.9563

MISSILE VALUES

ALT	R	RX	RY	RZ
904.2944	7275.6094	681.7127	0.0000	7243.6013
VMAG	VX	VY	VZ	ACCELGRAV
6.8021	6.7934	0.0000	0.3441	7.5206

TARGET VALUES

ALT	R	RX	RY	RZ
800.0024	7171.3174	-743.7294	-5.8841	7132.6451
VMAG	VX	VY	VZ	ACCELGRAV
7.4507	-7.4105	-0.0085	-0.7727	7.7409

CURRENT TIME

TIME	RREL	RRELX	RRELY	RRELZ
300.0000	2843.8444	-2834.9553	3.0801	-224.6545

MISSILE VALUES

ALT	R	RX	RY	RZ
110.0000	6926.3331	-1355.5167	0.0000	6792.3976
VMAG	VX	VY	VZ	ACCELGRAV
7.1963	6.6719	0.0000	2.6967	8.2982

TARGET VALUES

ALT	R	RX	RY	RZ
800.0000	7171.3156	1479.4387	-3.0801	7017.0521
VMAG	VX	VY	VZ	ACCELGRAV
7.4507	-7.2904	-0.0100	1.5371	7.7410

PREDICTED TIME

TIME	RREL	RRELX	RRELY	RRELZ
700.0000	2844.7047	2835.8654	6.7047	223.9803

MISSILE VALUES

ALT	R	RX	RY	RZ
995.6687	7366.9837	1356.4273	0.0000	7241.0327
VMAG	VX	VY	VZ	ACCELGRAV
6.7016	6.6902	0.0000	-0.3909	7.3352

TARGET VALUES

ALT	R	RX	RY	RZ
800.0033	7171.3183	-1479.4381	-6.7047	7017.0524
VMAG	VX	VY	VZ	ACCELGRAV
7.4507	-7.2904	-0.0079	-1.5371	7.7409

CURRENT TIME

TIME	RREL	RRELX	RRELY	RRELZ
400.0000	1429.7065	-1425.3854	4.0620	-110.9989

MISSILE VALUES

ALT	R	RX	RY	RZ
110.0000	7054.6558	-681.6554	0.0000	7021.6461
VMAG	VX	VY	VZ	ACCELGRAV
7.0495	6.7911	0.0000	1.8913	7.9991

TARGET VALUES

ALT	R	RX	RY	RZ
800.0000	7171.3161	743.7300	-4.0620	7132.6450
VMAG	VX	VY	VZ	ACCELGRAV
7.4507	-7.4105	-0.0096	0.7727	7.7409

PREDICTED TIME

TIME	RREL	RRELX	RRELY	RRELZ
800.0000	4230.6087	4216.8694	7.4531	340.5978

MISSILE VALUES

ALT	R	RX	RY	RZ
1073.6865	7445.0015	2017.6778	0.0000	7166.3814
VMAG	VX	VY	VZ	ACCELGRAV
6.6165	6.5249	0.0000	-1.0972	7.1823

TARGET VALUES

ALT	R	RX	RY	RZ
800.0044	7171.3194	-2199.1916	-7.4531	6825.7836
VMAG	VX	VY	VZ	ACCELGRAV
7.4507	-7.0917	-0.0071	-2.2849	7.7409

CURRENT TIME

TIME	RREL	RRELX	RRELY	RRELZ
500.0000	5.0000	-0.0003	5.0000	0.0000

MISSILE VALUES

ALT	R	RX	RY	RZ
110.0000	7171.3150	0.0001	0.0000	7171.3150
VMAG	VX	VY	VZ	ACCELGRAV
6.9181	6.8291	0.0000	1.1058	7.7410

TARGET VALUES

ALT	R	RX	RY	RZ
800.0000	7171.3168	0.0004	-5.0000	7171.3151
VMAG	VX	VY	VZ	ACCELGRAV
7.4507	-7.4507	-0.0091	0.0000	7.7409

PREDICTED TIME

TIME RREL RRELX RRELY RRELZ
900.0000 5573.8875 5554.7263 8.1210 461.7062

MISSILE VALUES

ALT R RX RY RZ
1138.0093 7509.3243 2659.4985 0.0000 7022.6077

VMAG VX VY VZ ACCELGRAV
6.5469 6.3023 0.0000 -1.7731 7.0598

TARGET VALUES

ALT R RX RY RZ
800.0056 7171.3206 -2895.2277 -8.1210 6560.9016

VMAG VX VY VZ ACCELGRAV
7.4507 -6.8165 -0.0063 -3.0080 7.7409

CURRENT TIME

TIME RREL RRELX RRELY RRELZ
600.0000 1429.7656 1425.4416 5.8841 110.9563

MISSILE VALUES

ALT R RX RY RZ
110.0000 7275.6096 681.7125 0.0000 7243.6016

VMAG VX VY VZ ACCELGRAV
6.8021 6.7934 0.0000 0.3442 7.5206

TARGET VALUES

ALT R RX RY RZ
800.0000 7171.3176 -743.7291 -5.8841 7132.6453

VMAG VX VY VZ ACCELGRAV
7.4507 -7.4105 -0.0085 -0.7727 7.7409

PREDICTED TIME

TIME RREL RRELX RRELY RRELZ
1000.0000 6861.5939 6836.3856 8.7014 587.5602

MISSILE VALUES

ALT R RX RY RZ

1188.3807	7559.6957	3276.3456	0.0000	6812.8230
VMAG	VX	VY	VZ	ACCELGRAV
6.4928	6.0260	0.0000	-2.4172	6.9660

TARGET VALUES

ALT	R	RX	RY	RZ
800.0069	7171.3219	-3560.0400	-8.7014	6225.2628
VMAG	VX	VY	VZ	ACCELGRAV
7.4507	-6.4678	-0.0053	-3.6987	7.7409

MISSILE SUCCESSFULLY EVADED

FINAL ORBITAL ELEMENTS FOR THE TARGET

H	P	A	E	I
53431.3158	7171.3276	7171.3276	0.0000	89.9601

FINAL ORBITAL ELEMENTS FOR THE MISSILE

H	P	A	E	I
48973.8689	6024.7170	6302.4626	0.2099	90.0000

B.6 Delta V Required vs. Separation Distance

DIRECT INTERCEPT OR CO-ORBITAL INJECTION? (D OR C) C

INPUT DATA FOR NEW SETUP

TALT1	TN2	ECCENTM	FIXTIME	TRTIME	ORBINCL	RETROGRADE
900.0000	90.0000	0.8000	1.0000	400.0000	0.0000	N

INTERCEPT OR NEAR-MISS TRAJECTORY? (I OR M) I

INPUT INTSTEP, BURNSTEP, THOUTSTEP, OUTSTEP, NRUNS: 1.000 0.100 1.000 50.000 10

AXISYMMETRIC GRAVITY, DRAG? (Y OR N) N, Y

INITIAL INPUT VECTORS FOR THIS RUN

(TIME BETWEEN MISSILE FIXES: 1.0000)

RMOX	RMOY	RMOZ	RM1X	RM1Y	RM1Z
1288.0739	6653.6568	0.0000	1285.0656	6656.7972	0.0000
RT1X	RT1Y	RT1Z	VT1X	VT1Y	VT1Z
2878.6592	6677.2257	0.0000	-6.7947	2.9293	0.0000

MISSILE AND TARGET TRAJECTORIES

TIME IN SEC, DISTANCE IN KM, VELOCITY IN KM/S
ACCELERATION DUE TO DRAG AND GRAVITY IN M/S**2, DENSITY IN KG/M**3
THRUST ACCELERATION IN KM/S**2, MASS IN KG, THRUST IN NEWTONS
VACISP IN SEC, MASSFLOW IN KG/S

INITIAL PREDICTED INTERCEPT TIME	MISSILE APOGEE ALTITUDE
400.0000	900.0000

CURRENT TIME

TIME	RREL	RRELX	RRELY	RRELZ
0.0000	1593.7246	-1593.5937	-20.4285	0.0000

MISSILE VALUES

ALT	R	RX	RY	RZ
408.3857	6779.7007	1285.0656	6656.7972	0.0000

VMAG	VX	VY	VZ	ACCELGRAV
4.3463	-3.0091	3.1361	0.0000	8.6611
DECCELDRAG	RHO			
0.1859E-12	0.2531E-11			

TARGET VALUES

ALT	R	RX	RY	RZ
900.0000	7271.3150	2878.6592	6677.2257	0.0000
VMAG	VX	VY	VZ	ACCELGRAV
7.3993	-6.7947	2.9293	0.0000	7.5295
DECCELDRAG	RHO			
0.5202E-15	0.5759E-14			

PREDICTED TIME

TIME	RREL	RRELX	RRELY	RRELZ
400.0000	0.0001	-0.0001	0.0000	0.0000

MISSILE VALUES

ALT	R	RX	RY	RZ
900.0000	7271.3150	0.0001	7271.3150	0.0000
VMAG	VX	VY	VZ	ACCELGRAV
3.3091	-3.3091	0.0000	0.0000	7.5295
DECCELDRAG	RHO			
0.4230E-15	0.5759E-14			

TARGET VALUES

ALT	R	RX	RY	RZ
900.0000	7271.3150	0.0001	7271.3150	0.0000
VMAG	VX	VY	VZ	ACCELGRAV
7.3993	-7.3993	0.0000	0.0000	7.5295
DECCELDRAG	RHO			
0.5202E-15	0.5759E-14			

EVASIVE MANEUVER REQUIRED

INPUT MANEUVER OPTION (R,V,H,E,C), DESIRED MISS DISTANCE (KM): R 2.0000

REQUIRED IMPULSIVE DELV = 0.004754

REQUIRED IMPULSIVE DELV VECTOR (DELVX,DELVY,DELVZ) = -0.000079 0.004754 0.000000

SELECT IMPULSIVE DELV, ENGINE BURN OR NO EVASION: (I,E OR N) N

CURRENT TIME

TIME	RREL	RRELX	RRELY	RRELZ
50.0000	1402.7223	-1402.6717	-11.9074	0.0000

MISSILE VALUES

ALT	R	RX	RY	RZ
525.4121	6896.7271	1132.6719	6803.0801	0.0000

VMAG	VX	VY	VZ	ACCELGRAV
4.1106	-3.0844	2.7173	0.0000	8.3696

DECCELDRAG	RHO
0.2481E-13	0.3776E-12

TARGET VALUES

ALT	R	RX	RY	RZ
900.0000	7271.3150	2535.3436	6814.9875	0.0000

VMAG	VX	VY	VZ	ACCELGRAV
7.3993	-6.9349	2.5800	0.0000	7.5295

DECCELDRAG	RHO
0.5202E-15	0.5759E-14

PREDICTED TIME

TIME	RREL	RRELX	RRELY	RRELZ
400.0000	0.0001	-0.0001	0.0000	0.0000

MISSILE VALUES

ALT	R	RX	RY	RZ
900.0000	7271.3150	0.0001	7271.3150	0.0000

VMAG	VX	VY	VZ	ACCELGRAV
3.3091	-3.3091	0.0000	0.0000	7.5295

DECCELDRAG	RHO
0.3784E-15	0.5759E-14

TARGET VALUES

ALT	R	RX	RY	RZ
900.0000	7271.3150	0.0001	7271.3150	0.0000
VMAG	VX	VY	VZ	ACCELGRAV
7.3993	-7.3993	0.0000	0.0000	7.5295
DECCELDRAG	RHO			
0.5202E-15	0.5759E-14			

EVASIVE MANEUVER REQUIRED

INPUT MANEUVER OPTION (R,V,H,E,C), DESIRED MISS DISTANCE (KM): R 2.0000

REQUIRED IMPULSIVE DELV = 0.005493

REQUIRED IMPULSIVE DELV VECTOR (DELVX,DELVY,DELVZ) = -0.000061 0.005493 0.000000

SELECT IMPULSIVE DELV, ENGINE BURN OR NO EVASION: (I,E OR N) N

CURRENT TIME

TIME	RREL	RRELX	RRELY	RRELZ
100.0000	1208.6469	-1208.6300	-6.3966	0.0000

MISSILE VALUES

ALT	R	RX	RY	RZ
625.9193	6997.2343	976.8360	6928.7141	0.0000
VMAG	VX	VY	VZ	ACCELGRAV
3.9037	-3.1470	2.3098	0.0000	8.1309
DECCELDRAG	RHO			
0.4999E-14	0.8437E-13			

TARGET VALUES

ALT	R	RX	RY	RZ
900.0000	7271.3150	2185.4660	6935.1107	0.0000
VMAG	VX	VY	VZ	ACCELGRAV
7.3993	-7.0572	2.2239	0.0000	7.5295
DECCELDRAG	RHO			

0.5202E-15 0.5759E-14

PREDICTED TIME

TIME RREL RRELX RRELY RRELZ
400.0000 0.0001 -0.0001 0.0000 0.0000

MISSILE VALUES

ALT R RX RY RZ
900.0000 7271.3150 0.0000 7271.3150 0.0000

VMAG VX VY VZ ACCELGRAV
3.3091 -3.3091 0.0000 0.0000 7.5295

DECCELDRAG RHO
0.3413E-15 0.5759E-14

TARGET VALUES

ALT R RX RY RZ
900.0000 7271.3150 0.0001 7271.3150 0.0000

VMAG VX VY VZ ACCELGRAV
7.3993 -7.3993 0.0000 0.0000 7.5295

DECCELDRAG RHO
0.5202E-15 0.5759E-14

EVASIVE MANEUVER REQUIRED

INPUT MANEUVER OPTION (R,V,H,E,C), DESIRED MISS DISTANCE (KM): R 2.0000

REQUIRED IMPULSIVE DELV = 0.006473

REQUIRED IMPULSIVE DELV VECTOR (DELVX,DELVY,DELVZ) = -0.000046 0.006472 0.000000

SELECT IMPULSIVE DELV, ENGINE BURN OR NO EVASION: (I,E OR N) N

CURRENT TIME

TIME RREL RRELX RRELY RRELZ
150.0000 1011.7787 -1011.7740 -3.0725 0.0000

MISSILE VALUES

ALT	R	RX	RY	RZ
710.3174	7081.6324	818.1579	7034.2118	0.0000
VMAG	VX	VY	VZ	ACCELGRAV
3.7260	-3.1983	1.9115	0.0000	7.9383
DECCELDRAG	RHO			
0.1514E-14	0.2805E-13			

TARGET VALUES

ALT	R	RX	RY	RZ
900.0000	7271.3150	1829.9319	7037.2843	0.0000
VMAG	VX	VY	VZ	ACCELGRAV
7.3993	-7.1611	1.8621	0.0000	7.5295
DECCELDRAG	RHO			
0.5202E-15	0.5759E-14			

PREDICTED TIME

TIME	RREL	RRELX	RRELY	RRELZ
400.0000	0.0001	-0.0001	0.0000	0.0000

MISSILE VALUES

ALT	R	RX	RY	RZ
900.0000	7271.3150	0.0000	7271.3150	0.0000
VMAG	VX	VY	VZ	ACCELGRAV
3.3091	-3.3091	0.0000	0.0000	7.5295
DECCELDRAG	RHO			
0.3109E-15	0.5759E-14			

TARGET VALUES

ALT	R	RX	RY	RZ
900.0000	7271.3150	0.0001	7271.3150	0.0000
VMAG	VX	VY	VZ	ACCELGRAV
7.3993	-7.3993	0.0000	0.0000	7.5295
DECCELDRAG	RHO			
0.5202E-15	0.5759E-14			

EVASIVE MANEUVER REQUIRED

INPUT MANEUVER OPTION (R,V,H,E,C), DESIRED MISS DISTANCE (KM): R 2.0000

REQUIRED IMPULSIVE DELV = 0.007835

REQUIRED IMPULSIVE DELV VECTOR (DELVX,DELVY,DELVZ) = -0.000032 0.007835 0.000000

SELECT IMPULSIVE DELV, ENGINE BURN OR NO EVASION: (I,E OR N) N

CURRENT TIME

TIME RREL RRELX RRELY RRELZ
200.0000 812.4790 -812.4781 -1.2545 0.0000

MISSILE VALUES

ALT R RX RY RZ
778.9396 7150.2546 657.1836 7119.9895 0.0000

VMAG VX VY VZ ACCELGRAV
3.5782 -3.2390 1.5207 0.0000 7.7866

DECCELDRAG RHO
0.7023E-15 0.1411E-13

TARGET VALUES

ALT R RX RY RZ
900.0000 7271.3150 1469.6616 7121.2440 0.0000

VMAG VX VY VZ ACCELGRAV
7.3993 -7.2466 1.4955 0.0000 7.5295

DECCELDRAG RHO
0.5202E-15 0.5759E-14

PREDICTED TIME

TIME RREL RRELX RRELY RRELZ
400.0000 0.0001 -0.0001 0.0000 0.0000

MISSILE VALUES

ALT R RX RY RZ
900.0000 7271.3150 0.0000 7271.3150 0.0000

VMAG VX VY VZ ACCELGRAV
3.3091 -3.3091 0.0000 0.0000 7.5295

DECCELDRAG RHO
0.2867E-15 0.5759E-14

TARGET VALUES

ALT R RX RY RZ
900.0000 7271.3150 0.0001 7271.3150 0.0000

VMAG VX VY VZ ACCELGRAV
7.3993 -7.3993 0.0000 0.0000 7.5295

DECCELDRAG RHO
0.5202E-15 0.5759E-14

EVASIVE MANEUVER REQUIRED

INPUT MANEUVER OPTION (R,V,H,E,C), DESIRED MISS DISTANCE (KM): R 2.0000

REQUIRED IMPULSIVE DELV = 0.009866

REQUIRED IMPULSIVE DELV VECTOR (DELVX,DELVY,DELVZ) = -0.000021 0.009866 0.000000

SELECT IMPULSIVE DELV, ENGINE BURN OR NO EVASION: (I,E OR N) N

CURRENT TIME

TIME RREL RRELX RRELY RRELZ
250.0000 611.1702 -611.1701 -0.3960 0.0000

MISSILE VALUES

ALT R RX RY RZ
832.0492 7203.3642 494.4175 7186.3765 0.0000

VMAG VX VY VZ ACCELGRAV
3.4616 -3.2700 1.1356 0.0000 7.6722

DECCELDRAG RHO
0.4237E-15 0.9093E-14

TARGET VALUES

ALT R RX RY RZ
900.0000 7271.3150 1105.5875 7186.7724 0.0000

VMAG VX VY VZ ACCELGRAV
7.3993 -7.3133 1.1250 0.0000 7.5295

DECCELDRAG RHO
0.5202E-15 0.5759E-14

PREDICTED TIME

TIME	RREL	RRELX	RRELY	RRELZ
400.0000	0.0001	-0.0001	0.0000	0.0000

MISSILE VALUES

ALT	R	RX	RY	RZ
900.0000	7271.3150	0.0000	7271.3150	0.0000
VMAG	VX	VY	VZ	ACCELGRAV
3.3091	-3.3091	0.0000	0.0000	7.5295

DECCELDRAG RHO
0.2683E-15 0.5759E-14

TARGET VALUES

ALT	R	RX	RY	RZ
900.0000	7271.3150	0.0001	7271.3150	0.0000
VMAG	VX	VY	VZ	ACCELGRAV
7.3993	-7.3993	0.0000	0.0000	7.5295

DECCELDRAG RHO
0.5202E-15 0.5759E-14

EVASIVE MANEUVER REQUIRED

INPUT MANEUVER OPTION (R,V,H,E,C), DESIRED MISS DISTANCE (KM): R 2.0000

REQUIRED IMPULSIVE DELV - 0.013231

REQUIRED IMPULSIVE DELV VECTOR (DELVX,DELVY,DELVZ) - -0.000012 0.013231 0.000000

SELECT IMPULSIVE DELV, ENGINE BURN OR NO EVASION: (I,E OR N) N

CURRENT TIME

TIME	RREL	RRELX	RRELY	RRELZ
300.0000	408.3189	-408.3189	-0.0781	0.0000

MISSILE VALUES

ALT	R	RX	RY	RZ
869.8455	7241.1605	330.3330	7233.6219	0.0000
VMAG	VX	VY	VZ	ACCELGRAV
3.3773	-3.2918	0.7548	0.0000	7.5923
DECCELDRAG	RHO			
0.3107E-15	0.7004E-14			

TARGET VALUES

ALT	R	RX	RY	RZ
900.0000	7271.3150	738.6519	7233.7000	0.0000
VMAG	VX	VY	VZ	ACCELGRAV
7.3993	-7.3610	0.7517	0.0000	7.5295
DECCELDRAG	RHO			
0.5202E-15	0.5759E-14			

PREDICTED TIME

TIME	RREL	RRELX	RRELY	RRELZ
400.0000	0.0001	-0.0001	0.0000	0.0000

MISSILE VALUES

ALT	R	RX	RY	RZ
900.0000	7271.3150	0.0000	7271.3150	0.0000
VMAG	VX	VY	VZ	ACCELGRAV
3.3091	-3.3091	0.0000	0.0000	7.5295
DECCELDRAG	RHO			
0.2554E-15	0.5759E-14			

TARGET VALUES

ALT	R	RX	RY	RZ
900.0000	7271.3150	0.0001	7271.3150	0.0000
VMAG	VX	VY	VZ	ACCELGRAV
7.3993	-7.3993	0.0000	0.0000	7.5295
DECCELDRAG	RHO			
0.5202E-15	0.5759E-14			

EVASIVE MANEUVER REQUIRED

INPUT MANEUVER OPTION (R,V,H,E,C), DESIRED MISS DISTANCE (KM): R 2.0000

REQUIRED IMPULSIVE DELV = 0.019931

REQUIRED IMPULSIVE DELV VECTOR (DELVX,DELVY,DELVZ) = -0.000006 0.019931 0.000000

SELECT IMPULSIVE DELV, ENGINE BURN OR NO EVASION: (I,E OR N) N

CURRENT TIME

TIME RREL RRELX RRELY RRELZ
350.0000 204.4230 -204.4230 -0.0049 0.0000

MISSILE VALUES

ALT R RX RY RZ
892.4682 7263.7832 165.3815 7261.9003 0.0000

VMAG VX VY VZ ACCELGRAV
3.3262 -3.3048 0.3767 0.0000 7.5451

DECCELDRAG RHO
0.2611E-15 0.6070E-14

TARGET VALUES

ALT R RX RY RZ
900.0000 7271.3150 369.8045 7261.9052 0.0000

VMAG VX VY VZ ACCELGRAV
7.3993 -7.3897 0.3763 0.0000 7.5295

DECCELDRAG RHO
0.5202E-15 0.5759E-14

PREDICTED TIME

TIME RREL RRELX RRELY RRELZ
400.0000 0.0001 0.0000 0.0000 0.0000

MISSILE VALUES

ALT R RX RY RZ
900.0000 7271.3150 0.0000 7271.3150 0.0000

VMAG VX VY VZ ACCELGRAV

3.3091 -3.3091 0.0000 0.0000 7.5295
 DECCELDRAG RHO
 0.2478E-15 0.5759E-14

TARGET VALUES

ALT R RX RY RZ
 900.0000 7271.3150 0.0001 7271.3150 0.0000
 VMAG VX VY VZ ACCELGRAV
 7.3993 -7.3993 0.0000 0.0000 7.5295
 DECCELDRAG RHO
 0.5202E-15 0.5759E-14

EVASIVE MANEUVER REQUIRED

INPUT MANEUVER OPTION (R,V,H,E,C), DESIRED MISS DISTANCE (KM): R 2.0000

REQUIRED IMPULSIVE DELV = 0.039965

REQUIRED IMPULSIVE DELV VECTOR (DELVX,DELVY,DELVZ) = -0.000002 0.039965 0.000000

SELECT IMPULSIVE DELV, ENGINE BURN OR NO EVASION: (I,E OR N) I

CURRENT TIME

 TIME RREL RRELX RRELY RRELZ
 350.0000 204.4230 -204.4230 -0.0049 0.0000

MISSILE VALUES

ALT R RX RY RZ
 892.4682 7263.7832 165.3815 7261.9003 0.0000
 VMAG VX VY VZ ACCELGRAV
 3.3262 -3.3048 0.3767 0.0000 7.5451
 DECCELDRAG RHO
 0.2611E-15 0.6070E-14

TARGET VALUES

ALT R RX RY RZ
 900.0000 7271.3150 369.8045 7261.9052 0.0000

VMAG	VX	VY	VZ	ACCELGRAV
7.4014	-7.3897	0.4163	0.0000	7.5295
DECCELDRAG	RHO			
0.5205E-15	0.5759E-14			

PREDICTED TIME

TIME	RREL	RRELX	RRELY	RRELZ
400.0000	2.0000	0.0000	-2.0000	0.0000

MISSILE VALUES

ALT	R	RX	RY	RZ
900.0000	7271.3150	0.0000	7271.3150	0.0000
VMAG	VX	VY	VZ	ACCELGRAV
3.3091	-3.3091	0.0000	0.0000	7.5295
DECCELDRAG	RHO			
0.2478E-15	0.5759E-14			

TARGET VALUES

ALT	R	RX	RY	RZ
902.0000	7273.3150	0.0000	7273.3150	0.0000
VMAG	VX	VY	VZ	ACCELGRAV
7.3994	-7.3993	0.0401	0.0000	7.5254
DECCELDRAG	RHO			
0.5158E-15	0.5707E-14			

CURRENT TIME

TIME	RREL	RRELX	RRELY	RRELZ
400.0000	2.0000	0.0000	-2.0000	0.0000

MISSILE VALUES

ALT	R	RX	RY	RZ
900.0000	7271.3150	0.0000	7271.3150	0.0000
VMAG	VX	VY	VZ	ACCELGRAV
3.3091	-3.3091	0.0000	0.0000	7.5295
DECCELDRAG	RHO			
0.2452E-15	0.5759E-14			

TARGET VALUES

ALT	R	RX	RY	RZ
902.0000	7273.3150	0.0000	7273.3150	0.0000
VMAG	VX	VY	VZ	ACCELGRAV
7.3994	-7.3993	0.0401	0.0000	7.5254
DECCELDRAG	RHO			
0.5155E-15	0.5707E-14			

PREDICTED TIME

TIME	RREL	RRELX	RRELY	RRELZ
450.0000	204.4626	204.4231	-4.0152	0.0000

MISSILE VALUES

ALT	R	RX	RY	RZ
892.4682	7263.7832	-165.3815	7261.9002	0.0000
VMAG	VX	VY	VZ	ACCELGRAV
3.3262	-3.3048	-0.3767	0.0000	7.5451
DECCELDRAG	RHO			
0.2585E-15	0.6070E-14			

TARGET VALUES

ALT	R	RX	RY	RZ
904.0051	7275.3201	-369.8047	7265.9154	0.0000
VMAG	VX	VY	VZ	ACCELGRAV
7.3974	-7.3897	-0.3359	0.0000	7.5212
DECCELDRAG	RHO			
0.5108E-15	0.5654E-14			

MISSILE SUCCESSFULLY EVADED

FINAL ORBITAL ELEMENTS FOR THE TARGET

H	P	A	E	I
53817.3088	7275.3146	7275.5286	0.0054	0.0000

FINAL ORBITAL ELEMENTS FOR THE MISSILE

H	P	A	E	I
24061.2152	1454.2629	4039.6194	0.8000	0.0000

B.7 Scenario Demonstrating Options Available in EVADER

DIRECT INTERCEPT OR CO-ORBITAL INJECTION? (D OR C) D

INPUT DATA FOR NEW SETUP

TALT1	MALT1	TN2	MN1	FIXTIME	TRTIME	ORBINCL
300.0000	105.0000	80.0000	85.0000	2.0000	125.0000	28.5000

INTERCEPT OR NEAR-MISS TRAJECTORY? (I OR M) M

INPUT DESIRED MISS DISTANCE: 0.0100

INPUT INTSTEP, BURNSTEP, THOUTSTEP, OUTSTEP, NRUNS: 1.000 0.100 5.000
25.000 8

AXISYMMETRIC GRAVITY, DRAG? (Y OR N) Y, Y

INPUT CROSS-SECT AREAS FOR MISSILE AND TARGET (SQUARE METERS): 5.0000 30.0000

INPUT TOTAL MISSILE AND TARGET MASSES (KG): 1000.0000 20000.0000

INPUT NEW ENGINE THRUST (NEWTONS): 30000.0000

INITIAL INPUT VECTORS FOR THIS RUN

(TIME BETWEEN MISSILE FIXES: 2.0000)

RMOX	RMOY	RMOZ	RM1X	RM1Y	RM1Z
554.8073	5667.1460	3077.0092	564.4480	5669.8386	3078.4712
RT1X	RT1Y	RT1Z	VT1X	VT1Y	VT1Z
2093.9780	5566.5763	3022.4043	-7.3345	2.1308	1.1569

MISSILE AND TARGET TRAJECTORIES

TIME IN SEC, DISTANCE IN KM, VELOCITY IN KM/S
ACCELERATION DUE TO DRAG AND GRAVITY IN M/S**2, DENSITY IN KG/M**3
THRUST ACCELERATION IN KM/S**2, MASS IN KG, THRUST IN NEWTONS
VACISP IN SEC, MASSFLOW IN KG/S

INITIAL PREDICTED INTERCEPT TIME	MISSILE APOGEE ALTITUDE
125.0000	422.0629

CURRENT TIME

TIME	RREL	RRELX	RRELY	RRELZ
0.0000	1534.0367	-1529.5300	103.2623	56.0668

MISSILE VALUES

ALT	R	RX	RY	RZ
105.0000	6476.3150	564.4480	5669.8386	3078.4712
VMAG	VX	VY	VZ	ACCELGRAV
5.0543	4.8195	1.3380	0.7265	9.4915
DECCELDRAG	RHO			
0.7089E-07	0.5046E-06			

TARGET VALUES

ALT	R	RX	RY	RZ
300.0000	6671.3150	2093.9780	5566.5763	3022.4043
VMAG	VX	VY	VZ	ACCELGRAV
7.7249	-7.3345	2.1308	1.1569	8.9448
DECCELDRAG	RHO			
0.1887E-11	0.1916E-10			

PREDICTED TIME

TIME	RREL	RRELX	RRELY	RRELZ
125.0000	0.0100	-0.0098	0.0015	0.0008

MISSILE VALUES

ALT	R	RX	RY	RZ
300.0000	6671.3150	1158.4617	5773.7957	3134.9153
VMAG	VX	VY	VZ	ACCELGRAV
4.6853	4.6696	0.3371	0.1831	8.9448
DECCELDRAG	RHO			
0.2692E-11	0.1916E-10			

TARGET VALUES

ALT	R	RX	RY	RZ
300.0000	6671.3150	1158.4715	5773.7942	3134.9144
VMAG	VX	VY	VZ	ACCELGRAV
7.7249	-7.6075	1.1789	0.6401	8.9448

DECCELDRAG RHO
0.1887E-11 0.1916E-10

EVASIVE MANEUVER REQUIRED

INPUT MANEUVER OPTION (R,V,H,E,C), DESIRED MISS DISTANCE (KM): E 1.0000

REQUIRED IMPULSIVE DELV = 0.008107

REQUIRED IMPULSIVE DELV VECTOR (DELVX,DELVY,DELVZ) = -0.007984 0.001240 0.000673

SELECT IMPULSIVE DELV, ENGINE BURN OR NO EVASION: (I,E OR N) N

CURRENT TIME

TIME	RREL	RRELX	RRELY	RRELZ
25.0000	1228.7688	-1225.1168	83.1943	45.1708

MISSILE VALUES

ALT	R	RX	RY	RZ
151.5052	6522.8202	684.6478	5700.7018	3095.2285

VMAG	VX	VY	VZ	ACCELGRAV
4.9660	4.7961	1.1317	0.6145	9.3567

DECCELDRAG	RHO
0.2741E-09	0.2021E-08

TARGET VALUES

ALT	R	RX	RY	RZ
300.0000	6671.3150	1909.7646	5617.5075	3050.0577

VMAG	VX	VY	VZ	ACCELGRAV
7.7249	-7.4016	1.9434	1.0552	8.9448

DECCELDRAG	RHO
0.1887E-11	0.1916E-10

PREDICTED TIME

TIME	RREL	RRELX	RRELY	RRELZ
125.0000	0.1070	-0.1036	-0.0236	-0.0128

MISSILE VALUES

ALT	R	RX	RY	RZ
299.9555	6671.2705	1158.3679	5773.7705	3134.9013
VMAG	VX	VY	VZ	ACCELGRAV
4.6845	4.6688	0.3369	0.1829	8.9449
DECCELDRAG	RHO			
0.2604E-11	0.1920E-10			

TARGET VALUES

ALT	R	RX	RY	RZ
300.0000	6671.3150	1158.4715	5773.7942	3134.9144
VMAG	VX	VY	VZ	ACCELGRAV
7.7249	-7.6075	1.1789	0.6401	8.9448
DECCELDRAG	RHO			
0.1887E-11	0.1916E-10			

EVASIVE MANEUVER REQUIRED

INPUT MANEUVER OPTION (R,V,H,E,C): C

INPUT DESIRED MISS DISTANCES IN THE H,R, AND V DIRECTIONS: (KM)
 -4.0000 3.0000 -1.0000

RESULTING MISS DISTANCE = 5.0990

REQUIRED IMPULSIVE DELV = 0.050541

REQUIRED IMPULSIVE DELV VECTOR (DELVX,DELVY,DELVZ) = 0.014007 0.043213 -0.022155

SELECT IMPULSIVE DELV, ENGINE BURN OR NO EVASION: (I,E OR N) E

CURRENT TIME

TIME	RREL	RRELX	RRELY	RRELZ
25.0000	1228.7688	-1225.1168	83.1943	45.1708

MISSILE VALUES

ALT	R	RX	RY	RZ
151.5052	6522.8202	684.6478	5700.7018	3095.2285
VMAG	VX	VY	VZ	ACCELGRAV
4.9660	4.7961	1.1317	0.6145	9.3567
DECCELDRAG	RHO			
0.2741E-09	0.2021E-08			

TARGET VALUES

ALT	R	RX	RY	RZ
300.0000	6671.3150	1909.7646	5617.5075	3050.0577
VMAG	VX	VY	VZ	ACCELGRAV
7.7249	-7.4016	1.9434	1.0552	8.9448
DECCELDRAG	RHO			
0.1887E-11	0.1916E-10			

CURRENT TARGET ENGINE VALUES

TIME	TOTBTIME	BTAVAIL	DELVUSED	DVAVAIL
25.0000	0.0000	1105.5870	0.000000	2.041149
FUELUSED	FUELAVAIL	THDIRX	THDIRY	THDIRZ
0.0000	7000.0000	0.2771	0.8550	-0.4384
VTBGAIED	THACCEL	THRUST	MASSFLOW	VACISP
0.0505411	0.001500	30000.00	6.3315	483.0000

PREDICTED TIME

TIME	RREL	RRELX	RRELY	RRELZ
125.0000	0.1070	-0.1036	-0.0236	-0.0128

MISSILE VALUES

ALT	R	RX	RY	RZ
299.9555	6671.2705	1158.3679	5773.7705	3134.9016
VMAG	VX	VY	VZ	ACCELGRAV
4.6845	4.6688	0.3369	0.1829	8.9449
DECCELDRAG	RHO			
0.2604E-11	0.1920E-10			

TARGET VALUES

ALT	R	RX	RY	RZ
300.0000	6671.3150	1158.4715	5773.7942	3134.9144

VMAG	VX	VY	VZ	ACCELGRAV
7.7249	-7.6075	1.1789	0.6401	8.9448
DECCELDRAG	RHO			
0.1887E-11	0.1916E-10			

CURRENT TARGET ENGINE VALUES

TIME	TOTBTIME	BTAVAIL	DELVUSED	DVAVAIL
30.0000	5.0000	1100.5870	0.007506	2.033643
FUELUSED	FUELAVAIL	THDIRX	THDIRY	THDIRZ
31.6574	6968.3426	0.2772	0.8551	-0.4381
VTBGAINED	THACCEL	THRUST	MASSFLOW	VACISP
0.0454984	0.001502	30000.00	6.3315	483.0000

CURRENT TARGET ENGINE VALUES

TIME	TOTBTIME	BTAVAIL	DELVUSED	DVAVAIL
35.0000	10.0000	1095.5870	0.015024	2.026125
FUELUSED	FUELAVAIL	THDIRX	THDIRY	THDIRZ
63.3148	6936.6852	0.2772	0.8553	-0.4378
VTBGAINED	THACCEL	THRUST	MASSFLOW	VACISP
0.0403000	0.001505	30000.00	6.3315	483.0000

CURRENT TARGET ENGINE VALUES

TIME	TOTBTIME	BTAVAIL	DELVUSED	DVAVAIL
40.0000	15.0000	1090.5870	0.022554	2.018595
FUELUSED	FUELAVAIL	THDIRX	THDIRY	THDIRZ
94.9722	6905.0278	0.2772	0.8554	-0.4376
VTBGAINED	THACCEL	THRUST	MASSFLOW	VACISP
0.0349198	0.001507	30000.00	6.3315	483.0000

CURRENT TARGET ENGINE VALUES

TIME	TOTBTIME	BTAVAIL	DELVUSED	DVAVAIL
45.0000	20.0000	1085.5870	0.030095	2.011053
FUELUSED	FUELAVAIL	THDIRX	THDIRY	THDIRZ
126.6296	6873.3704	0.2773	0.8555	-0.4373
VTBGAINED	THACCEL	THRUST	MASSFLOW	VACISP
0.0293252	0.001510	30000.00	6.3315	483.0000

CURRENT TIME

 TIME RREL RRELX RRELY RRELZ
 50.0000 922.5986 -919.8537 62.3183 34.2601

MISSILE VALUES

ALT R RX RY RZ
 194.2177 6565.5327 804.2276 5726.4520 3109.2097

VMAG VX VY VZ ACCELGRAV
 4.8854 4.7697 0.9288 0.5043 9.2353

DECCELDRAG RHO
 0.6101E-10 0.4648E-09

TARGET VALUES

ALT R RX RY RZ
 300.2801 6671.5951 1724.0813 5664.1336 3074.9496

VMAG VX VY VZ ACCELGRAV
 7.7201 -7.4520 1.7866 0.9360 8.9440

DECCELDRAG RHO
 0.1893E-11 0.1909E-10

CURRENT TARGET ENGINE VALUES

 TIME TOTBTIME BTAVAIL DELVUSED DVAVAIL
 50.0000 25.0000 1080.5870 0.037649 2.003499

FUELUSED FUELAVAIL THDIRX THDIRY THDIRZ
 158.2870 6841.7130 0.2773 0.8556 -0.4371

VTBGAINED THACCEL THRUST MASSFLOW VACISP
 0.0234750 0.001512 30000.00 6.3315 483.0000

PREDICTED TIME

 TIME RREL RRELX RRELY RRELZ
 125.0000 3.3389 -1.0177 -2.8446 1.4216

MISSILE VALUES

ALT R RX RY RZ
 299.9554 6671.2704 1158.3676 5773.7705 3134.9016

VMAG VX VY VZ ACCELGRAV

4.6845 4.6688 0.3369 0.1829 8.9449
 DECCELDRAG RHO
 0.2520E-11 0.1920E-10

TARGET VALUES

ALT R RX RY RZ
 301.9266 6673.2416 1159.3853 5776.6151 3133.4800
 VMAG VX VY VZ ACCELGRAV
 7.7182 -7.5970 1.2112 0.6238 8.9396
 DECCELDRAG RHO
 0.1853E-11 0.1869E-10

CURRENT TARGET ENGINE VALUES

 TIME TOTBTIME BTAVAIL DELVUSED DVAVAIL
 55.0000 30.0000 1075.5870 0.045215 1.995933
 FUELUSED FUELAVAIL THDIRX THDIRY THDIRZ
 189.9443 6810.0557 0.2773 0.8557 -0.4369
 VTBGAINED THACCEL THRUST MASSFLOW VACISP
 0.0173159 0.001514 30000.00 6.3315 483.0000

CURRENT TARGET ENGINE VALUES

 TIME TOTBTIME BTAVAIL DELVUSED DVAVAIL
 60.0000 35.0000 1070.5870 0.052793 1.988356
 FUELUSED FUELAVAIL THDIRX THDIRY THDIRZ
 221.6017 6778.3983 0.2773 0.8558 -0.4367
 VTBGAINED THACCEL THRUST MASSFLOW VACISP
 0.0107787 0.001517 30000.00 6.3315 483.0000

CURRENT TARGET ENGINE VALUES

 TIME TOTBTIME BTAVAIL DELVUSED DVAVAIL
 65.0000 40.0000 1065.5870 0.060383 1.980765
 FUELUSED FUELAVAIL THDIRX THDIRY THDIRZ
 253.2591 6746.7409 0.2773 0.8559 -0.4365
 VTBGAINED THACCEL THRUST MASSFLOW VACISP
 0.0037707 0.001519 30000.00 6.3315 483.0000

CURRENT TARGET ENGINE VALUES

TIME	TOTBTIME	BTAVAIL	DELVUSED	DVAVAIL
67.5000	42.5000	1063.0870	0.064183	1.976966
FUELUSED	FUELAVAL	THDIRX	THDIRY	THDIRZ
269.0878	6730.9122	0.2773	0.8559	-0.4364
VTBGAINED	THACCEL	THRUST	MASSFLOW	VACISP
0.0000524	0.000524	10341.48	2.1826	483.0000

CURRENT TARGET ENGINE VALUES

TIME	TOTBTIME	BTAVAIL	DELVUSED	DVAVAIL
67.6000	42.6000	1063.0525	0.064235	1.976913
FUELUSED	FUELAVAL	THDIRX	THDIRY	THDIRZ
269.3061	6730.6939	0.2732	0.8565	-0.4379
VTBGAINED	THACCEL	THRUST	MASSFLOW	VACISP
0.0000000	0.000000	0.00	0.0000	483.0000

EVASIVE MANEUVER COMPLETED - THRUST TERMINATED

CURRENT TIME

TIME	RREL	RRELX	RRELY	RRELZ
75.0000	615.8812	-614.1032	40.3808	23.5865

MISSILE VALUES

ALT	R	RX	RY	RZ
233.1758	6604.4908	923.1006	5747.1672	3120.4572
VMAG	VX	VY	VZ	ACCELGRAV
4.8116	4.7396	0.7289	0.3957	9.1267
DECCELDRAG	RHO			
0.1602E-10	0.1258E-09			

TARGET VALUES

ALT	R	RX	RY	RZ
301.0920	6672.4070	1537.2037	5706.7864	3096.8707
VMAG	VX	VY	VZ	ACCELGRAV
7.7158	-7.4993	1.6187	0.8210	8.9418
DECCELDRAG	RHO			
0.1881E-11	0.1889E-10			

PREDICTED TIME

TIME	RREL	RRELX	RRELY	RRELZ
125.0000	5.0992	-1.5062	-4.3525	2.1884

MISSILE VALUES

ALT	R	RX	RY	RZ
299.9554	6671.2704	1158.3675	5773.7705	3134.9016

VMAG	VX	VY	VZ	ACCELGRAV
4.6845	4.6688	0.3369	0.1829	8.9449

DECCELDRAG	RHO
0.2444E-11	0.1920E-10

TARGET VALUES

ALT	R	RX	RY	RZ
302.9568	6674.2718	1159.8737	5778.1230	3132.7132

VMAG	VX	VY	VZ	ACCELGRAV
7.7137	-7.5897	1.2340	0.6123	8.9368

DECCELDRAG	RHO
0.1836E-11	0.1844E-10

CURRENT TIME

TIME	RREL	RRELX	RRELY	RRELZ
100.0000	308.7263	-307.9270	18.0589	12.9130

MISSILE VALUES

ALT	R	RX	RY	RZ
268.4121	6639.7271	1041.1765	5762.9183	3129.0093

VMAG	VX	VY	VZ	ACCELGRAV
4.7446	4.7059	0.5316	0.2887	9.0301

DECCELDRAG	RHO
0.5624E-11	0.4542E-10

TARGET VALUES

ALT	R	RX	RY	RZ
302.0309	6673.3459	1349.1035	5744.8594	3116.0963

VMAG	VX	VY	VZ	ACCELGRAV
7.7147	-7.5477	1.4269	0.7169	8.9393

DECCELDRAG RHO
0.1858E-11 0.1867E-10

PREDICTED TIME

TIME RREL RRELX RRELY RRELZ
150.0000 306.2065 304.9146 -26.7675 -8.5421

MISSILE VALUES

ALT R RX RY RZ
327.8315 6699.1465 1274.5880 5779.7838 3138.1665

VMAG VX VY VZ ACCELGRAV
4.6312 4.6283 0.1445 0.0785 8.8706

DECCELDRAG RHO
0.1535E-11 0.1240E-10

TARGET VALUES

ALT R RX RY RZ
303.8689 6675.1839 969.6734 5806.5513 3146.7086

VMAG VX VY VZ ACCELGRAV
7.7126 -7.6253 1.0401 0.5072 8.9344

DECCELDRAG RHO
0.1814E-11 0.1822E-10

CURRENT TIME

TIME RREL RRELX RRELY RRELZ
125.0000 5.0992 -1.5062 -4.3525 2.1884

MISSILE VALUES

ALT R RX RY RZ
299.9554 6671.2704 1158.3675 5773.7705 3134.9016

VMAG VX VY VZ ACCELGRAV
4.6845 4.6688 0.3369 0.1829 8.9449

DECCELDRAG RHO
0.2317E-11 0.1920E-10

TARGET VALUES

ALT R RX RY RZ
302.9568 6674.2718 1159.8737 5778.1230 3132.7132

VMAG	VX	VY	VZ	ACCELGRAV
7.7137	-7.5897	1.2340	0.6123	8.9368
DECCELDRAG	RHO			
0.1835E-11	0.1844E-10			

PREDICTED TIME

TIME	RREL	RRELX	RRELY	RRELZ
175.0000	613.3637	611.0918	-49.1092	-19.2377

MISSILE VALUES

ALT	R	RX	RY	RZ
352.0630	6723.3780	1389.7537	5781.0134	3138.8342
VMAG	VX	VY	VZ	ACCELGRAV
4.5847	4.5844	-0.0458	-0.0249	8.8068
DECCELDRAG	RHO			
0.8256E-12	0.6840E-11			

TARGET VALUES

ALT	R	RX	RY	RZ
304.7663	6676.0813	778.6619	5830.1226	3158.0719
VMAG	VX	VY	VZ	ACCELGRAV
7.7116	-7.6545	0.8455	0.4018	8.9320
DECCELDRAG	RHO			
0.1792E-11	0.1800E-10			

CURRENT TIME

TIME	RREL	RRELX	RRELY	RRELZ
150.0000	306.2064	304.9146	-26.7675	-8.5421

MISSILE VALUES

ALT	R	RX	RY	RZ
327.8315	6699.1465	1274.5880	5779.7838	3138.1665
VMAG	VX	VY	VZ	ACCELGRAV
4.6312	4.6283	0.1445	0.0785	8.8706
DECCELDRAG	RHO			
0.1463E-11	0.1240E-10			

TARGET VALUES

ALT	R	RX	RY	RZ
303.8689	6675.1839	969.6734	5806.5513	3146.7086
VMAG	VX	VY	VZ	ACCELGRAV
7.7126	-7.6253	1.0401	0.5072	8.9344
DECCELDRAG	RHO			
0.1813E-11	0.1822E-10			

PREDICTED TIME

TIME	RREL	RRELX	RRELY	RRELZ
200.0000	920.0362	916.7824	-71.3092	-29.8626

MISSILE VALUES

ALT	R	RX	RY	RZ
372.6691	6743.9841	1503.7818	5777.5099	3136.9319
VMAG	VX	VY	VZ	ACCELGRAV
4.5451	4.5373	-0.2342	-0.1271	8.7530
DECCELDRAG	RHO			
0.6022E-12	0.5105E-11			

TARGET VALUES

ALT	R	RX	RY	RZ
305.6485	6676.9635	586.9994	5848.8191	3166.7946
VMAG	VX	VY	VZ	ACCELGRAV
7.7105	-7.6774	0.6502	0.2960	8.9296
DECCELDRAG	RHO			
0.1770E-11	0.1779E-10			

MISSILE SUCCESSFULLY EVADED

FINAL ORBITAL ELEMENTS FOR THE TARGET

H	P	A	E	I
51482.5273	6657.7509	6657.9422	0.0054	28.4029

FINAL ORBITAL ELEMENTS FOR THE MISSILE

H	P	A	E	I
30229.5800	2295.4723	4087.1454	0.6621	28.5000

Bibliography

- [1] Anderson, G. M. and G. D. Bohn. *A Near-Optimal Control Law for Pursuit-Evasion Problems Between Two Spacecraft*. AIAA Paper 76-794, American Institute of Aeronautics and Astronautics, New York, NY, August 1976.
- [2] Angell, Lt Col John E. United States Air Force Perspective of Space Operations. In *AIAA Computers in Aerospace Conference*, pp. 263-267, American Institute of Aeronautics and Astronautics, New York, NY, October 1983.
- [3] Ash, M. E. *Velocity Requirements for Rapid Intercept with Midcourse Corrections*. Technical Note 1970-32, MIT Lincoln Laboratory, Lexington, MA, October 1970. ESD-TR-70-320.
- [4] Battin, Richard H., Charles Stark Draper Laboratory, Adjunct Professor of Aeronautics and Astronautics, MIT. *An Introduction to the Mathematics and Methods of Astrodynamics*. 1984. in publication.
- [5] Battin, Richard H., and Robin M. Vaughan. An Elegant Lambert Algorithm. In *34th Congress of the International Astronautical Federation, Selected Papers, Volume 2*. IAF Paper 83-325, American Institute of Aeronautics and Astronautics, New York, NY, October 1983.
- [6] Brown, J. R., Pratt & Whitney Aircraft Co. Advanced OTV Engines and Issues. In *OTV Propulsion Issues*, pp. 127-134, NASA Lewis Research Center, Cleveland, OH, April 1984. NASA Conference Publication 2347.
- [7] Ethell, Jeff. To Kill or Not To Kill Satellites. *Aerospace America*, Vol. 23 No. 11, pp. 10-13, November 1985.
- [8] Fitzgerald, Dennis E. *Minimum Energy Intercept of a Deorbiting Target*. AIAA Paper 70-1019, American Institute of Aeronautics and Astronautics, New York, NY, August 1970.
- [9] Garwin, Richard L., Kurt Gottfried, and Donald L. Hafner. Antisatellite Weapons. *Scientific American*, Vol. 250 No. 6, pp. 45-55, June 1984.
- [10] Henderson, Col Donald W. Defending Our Space Assets - The Issues and the Challenges. AAS Paper 81-304, In *Leadership in Space for Benefits on Earth*, pp. 45-51, William F. Rector, III, ed., American Astronautical Society, October 1981.
- [11] Jezewski, D. J. An Analytic Solution For the J_2 Perturbed Equatorial Orbit. *Celestial Mechanics*, 30(4):363-371, August 1983.
- [12] Jezewski, D. J. A Noncanonical Analytic Solution to the J_2 Perturbed Two-Body Problem. *Celestial Mechanics*, 30(4):343-361, August 1983.

- [13] Kelley, Henry J., Eugene M. Cliff, and Frederick H. Lutze. Pursuit/Evasion in Orbit. *The Journal of the Astronautical Sciences*, 29(3):277-288, July-September 1981.
- [14] Lerner, Eric J. SDI: Part II - Survivability and Stability. *Aerospace America*, Vol. 23 No. 9, pp. 80-84, September 1985.
- [15] Lerner, Eric J. SDI: Part III - Who Wins the Cost Exchange. *Aerospace America*, Vol. 24 No. 10, pp. 62-66, October 1985.
- [16] Mordoff, Keith F. Test Asat Launched Autonomously From USAF Carrier Aircraft. *Aviation Week & Space Technology*, Vol. 123 No. 14, pp. 18-19, October 7, 1985.
- [17] Morishige, Lt Col Ronald I., and Lt Col John Retelle. Air Combat and Artificial Intelligence. *Air Force Magazine*, Vol. 68 No. 10, pp. 91-93, October 1985.
- [18] Muckley, Edwin T. Shuttle/Centaur Project Perspective. In *OTV Propulsion Issues*, pp. 15-28, NASA Lewis Research Center, Cleveland, OH, April 1984. NASA Conference Publication 2347
- [19] Pope, David Edward. *An Expert System for Airborne Object Analysis*. Massachusetts Institute of Technology, January 1985. Master's Thesis.
- [20] Reiss, Martin H. Guidance and Control Considerations for Guided Interceptor Vehicles in Space. In *Advances in the Astronautical Sciences*, pp. 212-228, Eric Burgess, ed., American Astronautical Society, New York, NY, August 1961.
- [21] Robinson, Jr., Clarence A. BMD Homing Interceptor Destroys Reentry Vehicle. *Aviation Week & Space Technology*, Vol. 120 No. 25, pp. 19-20, June 18, 1984.
- [22] Rosenbaum, Richard. *Minimum-Time Intercept of a Maneuvering Orbital Target with Constant Thrust Acceleration*. AAS 68-082, American Astronautical Society, Washington, D. C., September 1968.
- [23] Salkeld, Robert. Space Interceptors: An Investigation of Seven Main Parameters. *Journal of Spacecraft and Rockets*, 8(5):541-543, May 1971.
- [24] Schoenman, L., Aerojet TechSystems Co. Aerojet Advanced Engine Concept. In *OTV Propulsion Issues*, pp. 113-126, NASA Lewis Research Center, Cleveland, OH, April 1984. NASA Conference Publication 2347.
- [25] Shoup, Terry E. *A Practical Guide to Computer Methods for Engineers*. Chapter 4, Prentice-Hall, Englewood Cliff, NJ, 1979.
- [26] Stuart, Dale Gordon. A Simple Targeting Technique for Two-Body Spacecraft Trajectories. *Journal of Guidance, Control, and Dynamics*, 9(1):27-31, January-February 1986.

- [27] Taylor, John W. R. Gallery of Soviet Aerospace Weapons. *Air Force Magazine*, Vol. 69 No. 3, p. 97, March 1986.
- [28] Zachary, A. T., Rockwell International, Rocketdyne Division. Advanced OTV Engine Concepts. In *OTV Propulsion Issues*, pp. 135-148, NASA Lewis Research Center, Cleveland, OH, April 1984. NASA Conference Publication 2347.
- [29] DARPA's Pilot's Associate Program Provides Development Challenges. *Aviation Week & Space Technology*, Vol. 124 No. 7, pp. 45-52, February 17, 1986.
- [30] Defense Dept. Plans Next Test Firing of Air-Launched Asat System. *Aviation Week & Space Technology*, Vol. 123 No. 12, pp. 20-21, September 23, 1985.
- [31] Soviet Aerospace Almanac 1986. *Air Force Magazine*, Vol. 69 No. 3, p. 78, March 1986.
- [32] Soviets Launch Antisatellite Targetlike Vehicle. *Aviation Week & Space Technology*, Vol. 116 No. 24, p. 19, June 14, 1982.
- [33] Soviets Orbit Large New Military Electronic Intelligence Satellite. *Aviation Week & Space Technology*, Vol. 122 No. 2, pp. 19-20, January 14, 1985.
- [34] Soviets Stage Integrated Test of Weapons. *Aviation Week & Space Technology*, Vol. 116 No. 26, pp. 20-21, June 28, 1982.
- [35] USAF Selects Nuclear-Powered Warning Sensor. *Aviation Week & Space Technology*, Vol. 124 No. 11, p. 74, March 17, 1986.
- [36] USAF Vehicle Designed for Satellite Attack. *Aviation Week & Space Technology*, Vol. 122 No. 2, p. 21, January 14, 1985.
- [37] *U.S. Standard Atmosphere, 1976*. U.S. Committee on Extension to the Standard Atmosphere, U.S. Government Printing Office, Washington, D.C., October 1976.
- [38] *U.S. Standard Atmosphere Supplements, 1966*. U.S. Committee on Extension to the Standard Atmosphere, U.S. Government Printing Office, Washington, D.C., 1966. p. 61.

ATE
LMED
-8